이학박사학위논문

애기장대 히스톤 탈아세틸화 효소 HDA9의 개화 및 발아 관련 기능에 대한 연구

A Study on the Role of Histone Deacetylase HDA9 in Arabidopsis Flowering and Germination

2016년 2월

서울대학교 대학원

생명과학부

강 민 정

Abstract

A Study on the Role of Histone Deacetylase HDA9 in Arabidopsis Flowering and Germination

Min-Jeong Kang

Department of Biological Sciences

The Graduate School

Seoul National University

Posttranslational acetylation of histones is reversibly regulated by histone deacetylases (HDACs). Despite the evident significances of HDACs in Arabidopsis development, the biological roles and underlying molecular mechanisms of many HDACs are yet to be elucidated. In this study, I revealed the biological role of the RPD3/HDA1-class histone deacetylase HDA9 in resetting histone acetylation levels during active transcription to maintain proper transcription activity in two major phase transition of plants; seed germination and flowering.

Loss-of-function in *HDA9* flowered early under non-inductive short-day

(SD) condition and showed increased expression of the floral integrator, *FT* and floral activator, *AGL19*. The *hda9* mutation increased histone H3 acetylation and RNA polymerase II occupancy at *AGL19* chromatin but not *FT* during active transcription. In addition, HDA9 directly targeted *AGL19*, and *AGL19* expression was higher in SD than LD condition. The *agl19* mutation is epistatic to the *hda9* mutation, masking the early flowering and increased *FT* expression of *hda9*. Taken together, my data indicates that HDA9 prevents precocious flowering in SD by curbing the hyper-activation of *AGL19*, an upstream activator of *FT*, through resetting local chromatin environment.

Epigenetic regulation network through HAT and HDAC is known to play crucial roles in seed development. Timing of seed germination is controlled by various environmental factors in order to initiate a successful new life cycle under favorable environment. Light is the most critical environmental factor to promote seed germination. Light-induced germination process involves the perception of light mainly by phytochrome B (phyB) and degradation of the germination repressor PHYTOCHROME INTERACTING FACTOR (PIF1) resulted from its interaction with phyB.

Through this study, I found out that HDA9 adds a new layer of regulation for phyB-dependent germination process. Loss-of-*HDA9* activity caused rapid germination after red-light pulse treatment and under continuous white light. The expressin of *HECs*, previously known repressors of PIF1 transcription activity was also increased in the *hda9* mutant. Epistatic analysis between the *hda9* mutant and

hec1hec2 RNAi showed that rapid seed germination of the *hda9* mutant was caused by the increased *HECs* expression. Histone H3 acetylation level and RNA polymerase II occupancy at *HECs* were more elevated in *hda9-1* than in wt after red light pulse but not after far-red light pulse. The direct association of HDA9 with *HECs* chromatin was also observed after red light pulse but not after far-red light pulse. Furthermore, HDA9 also affect the expression of *GA-INSENSITIVE (GAI)* and *REPRESSOR OF GA1-3 (RGA/RGA1),* downstream target genes of *PIF1*. Taken together, my results indicate that HDA9 plays a role in the prevention of the hyper light-sensitive germination by inhibiting the hyper-activation of *HECs* transcription by light through deacetylating *HEC* chromatin during active transcription. Thus, HDA9 acts as a fine-tuning mechanism of phyB-dependent germination ensuring the beginning of germination under proper light condition.

In conclusion, throughout my research, I focused on the identification of the novel roles of HDA9 during seed germination and flowering. The role of HDA9 in transcription, unlike the conventional idea of HDACs is to modulate the transcription activity of target chromatin (*AGL19* and *HECs*) by resetting the landscape of chromatin during active transcription.

Key words: histone deacetylation, histone deacetylase (HDA9), HECATE (HEC), seed germination, AGAMOUS-LIKE 19 (AGL19), flowering.

Student Number: 2008-30102

Contents

List of tables

Chapter II.

Chapter III.

List of figures

Chapter I. General introduction

Chapter II.

Chapter III.

Abbreviations

AGL19	AGAMOUS-LIKE 19
bP	base pair
ChIP	chromatin immunoprecipitation
DAP	days after planting
DNA	deoxyribonucleic acid
FLC	FLOWERING LOCUS C
FT	FLOWERING LOCUS T
Fp	far-red light pulse
GAI	GA-INSENSITIVE
GUS	β-glucuronidase
HA	hemagglutinin
HDAC	Histone deacetylation
HDA9	Histone deacetylase 9
HEC	HECATE
K	lysine
kD	kilodalton
LD	long day
LN	leaf number

MS	Murashige-skoog
mRNA	messenger ribonucleic acid
N	nuclear protein
NN	nonnuclear protein
NV	nonvernalization
PAGE	polyacrylamide gel
PCR	polymerase chain reaction
phyB	phytochrome B
PIF1	PHTOCHROME INTERACTING FACTOR 1
qPCR	quantitative polymerase chain reaction
RAM	root apical meristem
RGA	REPRESSOR OF GA1-3
Rp	red light pulse
RT	reverse-transcription
SAM	shoot apical meristem
SD	short day
SDS	sodium dodecyl sulfate
S.E	standard error
UTR	untranslated region
V	vernalization

General introduction

1. Epigenetics and gene regulation

Multicellular eukaryotes are composed of structurally distinctive and membrane-enclosed organelles. They have developed well-organized systems for the regulation of gene expression. Eukaryotic organs and tissues are affected by differential gene expression during development. Gene-expression control in eukaryotes begins with an access to DNA before transcription initiation. The DNA accessibility is related with epigenetics, which allows stable differential gene expressions without changes in DNA sequence. These epigenetically regulated expression patterns are heritable through mitotic and/or meiotic cell divisions.

Hitherto, three main mechanisms are acknowledged underlying epigenetic gene regulations: histone modification, DNA methylation, and ATP-dependent chromatin remodeling. In addition, small or long non-coding RNAs are recently ascertained to affect chromatin structure and transcription control via RNA interference (RNAi) pathways (Holoch and Moazed, 2015). Moreover, crosstalks between these mechanisms also exist. Occurrence of one mechanism may promote another to arise in cooperative manner or may also be disrupted by another due to antagonistic effects between them. Therefore, multiple epigenetic mechanisms provide a higher level of complexity and more fine-tuned control for the regulation of gene expression.

1.1 Histone modification

Chromatin modification exerts critical roles in cell proliferation, differentiation, cell-cycle regulation, and cell function in all eukaryotes. Generally, 147 base pairs (bp) of DNA wraps around a compact histone octamer, which is assembled by two H2A-H2B histone heterodimers and two H3-H4 histone heterodimers, forming 'beads-on-a-string'-like structure. The histone octamer and the surrounding DNA make interactions through the core histone fold and its N-terminal tails. Indeed, N-terminal tails of each histone proteins are exposed to the outer surface of histone octamer in such way that many chemical modifications can frequently occur on those tails and thus easily modulate the transcription of the adjacent DNA (Strahl and Allis, 2000; Zhang and Reinbag, 2001; Berger, 2002).

The compaction of chromatin changes depending on the stage of cell cycle, and its conformational change alters the accessibility of RNA polymerase and transcription regulatory proteins to the DNA strand. Chromatin loosening during interphase allows RNA and DNA polymerases to approach for transcription and replication. Genes within the relaxed state of chromatin, called euchromatin, are actively transcribed and associated with RNA polymerases. On the other hand, heterochromatin, more condensed state of chromatin, is responsible for repression of gene expression during the remaining of cell cycles and serves to protect chromosome integrity.

Histone modification has been widely studied, and different types of histone modification mechanisms have been examined. Covalent histone posttranslational modifications, including acetylation, methylation, phosphorylation, sumoylation,

ubiquitination, and ADP-ribosylation, play critical roles in epigenetic control of transcription. Among them, acetylation and methylation are the most profoundly studied histone modifications. The first one will be further discussed in detail in the following sections. Briefly, histone methylation can either increase or decrease transcription activity depending on which lysine or arginine on the N-terminal tails of the histones is modified. Histone phosphorylation is associated with chromatin compaction during mitosis and meiosis. Histone ubiquitination is a covalent modification on lysine residues, and its function is determined upon the substrate specificity or the degree of ubiquitination. Sumoylation also involves a covalent attachment of small ubiquitin-like modifier to lysine residues and is responsible for the repression of its target gene. ADP-ribosyltransferases catalyze mono- and poly-ADP ribosylation at glutamate and arginine residues, and this type of posttranslational modification occurs reversibly in various cellular processes (Bannister and Kouzarides, 2011).

1.1.1 Histone acetylation

It has been demonstrated that histone acetylation is associated with transcriptional activation in various cellular processes such as chromatin dynamics, cell cycle progression, DNA repair, and many others. This type of modification is catalyzed by histone acetyltransferases (HATs), which are also known as transcriptional co-activators. These enzymes neutralize the positive charge on the lysine residues at N-terminal tails of histone proteins by transferring an acetyl group from acetyl-coenzyme A (acetyl-CoA) to the NH_3^+ of the amino group on

the histone tails. Neutralization of the lysine residues leads to a weaker binding between the core histone proteins and the negatively charged DNA, and this allows the chromatin to be in an open conformation. Moreover, transferred acetyl group can be recognized by a reader module, such as bromodomain, of other proteins that finally allow additional loosening of chromatin. As a result, RNA polymerase and transcription factors are prone to access the euchromatin region. Generating binding sites for protein-protein interaction ensues in gene activation located on the chromatin. Indeed, expression of transcribed gene is correlated with enriched HATs on the gene locus. Several studies have demonstrated that HATs are preferentially associated with promoters or exonic regions of target genes. In addition, from studies on genome-wide distribution maps, it is revealed that recruitment of HATs and RNA polymerase II binding are positively correlated each other, supporting the idea that histone acetylation serves as an important positive regulator of its target gene expression (Barski et al., 2007; Shahbazian and Grunstein, 2007; Wang et al., 2009).

HATs are classified into two families depending on their subcellular localizations: type-A in the nucleus and type-B in the cytoplasm. Type-A HATs are diverse and function within context. They often recognize acetylated lysine residues with their conserved bromodomain. According to their structural features and functional roles, type-A HATs are subdivided into separate groups of the cAMP Responsive Element-Binding Protein (CREB)-Binding Protein (CBP)/p300 family, the MOZ, Ybf2/Sas3, Sas2, and Tip60 (MYST) family, the GCN5-Related N-terminal Acetyltransferase (GNAT) family, the TATA-Binding Protein-

Associated Factor $(TAF)_{II}250$ family, and the mammalian-specific nuclear hormone-related HAT family, ACTR/AIB1 and SRC1 (Neuwald and Landsman, 1997: Goodman and Smolik, 2000; Sterner and Berger, 2000; Roth et al., 2001; Kalkhoven, 2004; Hodawadekar and Marmorstein, 2007; Lee and Workman, 2007). Type-B HATs, on the other hand, acetylate free histones prior to their assembly into nucleosomes (Hodawadekar and Marmorstein, 2007; Yang and Seto, 2007; Bannister and Kouzarides, 2011). They function on newly synthesized histone H3 and histone H4, while type-A members act on H2A, H2B, H3 and H4. Moreover, they share higher amino-acid sequence similarity than type-A HATs (Parthun, 2007; Bannister and Kouzarides, 2011).

In Arabidopsis, 12 genes are identified to encode HATs, and they are classified into four groups as summarized in Fig.1-1(a) (Pandey et al., 2002; Liu et al., 2012). Moreover, N-terminal lysine residues of histone H3 (K9, K14, K18, K23, and K27) and H4 (K5, K8, K12, K16, and K20) are well conserved as acetylation or de-acetylation sites in Arabidopsis (Servet et al., 2010). Five proteins, named as HACs in Arabidopsis, are members of CBP/P300 family: HAC1, HAC2, HAC4, HAC5, and HAC12. In plant, there are more number of this type of HATs than animals which usually possess only one or two homologs. MYST-family members are called as HAM1/HAG4 and HAM2/HAG5. HAG1/GCN5, HAG2, and HAG3/ELP3 belong to the GNAT family. Moreover, two of the TATA-binding protein-associated factor (TAFII 250)-family members are renamed as HAF1 and HAF2/TAF1 in Arabidopsis. The classification of Arabidopsis HATs are summarized in Fig1-1(a).

HATs play critical roles in many cellular processes in Arabidopsis. Among the CBP/p300-family members, HAC1 functions in flowering-time control (Deng et al., 2007; Han et al., 2007) and immune response (Singh et al., 2014). In addition, HAC1 and HAC5 are involved in the ethylene-signaling pathway (Li et al., 2014). In the TAFII family, HAF2 is required to integrate light response such as in chlorophyll accumulation (Bertrand et al., 2005; Renhamed et al., 2006). The GNAT/MYST family, the most extensively studied group of HATs, function in developmental processes, cell differentiation, leaf or floral organogenesis, and meristem function (Servet et al., 2010). Moreover, HAG1/GCN5 mutations result in various pleiotropic defects during developmental process. The role of HAG1/GCN5 is well characterized in root and shoot development, flower development, micro RNA (miRNA) production, light signaling and response, and low-temperature response (Bertrand et al., 2003; Renhamed et al., 2006; Earley et al., 2007; Servet et al., 2010; Wang et al., 2014; Kim et al., 2015). HAG2 is necessary for DNA replication and cell cycle progression (Ramirez-Parra et al., 2003; Vandepoele et al., 2005). HAG3 is involved in ABA response, oxidative stress, cell-cycle progression, immune responses, and leaf patterning (Nelissen et al., 2005; Chen et al., 2006; Zhou et al., 2009; Defraia et al., 2010; Xu et al., 2012). In short, histone acetylation is one of the most important posttranslational modification that affect transcription activities in various developmental aspects and environmental responses.

1.1.2 Histone deacetylation

Conformation change of chromatin via histone acetylation is reversible by histone deacetylases (HDACs), which have an opposite role against HATs. They remove the acetyl group from N-acetyl lysine residues in both histone and non-histone proteins. Histone deacetylation turns neutralized histone tail back into positively charged one and tight binding between the histone tail and the DNA backbone is reestablished, resulting in heterochromatin state of the modulated chromatin. The compacted chromatin structure prevents access of transcription factors and RNA polymerases to the target DNA, and thus transcription repression occurs (Cress and Seto, 2000; Yang and Seto, 2003).

HDACs, also known as transcriptional co-repressors, are traditionally considered to be recruited to mainly repressed genes replacing HATs. However, based on recent findings, it has been revealed that HDAC-enrichment patterns are more dynamic than anticipated through transient bindings of HATs and HDACs and via crosstalk with other types of histone modifications. Three association models of HDAC-binding mechanisms were established through genome-wide studies (Wang et al., 2009). First, as a contradiction to the traditional hypothesis, HDACs are more enriched on active genes rather than repressed ones. HDACs are recruited on active genes to maintain a suitable level of histone acetylation. After transcription activation followed by acetylation, chromatin status is normally required to be reset. Then, HDACs are recruited and function on those genes to reset their acetylation levels. Moreover, excessive acetylation of histones in

transcribed regions may result in cryptic initiation of transcription due to the destabilized chromatin status. Hence, it is a requisite for active genes to be controlled by HDACs for their adequate acetylation levels. In addition, both HATs and HDACs are detected at the highest levels on actively transcribed genes. In other words, the binding patterns of HDACs are positively correlated with transcription, RNA polymerase II occupancy, and histone acetylation levels. Second, HDACs are associated with poised genes, which are primed by histone H3 lysine 4 (H3K4) methylation or histone H2A.Z variant. H3K4 methylation or H2A.Z priming prepares yet-to-be expressed genes for activation by modulating the chromatin architecture to facilitate acetylation. HATs then transiently bind on the chromatin regions, transfer acetyl groups and potentiate future activation upon activation signals. Simultaneously and dynamically, HDACs function to reduce acetylation to keep the primed gene unexpressed until signaling. Low level distribution patterns of both HATs and HDACs on primed genes were observed genome-widely (Wang et al., 2009). In short, transient acetylation and deacetylation occur concurrently and sporadically to poise silent genes adept for further activation. Third, HDACs are recruited on silent genes with unexpectedly low frequency at undetectable levels. Unlike silenced but primed genes, neither histone acetylation nor deacetylation activities were detected on these repressive non-primed genes. It is clear that enriched level of histone H3 lysine 27 (H3K27) trimethylation, generated by the Polycomb Group (PcG) complex, is related with the gene silencing. However, it is not evident that HATs or HACs function on those genes for transcriptional regulation. Therefore, depending on target genes and

their chromatin status, role of HDACs may vary.

HDACs can be classified into 4 different classes, from I to IV, based on sequence similarity among them (Yang and Seto, 2007). Depending on species, entitlement can be differed. Fig1-1(b) shows the phylogenetic trees of Arabidopsis HDACs, illustrating the similarity of HDAC domains using neighbor-joining algorithm. In Arabidopsis, 18 HDAC proteins are categorized into three large groups. 12 of the Arabidopsis 18 HDACs belong to the yeast Reduced Potassium Deficiency (RPD3/HDA1) superfamily, which are named as HDAs in Arabidopsis. Other 4 belong to the plant-specific Histone Deacetylase 2 (HD2) family, known as HD-tuins (HDT), and the other 2 belong to the yeast Silent Information Regulator 2 (SIR2) family and are termed as SiRTuin 1 (SRT). Then, RPD3/HDA1 superfamily of plant HDACs is further divided into three subclades, Class I, II, and III, based on their homology to yeast HDAC proteins. Arabidopsis Class I HDAC proteins are most closely related to the yeast RPD3 family, and Arabidopsis Class II to the yeast HDA1 family. Class III members share no sequence homology with yeast HDACs. (Rundlett et al., 1996; Grozinger et al., 1999; Gao et al., 2002; Pandey et al., 2002). In Arabidopsis, 6 HDA proteins belong to Class I: HDA6, HDA7, HDA9, HDA10, HDA17, and HDA19. This class of the RPD3/HDA1 includes most of identified Arabidopsis HDA proteins. Of the 6 Class I proteins, HDA6 and HDA19 are most profoundly investigated for their function and mechanism. HDA6 functions in the acceleration of flowering, repression of embryonic trait, and light-induced chromatin compaction (Tanaka M et al., 2008; Snoek LB et al., 2009; Yu CW et al., 2011). HDA19 is involved in light-mediated hypocotyl elongation,

repression of salicylic acid (SA) biosynthesis and SA-dependent defense response (Benhamed et al., 2006; Choi et al., 2012). Moreover, HDA9, HDA10, and HDA17 are proposed to be involved in disease resistance because the intergenic sequence between *HDA9* and *HDA10* genes and *HDA17* gene is annotated as 'disease-resistance-like' gene in the Genebank database. Yet, Class I members, other than HDA6 and HDA19, are not extensively characterized for their function and mechanism. In the Chapter II and III of this thesis, I will demonstrate the mechanism and biological role of HDA9 in photoperiodic flowering and seed germination in detail. Class II proteins include the following three HDACs that contain subcellular localization signals: HDA5, HDA15, and HDA18. Among them, HDA5 and HDA18 possess putative nuclear export signals and may be shuttled between nucleus and cytoplasm (Grozinger and Schreiber, 2000; Verdel et al., 2000). HDA15 encompasses a RanBP zinc-finger domain which was shown to function in nucleocytoplasmic transport and nuclear envelope localization (Vetter et al., 1999). HDA2 is a sole member of Class III and has an incomplete HDAC domain. Class III proteins contain sequences similar to bacterial acetoin utilization proteins and cyanobacteria glutamine syntheses, suggesting that class III HDACs may have a novel function derived from bacterial origin (Pandey et al., 2002). Moreover, the Arabidopsis genome encodes plant-specific HDAC proteins which are categorized as the HD2 superfamily: HDT1, HDT2, HDT3, and HDT4 (Danql et al., 2001; Pandey et al., 2002; Wu et al., 2003). Two members of this family, HDT1 and HDT3, have antagonistic effects in seed development (Wu et al., 2000; Colville et al., 2011). In addition, there are two members (SRT1 and SRT2) in the

SRT superfamily which are NAD-dependent HDACs. These HDACs were identified to have a distinctive NAD-dependent ADP-ribosyltransferase activity in addition to the HDAC activity (Frye, 1999; Imai et al., 2000). Arabidopsis SRT2, a homolog of yeast Sir2, functions as a negative regulator in basal defense by suppressing SA biosynthesis (Wang et al., 2010).

It is clear that identified HDACs play critical roles in the regulation of various biological processes in Arabidopsis, including seed germination, development, and defense against diverse pathogen infections. As briefly mentioned above, HDA6 and HDA19 are the most studied HDACs in Arabidopsis. HDA6 acts as a global repressor in jasmonate (JA) signaling, senescence, embryonic-fate suppression, transgene and transposon silencing, RNA-directed DNA methylation, and flowering (Aufsatz et al., 2002; Probst et al., 2004; Tanaka et al., 2008; Hollender and Liu, 2008; Wu et al., 2008; Earley et al., 2010; To et al., 2011; Yu et al., 2011; Liu et al., 2012). The closest homolog of HDA6, HDA19, also functions as a global repressor during embryonic and flower development, immune response, JA and ethylene response, and light signaling (Tian et al., 2003; Zhou et al., 2005; Benhamed et al., 2006; Long et al., 2006; Kim et al., 2008; Hollender and Liu., 2008; Choi et al., 2012). Loss of *HDA19* also results in developmental abnormalities (Tanaka et al., 2008). HDA7, another member of the Class I RPD3/HDA1 Superfamily, is required for female-gametophyte development and embryogenesis (Cigliano RA et al., 2013). Moreover, an alteration of *HDA7* expression may lead to delay in post-germination and later developmental growth (Ciqliano et al., 2013). HDA5, belonging to the Class II

RPD3/HDA1 Superfamily, is involved in flowering regulation by repressing *FLOWERING LOCUS C (FLC)* and *MADS AFFECTING FLOWERING 1 (MAF1)/ FLOWERING LOCUS M (FLM)* expression (Luo M et al., 2015). Moreover, HDA5 and HDA6 form a complex with FLOWERING LOCUS D (FLD) and FVE to control flowering and gene expression (Luo et al., 2015). It is now more and more evident that multiple HDAC complexes are involved in higher level regulation of target gene expression. HDA15, belonging to the Class II of RPD3/HDA1 Superfamily of Arabidopsis, is involved in repression of chlorophyll biosynthesis and photosynthesis in etiolated seedlings (Liu X et al., 2013). Furthermore, a proper HDA15 activity requires PIF3 recruitment on their co-target genes for chlorophyll biosynthesis and photosynthesis in the dark (Liu et al., 2013). Deciphering an HDAC complex, formed not only by HDAC-multiplex but also with transcription factors or other proteins, provides deeper understanding of epigenetic regulatory mechanisms of histone deacetylation.

In my dissertation, I will specifically focus on the understanding of the biological roles and the mechanism of HDA9. Throughout my research, HDA9 has been anticipated to play pivotal roles in various biological responses from seed germination to flowering regulation upon environmental signals through epigenetic mechanisms on its target genes. As depicted in the phylogenetic tree (Fig.1), HDA9 shares high sequence similarity with HDA10 and HDA17, which might represent endoduplication and rearrangement of an important gene during evolution. Therefore, the purpose of this study is to elucidate biochemical function of HDA9 and to find its target genes underlying plasticity of plants upon external

signals.

1.2 DNA methylation

DNA methylation occurs when a methyl group ($-CH_3$) is covalently added to the cytosine bases of DNA and, without alteration of DNA sequence, forms 5-methylcytosine. It arises in both prokaryotes and eukaryotes. Bacterial DNA methylation differentiates genomic DNA from invading phage DNA. The foreign phage DNA is then fragmented by the host restriction enzymes so that the intruding DNA cannot be replicated (Chinnusamy and Zhu, 2009). DNA methylation is a well-conserved epigenetic mechanism in most eukaryotes, from fungi to animals and plants. Moreover, transposons, other repetitive elements, and DNA in centromeric, peri-centromeric, and some genic regions are highly methylated intendedly for inactivation of the methylated DNA loci within the genome.

In mammals, most DNA methylation occurs exclusively in CG context while non-CG methylation is observed only in embryonic stem cells. Moreover, *de novo* DNA methylation is established by DNA methyltransferase 3 (DNMT3) during the development of germ cells whereas methylated DNA pattern is maintained via DNA methyltransferase 1 (DNMT1) during replication (Zhao and Chen, 2014). Unlike animals, DNA methylation *in planta* occurs in all possible cytosine contexts, such as CG, CHG, and CHH (where H is A, C, or T) (Pikaard and Scheid, 2014). Although animals and plants share common features of dynamic regulation mechanism of DNA methylation and demethylation, there are more evidences that

DNA methylation is elaborated involving RNA interference (RNAi) pathway in plants.

De novo DNA methylation in Arabidopsis is mediated by the RNA-directed DNA methylation (RdDM) pathway. Small RNAs generated via RNAi pathway, such as 24-nucleotide (nt) small-interfering RNAs (siRNAs), or long non-coding RNAs (lncRNAs) may guide the DNA methylation to occur.

At RdDM target loci, single-stranded RNAs are transcribed and converted into double-stranded RNAs (dsRNAs). DICER-LIKE 3 (DCL3) then generates primary 24-nt siRNAs by cleaving the long dsRNA precursors, and HUA ENHANCER 1 (HEN1) assists maturation of the siRNAs. The mature siRNAs are loaded onto ARGONAUTE 4 (AGO4) (Law and Jacobsen, 2010). Next, via the sequence complementarity between the AGO4-bound siRNA and the scaffold RNA transcribed from an intergenic non-coding region, the RdDM effector complex, including DOMAINS REARRANGED METHYLTRANSFERASE 2 (DRM2), is recruited to RdDM target genes establishing *de novo* DNA methylation (He et al., 2011; Zhao and Chen, 2014).

To maintain DNA methylation patterns after replication, the nascent strand of hemimethylated double-stranded DNA becomes the target of metyltransferases. Maintenance of DNA methylation in plants is carried out via three distinctive pathways using different methyltransferases subject to cytosine sequence contexts (Law and Jacobsen, 2010). First, DNA methylation in CG context is the most frequently observed modification in plant genome as in animals (Chan et al., 2005).

DNA METHYLTRANSFERASE 1 (MET1), which is the ortholog of mammalian DNMT1, governs the maintenance CG methylation. Furthermore, it is recently revealed that VARIANTION IN METHYLATION/ORTHRUS (VIM/ORTH) family proteins and DECREASE IN DNA METHYLATION 1 (DDM1) are also required for this mechanism (Law and Jacobsen, 2010; Zhao and Chen, 2014). Next, the maintenance CHG methylation is implemented by a plant-specific DNA methyltransferase, CHROMOMETHYLASE 3 (CMT3), involving dimethylated histone H3 lysine 9 (H3K9me2) (Cao et al., 2003). In Arabidopsis, H3K9me2 is enriched by a histone methyltransferase, KRYPTONITE (KYP), and its homologs SU(VAR)3-9 HOMOLOG 5 (SUVH5) and SUVH6. Then, CMT3 is guided by H3K9me2 at target loci (Law and Jacobsen, 2010; Zhao and Chen, 2014). Occasionally, in CHG methylation, another DNA methyltransferase, DRM2, is also involved through the RdDM pathway (Stroud et al., 2013). Lastly, asymmetric CHH methylation is predominantly sustained by DDM1 and CMT2 in cooperation with the RdDM pathway (Zemach et al., 2013). DDM1 is required for DNA methylation on linker histone H1. CMT2 preferentially binds to enriched H3K9me2, just like its homolog CMT3. In other words, CMT2 and CMT3 methylate CHG sites in a redundant manner. However, CMT2 is only functional on large transposable elements (TEs) at heterochromatin region unlike CMT3 that also function on protein-coding genes (Stroud et al., 2014).

1.3 ATP-dependent chromatin remodeling

Another eminent epigenetic regulation occurs via ATP-dependent chromatin remodeling mechanism. It uses an energy derived from ATP hydrolysis to alter histone-DNA interactions by sliding, ejecting, or restructuring the nucleosome. In this manner, the accessibility of transcription factors or the recruitment of transcription machinery to the genomic region in chromatin is controlled (Cairns, 2005; Ho and Crabtree, 2010; Zhao et al., 2015).

There are four classes of ATP-dependent chromatin remodelers in eukaryotes: SWItching defective/Sucrose Non-Fermenting (SWI/SNF), Imitation SWI (ISWI), Chromodomain (CHD), and INO80 groups (Eisen et al., 1995; Vignali et al., 2000; Varga-Weisz, 2001; Jerzmanowski, 2007). In addition to their catalytic ATPase domains, these remodelers have unique structures that allow specific association with their targets within the biological context. They act in diverse processes and associate with other types of epigenetic modification mechanism.

First, SWI/SNF is the most characterized group among the ATP-dependent chromatin remodelers. Members of this family consist of a highly conserved ATPase subunit, which includes a helicase-SANT (HSA), a post-HSA, and a bromodomain within the structure. When actin or actin-related proteins (ARPs) are associated with the HSA domain and acetylated target loci is recognized by their c-terminal bromodomain, the ATPase activity is modulated. Second, the ATPase subunit of ISWI family has a SANT (ySWI3, yADA2, hNCoR, and hTFIIIB) or SLIDE (SANT-like ISWI) domain at the C-terminus of the catalytic ATPase domain. The C-terminal module is able to interact with a DNA-binding histone-

fold motif, plant homeodomain (PHD), or bromodomain of other proteins. This group of chromatin remodeler binds to an unmodified histone tail and DNA and provides an optimized space to promote chromatin assembly and repression of transcription. Third, CHD family includes two tandem chromodomains at the N-terminus of its ATPase domain. The tandemly arranged chromodomain binds to methylated lysine or forms a complex with deacetylases and methyl CG-binding domain (MBD) proteins. CHD remodelers promote or repress transcription by sliding or ejecting nucleosomes. Last, INO80 remodelers include more than 10 subunits. The prominent feature of this family is that its ATPase domain is split by a long insertion, to which ARPs and AAA-ATPases can bind. This group of remodelers functions by either sliding nucleosome along the DNA or exchanging histones with their variants to promote transcriptional activation or DNA repair.

Arabidopsis genome also encodes a number of characterized ATPase chromatin remodelers. PHOTOPERIOD-INDEPENDENT EARLY FLOWERING 1 (PIE1) is most homologous to SWR1, a member of INO80 class remodeler, although it harbors SANT domain which is normally found in ISWI family members (Noh and Amasino, 2003). As an SWR1 complex, PIE1 plays a key role in repression of floral transition and in ambient temperature response through interaction with ACTIN-RELATED PROTEIN 6 (ARP6) (Noh and Amasino, 2003; Kumar and Wigge, 2010). SPLAYED (SYP) and BRAHMA (BRM) are identified as possible SWI/SNF ATPase remodelers associated with developmental processes in Arabidopsis (Wagner and Meyerowitz, 2002; Bezhani et al., 2007). Loss of SYP and BRM exhibits pleiotropic developmental defects such as slow growth,

dwarfism, abnormal separation of cotyledons, and reduced apical dominance (Wagner and Meyerowitz, 2002; Hurtado et al., 2006; Kwon et al., 2006). DECREASE IN DNA METHYLATION (DDM1) also belongs to the SWI/SNF family and causes DNA methylation (Shaked et al., 2006). BUSHY (BSH) is a plant-specific ATPase that is involved in control of auxin response (Brzeski et al., 1999). Moreover, PICKLE (PKL), a CHD3 group remodeler, represses expression of seed-associated genes during germination and regulates the post-embryonic transition via histone H3 lysine 27 methylation (Jerzmanowski, 2007; Zhang et al., 2008). Concisely, plant chromatin-remodeling factors perform important functions in epigenetic control of plant growth and development.

1.4 RNA interference (RNAi)

Only recently, a highly complex and diverse network of noncoding RNAs (ncRNAs) has been revealed. Large-scale and genome-wide analyses have indicated that only 1~2% of the genome can actually encode proteins, although approximately 90% of eukaryotic genomes are transcribed. This implies that a large portion of the eukaryotic genome produces unexpected RNAs that do not have protein-coding potential and are thus called ncRNAs.

NcRNAs are classified into either housekeeping or regulatory ncRNAs. Housekeeping ncRNAs are constitutively expressed, which include transfer RNAs (tRNAs), ribosomal RNAs (rRNAs), small nuclear RNAs (snRNAs), and small nucleolar RNAs (snoRNAs). Regulatory ncRNA can be further divided into two

groups according to the size of transcripts, short ncRNAs and long noncoding RNAs (lncRNAs).

Short ncRNAs are less than 200 nucleotides comprising micro RNAs (miRNAs), small interfering RNAs (siRNAs), and piwi-interacting RNAs (piRNAs). Among short ncRNAs, miRNA and siRNA are extensively investigated. MiRNAs are derived from short hairpins, whereas siRNAs are derived from longer regions of double strand RNAs. However, both miRNAs and siRNAs are about 22 nt long as they are cleaved by an endoribonuclease, DICER. These small ncRNAs are loaded onto AGO or RNA-induced silencing complex (RISC) (Ramachandran and Chen, 2009). RISC then binds to the target messenger RNAs (mRNAs) through partial base paring with the loaded small ncRNAs. These bindings negatively regulate target-gene expression via mRNA degradation or repression of translation (Guo et al., 2014). On the other hand, long non-protein coding transcripts are termed as lncRNAs (Heo et al., 2013; Cao, 2014; Shafiq et al., 2015). LncRNAs were initially thought to be non-functional junk transcripts. However, their significances have been emerged and it is now considered that many lncRNAs actually function as key regulators of transcription and translation in various biological pathways, for instances, genomic imprinting, nuclear organization, alternative splicing, and chromatin regulation. More and more lncRNAs have been identified through different approaches in plants and yet their exact functions are still abstruse.

In Arabidopsis, best-known lncRNAs are COLD INDUCED LONG

ANTISENSE INTRAGENIC RNA (COOLAIR) (Swiezewski et al., 2009) and COLD ASSISTED INTRONIC ncRNA (COLDAIR) (Heo and Sung, 2011). Both COOLAIR and COLDAIR were found based on analogy from human HOX TRANSCRIPT ANTISENSE RNA (HOTAIR) (Rinn et al., 2007). These plant lncRNAs are involved in the repression of *FLC* expression during vernalization. COOLAIR is transcribed from the 3-end heterochromatic region of *FLC* in an antisense direction compared to *FLC* mRNA. COOLAIR lncRNA transcript covers the whole *FLC* gene locus, which is 7 kb long, and can be alternatively spliced and polyadenylated (Swiezewski et al., 2009). On the hand, COLDAIR lncRNA does not have any alternative isoforms and is transcribed from the first intron of *FLC*. 5'-end of COLDAIR is capped but not polyadenylated unlike COOLAIR. Although they originate differently, both COOLAIR and COLDAIR function in *FLC* repression during vernalization. Vernalization intervenes the epigenetic regulation of *FLC* through decreased histone H3 lysine 36 trimethylation (H3K36me3) and increased histone H3 lysine 27 trimethylation (H3K27me3) by recruiting the PLANT HOMEODOMAIN (PHD) protein, VERNALIZATION INSENSITIVE 3 (VIN3) and POLYCOMB REPRESSVIE COMPLEX 2 (PRC2) (Sung and Amasino, 2004; Song et al., 2012). During this process, COLDAIR transcription is increased after COOLAIR induction but before the elevation of *VIN3* transcription. COLDAIR physically interacts with PRC2 complex to promote H3K27me3 accumulation during vernalization. It is considered that COLDAIR functions as a scaffold RNA to recruit the PRC2 complex and to epigenetically repress *FLC* expression during vernalization.

Moreover, a 236-nt lncRNA called HIDDEN TREASURE1 (HID1) was newly identified through transcriptome analysis (Wang et al., 2014). HID1 is characterized to be involved in both transcriptional and post-transcriptional regulation of photomorphogenesis-related gene expression. Transcription level of HID1 itself is not regulated by light. However, it promotes photomorphogenic response through the repression of PHYTOCHROME-INTERACTING FACTOR (PIF3) activity under continuous red light. PIF3 is a well-known transcription factor that triggers hypocotyl elongation. HID1, as the first identified lncRNA to be involved in the control of light-mediated plant development, is still required to be clarified for its precise function and mechanism.

Further studies connecting the posttranslational regulatory networks of histones and DNA to ncRNA-based transcriptional regulation will bring better understandings of cellular processes and developments in eukaryotes. Ultimately, studies in epigenetics will enlighten the fine regulatory mechanisms underlying gene expression as a whole.

2. Photoperiod regulates floral transition

Transition from vegetative to reproductive phase is very crucial process for reproductive success in higher plants. Arabidopsis has been well characterized for decades with regard to the genetic and molecular mechanisms of flowering. Floral transition in Arabidopsis is controlled by environmental stimuli (including

photoperiod, circadian rhythm, and vernalization) gibberellin (GA) pathway, and by internal cues including developmental and autonomous signals. Signals from these pathways are finely tuned by other mechanisms.

2.1 Photoperiod and circadian rhythm

Photoperiod and circadian rhythm are crucial factors for seasonal plant growth and flowering. Higher plants, animals, and fungi have their own endogenous biological clocks, and they can auto-regulate through their negative-feedback loops. In Arabidopsis, the central oscillator depends on multiple interconnected loops to generate biological rhythm. These multiple loops comprise three feedback loops, two morning MYB transcription factors, and an evening-phased pseudo response regulator. The morning-expressed MYB transcription factors include CIRCADIAN CLOCK ASSOCIATED 1 (CCA1) and LATE ELONGATED HYPOCOTYL (LHY) (Schaffer et al., 1998; Wang and Tobin, 1998; Makino et al., 2000). The evening-phased PSEUDO RESPONSE REGULATOR (PRR), TIMING OF CAB2 EXPRESSION1 (TOC1), is a member of the PRR family (Nagel and Kay, 2012; McClung et al., 2013). Light activates transcript levels of *LHY* and *CCA1*, and represses *TOC1* expression in the morning. LHY and CCA1 proteins inhibit *TOC1* transcription through binding with the evening element in the *TOC1* promoter (Schaffer et al., 1998; Wang and Tobin, 1998; Green and Tobin, 1999, 2002; Alabadi et al., 2001, 2002). At night, TOC1 protein up-regulates the transcription of *LHY1* and *CCA1* (Alabadi et al., 2001 and 2002; Pruneda-Paz et al., 2009). In addition, *TOC1* is repressed by TOC1 protein

itself, forming a second loop (Locke et al., 2005). LHY and CCA1 function as positive regulators of three *TOC1* relatives (*PRR5*, *PRR7*, and *PRR9*), and this forms the third loop (Farre´ et al., 2005; Harmer and Kay, 2005; Mizuno and Nakamichi, 2005).

Moreover, GIGANTA (GI), EARLY FLOWERING 3 (ELF3), ELF4, and LUX are also required for *LHY* and *CCA1* expression (Park et al., 1999; Doyle et al., 2002; Mizoguchi et al., 2002; Hazen et al., 2005). ELF3, ELF4, and LUX act together in a transcription complex called EVENING COMPLEX (EC) (Hicks et al., 2001; Doyle et al., 2002; Dixon et al., 2011; Helfer et al., 2011; Nusinow et al., 2011; Herrero et al., 2012).

The connection between the circadian clock and photoperiod (day length) has been developed into the external coincidence model. The photoperiodic response is controlled by light at certain times of the day (Bünning, 1936; Pittindrigh and Minis, 1964). Arabidopsis behaves as a facultative long-day plant because its flowering is accelerated during long days (16 hr light and 8 hr dark photoperiod). The output of photoperiod depends on *CONSTANS* (*CO*) gene. The circadian clock regulates *CO* mRNA expression in late afternoon, and then CO protein is accumulated and stabilized. Stabilized CO protein can bind directly to a *cis*-element (CCAAT box) in the distal promoter of *FLOWERING LOCUS T* (*FT*) (Wenkel et al., 2006; Kumimoto et al., 2008 and 2010). Hence, light promotes *FT* expression in the phloem companion cells at the end of the day, and FT protein is translocated to the shoot apical meristem and facilitates flowering (Michaels, 2009; Amasino and Michaels, 2010; Pruneda-Paz and Kay, 2010). Whereas, at night, CO

protein is degraded by 26S proteasome. Thus, the mobile FT protein is considered a florigen. FT forms a complex with FD, a bZIP transcription factor, in the shoot apical meristem. The FT–FD module initiates flowering by activating a floral integrator, *SUPPRESSOR OF OVEREXPRESSION OF CONSTANS 1* (*SOC1*; Michaels, 2009).

Although CO-mediated regulation accounts for most of the activation of *FT*, CO-independent mechanisms function in parallel (Liu el al., 2008; Sawa and Kay, 2011; Iñigo et al., 2012; Kumar et al., 2012; Pin and Nilsson, 2012). *FT* expression is also controlled by various repressive signals: *FLOWERING LOCUS C* (*FLC*) and *SHORT VEGETATIVE PHASE* (*SVP*), two MADS-box proteins. They repress *FT* expression by directly binding to the CArG motifs in the promoter and intron of *FT*. *FLC* directly represses transcription of floral integrators, *SOC1* and *FT*, which combine the signals from several pathways to promote flowering (Borner et al., 2000; Lee et al., 2000; Michaels and Amasino, 2001; Helliwell et al., 2006; Schörock et al., 2006). Another negative transcriptional regulator of *FT* is *TEMPRANILLO 1* (*TEM1*), a RAV-like AP2 domain-containing protein that directly interacts with the 5'UTR of *FT* chromatin (Castillejo and Pelaz, 2008). In addition, miR172-targeted AP2-like transcription factors, including *TARGET OF EAT 1* (*TOE1*), *TOE2*, *SCHLAFMÜTZE* (*SMZ)*, and *SCH ARCHZAPFEN (SNZ)*, negatively affect *FT* expression in an age-dependent manner and reduce miR156 but increase miR172 expression levels (Jung et al., 2007; Mathieu et al., 2009; Wu et al., 2009; Huijser and Schmid, 2011). It has been reported that *FT* transcription is also controlled by epigenetic mechanisms. Tri-methylation of H3K27

(H3K27me3) within *FT* chromatin, a representative repressive mark, is established by *CURLY LEAF* (*CLF*) of the polycomb repressive complex 2 (PRC2) (Coupland and Turck, 2008; Jiang et al., 2008; Pazhouhandeh et al., 2011). LIKE HETEROCHROMATIN PROTEIN 1 (LHP1), a component of the plant PRC1, is associated with the H3K27me3 within *FT* chromatin, leading to *FT* repression (Turck et al., 2007; Adrian et al., 2010). H3K4me3 in the *FT* promoter region is influenced by Jumonji (Jmj)-family histone demethylases, AtJmj4 and EARLY FLOWERING 6 (ELF6), which also lead to reduced *FT* transcription (Jeong et al., 2009).

2.2 Vernalization pathway

Winter-annual Arabidopsis accessions flower late without winter exposure and show accelerated flowering after prolonged exposure to low temperature. This process is called vernalization, and *FLC* is largely responsible for this process (Koornneef et al., 1994; Lee et al., 1994; Sanda and Amasino, 1996; Michaels and Amasino, 1999 and 2001, Sheldon et al., 1999, 2000 and 2002; Rouse et al., 2002). *FLC* encodes a MADS-box transcription factor. Its transcript and protein levels are high in winter-annual accessions, resulting in delayed flowering. However, *FLC* is repressed when plants are exposed to prolonged cold or by the autonomous pathway.

In Arabidopsis, vernalization results in mitotically stable repression of *FLC* chromatin through the PRC2 complex and long noncoding RNAs (Gendall et al., 2001; Levy et al., 2002; Sung and Amasino, 2004; Helliwell et al.,2011; Heo and

Sung, 2011).

Before cold exposure, *FLC* chromatin is at active state, with active histone marks, such as H3K4, H3K36, and H3Ac (Zografos and Sung, 2012). Many histone modifying complexes, including yeast RNA pol II Associated Factor 1 (PAF1) complex and COMPASS- complex are involved in *FLC* activation before cold (He et al., 2004; Tamada et al., 2009; Jiang et al., 2011; Kim et al., 2014).

During winter, the repression of *FLC* chromatin is initiated by VERNALIZATION INSENSITIVE 3 (VIN3), the plant homeodomain (PHD)- and fibronectin type III domain-containing protein. VIN3 and VIL1/VRN5 act together with PRC2 and enhance their activity (Kim and Sung, 2014). Among Arabidopsis PRC2 components, CURLY LEAF (CLF) and SWINGER (SWN), two homologs of E(z), and VRN2, the homolog of Su(z)12, are involved in the repression of FLC during vernalization (Chanvivattana et al., 2004). The enrichment of PRC2 to the *FLC* chromatin increases by vernalization. PRC2 contributes to the repression of FLC by mediating tri-methylation of H3K27 at *FLC* chromatin.

Components of another Polycomb group complex, PRC1 which include VIL1, LHP1, EMF1, AtBMI1A, AtBMI1B, and AtBMI1C also contributes to the repression of FLC. After cold, the components of the PRC1 complex such as LHP1, PRC2, and VIL1 act with the PRC2 complex for the stable silencing of the *FLC* chromatin.

Recently studies indicate that long noncoding RNAs (lncRNAs) also play a role in the epigenetic repression of *FLC*. One such lncRNA, *COOLAIR* is increased by cold exposure and its antisense transcript does not affect *FLC* repression during

vernalization (Helliwell et al.,2011). However, another lncRNA, COLDAIR physically interacts with the CLF and is required for establishing stable *FLC* repression through direct interaction with PRC2 during vernalization (Heo and Sung, 2011; Zografos and Sung, 2012).

MADS AFFECTING FLOWERING (MAF1~5) proteins are paralogs of FLC. Their genes are arranged in tandem clusters on Arabidopsis chromosome V. *MAF* genes have 53~98% nucleotide-sequence identities with *FLC* (Bodt et al., 2003; Raccliffe et al., 2003). Vernalization also represses *MAF1*, *MAF2*, and *MAF3* expression but not *MAF5*. *MAF4* is not strongly affected by vernalization either. MAF1/FLOWERING LOCUS M (FLM) acts as a floral repressor such that its repression by vernalization contributes to accelerated flowering (Sung et al., 2006). MAF1 has also been reported to be involved in the acceleration of flowering by elevated temperature (Werner et al., 2005; Li et al., 2006; Sung et al., 2006). MAF2, another floral repressor reacts to a relatively short cold period (Raccliffe et al., 2003). MAF3 has a redundant function with MAF1 in repressing *FT* expression and delaying flowering. It has also been reported that MAF1 acts redundantly with FLC, MAF2, and MAF4 in floral repression (Raccliffe et al., 2001 and 2003; Sheldon et al., 2009; Gu et al., 2012). Transcript levels of *MAF4* and *MAF5* are increased transiently by short-term cold, and these increases have roles in inhibiting precocious response to vernalization (Kim and Sung, 2013).

In addition to *FLC*, other genes of the MADS-box family also respond to the vernalization pathway (Alexander and Hennig, 2008). AGOMOUS-LIKE 19 (AGL19) belongs to the TM3 clade of the MADS-box family, and is highly similar

to SOC1. *AGL19* was originally characterized as a root-specific gene (Alvarez-Buylla et al., 2000). However, *AGL19* is also involved in flowering control through the vernalization pathway. Ectopically expressed *AGL19* promotes flowering under both LD and SD, suggesting that AGL19 acts as a floral activator (Schönrock et al., 2006). In the absence of cold, *AGL19* expression is maintained at very low levels by the PRC2 complex, which is composed of MSI1, CLF, FERTILISATION INDEPENDENT ENDOSPERM (FIE), and EMBRYONIC FLOWER 2 (EMF2). It has been reported that *AGL19* chromatin is associated with H3K27me3 but not with H3K9me2 (Schönrock et al., 2006). When the plant is exposed to prolonged cold, H3K27me3 level within *AGL19* chromatin is reduced by decreased PRC2 occupancy, and thus, *AGL19* is relieved from PRC2 repression and promotes flowering. Therefore, the vernalization pathway in Arabidopsis has two branches, FLC- dependent and FLC-independent. Both branches are dependent on the PRC2 complex. While *FLC* is repressed by VRN2-containing PRC2 after vernalization, *AGL19* is repressed by EMF2-containing PRC2 before vernalization. In sum, different polycomb group (PcG) proteins have been recruited to synchronize the vernalization response and to regulate the transition from developmental growth to reproductive growth (Alexandre and Hennig, 2008).

AGAMOUS LIKE 24 (AGL24) belongs to the MADS-box family and functions as an activator of floral transition (Yu et al., 2002; Bodt et al., 2003; Michaels et al., 2003). *AGL24* is regulated by multiple flowering pathways such as the photoperiod pathway, the autonomous pathway and vernalization (Yu et al., 2004; Liu et al., 2007 and 2008; Lee J et al., 2008).Previous studies have reported

that *AGL24* and *SOC1* affect expression of each other (Yu et al., 2002; Michaels et al., 2003). However, *AGL24* and *SOC1* are also regulated differently in several aspects during flowering. During vernalization, *AGL24* but not *SOC1* is controlled in a manner independent of *FLC* (Michaels et al., 2003). In the photoperiod pathway, *AGL24* is influenced by *CO* but not by *FT*, whereas *SOC1* is affected directly by *FT* and indirectly by *CO* (Lee et al., 2000; Samach et al., 2000; Hepworth et al., 2002). These results suggest that *AGL24* and *SOC1* may have an interdependent or independent effect on each other in the perception of flowering cues.

2.3 Autonomous pathway

The autonomous-pathway proteins are characterized as a combination of proteins that affect late flowering under the influence of photoperiod, the vernalization pathway, and even in summer-annual accessions that are defective in the functional allele of *FRI* (Koornneef et al., 1991; Simpson, 2004). When the autonomous-pathway genes are mutated, the resulting mutant plants flower later than wild-type plants in both LD and SD conditions (Simpson, 2004). This occurs because the components of the autonomous pathway inhibit the accumulation of FLC, the major floral repressor. Therefore, the autonomous pathway can promote flowering independent of day length.

The autonomous-pathway proteins include FCA, FY, FLOWERING LATE KH MOTIF (FLK), FPA, LUMININDEPENDENS (LD), FLOWERING LOCUS D (FLD), FVE, and RELATIVE OF EARLY FLOWERING 6 (REF6) (Michaels

and Amasino, 1996; Koorneef et al., 1998; Lim et al., 2004; Noh et al., 2004). FCA, FPA, and FLK encode RNA-binding proteins (Macknight et al., 1997; Schomburg et al., 2001; Lim et al., 2004). FCA has two RNA Recognition Motifs (RRMs) and a WW protein-interaction domain, whereas FPA has three RRMs (Macknight et al., 1997; Schomburg et al., 2001). FLK is a plant-specific protein that has three K-homology (KH)-type RNA-binding domains (Lim et al., 2004). FY is homologous to the *Saccharomyces cerevisiae* protein Rfs2p (polyadenylation factor 1 subunit 2), a component of RNA-processing factors and required for FCA to promote flowering (Simpson et al., 2003; Amasino and Michaels, 2010). FVE, FLD, and REF6 epigenetically regulate *FLC* expression. FVE is a plant homolog of the yeast protein MULTIPLE SUPPRESSOR OF IRA1 (MSI) and the mammalian retinoblastoma associated proteins RbAp46 and RbpA48. FVE is required for a protein complex repressing *FLC* transcription via histone deacetylation (Ausin et al., 2004). FLD and RFF6 have histone demethylase activities and play roles in histone demethylation within *FLC* chromatin. FLD is homologous to human LYSINE-SPECIFIC HISTONE DEMETHYLASE1 (LSD1), whereas REF6 is one of the plant Jumonji-family proteins (He et al., 2003; Noh et al., 2004). LD encodes a homeodomain-containing protein (Lee et al., 1994), although the mechanism how LD represses *FLC* expression is yet to be elucidated.

In sum, numerous studies indicate that the autonomous pathway represses *FLC* expression mainly through RNA processing or chromatin modifications (Kim et al., 2009; Michaels, 2009).

2.4 GA pathway

Gibberellic acid (GA), one of the phytohormones, has an effect on plant development and growth, including seed germination, stem elongation, floral development, and flowering. A GA biosynthesis mutant, *ga1-3*, did not promote flowering in SD, but promoted late flowering in LD (Wilson et al., 1992). This stronger effect of GA in SD is perhaps due to the photoperiod pathway masking the effect of loss of GA signaling under LD (Reeves and Coupland, 2001; Mouradov et al., 2002; Porri et al., 2012).

GA promotes the expression of *SOC1* (Bonhomme et al., 2000; Moon et al., 2003) and *LFY* (Blazquez et al., 1998) that are involved in flowering at the shoot apical meristem. In addition, GA upregulates the expression of miR159 and its target *MYB33* mRNA that encode the MYB transcription factor and regulate *LFY* expression (Gocal et al., 2001; Woodger et al., 2003; Achard et al., 2004). The *GATA NITRATE INDUCIBLE CARBON METABOLISM INVOLVED* (*GNC*) *and GNC LIKE* (*GNL*) genes are GATA transcription factors that inhibit flowering, and GA represses *GNC* and *GNL* expressions (Richter et al., 2010).

DELLA proteins, GIBBERELLIC ACID INSENSITIVE (GAI), REPRESSOR OF GA1-3 (RGA), and RGA-LIKE 1 (RGL1), have a negative role in GA signaling, and the GA signal mediates flowering primarily through degradation of these DELLA proteins (Dill and Sun., 2001; King et al., 2001; Mouradov et al., 2002; Cheng et al., 2004).

3. Light regulates seed germination

Higher plants such as Arabidopsis are well adapted to optimizing their survival and reproductive success through environmental and endogenous signals. Light is an important environmental signal that influences plant developmental processes differently at tissue- and organ-dependent levels.

Seed germination is a physiological process in which the radicle surrounded by the seed coat emerges after the absorption of water by dry seed (Bewley, 1997b; Baskin and Baskin 2004; Finch-Savage and Leubner-Metzger, 2006). Arabidopsis has two layers, an outer dead testa, also called the seed coat, and an inner layer with living endosperm cells, called the aleurone layer (Linkies et al., 2009; Morris et al., 2011). In Arabidopsis, seed germination takes place in two visible steps. The first step is the testa rupture, and one or several slits form at the seed surface (Debeaujon et al., 2000; Piskurewicz and Lopez-Molina, 2009). The second step is the endosperm rupture and the hypocotyl and radicle break through the micropylar endosperm layer (Morris et al., 2011). Seed germination is affected by numerous environmental factors, including water, temperature, oxygen, nutrients, and light. Among them, light is a crucial factor in plants with small seeds such as Arabidopsis and lettuce (Shinomura, 1997). These plant species use phytochrome, a photoreceptor, to sense light and ultimately initiate seed germination. The phytohormones, including GA and abscisic acid (ABA), are also involved in the seed germinating process. Endosperm rupture is antagonistically controlled by GA and ABA (Piskurewicz and Lopez-Molina, 2009). The mutual negative regulation between GA and ABA might contribute to an effective change in the balance of

GA and ABA hormones in response to an external signal (Toyomasu et al., 1998; Yamaguchi et al., 1998; Seo et al., 2006). Hence, phytochrome regulates endogenous GA and ABA levels to optimize seed germination.

3.1 Light regulates phytochrome signaling

Light signaling in plants begins with perception of light through a photoreceptor, which induces modulation of the transcriptional regulatory networks. Plants are well adapted in this regard and react to a combination of cues, including light quality, quantity, and duration. Light quality is recognized by different light receptors for specific light wavelengths (Jiao et al., 2007). Phytochromes (phys) absorb red (660 nm) and far-red light (730 nm) (Wang and Deng, 2002; Lau and Deng, 2010). Arabidopsis phytochromes are designated phyA to phyE (Fankhauser and Staiger, 2002; Quail, 2002). Cryptochromes (CRYs), including CRY1 and CRY2, are flavin-type blue-light receptors (Cashmore, 1997; Fankhauser and Staiger, 2002). Arabidopsis possesses two UV-A light photoreceptors, PHOT1 and PHOT2 (Briggs et al., 2001; Christie and Briggs, 2001; Fankhauser and Staiger, 2002).

Phytochrome holoproteins are assembled in the cytosol. During this process, apoproteins are conjugated with linear tetrapyrrole chromophores. Light causes conversion of phytochrome structure based on whether the phytochrome absorbs red light (Pfr) or far-red light (Pr), and these forms determine biological activation and inactivation, respectively. Phytochrome is composed of two domains, N-terminal chromophore-binding photo sensory domain and C-terminal regulatory

domain. The C-terminal domain interacts with phytochrome-interacting factors (PIFs) (Wang and Deng, 2002; Lau and Deng, 2010). Conformation change of phytochrome is a reversible process that occurs upon absorbing red or far-red light. The Pfr form translocates into the cell nucleus where it binds to PIFs, and then regulates physiological processes (Sakamoto and Nagatani, 1996; Nagatani, 2004; Kircher et al., 1999, 2002; Frankin and Quail, 2009). There are five phytochromes (phyA to phyE) in Arabidopsis. Of the five phytochromes, phyA is a light-labile protein that belongs to the photo-irreversible 'type I phytochrome'. phyA reacts to very low fluence responses (VLFRs) and far-red high irradiance response (FR-HIR). The activated Pfr form of phyA is responsible for far-red light reception, and it is rapidly degraded upon light illumination. phyA influences diverse plant growth and developmental processes, such as seed germination and seedling de-etiolation.

phyB, a 'type II phytochrome', is involved in low fluence responses (LFRs). phyB is a light-stable protein and senses the red light necessary for seed germination. phyB, phyD, and phyE show different expression patterns, but their functions partially overlap each other.

3.2 Phytochrome-interacting factors (PIFs)

PIF, a bHLH transcription factor, has been known as a negative regulator of photomorphogeneis. The structure of the bHLH protein is comprised of the N-terminal DNA-binding basic domain (b) and the C-terminal dimerization region (HLH). The DNA-binding region possesses 15 amino acids with high numbers of basic residues, and the HLH region contains two alpha helices of a variable loop

that homo- or hetero-dimerizes with other bHLH proteins via their *cis*-acting regulatory motifs (Ortiz et al., 2003). These *cis*-acting regulatory elements have a conserved E-box (5'-CANNTG-3') and G-box (5'-CACGTG-3'). There are 15 PIF proteins in Arabidopsis, and each PIF has distinct or redundant biological function during plant development. Of the PIF family, PIF3 is the first characterized bHLH transcription factor that favorably binds to the Pfr form of phyA and phyB. In addition, PIF3 negatively controls phyB-mediated inhibition of hypocotyl elongation, cotyledon opening, and anthocyanin accumulation (Kim et al., 2003). PIF4 is the negative regulator of phyB-mediated inhibition of hypocotyl elongation and cotyledon opening (Huq and Quail, 2002). PIF1, also known as PHTYOCHROME INTERACTING FACTOR 3-LIKE 5 (PIL5), plays a negative role in seed germination, inhibition of hypocotyl elongation, negative hypocotyl gravitropism in the dark, and chlorophyll accumulation in the light (Huq et al., 2004; Oh et al., 2004).

HECATE (HEC) protein belongs to the HLH subfamily. HECATE lacks the basic DNA-binding region of the bHLH proteins, and therefore is referred to as HLH protein (Benezra et al., 1990). There are three *HECATE* genes (*HEC1*, *HEC2*, and *HEC3*) in Arabidopsis, and they function redundantly in the processes of germination and floral development. Because of the lack of a DNA-binding motif, these proteins are only able to interact with other bHLH proteins. The heterodimerization between HLH and bHLH proteins inhibits the DNA-binding activity of bHLH proteins. Accordingly, HLH proteins are considered to have a dominant negative effect on bHLH proteins. Mutation in *HEC* genes has resulted in

phenotypes defective in transmitting tract and stigma development. The dimerization between HEC and other bHLH proteins might be involved in gynoecium development (Gremski et al., 2007). A recent study showed that HEC proteins interact with PIF1 in the light and remove residual PIF1 which was not degraded by the 26S proteasome pathway, and then subsequently promote photo-morphogenesis (Zhu PhD thesis, 2012).

LONG HYPOCTYL IN FAR-RED 1 (HFR1) also belongs to the HLH subfamily and cannot bind directly to the DNA (Fairchild et al., 2000). HFR1 protein functions as a positive regulator in phyA-mediated inhibition of hypocotyl elongation and negative gravitropism (Fairchild et al., 2000; Fankhauser and Chory, 2000; Soh et al., 2000). HFR1 accumulates in the light but not in the dark, and is targeted by the E3 ubiquitin ligase, CONSTITUTIVE PHOTOMORPHOGENESIS 1 (COP1). HFR1 was reported to sequester PIF1 transcriptional activity by forming a heterodimer with PIF1, blocking PIF1 from binding to DNA. The light–HFR1–PIF1 module regulates PIF1-target genes, including *PIF3*, *EXP9*, *XTH4*, and *XTH33*, that mediate cell-wall loosening and cell-cycle initiation, (Shi et al., 2013). In addition, an overexpression of N-terminus truncated HFR1 resulted in constitutive germination in the dark (Yang et al., 2003).

3.3 Phytochrome modulates PIF1 during seed germination

PIFs can bind directly with activated phytochrome (with a stronger preference to phyB than phyA). In seed germination, PIF1 preferentially binds with Pfr form of phyB (also Pfr phyA), and the phyB–PIF1 interaction leads to

degradation of PIF1 through the 26S proteasome pathway (Oh et al., 2004, 2006). Previous data indicated that the *pif1* mutant seeds produce a constitutive germination phenotype in both inductive red light and non-inductive far-red light conditions. Conversely, constitutive *PIF1* expressors require much higher red light irradiation than wild type to initiate seed germination. PIF1 also regulates the increasing expression of ABA anabolic genes (*ABA1*, *NCED6*, and *NCED9*) and a GA catabolic gene (*GA2ox2*), whereas it represses an ABA catabolic gene (*CYP707A2*) and GA anabolic genes (*GA3ox1* and *GA3ox2*). As a result, seed germination is affected by increasing ABA and decreasing GA levels. PIF1 also activates the transcription of *RGA* and *GAI*, DELLA protein-encoding genes. A chromatin immunoprecipitation assay has shown that PIF1 binds directly to the promoters within *RGA* and *GAI* chromatin via G-box motifs (CACGTG). However, it does not bind to the promoters of other GA and ABA metabolic genes (Oh et al., 2007). Therefore, *RGA* and *GAI* may be the target genes of PIF1. It has also been reported that SOMNUS (SOM) regulates GA and ABA metabolic genes at the downstream of PIF1. *SOM* encodes a CCCH-type zinc finger protein (Kim et al., 2008).

3.4 Light regulates GA pathway during seed germination

Seed germination is determined by a balance between ABA and GA levels. Increased endogenous ABA levels inhibit seed germination. Previous studies have reported that GA functions in promoting seed germination, because GA-deficient mutants (*ga1-3* and *ga2-1*) were shown to be defective in seed germination

(Koornneef and van der Veen, 1980). In addition, treatment with GA inhibitors, paclrobutrazol or uniconazole, produced a phenotype with reduced seed germination (Nambara et al., 1991; Jacobsen and Olszewski, 1993; Ogawa et al., 2003). GA catabolism and anabolism influence seed germination through the alteration of endogenous GA levels. GA1 (the amount of which is usually ~10% that of GA4) and GA4 (the major bioactive GA in Arabidopsis), the precursors of GA biosynthesis, increase the bioactive GA level and promote seed germination. Bioactive GA1 and GA4 are produced in later steps during GA metabolism. Their productions are catalyzed by GA 3-oxidase (GA3ox) and GA 20-oxidase (GA20ox). These catalytic enzymes belong to 2-oxoglutarate-dependent dioxygenases (2ODDs), a family of the small multigene proteins. The 2ODDs are known as primary targets in the regulation of bioactive GA (Yamaguchi, 2008; Seo et al., 2009). GA 2-oxidase (GA2ox) was identified as a GA deactivation enzyme, and is a member of the 2ODDs (Yamaguchi, 2008; Seo et al., 2009). The transcript levels of endogenous *GA3ox* are increased after exposure to red light, whereas those of *GA2ox* are decreased. *GA3ox1* expression is induced sharply, peaks at 12 hr after light pulse, and then decreases rapidly. However, *GA3ox2* expression is gradually increased and peaks at 36 hr after light pulse. *GA3ox1* and *GA3ox2* transcript levels increase more with a pulse of red light than with far-red light. However, GA deactivating gene, *GA2ox2*, is increased at 12 hr after exposure to far-red light pulse. Therefore, bioactive GA levels are antagonistically regulated by GA3ox and GA2ox (Seo et al., 2009).

3.5 Light regulates ABA pathway

ABA, a phytohormone, regulates various environmental processes such as drought, cold, and conditions of high salinity (Leung and Giraudat, 1998). ABA controls light-dependent seed germination and maintains seed dormancy (Koornneef et al., 2002). Red-light activated phyB Pfr leads to repressed ABA levels, and subsequently it triggers seed germination. Alternatively, phyB Pr with far red light increases ABA levels and prohibits seed germination (Seo et al., 2006). Previous studies have shown that ABA inhibits GA biosynthetic genes (*GA3ox1* and *GA3ox2*) in imbibed seeds (Seo et al., 2006). Consistent with the changes in ABA levels, the transcript levels of ABA metabolic genes, *ZEAXANTHIN EPOXIDASE* (*ZEP)/ABA DEFICIENT 1(ABA1), 9-CIS EPOXYCAROTENOID DIOXYGENASE 6* (*NCED6*), and (*NCED9*), are decreased by red light, whereas the transcript levels of *ABSCISIC ACID 8'-HYDROXYLASE 2* (*CYO707A2)*, a gene encoding an ABA-deactivating enzyme, is increased (Seo et al., 2006; Oh et al., 2007; Sawada et al., 2008; Seo et al., 2009). Therefore, ABA levels in imbibed seeds are regulated in a manner opposite to GA levels (Seo et al., 2006).For these reasons, plant must carefully monitor to survive for their optimized seed germination through interaction with various environmental signals.

(a)

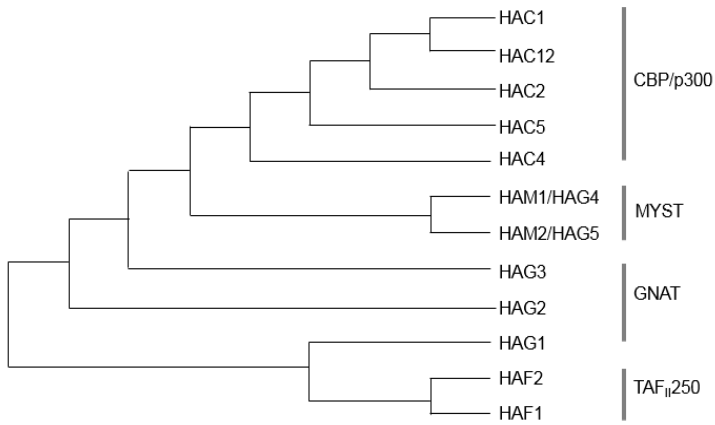

(b)

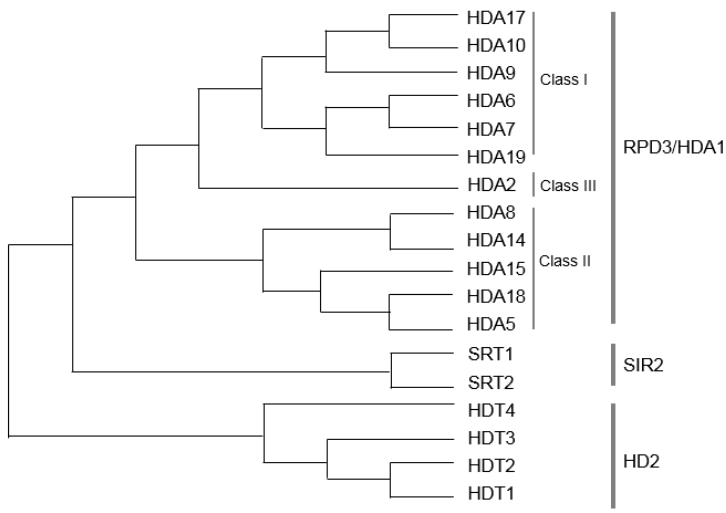

Figure 1-1. Phylogenetic tree for Arabidopsis HATs and HDACs.

The phylogenetic trees was generated using MEGA software (version 6.06) and displayed as neighbor-joining (NJ) tree. Arabidopsis HAT (a) and HDAC (b) amino-acid sequences were aligned with ClustalW.

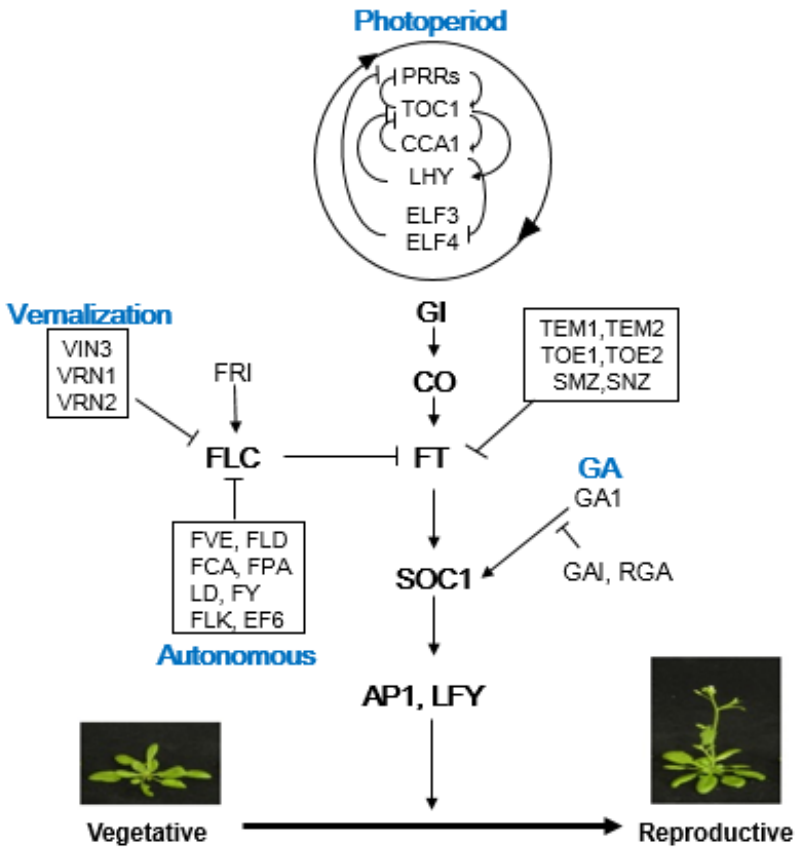

Figure 1-2. Flowering pathways in Arabidopsis

Chapter II.

Repression of flowering in non-inductive photoperiod by the *HDA9-AGL19-FT* module in Arabidopsis

---

This Chapter was published as ″Kang MJ, Jin HS, Noh YS, Noh B (2015) Repression of flowering in non-inductive photoperiod by the HDA9-AGL19-FT module in Arabidopsis. *New Phytol* **206:** 281-294″

2.1 Abstract

Posttranslational acetylation of histones is reversibly regulated by histone deacetylases (HDACs). Despite the evident significances of HDACs in Arabidopsis development, the biological roles and underlying molecular mechanisms of many HDACs are yet to be elucidated.

By reverse-genetic approach, I isolated an *hda9* mutant and performed phenotypic analyses on it. In order to address the role of HDA9 in flowering, genetic, molecular, and biochemical approaches were employed.

hda9 flowered early in non-inductive short days (SD) and had increased expression of the floral integrator *FLOWERING LOCUS T* (*FT*) and the floral activator *AGAMOUS-LIKE 19* (*AGL19*) compared to wild type. The *hda9* mutation increased histone acetylation and RNA polymerase II occupancy at *AGL19* but not at *FT* during active transcription, and HDA9 protein directly targeted *AGL19*. *AGL19* expression was higher in SD than in inductive long days, and an *AGL19* overexpression caused a strong upregulation of *FT*. A genetic analysis showed that an *agl19* mutation is epistatic to the *hda9* mutation, masking both the early flowering and the increased *FT* expression of *hda9*.

Taken together, my data indicate that HDA9 prevents precocious flowering in SD by curbing the hyper-activation of *AGL19*, an upstream activator of *FT*, through resetting local chromatin environment.

2.2 Introduction

Histone acetylation has been implicated in transcriptional activation. The addition of acetyl groups on lysine residues at the histone N-terminal tails by histone acetyltransferases (HATs) decreases the affinity of DNA to histones by increasing negative charges on histones, thereby relaxing the chromatin structure to be more accessible to transcription factors. The histone-tail acetylation also creates binding surfaces for other chromatin modifiers or transcription cofactors positively regulating transcription. Histone deacetylases (HDACs) remove acetyl groups from histone lysine residues, which results in the opposite effects to HATs on chromatin structure and transcription. In fact, HDACs have been found in various types of transcription repressor complexes in yeasts and higher eukaryotes (Cunliffe, 2008; Yang and Seto, 2008). Interestingly, genome-wide association studies in yeast and human have shown the presence of HDACs together with HATs in active as well as in inactive genes (Kurdistani *et al*., 2002; Wang *et al*., 2009b), suggesting the role of HDACs in controlling transcription that is beyond the traditional paradigm.

Arabidopsis has 12 putative HDACs belonging to the RPD3/HDA1 superfamily that is divided into four subgroups, namely Class I through III and an outlier group (Pandey *et al*., 2002). Genetic or pharmacological ablation of the HDAC function has shown that HDACs play diverse and important roles in many aspects of development and physiology in Arabidopsis. Antisense or T-DNA insertional knockout mutants of *HDA19*, a Class I *HDAC*, show multiple defects in

growth and development and altered responses to exogenous stimuli, such as light and pathogens, accompanied by deregulation of genes (Tian *et al*., 2003; Zhou *et al*., 2005; Benhamed *et al*., 2006; Long *et al*., 2006; Kim *et al*., 2008; Tanaka *et al*., 2008; Choi *et al*., 2012), reflecting the role of HDA19 as a global repressor (Tian *et al*., 2005). HDA6, the closest homolog of HDA19, plays key roles in the silencing of transgenes, transposable elements, and rRNA genes in association with RNA-directed DNA methylation (RdDM; Aufsatz *et al*., 2002; Probst *et al*., 2004; Earley *et al*., 2010) or RdDM-independent DNA methylation (To *et al*., 2011; Liu *et al*., 2012). Studies using *hda6* mutants have revealed that HDA6 has roles in flowering (Wu *et al*., 2008; Yu *et al*., 2011), embryonic-to-postembryonic transition (Tanaka *et al*., 2008), and senescence (Wu *et al*., 2008). Pharmacological studies employing trichostatin A (TSA), an inhibitor of the RPD3/HDA1 family of HDACs, have also revealed the importance of HDACs in directing the expression of root epidermal cell-patterning genes (Xu *et al*., 2005) and in controlling the rhythmic expression of the circadian clock gene, *TOC1* (Perales and Màs, 2007).

Flowering is controlled by environmental cues, such as photoperiod and temperature, and by developmental signals. In facultative long-day (LD) plants including Arabidopsis, inductive LD promotes rapid flowering, whereas non-inductive short-day (SD) represses the floral promotion activity and thus results in delayed flowering (Koornneef *et al*., 1998). There have been extensive studies on the signaling and mechanism of LD-induced floral promotion (Turck *et al*., 2008; reviewed in Amasino, 2010); however, the signaling and mechanistic detail of

floral repression and default flowering in SD are poorly understood. Gibberellic acid (GA) is known to allow default flowering in SD through activating *SUPPRESSOR OF OVEREXPRESSION OF CONSTANS 1* (*SOC1*) and *LEAFY* (*LFY*), two of the downstream floral activators (Blázquez and Weigel, 2000; Moon *et al*., 2003). VIN3-LIKE 1 (VIL1) and VIL2 have been reported to repress *FLOWERING LOCUS M* (*FLM*) and *MADS AFFECTING FLOWERING 5* (*MAF5*), two of the *FLOWERING LOCUS C* (*FLC*)-clade floral repressors, respectively in SD, leading to the promotion of floral transition (Sung *et al*., 2006; Kim and Sung, 2010). Lately, the micro RNA156 (miR156)-*SQUAMOSA PROMOTER BINDING PROTEIN LIKEs* (*SPLs*) regulatory module for vegetative phase transition has also been shown to play an important role in age-dependent flowering, especially under non-inductive SD conditions (Wang *et al*., 2009a).

Although there is evidence that indicates the significance of HDACs in the development and physiology of Arabidopsis, the biological roles and underlying molecular mechanisms of many HDACs have not yet been studied. Here, I report the *in vivo* roles of HDA9, a member of the RPD3/HDA1 family Class I HDACs. Loss of *HDA9* affects the development of several organs and caused early flowering in SD. Recently, an SD-specific early flowering of *hda9* mutants with increased *AGAMOUS-LIKE 19* (*AGL19*) expression and histone acetylation at the *AGL19* locus was reported (Kim et al., 2013). However, several important questions including whether *AGL19* is a direct target of HDA9, whether the increased expression of *AGL19* is a direct cause for the early flowering of *hda9*,

and how the loss of HDA9 activity results in SD-specific early flowering remain unanswered. Moreover, the pathway for which *AGL19* acts as a floral activator has not been elucidated. I demonstrate that HDA9 prevents precocious flowering in SD and during vernalization by directly targeting *AGL19* and repressing its expression during active transcription through histone deacetylation. Derepression of *AGL19* caused by the *hda9* mutation in turn induces the expression of *FLOWERING LOCUS T* (*FT*), which results in early flowering. I also show that *AGL19* expression is upregulated by SD photoperiod as well as by vernalization (Schönrock *et al*., 2006). These results indicate that the role of HDA9 in preventing the overstimulation of *AGL19* transcription by the inductive signals together with the photoperiod-dependent expression of *AGL19* are the basis of the SD-specific early flowering of *hda9*. My results suggest that the biochemical role of HDA9 might be to reset histone acetylation levels during active transcription to attain proper transcription activity and controlled gene expression.

2.3 Materials and Methods

2.3.1 Plant materials and growth conditions

The following T-DNA insertion mutants were obtained from the SALK collection (http://signal.salk.edu/): *hda9-1*, SALK_007123; *maf4*, SALK_028506; *maf5-1*, CS876411; and *maf5-2*, SALK_054770. The following mutants and transgenic plants were previously described as written in the text: *flc-3*, *fld-3*, *ld-1*, *FRI*, *hac1-1*, *ref6-3*; *co-101*, *ft-10*, *gi-2*, *agl19-1*, and *FT::GUS* plants. All the transgenic and mutant plants used in this study are in the Columbia (Col) background. All the plants were grown at 22℃ under 100 μmol m^{-2} s^{-1} of cool white fluorescent light with a 16 hours light/8 hours dark (LD) or an 8 hours light/16 hours dark (SD) photoperiod.

2.3.2 Histochemical β-glucuronidase (GUS) assay

For *HDA9:GUS*, a 3.9-kb genomic fragment of *HDA9* containing 0.9 kb promoter and the entire coding region was generated by polymerase chain reaction (PCR) using HDA9-GUS-F and HDA9-GUS-R as primers (Table S2). After restriction digestion with *Xho*I-*Sma*I, the PCR product was ligated to the *Sal*I-*Sma*I digested pPZP211G (Noh *et al*., 2001). *HDA9:GUS* was introduced into wt by the floral dip method (Clough and Bent, 1998) via *Agrobacterium tumefaciens* strain ABI, and

transformants were selected on MS media containing 50 μg ml^{-1} kanamycin. Histochemical GUS staining was performed as previously described (Noh *et al*., 2004). The GUS expression patterns in Fig. 2b,c were observed using a light microscope (Carl Zeiss Axioskop 40). *FT::GUS* from wt was introgressed into *hda9-1* through crossing, and the *hda9-1* mutants carrying *FT::GUS* (+/+) were selected. FT::GUS expression in wt and *hda9-1* was then compared.

2.3.3 Subcellular localization study

Nuclear fractionation was performed as previously described (Kinkema *et al*., 2000). Protein samples were quantified using a protein assay kit (Bio-Rad), subjected to SDS-PAGE, and transferred to nitrocellulose membranes (Millipore). For the detection of proteins, α-HA (Abcam ab9110), α-H3 (Abcam ab1791), and α-tubulin (Sigma-Aldrich T9026) were used at 1:3,000, 1:10,000, and 1:4,000, respectively.

2.3.4 HDA9 complementation construct and HDA9:HA

For the complementation construct (*HDA9g*), a 3.9 kb genomic fragment was amplified by PCR using HDA9-GUS-F and HDA9G-R (Table S2) as primers and cloned into the pPZP221-rbcsT which contains the transcriptional terminator of Arabidopsis *rbcS*. For the construction of *HDA9:HA*, a 3.9 kb *HDA9* genomic

fragment amplified using HDA9 gateway-F and HDA9 gateway-R as primers (Table S2) was cloned into the pENTR/SD/D-TOPO entry vector (Invitrogen) and then integrated into the pEarleyGate 301 destination vector (Earley *et al*., 2006) through recombination. The complementation construct and *HDA9:HA* were introduced into *hda9-1* as described for *HDA9:GUS*, and transformants were selected on MS media containing 100 μg ml^{-1} gentamycin (Sigma-Aldrich) or 25 μg ml^{-1} glufosinate ammonium (Sigma-Aldrich), respectively.

2.3.5 Flowering time analysis

Flowering times were measured as the means ± S.D. of the number of rosette and cauline leaves produced from the primary meristems at bolting. At least 15 plants were scored for each genotype and treatment. For vernalization treatment, plants were grown for 14 days (d) in SD and vernalized at 4℃ under SD conditions for 30 d. Vernalized samples were harvested immediately after the cold treatment.

2.3.6 RT-PCR and RT-qPCR analyses

Total RNA was isolated from plant tissues using TRI Reagent (Sigma-Aldrich) according to the manufacturer′s instructions. 4 μg of total RNA was reverse transcribed using MMLV Reverse Transcriptase (Fermentas) and the resulting first

strand was used as template for semi-quantitative PCR or quantitative real-time PCR (qPCR). The sequences of primers used for reverse transcription followed by PCR (RT-PCR) or qPCR (RT-qPCR) are provided in Table S3 or Table S4, respectively. qPCR was performed in 96-well blocks using an Applied Biosystems 7300 real-time PCR system (http://www.appliedbiosystems.com/) and SYBR Green I master mix (Kappa Biosystems). Absolute quantification was performed by generating standard curves using serial dilutions of a mixture of all cDNA samples to be analyzed. Normalization was to *Ubiquitin 10* (*UBQ10*). All the RT-qPCR results were presented as means ± S.E. of three biological replicates performed in triplicate.

2.3.7 ChIP assay

Chromatin immunoprecipitation (ChIP) was performed as previously described (Han *et al*., 2007; Kaufmann *et al*., 2010). Antibodies used for ChIP were α-H3Ac (Millipore 06-599), α-H3 (Abcam ab1791), α-RNA Pol II (Covance MMS-126R), and α-HA (Abcam ab9110). The α-H3Ac recognizes acetylated lysine 9 and 14 of H3, and the α-RNA Pol II recognizes both initiating and elongating forms of Pol II. The amount of immunoprecipitated chromatin was determined by qPCR (ChIP-qPCR) using primer pairs listed in Table S5, and the relative amounts of amplified

products were evaluated according to the $2^{\Delta\Delta CT}$ method (Livak and Schmittgen, 2001).

Table 2-1. Oligonucleotides used for genotyping

Gene	Name	Sequence
T-DNA border	SALK LB1.3	5'-ATTTTGCCGATTTCGGAAC-3'
	SAIL LB3	5'-TAGCATCTGAATTTCATAACCAATCTCGATACA-3'
HDA9	HDA9-F1	5'-GAAATGGCTAGATGTAAGTTTTGTGTCT-3'
	HDA9-R1	5'-TCGCCTGTCCCTGGAAAGAACTTATC-3'
AGL19	AGL19-1F	5'-TCACACCCTCTTCCCAAAATCTCGCC-3'
	AGL19-1R	5'-GGTGTCAAACTCATCTTTCTTACAAAC-3'
MAF4	MAF4-F	5'-GTTATTGGGTCTCATGGGCCAAAGAAACTG-3'
	MAF4-R	5'-GTTAACCAATAGTTTTTGCACTTCTCTAAC-3'
MAF5	MAF5-1F	5'-GGCGCCATCATACATAAGCTA -3'
	MAF5-1R	5'-TCTCCACAATAATAGGGCCCT-3'
	MAF5-2F	5'-AATTTGGCAACTACCATGCA-3'
	MAF5-2R	5'-TTGAATTGTTAGTTGTTCCGCTT-3'
HAC1	HAC1-3F	5'-ATGCAGAAGACCGTCATGCAGGTTC-3'
	HAC1-4R	5'-TTTTTAATCGAGCAAGGGACCGTGC-3'
REF6	T29H11-1	5'-CCTCCATGTTACATTGGTATGCTGCACATT-3'
	T29H11-2	5'-CAAATGTCTGATCCGCACAAGGGAATTATC-3'
FLD	FLD-3-1	5'-ACGGATCCATCAAATTTGTTCCCGAATTAC-3'
	FLD-3-2	5'-CTGAAGCTCCCACTGCAACATTAGAGTAAG-3'
LD	ld-1 MSEIF	5'-GCTGCGTAGCTTTCATCAATGCCA-3'
	ld-1 MSEIR	5'-GAATATCTTCCTGTTACGACACG-3'

FRI	FRI UJ26-F	5'-AGATTTGCTGGATTTGATAAGG-3'
	FRI UJ26-R	5'-GAAATTCACCGAGTGAGAACAGA-3'
GI	pGI2-1F	5'-CCACTAGTTGTAGCTTTGCTCAGAC-3'
	pGI2-1R	5'-ATGACTATTCGGAGCAATGGGCT-3'
CO	Constas R KO-F	5'-AGCTCCCACACCATCAAACTTACTACATC-3'
	Constas A-R	5'-AGTCCATACTCGAGTTGTAATCCAC-3'
FT	JH2295	5'-TAAGCTCAATGATATTCCCGTACA-3'
	JH2296	5'-CAGGTTCAAAACAAGCCAAGA-3'
	JH2297	5'-CCCATTTGACGTGAATGTAGACAC-3'
FLC	pFLC33	5'-CTCATGTATCTATCATGGTCGCAG-3'
	pFLC24	5'-CGTATCGTAGGGGAGGAAAGATAG-3'

Table 2-2. Oligonucleotides used for *HDA9g*, *HDA9:GUS*, and *HDA9:HA* constructs

Construct	Name	Sequence
HDA9:GUS	HDA9-GUS-F	5'-AGCTCGAGGGTCATCATTTCTCTCAACATTGTT-3'
	HDA9-GUS-R	5'-CAACCCGGGGATGACGCATCGTTATCGTTGTCTC-3'
HDA9:HA	HDA9 gateway-F	5'-CACCGGTCATCATTTCTCTCAACATTGT-3'
	HDA9 gateway-R	5'-TGACGCATCGTTATCGTTGTCTCC-3'
HDA9g	HDA9-GUS-F	5'-AGCTCGAGGGTCATCATTTCTCTCAACATTGTT-3'
	HDA9 GUS-R	5'-CCCGGGTTATGACGCATC GTTATCGTTGTCT-3'

Table 2-3. Oligonucleotides used for RT-PCR analysis

Gene	Name	Sequence
UBQ10	UBQ-F	5′-GATCTTTGCCGGAAAACAATTGGAGGATGGT-3′
	UBQ-R	5′-CGACTTGTCATTAGAAAGAAAGAGATAACAGG-3′
HDA9N	HDA9F	5'-GAGATGCGTTCCAAGGACAA-3'
	HDA9R-1	5'-GCCGGCGTAAAGTTGACAAAAT-3'
HDA9F	HDA9F	5'-GAGATGCGTTCCAAGGACAA-3'
	HDA9R-2	5'-TTATGACGCATCGTTATCGTTGTCT -3'
FT	FT-F	5'-GCTACAACTGGAACAACCTTTGGCAAT-3'
	FT-R	5'-TATAGGCATCATCACCGTTCGTTACTC-3'
TEM1	TEM1-F	5'-GCGTGTTGTTTCGGTATCACTA-3'
	TEM1-R	5'-ATTCAGAGAACGGCGTCGA-3'
TEM2	TEM2-F	5'-TTCCTCAGCCTAACGGAAGAT-3'
	TEM2-R	5'-TCCTTGACGAATCGACTCCAT-3'
TOE1	TOE1-F	5'-ACTCAGTACGGTGGTGACTC-3'
	TOE1-R	5'-CGAGGATCCATAAGGAAGAGG-3'
TOE2	TOE2-F	5'-CACTTTCTATCGGAGGACAG-3'

	TOE2-R	5'-CTTCCACATACGGAATTGTT-3'
TOE3	TOE3-F	5'-GTTACGTTTTACCGACGAAC-3'
	TOE3-R	5'-TGCTTGCAATATCAGACTTG-3'
SMZ	SMZ-F	5'-AATGGTGAAGAAGAGCAGAA-3'
	SMZ-R	5'-CTTTCCGATGATGATGAAAT-3'
SNZ	SNZ-F	5'-TTTGGAATCCTTAAACGAAA-3'
	SNZ-R	5'-TATCTCATTGCATTTTGCTG-3'
AGL15	AGL15-F	5'-TTATCTAGATGGGTCGTGGAAAAATCGAG-3'
	AGL15-R	5'-TTAGCGGCCGCAGAGAACCTTTGTCTTTTGGCTTC -3'
AGL18	AGL18-F	5'-ATGGGGAGAGGAAGGATTGAGATTAAGAA -3'
	AGL18-R	5'-TCAATCAGAAGCCACTTGACTCCCAGAGT -3'
AGL19	AGL19-F	5'-ATGGTGAGGGGCAAAACGGAGATG-3'
	AGL19-R	5'-TCCAGATGTTTCGTCTCTCGCTTGC-3'
AGL24	AGL24-F	5'-TCCATCGAAGTCAACTCTGCTGGATC-3'
	AGL24-R	5'-GTCTTCATGCAAGTAACATCAAC-3'
MAF4	MAF4-F	5'-ATTAGGTCAGAAGAATTAGTCGGAGAAAAC-3'
	MAF4-R	5'-CTTGGATGACTTTTCCGTAGCAGGGGGAAG-3'

MAF5	MAF5-F	5'-GGGGATTAGATGTGTCGGAAGAGTGAAG-3'
	MAF5-R	5'-GATCCTGTCTTCCAAGGTAACACAAAGG-3'

Table 2-4. Oligonucleotides used for RT-qPCR analyses

Gene	Name	Sequence
UBQ10	qUBQ-F	5′-GGCCTTGTATAATCCCTGATGAATAAG-3′
	qUBQ-R	5′-AAAGAGATAACAGGAACGGAAACATAGT-3′
CO	qCO-F	5'-AAACCCATTTGCACAACAG-3'
	qCO-R	5'-GAGCAAGGGTTCAACACGAT-3'
FT	qFT-F	5'-CCATTGGTTGGTGACTGATATCC-3'
	qFT-R	5'-TTGCCAAAGGTTGTTCCAGTT-3'
FLC	qFLC-F	5'-AGCAAGCTTGTGGGATCAAATGTC-3'
	qFLC-R	5'-TGGCTCTAGTCACGGAGAGGGC-3'
SOC1	qSOC1-F	5'-TCGAGCAAGAAAGACTCAAGTG-3'
	qSOC1-R	5'-TTGACCAAACTTCGCTTTCA-3'
SPL3	qSPL3-F	5′-CTTAGCTGGACACAACGAGAGAAGGC-3′
	qSPL3-R	5′-GAGAAACAGACAGAGACACAGAGGA-3′
SPL4	qSPL4-F	5′-GTAGCATCAATCGTGGTGGC-3′
	qSPL4-R	5′-CTTCGCTCATTGTGTCCAGC-3′
SPL5	qSPL5-F	5′-CCAGACTCAAGAAAGAAACAGGGTAGACAG-3′
	qSPL5-R	5′-TCCGTGTAGGATTTAATACCATGACC-3′

SPL9	qSPL9-F	5′-CAAGGTTCAGTTGGTGGAGGA-3′
	qSPL9-R	5′-TGAAGAAGCTCGCCATGTATTG-3′
SPL15	qSPL15-F	5′-TTGGGAGATCCTACTGCGTGGTCAACC-3′
	qSPL15-R	5′-AGCCATTGTAACCTTATCGGAGAATGAG-3′
MAF1	qMAF1-F	5'-TCACCTTAAACTCAAAGCCTGATTC-3'
	qMAF1-R	5'-CAAACTCTGATCTTGTCTCCGAAG-3'
MAF2	qMAF2-F	5'-CATTGTGGGTCTCCGGTGATTAG-3'
	qMAF2-R	5'-GATGAGACCATTGCGTCGTTTG-3'
MAF3	qMAF3-F	5'-TATCTTCCTCGCGCCAATG-3'
	qMAF3-R	5'-AGCACAAGAACTCTGATATTTGTCTAC-3'
MAF4	qMAF4-F	5'-GCTTCTCAAGTAACCACCATCAC-3'
	qMAF4-R	5'-CTTGGATGACTTTTCCGTAGCAG-3'
MAF5	qMAF5-F	5'-CATGGATTGTGCTAGAAAACAACTG-3'
	qMAF5-R	5'-GCTTCACTCTTCCGACACATCTAATC-3'
AGL6	qAGL6-F	5'-TTTCCGGTAGAGCCTTCTCA-3'
	qAGL6-R	5'-CCCAACCTTGGACGAAATTA-3'
AGL19	qAGL19-F	5'-TCAGCAAGCGAGAGACGAAACATC-3'
	qAGL19-R	5'-TGCATCAATGCCTTCTCCAAGCAA-3'
AGL24	qAGL24-F	5'-TCTCCGGCTTGAGAATTGTAACCTC-3'
	qAGL24-R	5'-TCCAGCCGCTGCAACTCTTC-3'

AGL15	qAGL15-F	5'-CTGCAGGGCAAGGGCTTGAA TCCT-3'
	qAGL15-R	5'-TGCTCGTTGTTCCTTGAGGCGTG-3'
AGL18	qAGL18-F	5'-ATGGGGAGAGGAAGGATTGAGATTAAGAA -3'
	qAGL18-R	5'-GATGATAAGAGCAACCTCGGCGTC-3'
VIN3	qVIN3-F	5'-ATCTTGCTTGAATCTCTTCTACTCT-3'
	qVIN3-R	5'-ATTGGGAGTGATGATCTTGATGGTA-3'

Table 2-5. Oligonucleotides used for ChIP assays

Locus	Name	Sequence
UBQ10	ChIP-F	5′-TTGCCAATTTTCAGCTCCAC-3′
	ChIP-R	5′-TGACTCGTCGACAACCACAA-3′
ACTIN2/7	ChIP-F	5′-GATCCGTTCGCTTGATTTTGC-3′
	ChIP-F	5′-ACAAGCACGGATCGAATCACA-3′
AGL19-A	AGL19-AF	5'-CCATTGATAGATTTTGGATATTAGATAA-3'
	AGL19-AR	5'-CAGGTGTCGCACGCTAGGAGAGGACCACA-3'
AGL19-B	AGL19-BF	5'-GTTACTGTTTTATTTGTGCGAAGGT-3'
	AGL19-BR	5'-TTCCACAGAAGAAGCAGAACTTTAT-3'
AGL19-C	AGL19-CF	5'-GTATCCATTTTTGTGTCGAAGTCTTTT-3'
	AGL19-CR	5'-TCGGACAAAATAAGTAGTTAGGACACAC-3'
AGL19-D	AGL19-DF	5'-CTATCCGTAGCCATAAGAGAAAATG-3'
	AGL19-DR	5'-AAGCCCTAGATTTATGATGAAGGAG-3'
AGL19-E	AGL19-EF	5'-TTTCTTTCTTTCTCTCCCCTCCTTCAT-3'
	AGL19-ER	5'-ATCTATCTTCTATAAGTGAGTGGAGAGT-3'
AGL19-I	AGL19-IF	5'-TCTTCCCAAAATCTCGCCTA-3'
	AGL19-IR	5'-CAACCACAAACAGAAGATGGAA-3'
AGL19-II	AGL19-IIF	5'-AAACGGAGATGAAGAGGATAGAGAAC-3'
	AGL19-IIR	5'-CATAGAGTTTGGATCTTGGAGAGAAG-3'
AGL19-III	AGL19-IIIF	5'-GCCATCCATTTTTTCGCTGTA-3'
	AGL19-IIIR	5'-GCCTAGCAGTAGCACTGGTGT-3'

AGL19-IV	AGL19-IVF	5'-TTTTGAGCAAACTCAAGAGAGG-3'
	AGL19-IVR	5'-GGACACGCTCAAATCGAAAT-3'
AGL19-V	AGL19-VF	5'-GGAATGGGAACAGCAACAAT-3'
	AGL19-VR	5'-GGAGGTCCAATGAACAAACC-3'
SOC1-1	SOC1-1F	5'-TATATCGGGAGGAGGACCACAC-3'
	SOC1-1R	5'-ATCCATACAGATTTTCGGACCT-3'
SOC1-2	SOC1-2F	5'-TCTCGTACCTATATGCCCCCACT-3'
	SOC1-2R	5'-TTTATCTGTTGGGATGGAAAGA-3'
SOC1-3	SOC1-3F	5'-GCAAAAGAAGTAGCTTTCCTCG-3'
	SOC1-3R	5'-AGCAGAGAGAGAAGAGACGAGTG-3'
SOC1-4	SOC1-4F	5'-GGATGCAACCTCCTTTCATGAG-3'
	SOC1-4R	5'-ATATGGGTTTGGTTTCATTTGG-3'
SOC1-5	SOC1-5F	5'-ATCACATCTCTTTGACGTTTGCTT-3'
	SOC1-5R	5'-GCCCTAATTTTGCAGAAACCAA-3'
SOC1-6	SOC1-6F	5'-TGTTTCAGACATTTGGTCCATTTG-3'
	SOC1-6R	5'-AGTCTTGTACTTTTTCCCCCTATTTTAG-3'
FT2	FT2-F	5'-TCTGATTTGGGGTTCAAAA -3'
	FT2-R	5'-TCGAACTGATTCCGATTGAA-3'
FT3	FT3-F	5'-GGCCAACATTAGAAGAAGATTCC-3'
	FT3-R	5'-TCTTGACATGGAGCGAAAGA -3'
FT7	FT7-F	5'-CTGCGACTGCGACCTATTTT-3'
	FT7-R	5'-GCCACTGTTCTACACGTCCA-3'

cArG VII	cArG VII-F	5'-GGTGGAGAAGACCTCAGGAA -3'
	cArG VII-R	5'-GTGGGGCATTTTTAACCAAG-3'

2.4 Results

2.4.1 Isolation of an *hda9* mutant

The amino acid sequence alignment of HDA9 (At3g44680) and other Arabidopsis Rpd3/HDA1 Class I HDACs (HDA6, HDA7, and HDA19) showed that the HDAC domain of HDA9 is highly similar to that of other HDACs, but its C-terminal region is quite divergent and varies in length compared with that of others (Fig. 1a). Interestingly, the C-terminal region of HDA9 (277 - 426) is nearly identical to the entire regions of HDA10 and HDA17, which belong to the outlier group (Fig. S1b; Pandey *et al*., 2002; Hollender and Liu, 2008). However, HDA10 and HDA17 possess partial HDAC domains and are thus unlikely to be functionally redundant with HDA9 (Fig. 1b). These structural features suggest that HDA9 might possess a unique role in Arabidopsis.

To address the biological role of HDA9 and determine if it is distinct from the roles of the well-characterized HDA6 and HDA19, I first isolated a mutant carrying a T-DNA insertion in the fourth exon of *HDA9* from the SALK collection and named it *hda9-1* (Fig. 2a). This mutant allele was also reported by Kim *et al.* (2013). RT-PCR analyses showed that the full-length *HDA9* transcript is not expressed at a detectable level, although a truncated transcript upstream of the T-DNA insertion site in *hda9-1* is expressed at a reduced level (Fig. 2b). Thus, *hda9-1* is believed to be a null allele.

The *hda9-1* mutants showed a normal morphology in most organs in contrast to *hda19* mutants, which display severely distorted morphological

phenotypes in many organs (Tian and Chen, 2001; Tian *et al*., 2003; Long *et al*., 2006). Nonetheless, subtle morphological differences between wild type (wt) and *hda9-1* were observed in a few organs. At the fully-developed stage, *hda9-1* flowers did not open as fully as wt flowers, and the petals and sepals were less tightly attached to the receptacles in *hda9-1* than in wt (Fig. 2c). In addition, the tips of the *hda9-1* siliques were wide and blunt, whereas those of the wt siliques were tapered and acute (Fig. 2d). The *hda9-1* silique phenotype was similar to that of *erecta* (*er*) mutants (Torii *et al*., 1996). However, unlike *er* mutation, the *hda9-1* mutation did not affect silique length (Fig. 2, 3). In addition, the size of adult *hda9-1*, especially when grown in SD, was smaller than wt mainly because of less elongated petioles and leaves (Figs. 2e,f, 3b). All the *hda9-1* phenotypes described above were restored to wt phenotypes when a genomic copy of *HDA9* was introduced into the *hda9* mutant plants (Fig. 2c,d,f), demonstrating that these phenotypes are indeed caused by the loss of *HDA9* function. Because the *hda9-1* phenotypes described here have not been reported for either *hda6* or *hda19*, it is likely that HDA9 has a distinct *in planta* role.

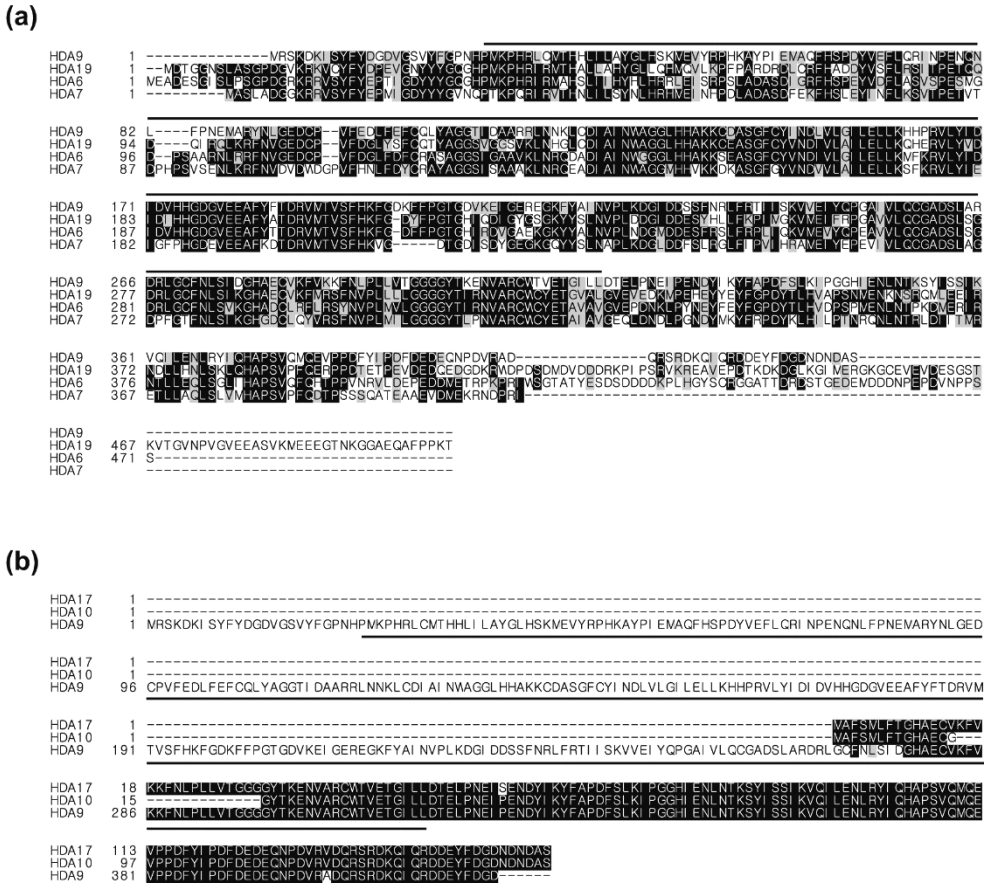

Fig. 1 Sequence comparison between Arabidopsis Class I HDAC proteins.

(a) Multiple sequence alignment of HDA9 (At3g44680), HDA19 (At4g38130), HDA6 (At5g63110), and HDA7 (At5g35600) generated using ClustalW. The numerals indicate amino acid positions, and HDAC domains are marked with solid lines (a,b). (b) Multiple sequence alignment of HDA17 (At3g44490), HDA10 (At3g44660), and HDA9 generated using ClustalW.

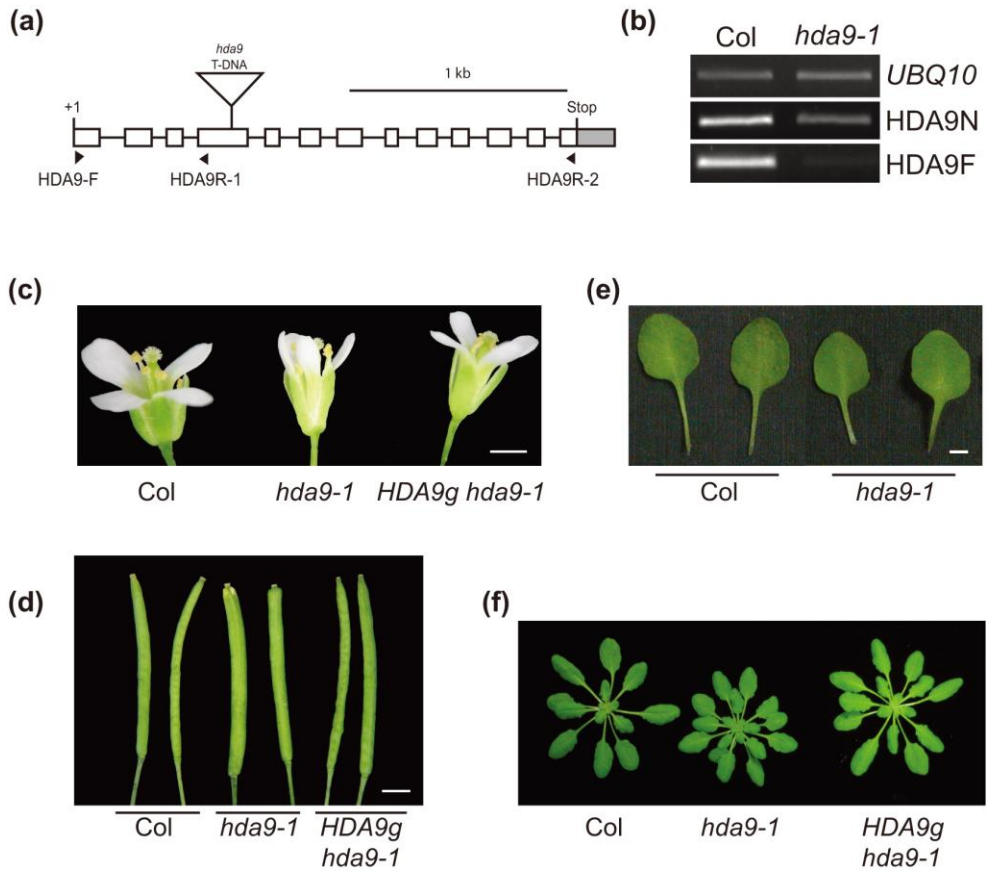

Fig. 2 Phenotype of *hda9-1* mutant

(a) Schematic illustration of the gene structure of *HDA9* and a T-DNA insertion in *hda9-1*. Exons and the 3′ untranslated region (UTR) are represented with white

boxes and a gray box, respectively. Introns are indicated as solid lines. ′+1′ refers to the transcription start site. The T-DNA insertion position in *hda9-1* is marked with a triangle. Arrows indicate the primers used for RT-PCR in (b). (b) RT-PCR analysis of a 5′ (HDA9N) and the full-length (HDA9F) *HDA9* transcript expression in wild type (Col) and *hda9-1*. HDA9-F/HDA9-R1 and HDA9-F/HDA9-R2 primer pairs (a; Table S3) were used for HDA9N and HDA9F, respectively. *UBQ10* was used as an expression control. (c, d) Flower (c) and silique (d) phenotype of wt, *hda9-1*, and *hda9-1* transformed with a genomic copy of *HDA9* (*HDA9g hda9-1*). Scale bars represent 1 mm. (e) Representative 5th and 6th rosette leaves with petioles of wt and *hda9-1* plants grown for 45 d in SD. Scale bars represent 5 mm. (f) Rosette development in wt, *hda9-1*, and *HDA9g hda9-1*. Shown are plants grown for 45 d in SD.

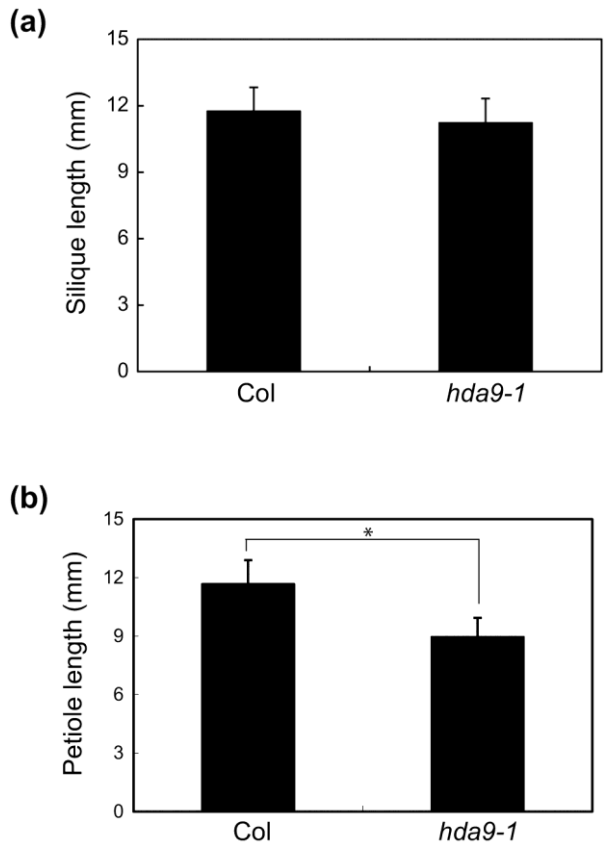

Fig. 3 Effect of the *hda9-1* mutation on silique and petiole lengths.

(a) Length of the 5th and 6th siliques from the primary inflorescence tips. At least fifteen wt or *hda9-1* plants were used for scoring, and values are the means±s.d. (a,b). Length was measured from digital images using UTHSCSA Image Tool (a,b). (b) Length of the petioles of the 5th and 6th rosette leaves. Asterisk denotes a statistically significant difference (P<0.001).

2.4.2 Spatial expression pattern and nuclear localization of HDA9

Because the expression pattern of *HDA9* has not been reported previously, we generated transgenic plants harboring the native promoter and genomic coding region of *HDA9* translationally fused to *GUS* (*HDA9:GUS*), and performed histochemical analyses to study the spatial expression pattern of *HDA9*. GUS staining was observed in the cotyledons, hypocotyls, and roots of the seedlings (Fig. 4a). The shoot apexes, leaf primordial, and root tips were the organs most strongly stained (Fig. 4b,c). In older developmental stages, GUS staining was detected in the entire rosette leaves, including the trichomes and petioles (Fig. 4d), floral organs such as the stigmas, anthers, filaments, pollens, and the siliques (Fig. 4e,f). The nearly ubiquitous spatial expression pattern of *HDA9* studied with the *HDA9:GUS* plants was confirmed by RT-qPCR using RNAs obtained from various tissues (Fig. 4g) and by analysis of the expression profile of *HDA9* exploiting publicly available microarray datasets (Fig. 5).

As shown in Fig. 4c, HDA9:GUS expression was dispersed but not restricted to any particular subcellular compartment. However, it was not clear whether this subcellular GUS-staining pattern reflects the real subcellular localization of the HDA9 protein because *HDA9:GUS* was not able to complement *hda9-1*. Therefore, I generated transgenic *hda9-1* plants expressing the HDA9 protein with a C-terminal HA tag (HDA9:HA) from the native *HDA9* promoter. Unlike *HDA9:GUS*, *HDA9:HA* was able to fully rescue the *hda9-1* mutant phenotypes (Fig. 6), indicating that HDA9:HA is functionally equivalent to HDA9.

To determine the subcellular localization of HDA9:HA, non-nuclear and nuclear proteins were fractionated from the *HDA9:HA hda9-1* plants and used for immunoblot analysis using an anti-HA antibody. A ~55 kilo-dalton protein corresponding to HDA9:HA was detected in the nuclear but not in the non-nuclear fraction (Fig. 4h). Thus, HDA9 seems to be localized predominantly in the nuclei like HDA6 and HDA19 (Earley *et al*., 2006; Fong *et al*., 2006; Long *et al*., 2006; Wu *et al*., 2008).

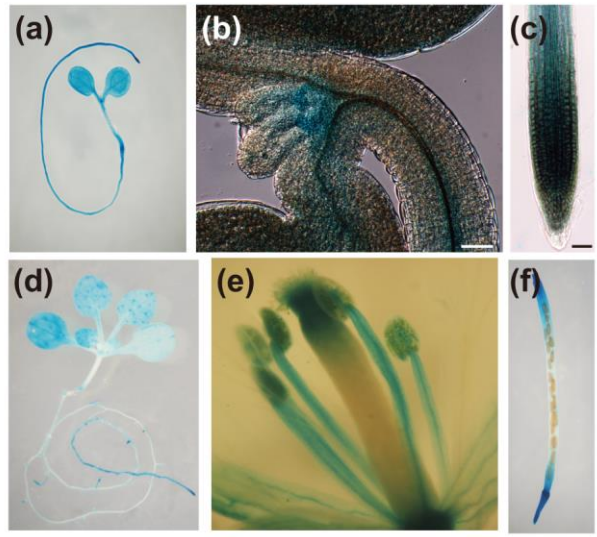
(a)
(b)
(c)
(d)
(e)
(f)

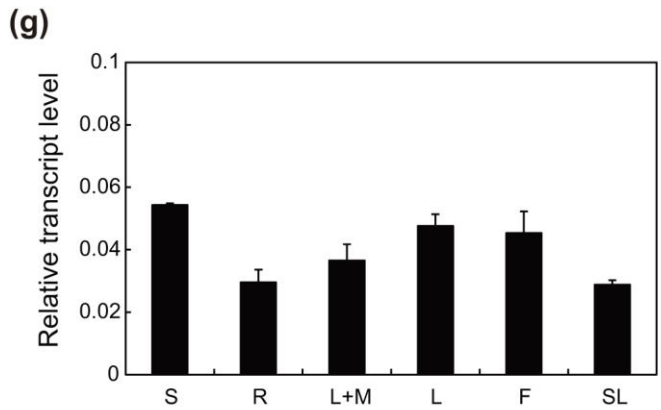
(g)
Relative transcript level
0.1
0.08
0.06
0.04
0.02
0
S
R
L+M
L
F
SL

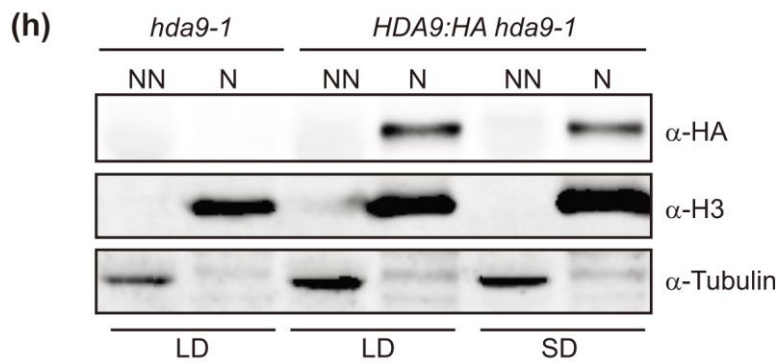
(h)
hda9-1
HDA9:HA hda9-1
NN
N
NN
N
NN
N
α-HA
α-H3
α-Tubulin
LD
LD
SD

Fig. 4 Expression pattern of *HDA9*.

(a-f) Histochemical GUS staining of *HDA9:GUS*-containing transgenic Arabidopsis. (a) 4 d-old seedling grown in SD. (b) Magnified shoot-apex of the seedling shown in (a). Scale bars represent 50 μm (b, c). (c) Primary root tip of 6 d-old seedling grown in SD. (d) 16 d-old whole seedling grown in SD. (e, f) Open flower (e) and silique (f) of LD-grown plant. (g) mRNA expression of *HDA9* in various tissues as studied by RT-qPCR. RNA was isolated from 10 d-old seedlings (S), roots (R), entire shoots including the shoot apical meristems (L+M), rosette leaves (L), flowers (F), and siliques (SL). *UBQ10* was used as an expression control. (h) Nuclear localization of HDA9. Nuclear (N) and nonnuclear (NN) proteins were extracted from *hda9-1* and *HDA9:HA*-containing *hda9-1* transgenic seedlings grown for 10 d in LD or for 14 d in SD and subjected to immunoblot analysis with anti-HA antibody. Histone H3 and tubulin were detected as nuclear and nonnuclear protein controls, respectively.

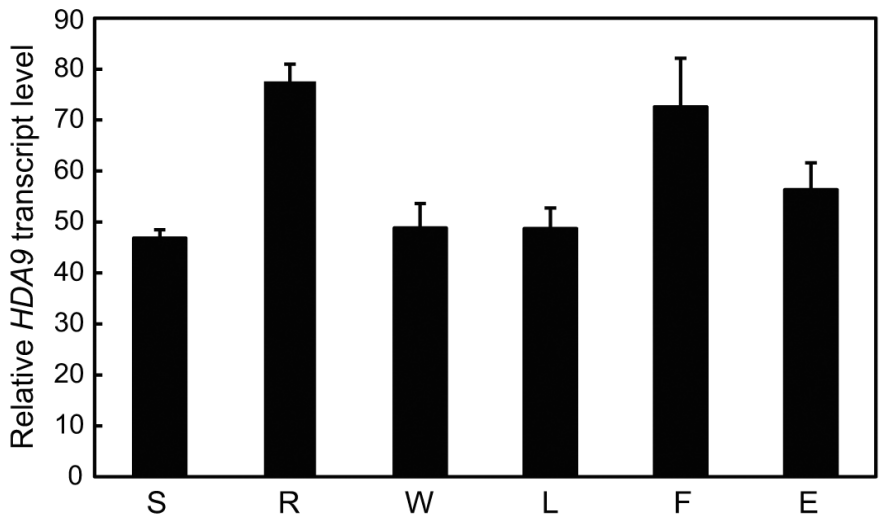

Fig. 5 Predicted spatial expression profile of *HDA9*.

Transcript levels of HDA9 in various tissues were obtained from publicly obtained microarray dataset http://www.arabidopsis.org/servlets/Search?action=new_search&type=expression). S, seedlings; R, roots; W, whole plants; L, leaves; F, flowers; E, embryos.

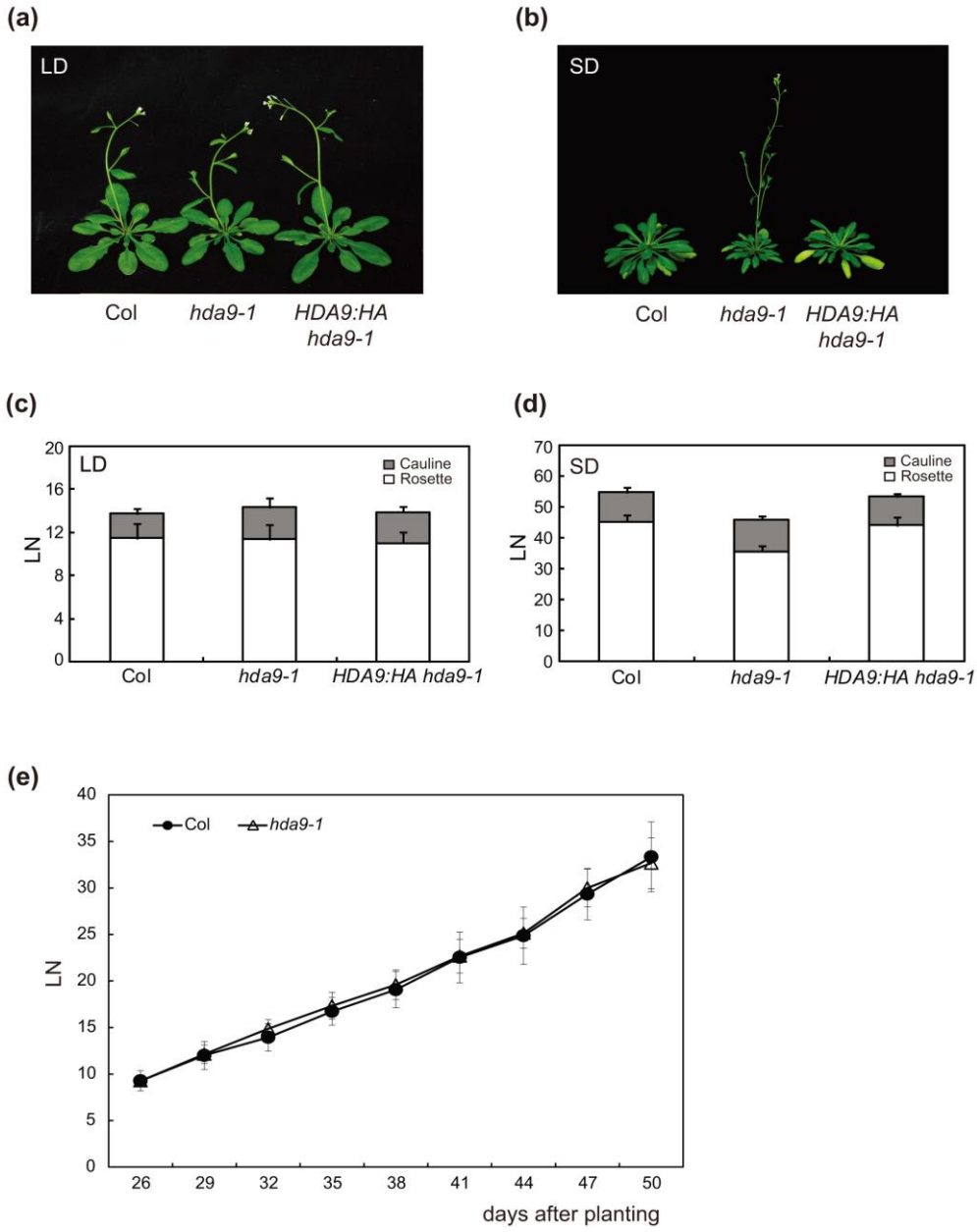
(a)
LD
Col
hda9-1
HDA9:HA hda9-1
(b)
SD
Col
hda9-1
HDA9:HA hda9-1
(c)
LD
Cauline
Rosette
LN
0
4
8
12
16
20
Col
hda9-1
HDA9:HA
hda9-1
(d)
SD
Cauline
Rosette
LN
0
10
20
30
40
50
60
70
Col
hda9-1
HDA9:HA
hda9-1
(e)
Col
hda9-1
LN
0
5
10
15
20
25
30
35
40
26
29
32
35
38
41
44
47
50
days after planting

Fig. 6 Complementation of the early-flowering phenotype of *hda9-1* by *HDA9:HA*.

(a,b) wt, *hda9-1*, and a representative complementation line of *hda9-1* harboring *HDA9:HA* (*HDA9:HA hda9-1*). Pictures were taken when plants were 28-day old in LD (a) or 84-day old in SD (b). (c,d) Flowering time of wt, *hda9-1*, and *HDA9:HA hda9-1* plants in LD (c) or SD (d) as determined by LN. (e) Leaf initiation rate of wt and *hda9-1* plants in SD. At least 15 individual plants per genotype were used for leaf number counting at indicated time until the appearance of primary inflorescence. Values are the means±s.d.

2.4.3 The *hda9-1* mutation causes early flowering in SD

The *hda9-1* mutants displayed another remarkable phenotype: an early flowering in non-inductive SD as evidenced by smaller number of rosette leaves at the onset of flowering (Fig. 7a,b) without change in leaf initiation rate (Fig. 6e). The early-flowering phenotype of *hda9-1* was rescued by the introduction of a genomic *HDA9* fragment (*HDA9g*; Fig. 7a,b) and by *HDA9:HA* (Fig. 6b,d). However, the early-flowering phenotype of *hda9-1* was not obvious in inductive LD (Figs. 6a,c, 7c,d).

I then analyzed the genetic interactions between *hda9-1* and mutations in the autonomous pathway, the photoperiod pathway, and the floral integrator group. The *hda9-1* mutation caused partial suppression of the late-flowering phenotypes of the autonomous-pathway mutants *hac1-1* (Han *et al*., 2007), *relative of early flowering 6-3* (*ref6-3*; Noh *et al*., 2004), *flowering locus d-3* (*fld-3*; He *et al*., 2003), *luminidependens-1* (*ld-1*; Lee *et al*., 1994), and *FRIGIDA* (*FRI*; Koornneef *et al*., 1994; Lee *et al*., 1994)-containing Col in LD (Fig. 7e) and to a greater extent in SD (Fig. 7f). The late-flowering phenotypes of the photoperiod-pathway mutants were also suppressed by *hda9-1* but not as effectively as those of the autonomous-pathway mutants: the *gigantea-2* (*gi-2*; Park *et al*., 1999) *hda9-1* and *constans-101* (*co-101*; Takada and Goto, 2003) *hda9-1* double mutants flowered slightly earlier than the *gi-2* and *co-101* single mutants, respectively (Fig. 7g,h). Notably, the *hda9-1* mutation was not capable of accelerating the floral transition of a floral integrator mutant, *flowering locus t-10* (*ft-10*; Yoo *et al*., 2005), both in LD and SD

(Fig. 7g,h), indicating that *FT* acts downstream of *HDA9*. These results indicate that *HDA9* negatively regulates flowering in parallel with the autonomous and photoperiod pathways and acts upstream of *FT*.

The day-length-dependent effect of the *hda9-1* mutation on flowering (Fig. 7a-d) raised a possibility of day-length dependent *HDA9* expression or nuclear-cytoplasmic shuttling of HDA9 protein as the mammal Class II HDACs (Grozinger *et al*., 2000; Verdel *et al*., 2000). However, HDA9:HA protein was accumulated to comparable levels in LD- and SD-grown plants and predominantly localized to nuclei in both photoperiodic conditions (Fig. 4h), excluding those possibilities.

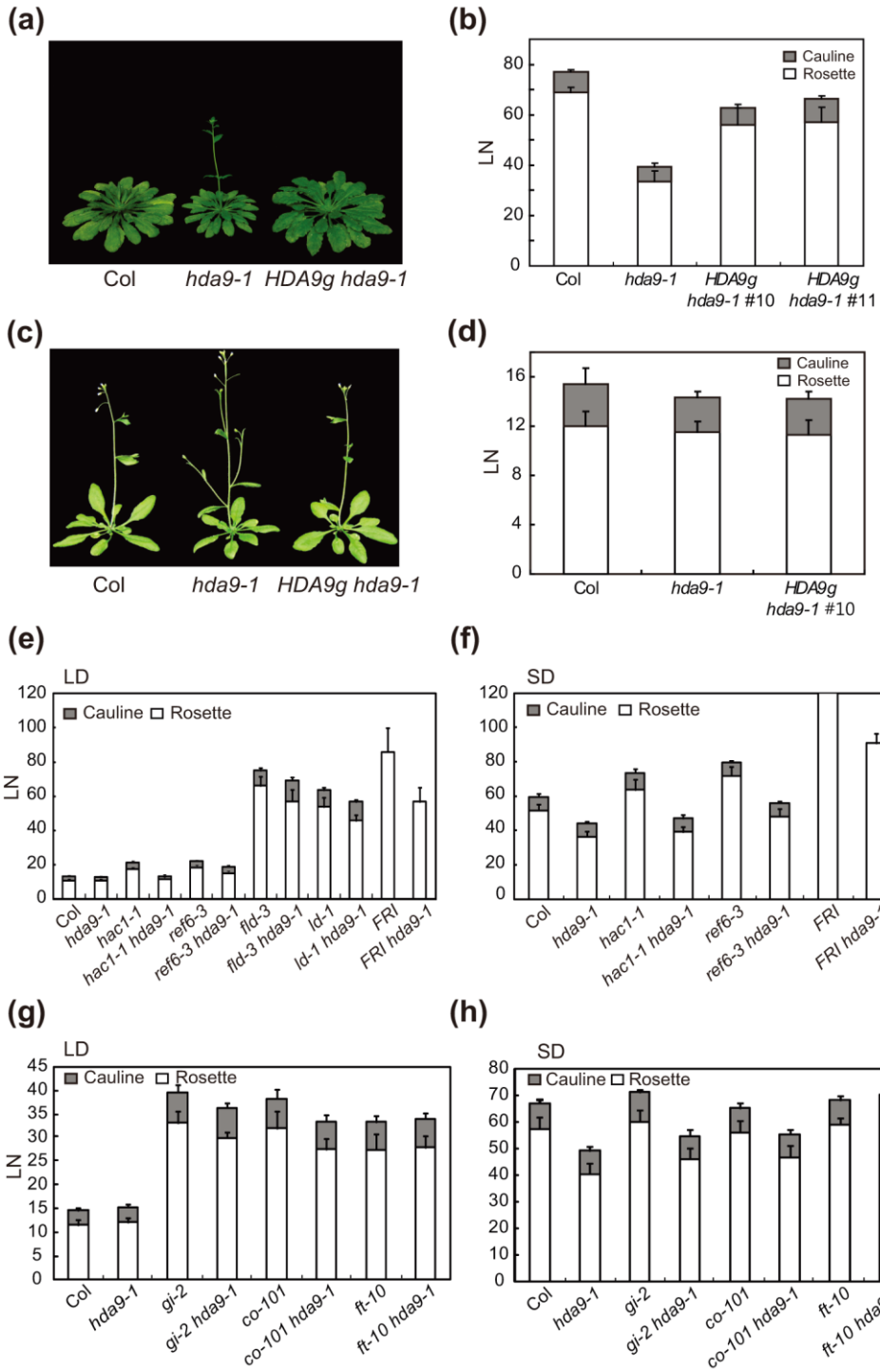
(a)
Col
hda9-1
HDA9g hda9-1
(b)
Cauline
Rosette
LN
Col
hda9-1
HDA9g hda9-1 #10
HDA9g hda9-1 #11
(c)
Col
hda9-1
HDA9g hda9-1
(d)
Cauline
Rosette
LN
Col
hda9-1
HDA9g hda9-1 #10
(e)
LD
Cauline
Rosette
LN
Col
hda9-1
hac1-1
hac1-1 hda9-1
ref6-3
ref6-3 hda9-1
fld-3
fld-3 hda9-1
ld-1
ld-1 hda9-1
FRI
FRI hda9-1
(f)
SD
Cauline
Rosette
Col
hda9-1
hac1-1
hac1-1 hda9-1
ref6-3
ref6-3 hda9-1
FRI
FRI hda9-1
(g)
LD
Cauline
Rosette
LN
Col
hda9-1
gi-2
gi-2 hda9-1
co-101
co-101 hda9-1
ft-10
ft-10 hda9-1
(h)
SD
Cauline
Rosette
Col
hda9-1
gi-2
gi-2 hda9-1
co-101
co-101 hda9-1
ft-10
ft-10 hda9-1

Fig. 7 The *hda9-1* mutation causes early flowering.

(a) Wt, *hda9-1*, and *HDA9g hda9-1* plants grown for 85 d in SD. (b) Flowering time of wt, *hda9-1*, and two independent *HDA9g hda9-1* transgenic lines in SD. Flowering times were determined as the numbers of rosette and cauline leaves formed at bolting (LN). (c) Wt, *hda9-1*, and *HDA9g hda9-1* plants grown for 25 d in LD. (d) Flowering time of wt, *hda9-1*, and an *HDA9g hda9-1* transgenic line in LD as determined by LN. (e-h) Double mutant analyses of *hda9-1* with various late flowering mutants of the autonomous (e, f) or photoperiod pathway (g, h). Flowering time was measured either in LD (e, g) or SD (f, h) by scoring LN. The *FRI* plants grown in SD (f) did not flower at the time of measurement and produced more than 130 rosette leaves.

2.4.4 Loss of *HDA9* affects the expression of *FLC*, *MAF4*, *MAF5*, and *FT*

Because HDA9 localizes to the nuclei and many Rpd3/HDA1 Class I HDACs in yeast, fly, and human are present within various transcriptional repressor complexes (reviewed in Hayakawa and Nakayama, 2010), I questioned whether the *hda9-1* mutation affects the expression of key flowering genes at their mRNA level: *CO*, a key floral promoter in the photoperiod pathway; *FLC*, a central floral repressor in the autonomous and vernalization pathways, and its five paralogs (*MAF1* through *MAF5*); and the floral integrators *FT* and *SOC1*. Under both LD and SD conditions, *FLC* mRNA levels were slightly reduced in *hda9-1*, whereas *CO* mRNA levels in wt and *hda9-1* were comparable (Fig. 8a,b). Downregulation of *MAF4* and *MAF5* mRNAs by *hda9-1* was also observed in SD (Fig. 8b). Consistent with the early-flowering phenotype of *hda9-1*, *FT* and, to a much lesser extent, *SOC1* mRNA levels were higher in *hda9-1* than in wt (Fig. 8a,b).

Because the genetic analysis positioned *FT* downstream of *HDA9*, I further examined the effect of *hda9-1* mutation on the spatial expression of *FT* using *FT::GUS* (Takada and Goto, 2003). In LD, GUS staining was detected mainly in the vascular tissues of the distal parts of both wt and *hda9-1* rosette leaves with similar staining intensity (Fig. 8c). In SD, GUS staining was detected in the primary veins and petioles of both wt and *hda9-1* leaves; however, a stronger intensity was observed in *hda9-1* than in wt, which indicates that *HDA9* affects the expression level but not the expression domain of *FT*. Collectively, these results show that *HDA9* is required for the full expression of *FLC*, *MAF4*, and, *MAF5*, and

for the negative regulation of *FT*.

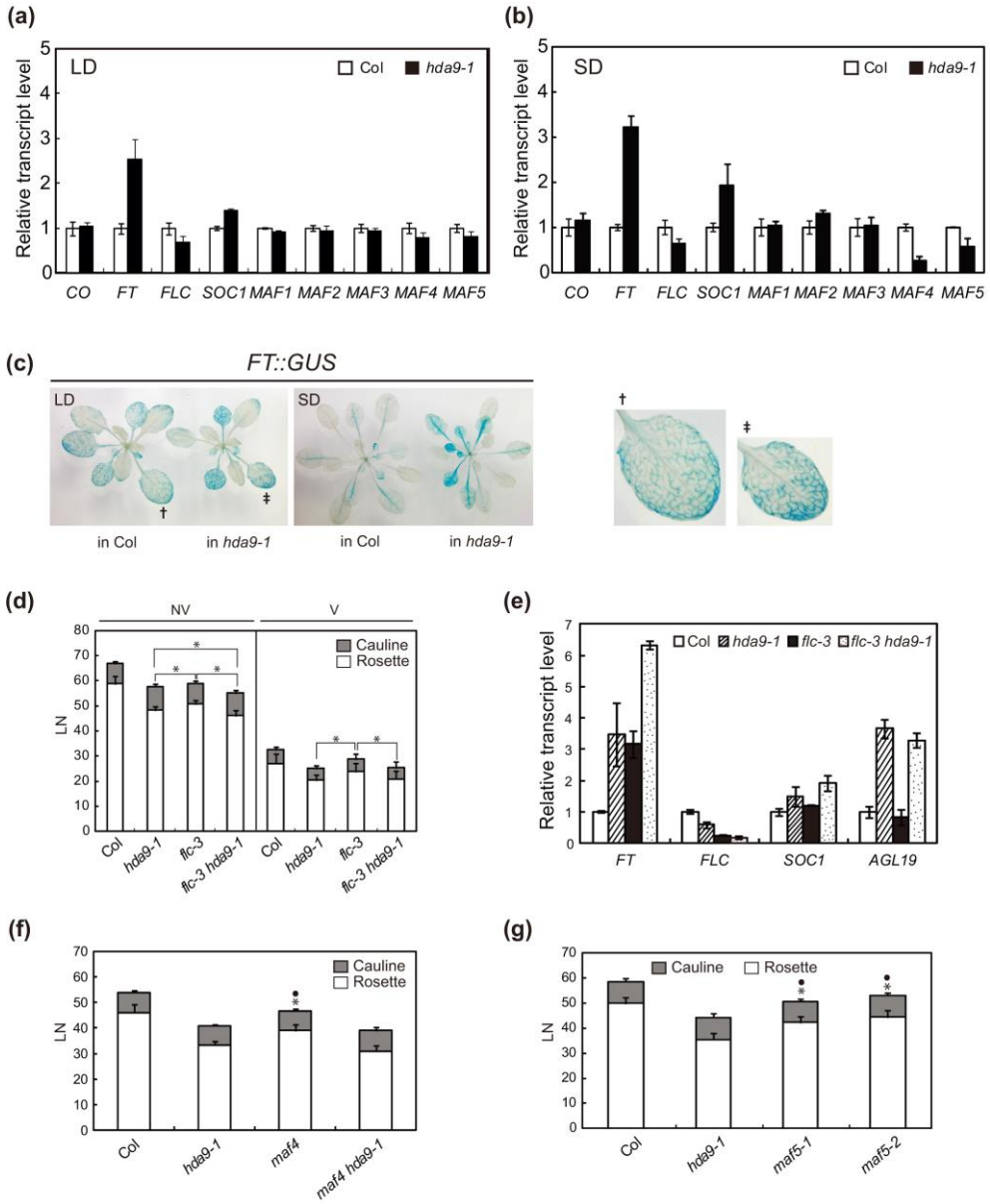

Fig. 8 The *hda9-1* mutation affects *FT* expression.

(a, b) RT-qPCR analyses of the transcript levels of various flowering genes in wt and *hda9-1* seedlings grown for 2 weeks in LD (a) or 4 weeks in SD (b). Wt levels

were set to 1 after normalization by *UBQ10*. Values are the means ± S.E. of three biological replicates. (c) Histochemical GUS staining of wt and *hda9-1* plants harboring *FT::GUS*. Plants were grown for 21 d in LD or for 45 d in SD before staining. All the plants were homozygous for *FT::GUS*. Right panel: 300% digital magnification of the marked leaves on the left to show vascular expression of FT::GUS. (d) Flowering time of *hda9-1*, *flc-3*, and *flc-3 hda9-1* without (NV) or with (V) vernalization as determined by LN. Vernalization was performed as described in the Materials and Methods, and the plants were subsequently grown in SD until bolting. Asterisks indicate statistically significant differences between the two comparisons marked by brackets ($P \leq 0.01$). (e) Additive effect of *flc-3* and *hda9-1* on *FT* expression. Plants were grown for 21 d in SD before being harvested for RNA extraction. Transcript levels of *FT*, *FLC*, *SOC1*, and *AGL19* were determined by RT-qPCR, and wt levels were set to 1 after normalization by *UBQ10*. Values are the means ± S.E. of three biological replicates. (f) Flowering time of *hda9-1*, *maf4*, and *maf4 hda9-1* in SD as determined by LN. Closed circles or asterisks indicate statistically significant differences from Col or *hda9-1*, respectively ($P < 0.001$; f, g). (g) Flowering time of *hda9-1* and *maf5* mutants in SD as determined by LN.

2.4.5 HDA9 controls flowering mostly independently of *FLC, MAF4,* and *MAF5*

FLC directly binds to the *FT* and *SOC1* promoters and represses the transcription of *FT* and *SOC1* (Helliwell *et al*., 2006). It is therefore possible that the upregulation of *FT* and *SOC1* in *hda9-1* might be the result of the reduced *FLC* expression. To test this possibility, I compared the flowering times of *hda9-1*, *flc-3* (an *FLC* null mutant; Michaels and Amasino, 2001), and the *flc-3 hda9-1* double mutants in SD. The flowering time of *hda9-1* was similar to that of *flc-3* (Fig. 8d), although a substantial amount of *FLC* transcript was present in *hda9-1* (Fig. 8b). Moreover, compared to both single mutants, the *flc-3 hda9-1* double mutant flowered slightly earlier and had a higher level of *FT* transcript (Fig. 8d,e). *SOC1* expression in *flc-3 hda9-1* compared to either of the single mutant was not increased as substantially as *FT* (Fig. 8e). These results indicate that the reduced *FLC* expression alone is not sufficient to cause the early flowering of *hda9-1*.

Similar to *FLC*, *MAF4* and *MAF5* have also been implicated in floral repression (Ratcliffe *et al*., 2003; Gu *et al*., 2008). Thus, to examine whether the decreased expression of *MAF4* and *MAF5* contributes to the accelerated flowering of *hda9-1*, T-DNA insertion mutants of *MAF4* and *MAF5* (Fig. 9) were isolated from the SALK collection, and their flowering time was analyzed. Both *maf4* and *maf5* flowered slightly earlier than wt but significantly later than *hda9-1* in SD (Fig. 8f,g). In addition, the *maf4 hda9-1* double mutants flowered slightly earlier than the *maf4* or the *hda9-1* single mutants (Fig. 8f). Moreover, *flc-3 hda9-1*

flowered earlier than *flc-3* even after vernalization (Fig. 8d), which should have decreased the expression of *MAF4* (Ratcliffe *et al*., 2003). Thus, although the decreased expression of *MAF4* and *MAF5* might contribute to the early flowering of *hda9-1*, it does not seem to fully account for the flowering behavior observed in *hda9-1*. In sum, these results suggest that HDA9 controls flowering time mostly independently of *FLC*, *MAF4*, and *MAF5*.

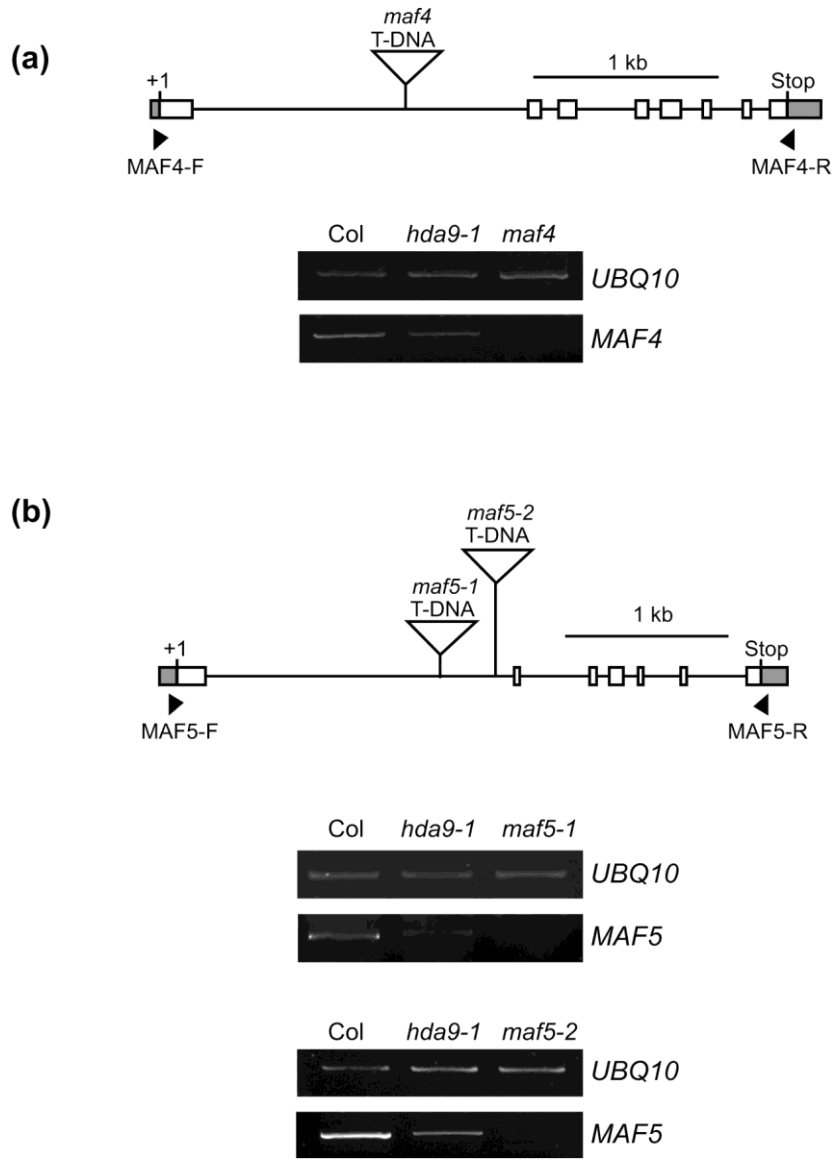

Fig. 9 T-DNA insertion mutants for *MAF4* and *MAF5*.

(a) Schematic gene structure of *MAF4* and its expression in the *maf4* mutants. The position of T-DNA insertion in *maf4* is marked with a triangle. White and gray boxes represent exons and UTRs, respectively, while introns are indicated as solid lines (a,b). *MAF4* mRNA expression in wt, *hda9-1*, and *maf4* was examined by RT-

PCR using MAF4-F and MAF4-R (supplementary material Table S3) as primers. *UBQ10* was used as an expression control (a,b). (b) Schematic gene structure of *MAF5* and its expression in the *maf5-1* and *maf5-2* mutants. The positions of T-DNA insertions in *maf5-1* and *maf5-2* are marked with triangles. *MAF5* mRNA expression in wt, *hda9-1*, *maf5-1*, and *maf5-2* was examined by RT-PCR using MAF5-F and MAF5-R (supplementary material Table S3) as primers.

2.4.6 The expression of *AGL19*, a floral activator, is increased in *hda9-1*

A number of MADS- and AP2-domain transcription factors that affect flowering in an *FLC*-independent manner have been identified (Yu *et al*., 2002; Aukerman and Sakai, 2003; Michales *et al*., 2003; Schmid *et al*., 2003; Schönrock *et al*., 2006; Adamczyk *et al*., 2007; Jung *et al*., 2007; Castillejo *et al*., 2008; Yoo *et al*., 2011). In addition, it was lately shown that SPL transcription factors promote flowering independently of *FLC* (Wang *et al*., 2009a). To study whether HDA9 affects flowering by regulating these factors, I compared their expression levels in wt and *hda9-1*. All the genes examined, with the exception of *AGL19*, were expressed at similar levels in wt and *hda9-1* (Figs. 10a, 11). Interestingly, in both LD and SD, the transcript level of *AGL19* was substantially higher in *hda9-1* than in wt (Figs. 10a, 11). The upregulation of *AGL19* is not thought to be related to the reduced *FLC* expression in *hda9-1* because the expression of *AGL19* was not affected by *flc-3* (Fig. 8e). I found that the transcript level of *AGL19*, similar to *FT*, was greatly elevated in 5-week-old plants compared with 1-week-old seedlings (Fig. 10b,c), consistently with previous report on the age-dependent induction of *AGL19* (Schönrock *et al*., 2006). Interestingly, the effect of the *hda9-1* mutation on the *AGL19* expression was barely detectable in young seedlings, although it became obvious in 5-week-old plants (Fig. 10b).

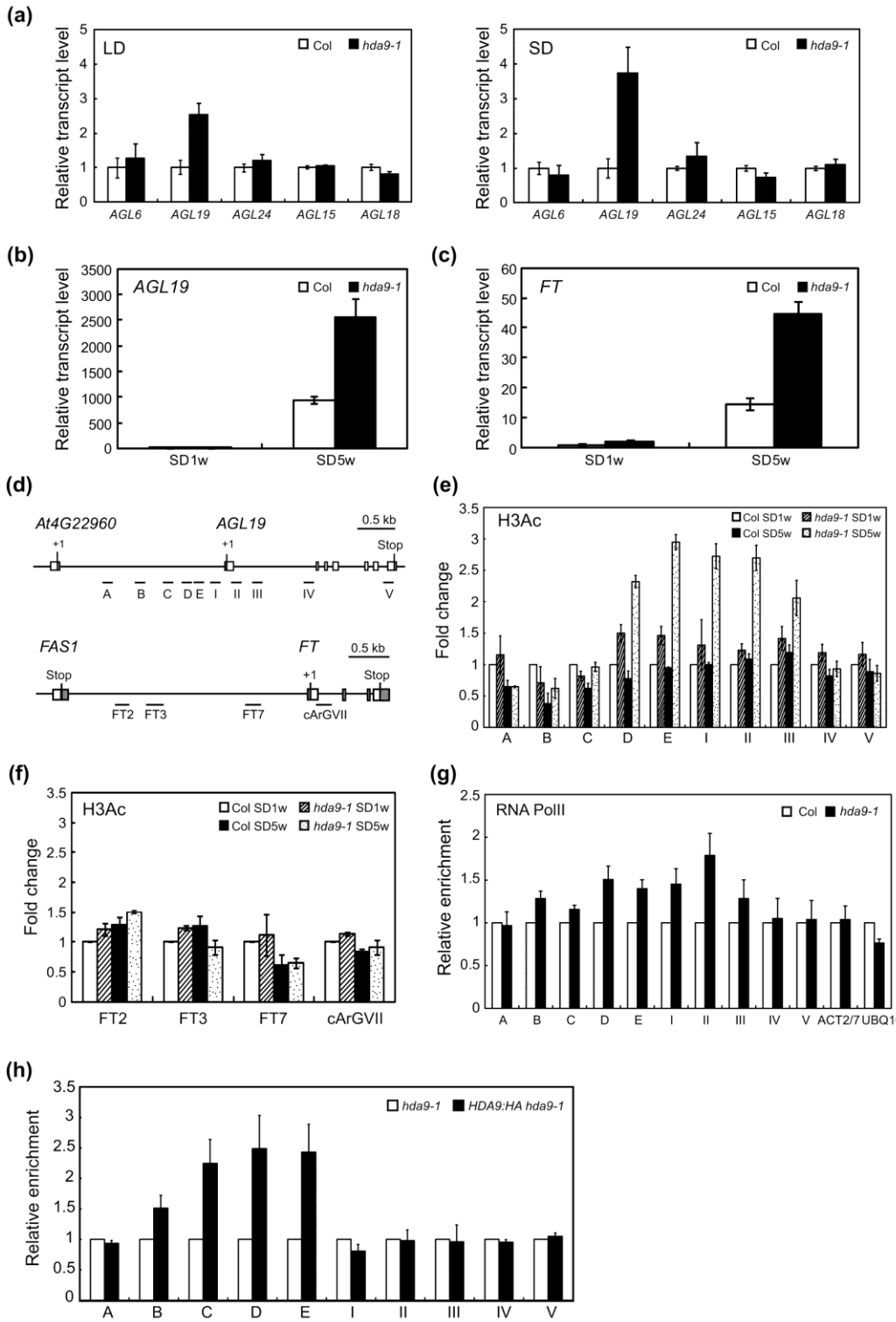

Fig. 10 HDA9 directly controls *AGL19* transcription through histone deacetylation.

(a) RT-qPCR analyses of the transcript levels of several *AGL* genes, which have floral regulatory roles, in wt and *hda9-1* seedlings grown for 2 weeks in LD (left) or for 4 weeks in SD (right). Wt levels were set to 1 after normalization by *UBQ10*, and values are the means ± S.E. of three biological replicates (a-c, h). (b, c) Transcript levels of *AGL19* (b) or *FT* (c) in 1- (SD1w) or 5-week (SD5w)-old wt and *hda9-1* plants grown in SD as determined by RT-qPCR. (d) Schematics of the genomic structures of *AGL19* and *FT*. Gray boxes represent 5′ and 3′ UTRs, and white boxes are exons. Solid lines indicate promoters, introns, or intergenic regions. ′+1′s refer to the transcription start sites. Regions amplified by primers used for ChIP (e-g) are shown for each gene. (e, f) ChIP-qPCR analyses of *AGL19* (e) and *FT* (f) chromatin using an anti-H3Ac antibody. Plants as grown in (b, c) were used for ChIP. Shown are the means ± S.E. of three biological replicates. SD1w wt levels were set to 1 after normalization by input and the internal control *UBQ10*. (g) ChIP-qPCR analyses of *AGL19* chromatin with an anti-PolII antibody. Plants grown for 5 weeks in SD were used for ChIP. Shown are the means ± S.E. of three biological replicates. Wt levels were set to 1 after normalization by input. *Actin 2/7* (*ACT2/7*) and *UBQ10* were used as internal controls. (h) ChIP-qPCR analyses of HDA9:HA enrichment at the *AGL19* locus using an anti-HA antibody. *HDA9:HA hda9-1* and *hda9-1* plants grown for 5 weeks in SD were used for ChIP. The amount of immunoprecipitated chromatin was normalized to the

corresponding input and compared with untagged plants. Shown are the means ± S.E. of three biological replicates.

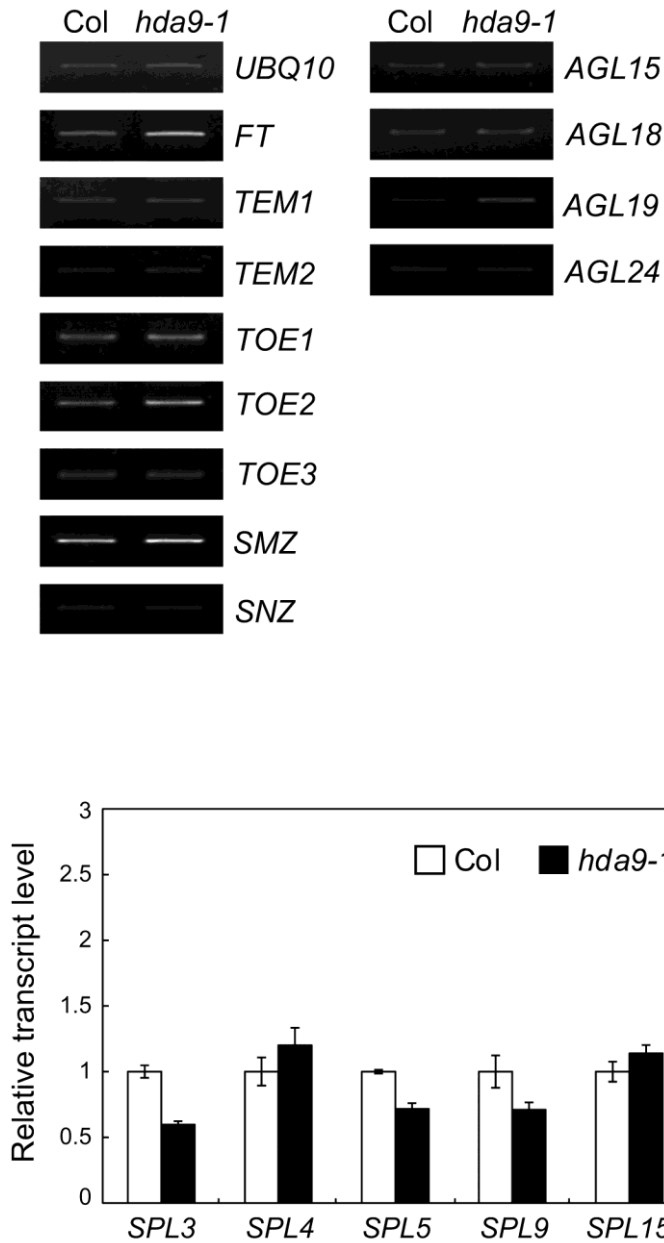

Fig. 11 Expression of genes encoding *FT* regulators and SPL-family transcription factors in *hda9-1*.

Plants were grown for 3 weeks in SD, harvested at zeitgeber 8, and used for RT-

PCR (upper panel) or RT-qPCR (lower panel) analysis. *UBQ10* was used as an expression control in the upper panel. In the lower panel, wt levels were set to 1 after normalization by *UBQ10*, and values are the means±s.e. of three biological replicates. The sequences of primers used to study the expression of each gene are in supplementary material Tables S3, S4.

2.4.7 HDA9 directly represses *AGL19* transcription through histone deacetylation

The increased expression of *AGL19*, *FT*, and *SOC1* by the loss of *HDA9* led us to test whether HDA9 directly represses the transcription of these genes by deacetylating histones within *AGL19* or *FT* chromatin. ChIP studies using anti-acetylated histone H3 (H3Ac) antibody showed that H3Ac levels at the *AGL19* locus were comparable between wt and *hda9-1* in 1-week-old seedlings (Fig. 10d,e). However, H3Ac levels around the transcription start site of *AGL19* (regions D, E, I, II, and III) were clearly increased in 5-week-old *hda9-1* but not in wt plants compared to the levels observed in 1-week-old seedlings (Fig. 10d,e). In contrast to *AGL19*, there was no clear difference in H3Ac levels at *FT* and *SOC1* loci between wt and *hda9-1* at both the seedling and mature stages (Figs. 10d,f, 12a,b). Given the fact that the transcript levels of both *AGL19* and *FT* were developmentally increased and upregulated by the loss of *HDA9* (Fig. 10b,c), these results suggest that the hyperacetylation of histones within *AGL19* chromatin in *hda9-1* is not merely a consequence of the increased *AGL19* transcription. Instead, it might be resulted from decreased HDAC activity caused by the loss of *HDA9*.

To study whether the increased *AGL19* mRNA levels and the hyperacetylation of histones within *AGL19* chromatin in *hda9-1* are related with increased transcriptional activity, I compared RNA Polymerase II (PolII) occupancies at *AGL19* in wt and *hda9-1* through ChIP assays using an anti-PolII antibody. The PolII occupancy at *AGL19* was higher in *hda9-1* than in wt; in

addition, the occupancy pattern was closely correlated with that of H3Ac (Fig. 10g). The PolII occupancy in the regions around the transcription start site (I, II, and III) but not in the elongation or termination regions (IV and V), was clearly higher in *hda9-1* than in wt. These results suggest that the histone hyperacetylation in the promoter and 5′ transcribed regions of *AGL19* might increase the accessibility of these regions to PolII, which in turn accelerates transcription.

Finally, in order to address whether HDA9 plays a direct role in the transcriptional regulation of *AGL19*, I performed ChIP assays using *HDA9:HA hda9-1* plants (Fig. 6). HDA9:HA protein was clearly enriched within *AGL19* (Fig. 10h) but not within *SOC1* chromatin (Fig. 12c), consistent with the effect of the *hda9-1* mutation on H3Ac levels at these loci (Figs. 10e, 12b). HDA9:HA enrichment was most obvious in regions upstream of the transcription start site of *AGL19*. Thus, HDA9 has a direct role in controlling and maintaining the transcription activity of *AGL19* at proper level by resetting the local chromatin environment through dynamic histone deacetylation.

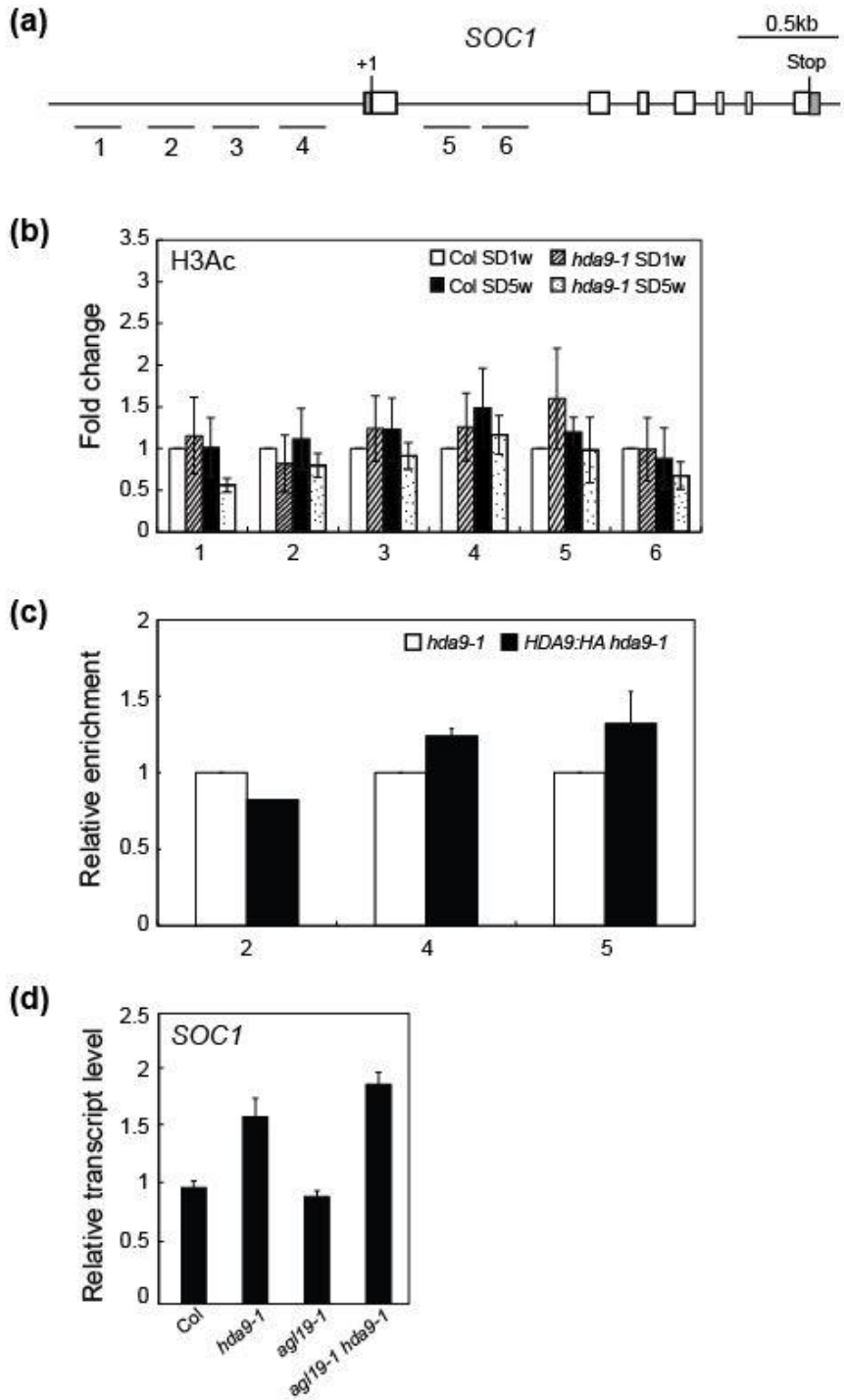
(a)
SOC1
0.5kb
+1
Stop
1
2
3
4
5
6
(b)
H3Ac
Col SD1w
hda9-1 SD1w
Col SD5w
hda9-1 SD5w
Fold change
3.5
3
2.5
2
1.5
1
0.5
0
1
2
3
4
5
6
(c)
hda9-1
HDA9:HA hda9-1
Relative enrichment
2
1.5
1
0.5
0
2
4
5
(d)
SOC1
Relative transcript level
2.5
2
1.5
1
0.5
0
Col
hda9-1
agl19-1
agl19-1 hda9-1

Fig. 12 *SOC1* is not a direct target of HDA9.

(a) Schematic of the genomic structure of *SOC1*. Gray boxes represent 5′ and 3′ UTRs, and white boxes are exons. Solid lines indicate promoters, introns, or intergenic regions. Lines with numbers indicate regions tested for ChIP-qPCR (b,c). (b) ChIP-qPCR analyses of *SOC1* chromatin with an anti-H3Ac antibody. Shown are the means±s.e. of three biological replicates performed in triplicate. Plants used for ChIP were grown as described in Fig. 5b,c. SD1w wt levels were set to 1 after normalization by input and the internal control *UBQ10*. (c) ChIP-qPCR analyses of HDA9:HA enrichment at the *SOC1* locus using an anti-HA antibody. ChIP samples used for Fig. 5H were also used here. Normalization was performed as in Fig. 5H. Shown are the means±s.e. of three biological replicates performed in triplicate. (d) RT-qPCR analyses of *SOC1* transcript levels in wt, *hda9-1*, *agl19-1*, and *agl19-1 hda9*. Plants grown for 5 weeks in SD were used for RNA extraction. Wt level was set to 1 after normalization by *UBQ10*, and values are the means±s.e. of three biological replicates.

2.4.8 HDA9 controls *FT* expression and flowering through *AGL19*

The correlation between the transcript and H3Ac levels of *AGL19* but not of *FT* and *SOC1* (Figs. 8b, 10b-f, 12b), led us to question whether the upregulation of *FT*/*SOC1* and the accelerated floral transition in *hda9-1* are caused by the increased *AGL19* expression. We thus measured the mRNA levels of *FT* and *SOC1* in wt, *hda9-1*, *agl19-1*, and transgenic plants overexpressing *AGL19* (*AGL19OE*; Schönrock *et al*., 2006). *FT* mRNA level was greatly increased when *AGL19* was overexpressed and was not largely affected by *agl19-1* (Schönrock *et al*., 2006; Fig. 13a). However, the mRNA levels of *FLC* and *SOC1* were barely affected by differential *AGL19* expression (Fig. 13a), indicating that the upregulation of *FT* in *AGL19OE* is independent of *FLC*. These results suggest that the repressive effect of *HDA9* on *FT* might be, at least in part, through the inhibition of *AGL19* transcription. Therefore, I analyzed the effect of the *agl19* mutation on the early flowering of *hda9-1* by measuring the flowering time of the *agl19-1 hda9-1* double mutants. *agl19-1 hda9-1* flowered at a similar time as wt but significantly later than the *hda9-1* single mutants (Fig. 13b), clearly demonstrating that *AGL19* is required for the early flowering of *hda9-1*. Furthermore, the increased expression of *FT* in *hda9-1* was strongly suppressed by the *agl19-1* mutation (Fig. 13c). By contrast, the upregulated *SOC1* expression in *hda9-1* was not suppressed by the *agl19-1* mutation (Fig. 12d). Thus, I concluded that HDA9 prevents precocious flowering in SD mostly by inhibiting *AGL19* upregulation, which otherwise would in turn activate *FT*.

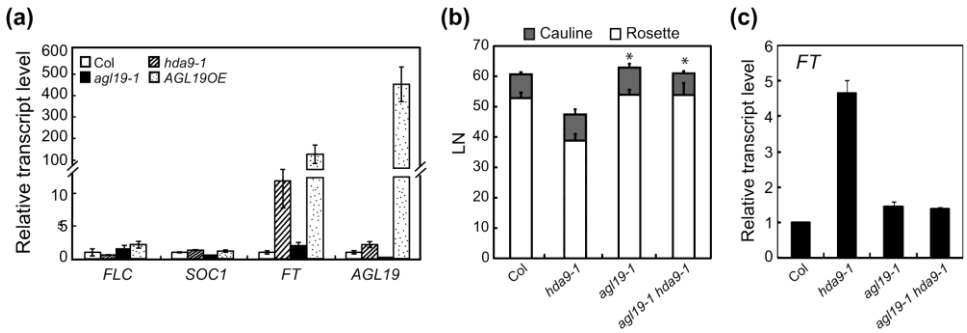

Fig. 13 HDA9 affects *FT* expression and flowering through *AGL19*.

(a) RT-qPCR analyses of the transcript levels of *FLC*, *SOC1*, *FT*, and *AGL19* in *hda9-1*, *agl19-1*, and *AGL19OE* plants. Plants grown for 3 weeks in SD were used for RNA extraction. (b) Flowering time of *hda9-1*, *agl19-1*, and *agl19-1 hda9-1* mutant plants in SD as determined by LN. Asterisks denote statistically significant differences from *hda9-1* ($P < 0.001$). (c) *FT* transcript levels as determined by RT-qPCR in *hda9-1*, *agl19-1*, and *agl19-1 hda9-1* mutant plants grown for 13 weeks in SD. Wt level was set to 1 after normalization by *UBQ10*, and values are the means ± S.E. of three technical replicates.

2.4.9 Loss of *HDA9* increases the levels of *AGL19* mRNA and H3Ac at *AGL19* in vernalized seedlings

Previous work showed that *AGL19* mRNA expression is induced by vernalization (Schönrock *et al*., 2006). Therefore, I examined the effect of the *hda9-1* mutation on the vernalization-induced *AGL19* expression (Fig. 14a). In non-vernalized seedlings, *AGL19* mRNA level was low and similar between wt and *hda9-1*. However, after 4 weeks of vernalization, it was increased in wt and, notably to a greater extent, in *hda9-1*. The hyperinduction of the vernalization-mediated *AGL19* expression by the *hda9-1* mutation might account for the accelerated floral transitions of *hda9-1* and *flc-3 hda9-1* compared to *flc-3* (Fig. 8d). I then studied H3Ac levels at *AGL19* in wt and *hda9-1* seedlings before and after vernalization (Fig. 14b). There was no detectable difference in H3Ac levels at *AGL19* between non-vernalized wt and *hda9-1* seedlings. However, an evident increase in H3Ac levels at *AGL19*, especially in regions around the transcription start site, was detected in *hda9-1* but not in wt after vernalization. Thus, the results in Fig. 14 indicate that HDA9 also prevents the hyper-activation of *AGL19* transcription during vernalization through a dynamic histone deacetylation.

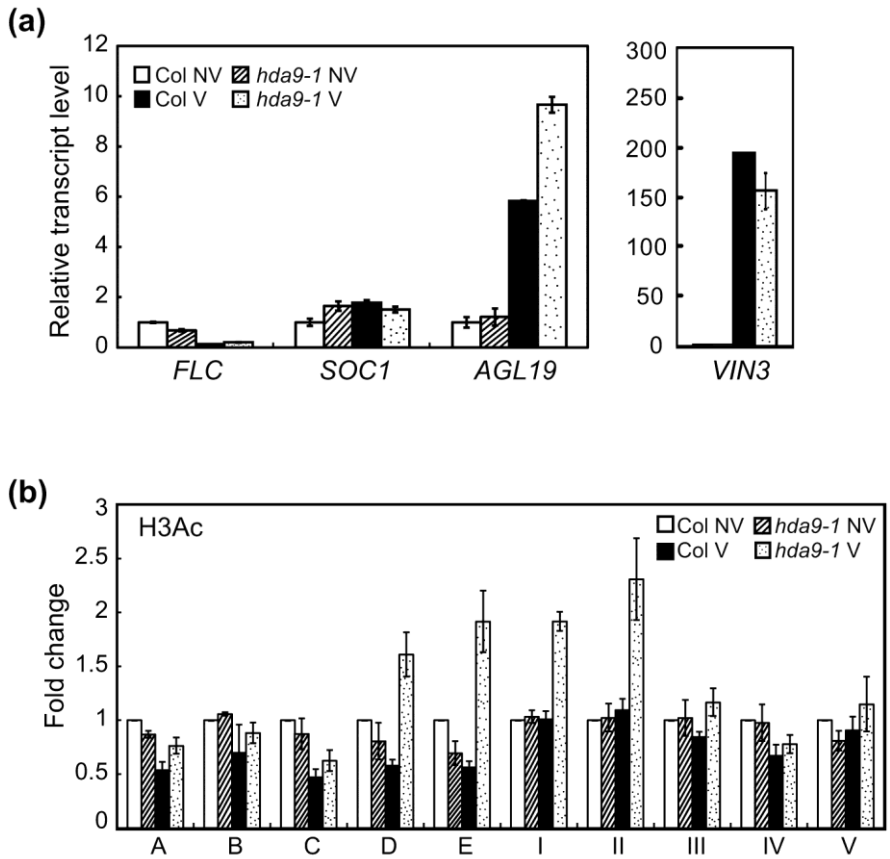

Fig. 14 Hyperacetylation of histones within *AGL19* chromatin by the *hda9-1* mutation in vernalized seedlings.

(a) RT-qPCR analyses of the transcript levels of *FLC*, *SOC1*, *AGL19*, and *VIN3* in wt and *hda9-1* seedlings vernalized for 30 d (V) or not vernalized (NV). NV wt levels were set to 1 after normalization by *UBQ10*. Values are the means ± S.E. of three biological replicates. (b) ChIP-qPCR analyses of *AGL19* chromatin using an anti-H3Ac antibody. Plants were grown as described in (a). NV wt levels were set to 1 after normalization by input and the internal control *UBQ10*. Shown are the

means ± S.E. of three biological replicates.

2.4.10 *AGL19* is differentially expressed in different photoperiods

We then questioned whether the regulation of *AGL19* by HDA9 is relevant to the photoperiod-dependent early-flowering phenotype of *hda9-1*. Interestingly, *AGL19* mRNA levels were ~10-fold higher in 5-week-old SD-grown plants than in 4-week-old LD-grown plants regardless of the *HDA9* genotype (Fig. 15a). This difference in *AGL19* expression is unlikely to be due to the age difference between the LD- and SD- grown plants because the 4-week-old LD-grown plants were rather developmentally more progressed than the 5-week-old SD-grown plants (Fig. 15a). Thus, *AGL19* might be expressed only in SD-grown *hda9-1* plants to the level required for the activation of *FT* and precocious flowering, and this might be the cause for the SD-specific early flowering of *hda9-1*.

Notably, *AGL19* expression was not as much affected by the loss of *CO* or *GI* under LD condition as by SD (Fig. 15b). The *AGL19* mRNA level in 3-week-old LD-grown *gi-2* or *co-101* mutants was moderately higher than that in 3-week-old LD-grown wt but substantially lower than that in 4-week-old SD-grown wt. Thus, unlike *FT* (Fig. 15b), the photoperiodic regulation of *AGL19* is largely independent of the GI-CO pathway. This result is in agreement with my observations that the suppressive effect of the *hda9-1* mutation on the late flowering of *co-101* or *gi-2* in LD (Fig. 7g) was weaker than its effect in SD (Fig.

7h). Taken together, these results suggest that the repressive role of HDA9 in *AGL19* expression together with the photoperiod-dependent expression of *AGL19* might underlie the SD-specific early flowering of the *hda9-1* mutants.

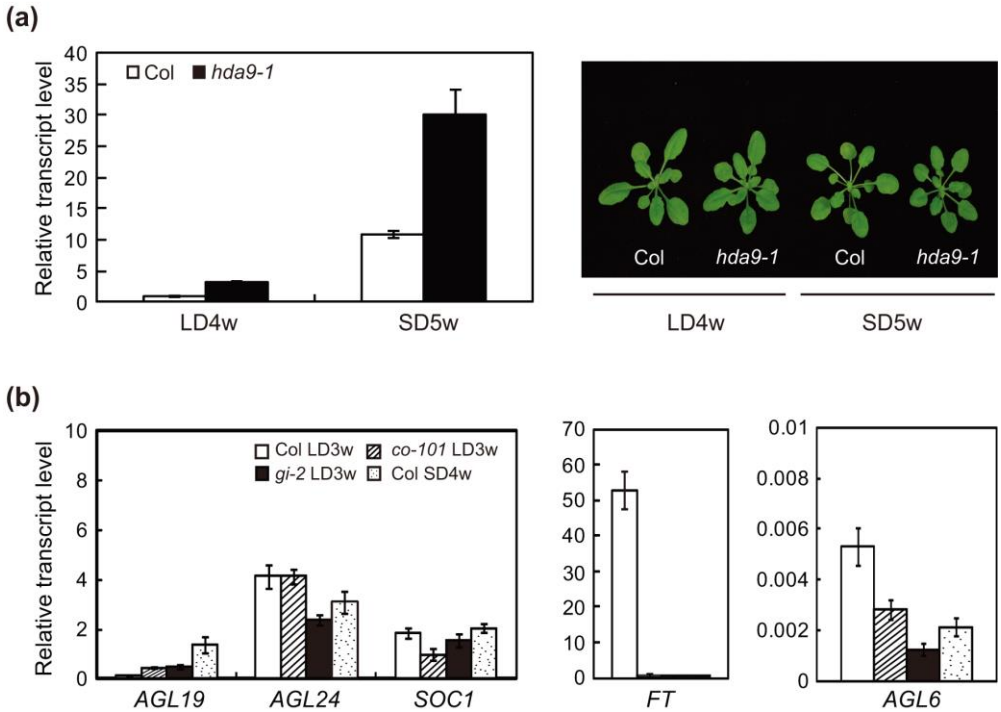

Fig. 15 Photoperiod-dependent expression of *AGL19*.

(a) RT-qPCR analyses of *AGL19* transcript levels in wt and *hda9-1* plants grown for 4 weeks in LD (LD4w) or for 5 weeks in SD (SD5w). The picture on the right shows representative wt and *hda9-1* plants. LD4w wt level was set to 1 after normalization by *UBQ10*. The values are the means ± S.E. of three biological replicates. (b) RT-qPCR analyses of the transcript levels of *AGL19*, *AGL24*, *SOC1*, *FT*, and *AGL6* in wt, *co-101*, and *gi-2* plants grown for 3 weeks in LD (LD3w) or for 4 weeks in SD (SD4w). Transcript levels of each gene were normalized by *UBQ10*, and values are the means ± S.E. of three biological replicates.

2.5 Discussion

Arabidopsis has a higher number of HDACs than other multicellular eukaryotes; however, to date, the biological roles of individual Arabidopsis HDACs, with the exception of HDA6 and HDA19, are mostly unknown. In this study, I show that HDA9, an Arabidopsis RPD3/HDA1 family Class I HDAC, plays distinct roles in plant development. The loss of *HDA9* causes several morphological alterations in a limited number of organs (Fig. 2), none of which are observed in the *hda6* or *hda19* mutants. These observations suggest that the *in planta* function of HDA9 might be localized and not global and that this function does not overlap with the functions of HDA6 or HDA19. It would be interesting to know how HDA9 and its phylogenetically close members, HDA6 and HDA19, perform distinct biological roles despite their conserved HDAC activity. The specificity of these HDACs might lie in their participation in different multi-protein complexes. Studies on animal and yeast HDACs have shown that most Class I HDACs perform their functions within a variety of multi-protein complexes, each of which has different target range (Cunliffe, 2008; reviewed in Yang and Seto, 2008). Although, to my knowledge, no HDAC complex has yet been biochemically purified from Arabidopsis, Arabidopsis HDACs are also likely to interact with different proteins or complexes, which might lead to different biological effects. Therefore, biochemical purification of HDA9-containing complexes will provide a better understanding of the action mechanisms of HDA9 and insights into its target

specificity.

My study using *hda9-1* revealed that HDA9 is involved in the control of flowering time, especially under non-inductive SD conditions. Floral repression in SD is as important as floral promotion in LD for the reproductive success of a facultative LD plant, such as Arabidopsis. Precocious flowering of a number of loss-of-function mutants in SD suggests that the repressive mechanisms to attenuate floral competence as well as the lack of floral promoter activity of the CO-FT pathway contribute to the repression of flowering in Arabidopsis under SD conditions. Our data indicate that HDA9 contributes to this floral repression mainly by negatively regulating the expression *AGL19*, an *FT* activator (Figs. 10, 13). *AGL19* appears to be responsible for the SD-specific early flowering of *hda9-1* as well. *AGL19* expression is higher in SD than LD (Fig. 15a), and its low level of expression in *hda9-1* under LD conditions may not be sufficient to effectively activate *FT* (Fig. 15b). Thus, in addition to strong CO activity, the low level of *AGL19* expression might be responsible for the normal flowering behavior of the *hda9-1* mutants in LD. The role of *AGL19* in promoting floral transition in wt is likely redundant or its expression level in wt is not sufficient for effective *FT* activation because its loss-of-function mutants displayed a normal flowering behavior without reduced *FT* expression (Fig. 13b,c). In either case, ensuring the proper expression of *AGL19* during the developmental time course is crucial for the prevention of precocious flowering in non-inductive SD. In sum, the control of *AGL19* expression by HDA9 adds a new layer to the mechanisms that prevent precocious flowering in SD.

Conventionally, the role of HDACs has been thought to be associated with inactive genes. However, the *hda9-1* mutation-induced increase of H3Ac levels at *AGL19* was clearly observed only at times when *AGL19* was actively expressed, such as in the adult stages or after vernalization (Figs. 10e, 14b). Thus, the role of HDA9 at *AGL19* is distinct from the conventional corepressor role of HDACs. Interestingly, a recent genome-wide mapping of HDACs in human CD4+ cells showed that HDACs associate more with transcriptionally active genes than with inactive genes (Wang *et al*., 2009b), which suggests a novel role of HDACs during transcription. Increased H3Ac levels at *AGL19* in *hda9-1* but not in wt during development in SD (Fig. 10e) implies that acetyl groups may be dynamically added to the histone tails and reversibly removed by HDA9 during the transcription of *AGL19*. This HDA9 function might be important in the prevention of hyperactive transcription by resetting the chromatin state. This postulate is supported by the *hda9-1* mutation-induced increased PolII occupancy, which is correlated with increased H3Ac levels in regions surrounding the *AGL19* transcription start site (Fig. 10g). Histone hyper-acetylation in these regions might cause hyperactive transcription at premature developmental stages. It will be of interest in the future to determine whether HDA9 has a similar role in the control of other genes during their transcription.

Chapter III.

HDA 9 plays a negative role in light-induced seed germination

3.1 Abstract

Timing of seed germination is controlled by various environmental factors in order to initiate a successful new life cycle under favorable environment. Light is the most critical environmental factor to promote seed germination. Light-induced germination process involves the perception of light mainly by phytochrome B (phyB) and then degradation of the germination repressor PHYTOCHROME INTERACTING FACTOR (PIF1) resulted from its interaction with phyB. In this study, I found the RPD3/HDA1-class histone deacetylase HDA9 is involved in a new layer of regulation for phyB-dependent germination process.

Loss-of-HDA9 activity caused rapid germination after a red-light pulse treatment as well as under continuous white light and had the increased expression of *HECs*, previously known repressors of PIF1 transcription activity. Epistatic analysis between the *hda9* mutant and *hec1hec2 RNAi* showed that rapid seed germination of the *hda9* mutant was caused by the increased *HECs* expression. Histone H3 acetylation level and RNA polymerase II occupancy at *HECs* were more elevated in *hda9-1* than in wt after red light pulse but not after far-red light pulse. The direct association of HDA9 with *HECs* chromatin was also observed after red light pulse but not after far-red light pulse. Furthermore, I found that mRNA levels of *GA-INSENSITIVE (GAI)* and *REPRESSOR OF GA1-3 (RGA/RGA1)* regulated positively by *PIF1* were decreased by the *hda9* mutation.

Taken together, my results indicate that HDA9 plays a role in the prevention of the hyper light-sensitive germination by inhibiting the hyper-

activation of HECs transcription by light through deacetylating HEC chromatin during active transcription. Thus, HDA9 acts as a fine-tuning mechanism of phyB-dependent germination ensuring the beginning of germination under proper light condition.

3.2 Introduction

Seed germination is a critical process to initiate a new life cycle of seed plants. Optimal timing of seed germination under favorable environmental condition is profoundly important since once seeds germinates, they have no other choice but to grow and reproduce in that environment. Indeed, seed germination is controlled by multiple environmental factors including light, oxygen, water, nutrient, and temperature as well as endogenous factors. In most seed plant species, light is one of the critical factors which affects seed germination. Among the various wavelengths of light, red and far-red wavelengths control the seed germination through phytochrome signaling (Shinomura et al., 1994; Oh et al., 2007). Among the identified phytochromes, phyB is known as a major phytochrome that is involved in the low influence response (LFR) and recognizes red light (R) to promote seed germination (Shinomura et al., 1994; Oh et al., 2007). Although the role of phyB in light-induced seed germination has long been known in plant biology, until recently the details of phyB downstream regulatory networks in seed germination have been mostly unknown. Recent studies showed that in seeds exposed to red light, phyB, converted to its active form, translocated into the nucleus. In nucleus, phyB interacts with PIF1 (Shen et al., 2005, 2008), also known as PIL5 (Oh et al., 2004). PIF1 is one of various basic helix-loop-helix (bHLH) transcription factor and is known to play a negative role in seed germination (Oh et al., 2004; Bae and Choi, 2008). Interaction of PIF1 with phyB (Pfr) causes PIF1 phosphorylation and rapid degradation through the ubiquitin/26S proteasome pathway (Oh et al., 2006). This event results in the decrease of the amount of PIF1

protein which is highly accumulated in seeds kept in dark and the diminution of PIF1-mediated repression of germination.

Recently, in addition to light-dependent degradation of PIF1, fine-tuning mechanisms of PIF1 activity by PIF1- interacting proteins have been reported. According to Zhu PhD thesis (2012), the closely related bHLH proteins HECATE 1 (HEC1) and HEC2 that are previously well known regulators of transmitting tract and stigma development (Gremski et al., 2007) also positively regulate germination and several aspects of photomorphogenesis. Zhu PhD thesis, (2012) demonstrated that HEC1 and HEC2 protein directly interacts with PIF1 and it reduces the DNA binding ability of PIF1, placing HECs as new positively acting components in phyB signaling (Zhu PhD thesis, 2012). Another HLH transcription factor, LONG HYPOCOTYL IN FAR-RED (HFR1) is also reported to heterodimerize with PIF1 and prevents the binding of PIF1 to its target genes related to germination (Shi et al., 2013).

Like other developmental transition in plants, transition to seed germination involves rapid changes in gene expression. Lately it has been reported that posttranslational modifications of histones functions in the transcriptional regulation of genes for appropriate light-induced germination. Histone arginine demethylase activity catalyzed by Jumonji C (JMJ) 20 and JMJ22 is required for the phyB-dependent seed germination while histone lysine methyltranseferase, EARLY FLOWERING IN SHORT DAYS (EFS) negatively regulates seed germination in the dark. Other histone mehyltransferases involved in repressive

chromatin states are also identified in seed germination. PHD-domain protein interacts with the Polycomb repressive complex 1 (PRC1), and this PHD-PRC1 complex promotes seed germination via changing the chromatin state (Cho et al., 2012; Lee et al., 2014; Molitor et al., 2014). Among diverse histone modifications, histone acetylation has been linked to the active transcription. Histone acetylases (HDACs) remove acetyl groups from histones which form the transcriptionally incompetent chromatin landscape. It was reported that two Arabidopsis HD2 family histone deacetylases HD2a and HD2C represses and enhance germination, respectively (Colville et al., 2011). The components of HDAC complex SIN3-LIKE1 (SNL1) and SNL2, together with HDAC19 modulate the transcription of genes involved in the ethylene and abscisic acid (ABA) pathways, consequently affecting seed dormancy and ABA sensitivity of germination (Wang et al., 2013). HISTONE DEACETYLATION COMPLEX1 (HDC1) was identified as a putative component of HDAC complexs and demonstrated to interact with the RPD3/HDA1 class I histone deacetylases HDA6 and HDA19. Studies using HDC1 overexpression and mutant lines showed that HDC1 plays a role in determining the ABA sensitivity of seed germination (Perrella et al., 2013). In addition, pharmacological prevention of histone deacetylases (Class I and Class II HDACs) with trichostatin (TSA) treatment delayed germination (Tanaka et al., 2008). Furthermore, recent study using the loss of function mutants of RPD3/HDA1 family class I HDA9 suggested that these HDA9 plays a role in seed dormancy and germination. Unlike the mutation in either HDA6 or HDA19 that affects germination only in the presence of ABA, the *hda9* mutation causes faster

germination in the absence of ABA (van Zanten et al., 2014). Although the accumulated evidences support the role of HDACs in the regulation of germination, the underlying molecular mechanisms by which each HDAC regulates seed germination remains to be elucidated.

Here, I report that HDA9, a member of RPD3/HDA1 family Class I HDACs plays a repressive role in the regulation of light-induced germination. I demonstrated HDA9 prevents phyB-dependent germination by directly targeting to *HECs* (*HEC1, HEC2, and HEC3*) and repressing their expression through histone deacetylation during active transcription induced by light. I further show that derepression of HECs by the hda9 mutation through blocking the transcriptional activity of PIF1 changes the expression of germination related PIF1 target genes. Thus HDA9 controls the light sensitivity of phyB-dependent germination and subsequently its speed through preventing the hyperactivation of HECs transcription by light which attenuates the blocking of PIF1 transcription activity by HECs.

3.3 Material and methods

3.3.1 Plant materials and growth conditions

The *hda9-1* mutant, *HDA9:HA hda9-1* line and *hfr1-201 (rep1)* mutant allele were previously described as written in Kang et al., 2014 and Soh et al., 2000. *hec1/3/hec2 RNAI* +/- and *HEC1p:HEC1:GUS* transgenic lines were provided by Martin F. Yanofsky. *35s:HEC2 GFP*, *35s:TAP:PIF1 pif1-2*, and *pPIF1:TAP:PIF1* lines were provided by Enamul Huq. *pif1-2* (SALK_072677), T-DNA insertion mutant was obtained from the SALK collection (http://signal.salk.edu/) and genotyped by using gene-specific primers (Table 1).

Seeds were sterilized with 75% EtOH containing 0.08% TritonX-100, washed with 95% EtOH, and plated on 1/2 Murashige-Skoog (MS) growth media containing 0.8% phyto-agar without sucrose (1/2MS-Suc).

For the germination assay, gene expression and ChIP experiments seeds were harvested from plants grown side by side in the same tray and shelf. Plants were grown at 22 ℃ under 100 umol/m^2s in long day condition (16 hr light/ 8 hr dark). Seeds were dried for at least 2 weeks at room temperature.

3.3.2 Light treatment and seed germination assay

For phyB-dependent germination assay, seeds were imbibed for 1hr at 22 ℃ in the dark to induce germination. Imbibed seeds were exposed to 1.8 μmol /m^2s of Fp for 5 min to inactivate phyB. Seeds were further exposed to 40 μmol /m^2s of Rp for 5 min to activate phyB. Then, seeds were kept in the dark at 22 ℃ for 4 additional

days.

For low light intensity germination assay, seeds were irradiated with 10 μmol /m^2s of Rp for 5 min instead of Rp 40 μmol /m^2s following the same procedure as phyB-dependent germination assay.

Germinated seeds were scored by counting the emergence of the radicles at the indicated time. At least 80-100 seeds of each genotype were used for the germination assay. Experiments were performed as triplicates for statistical analyses.

3.3.3 Histochemical β-glucuronidase (GUS) assay

For GUS assay, dry seeds were imbibed for 1hr in the dark, treated with Fp for 5 min or Rp for 5 min and further incubated for 12 in the dark hr at 22 ℃. Seeds were fixed by acetone on ice for 30 min in the dark and washed three times with KPO_4 buffer. The fixed seeds were dissected using forceps, and the extracted embryos were stained with X-Gluc solution for 2hr 30 min (HDA9:GUS) or overnight (HEC:GUS) at 37˚C. The stained embryos were photographed using AxioVison under optical microscope (Carl Zeiss, Germany). To observe HEC1:GUS expression in the wt and *hda9-1* background, HEC1:GUS was introgressed into *hda9-1* by crossing, and the *hda9-1* mutants carrying HEC1:GUS (+/+) were selected. HEC1:GUS expression between wt and *hda9-1* were then compared.

3.3.4 RNA extraction and RT-qPCR analysis

Total RNA was extracted from light treated seeds as previously described (Ling Meng and Lewis Feldman, 2010) with minor modifications. The RNA pellet was treated with RNase-Free DNase I set (Qiagen) to remove genomic DNA. Then, RNA was purified by using Qiagen RNeasy Plant mini kit (Qiagen). 3 ug of total RNA was reverse transcribed using MMLV Reverse Transcriptase (Fermentas, USA). The RT-qPCR analysis was performed with Rotor-Gene Q (Qiagen) using the SYBR Green Fast qPCR master mix (Kappa Biosystems). Absolute quantification was performed by generating standard curves using serial dilutions of mixture of all cDNA samples to be analyzed. *UBQ11* was used as a normalized control of the expression data. All RT-qPCR results were performed as means±SE of duplicate technical repeats and biological triplicates. Primers used for RT-qPCR analysis are listed in Table 2.

3.3.5 Protein extraction and western blot

Total 50 mg of light treated seed was ground in liquid nitrogen and resuspended in extraction buffer (4% SDS, 200mM dithiothreitol (DTT), 20% glycerol, 100mM Tris-HCl (pH 6.8)). The mixture was boiled for 10 min and then centrifuged at 13,000 rpm for 5 min at room temperature. The supernatant was resuspended in an equal volume of 2x SDS sample buffer (4% SDS, 200mM dithiothreitol (DTT), 20% glycerol, 100mM Tris-HCl (pH 6.8) and 0.02% bromophenol blue).

Nuclear protein was extracted by using Honda buffer as previously described (Xia et al., 1997 and Kinkema et al., 2000). Seeds were homogenized in liquid nitrogen and resuspended in Honda buffer (2.5% Ficoll 400, 5% dextran T40,

0.4M sucrose, 25mM Tris-HCl (pH 7.4), 10mM $MgCl_2$, 10 mM b-mercaptoethanol, and a proteinase inhibitor cocktail) and then filtered through miracloth (Milipore, 485855-1R). Triton X-100 was added to a final concentration of 0.5%, and the mixture was incubated on ice for 15 min. Then, the solution was centrifuged at 1500 g for 5 min and the pellet was washed with Honda buffer containing 0.1% Triton X-100. The pellet was resuspended gently in 1 mL of Honda buffer using a brush, and the resuspended fraction was transferred to a new tube. This nuclear-enriched preparation was centrifuged at 1000 rpm (or 100*g*) for 1 min to pellet starch and cell debris. The supernatant was centrifuged subsequently at 4000 rpm for 5 min at 4˚c to pellet the nuclei. Next, the nuclear enriched mixture was boiled for 10 min and then centrifuged at 13,000 rpm for 5 min at room temperature. The supernatant was resuspended in an equal volume of 2x SDS sample buffer.

Protein extracts were equally loaded on 8% or 15% polyacrylamide gel. Total or nuclear protein samples were subjected to sodium dodecyl sulfate-polyacrylamide gel (SDS-PAGE) and transferred to nitrocellulose membrane (Millipore). After blocking the membrane with blocking solution containing 10% non-fat milk in 1x TBS-T, the membrane was incubated with primary antibody (α – HA, Abcam ab9110; α –GUS, Life technologies A5790; α -H3, Abcam ab1791 at 1:4000, 1:1000, 1:10000, 1:5000 respectively) overnight. Following, the membrane was washed three times for 15 min with 1x TBS-T at room temperature. Then the membrane was incubated with horseradish peroxidase (HRP)- linked secondary antibody (α-Rabbit, Vector, PI-1000) in 10% non-fat milk in 1x TBS-T. Next, the membrane was washed three times for 15 min with 1x TBS-T and detected using

Lumi Femto ECL kit (Dogen). For protein visualization, proteins were stained with coomassie blue (0.1% coomassie brilliant blue R-250, 50% methanol and 10% glacial acetic acid) and ponceau S (0.1% (w/v) Ponceau S in 5% (v/v) acetic acid).

3.3.6 Chromatin immunoprecipitation (ChIP) assay

Light treated seeds (roughly 300ul dry seed) were cross-linked in 1% formaldehyde solution for 30 min with vacuum and quenched for 10 min by adding 0.2M glycine. Cross-linked seeds were washed three times with distilled water. Samples were quickly frozen in liquid nitrogen. The nuclei was isolated by using lysis buffer (50mM HEPES, 150mM NaCl, 1mM EDTA, 1% Triton X-100, 0.1% Sodium deoxycholate, 1mM PMSF, and protease inhibitor and 0.1% SDS) and the chromatin was sheared using ultra sonicator (Fisher scientific). Chromatin was pre-cleared to remove cell debris with salmon sperm DNA/Protein-A beads (50% slurry; Upstate 16-157). After overnight immunoprecipitation with the corresponding antibody, the antibody-protein/DNA complexes were isolated using salmon sperm DNA/Protein-A beads. After washing the chromatin mixture for five times with wash buffers (low salt, high salt, LiCl and TE x2) at 4 ℃, the immune-complex was eluted from beads using elution buffer (1% SDS and 0.1 M $NaHCO_3$). Finally the ChIPed DNA was purified using a PCR purification kit (Qiagen) after reverse crosslinking and treatment of proteinase K. Antibodies for ChIP assay were α-H3Ac (Millipore, 06-599), α -RNA PolII (Covance, MMS-126R), and α -HA (Abcam, ab9110). α-H3Ac recognizes acetylated lysine 9 and 14 of Histone 3. α -RNA PolII recognizes both initiating and elongating forms of PolII. The amount of

immunoprecipitated DNA was determined by qPCR using primer sets listed in Table 3. The relative amounts of ChIPed DNA were evaluated using the $2^{-\Delta\Delta ct}$ method (Livak and Schmittgen, 2001).

Table 3-1. Oligonucleotides used for genotyping.

Gene	Name	Sequence
SALK LB1.3		5'-ATTTTGCCGATTTCGGAAC-3'
HEC1	ghec1 oKG156	5'- ACCACAACAACACTTACCCTTTTC -3'
	ghec1oKG157	5'- GTTCC A CACCCTTTCATAACCACT -3'
	ghec1 GABI-KAT	5'- CCCATTTGGACGTGAATGTAGACAC -3'
HEC3	ghec3 C-X1	5'- GTGCTATTTCGTGAAGAGACAAGAGA -3'
	ghec3 C-X4	5'- TCCTAACAAACCCTTAT TTC GTATCCA -3'
	ghec3JMLB2	5'- TTGGGTGATGGTTCACGTAGTGGG -3'
PIL5	gPIL5 F	5'- ATGATTATGTCAACAACCATAATTCTTC -3'
	gPIL5 R	5'- CTTTCATTCTCTCATTGATCCTATCTC -3'
HFR1	gHFR1 F	5'- GCTACAAAGTTAACATTC -3'
	gHFR1 R	5'- CTCTTTAACTAACATGTAAGTA -3'
phyB	gphyB F	5’-GTGGAAGAAGCTCGACCAGGCTTG-3’
	gphyB R	5’-GCAAAACTCTTGCGTCTGTG-3’
	dCAPS	5’-GTGGAAGAAGCTCGACCAGGCTTTG-3’

Table 3-2. Oligonucleotides used for RT and RT-qPCR analyses.

Gene	Name	Sequence
UBQ10	UBQ-F	5’-GATCTTTGCCGGAAAACAATTGGAGGATGGT-3’
	UBQ-R	5’-CGACTTGTCATTAGAAAGAAAGAGATAACAGG-3’
UBQ11	qUBQ11-F	5’-GATCTTCGCCGGAAAGCAACTT-3’
	qUBQ11-R	5’-CCACGGAGACGGAGGACC-3’
PP2A	qPP2A-F	5’-TATCGGATGACGATTCTTCGTGCAG-3’
	qPP2A-R	5’-GCTTGGTCGACTATCGGAATGAGAG-3’
HFR1	qHFR1-F	5'-TACCACCGTTTACTAATATTTCATTCC-3'
	qHFR1-R	5'-AAAAATCCAAGAAACTTGGGAAATAAG-3'
HEC1	qHEC1-F	5'-ATTTCACTTGTAAGCTTTTCACCAG-3'
	qHEC1-R	5'-AGAGAAAAGGGTAAGTGTTGTTGTG-3'
HEC2	qHEC2-F	5'-CTTGGAAATGCACAGATTCTTAGAT-3'
	qHEC2-R	5'-TAATTAACCATCCCAAACATTATCG-3'
HEC3	qHEC3-F	5’-CTTCTCATTTCCCTCCTCTCTCTTCTTC-3’
	qHEC3-R	5’-CTTCTCATTTCCCTCCTCTCTCTTCTTC-3’
SPT	SPT-F	5’-AAGAAGCAGAGAGTGATGGG-3’
	SPT-R	5’-ACTACAGCTTCTCCTCCTTC-3’
PIF1	PIF1-F	5’-GATGTGGAATGATGCCAATGATG-3’
	PIF1-R	5’-GGAGACCGCGGAACTGCTGATATG-3’
PIF1	qPIF1-F	5’-ATGATTTCTGCTCAGATCTTCTCTTCT-3’
	qPIF1-R	5’-AGATTCACCACCTCTACCGTTATTAAA-3’
SOM	qSOM-F	5'-GCTCTTTCGCCTTCCACTCC-3'
	qSOM-R	5'-TCCTAGATCAGGGTCACCAC-3'
GA3OX1	qGA3ox1-F	5'-TCCCGGATTCTTACAAGTGGAC-3'
	qGA3ox1-R	5'-GCCGGAGGAGAAGGAGCA-3'

GA3OX2	qGA3ox2-F	5'-GACCCTCATGACAATTCTGTACC-3'
	qGA3ox2-R	5'-GTTAAAATGTGGAGCAAGTCACC-3'
GA2OX2	qGA2ox2-F	5’-AATAACACGGCGGGTCTTCAAATCT-3’
	qGA2ox2-R	5’-TCCTCGATCTCCTTGTATCGGCTAA-3’
GAI	qGAI-F	5'-GAAGACTATGATGATGAATGAAGAAGAC-3'
	qGAT-R	5'-TATAGTGAACAGTCTCAGTAGCGAGTT-3'
RGA	qRGA-F	5'-TACATCGACTTCGACGGGTA-3'
	qRGA-R	5'-GTTGTCGTCACCGTCGTTC-3'
ABA1	qABA1-F	5’- GATGCAGCCAAATATGGGTCAAGG-3’
	qABA1-R	5’- GCCATTGCATGGATAATAGCGACTC-3’
CYP707A2	qCYP707A2-F	5’-TGGTGGTTGCACTGGAAAGAGC-3’
	qCYP707A2-R	5’-TTGGCGAGTGGCGAAGAAGG-3’
NCED6	qNCED6-F	5’-ACCGGGTCGGATATAAATTGGGTTG-3’
	qNCED6-R	5’-CCCGGGTTGGTTCTCCTGATTC-3’
NCED9	qNCED9-F	5’-GCGGGCTATTTGGGTTAGTC-3’
	qNCED9-R	5’-CGGTAAATCGTCTTCGGACA-3’

Table 3-3. Oligonucleotides used for ChIP assays.

Locus	Name	Sequence
UBQ11	UBQ11-ChIP-F	5'-GGCCTTGTATAATCCCTGATGAATAAG -3'
	UBQ11-ChIP-R	5'-AAAGAGATAACAGGAACGGAAACATAGT-3'
PP2A	PP2A-ChIP-F	5'-GCCTTAAGCTCCGTTTCCTACTT-3'
	PP2A-ChIP-R	5'-CGGCTTTCATGATTCCCTCT-3'
HEC1	HEC1 A-F	5'-ACAAAACCAGTTGATAATCTTTTACTCC-3'
	HEC1 A-R	5'-TCCACCATTATTATTGTATTCATTTCAT-3'
	HEC1 B-F	5'-ATTTCACTTGTAAGCTTTTCACCAG-3'
	HEC1 B-R	5'-AGAGAAAAGGGTAAGTGTTGTTGTG-3'
	HEC1 C-F	5'-GCTAGGCATAGAAGGGAGAGAATAAG -3'
	HEC1 C-R	5'-TCTTTAAAAACTTCACATAATGAATTGC-3'
HEC2	HEC2 A-F	5'-CCATCCAGGTTAAAAGTTAAAATAAGAA-3'
	HEC2 A-R	5'-TTTGTTTATAATTGTTAATTACCCCACA-3'
	HEC2 B-F	5'-TAAAATAATAAGAATGGGTCACAAATG-3'
	HEC2 B-R	5'-AGTTATGTGCGAAATGTAAACTGTTACT-3'
	HEC2 C-F	5'-ATCTTCTTCTTCCTCCATACCTTATCTC -3'
	HEC2 C-R	5'-ATCATGTTCATTAGAATGTCGGAGTTAT-3'
	HEC2 D-F	5'-AAAGAGAAAGAACGTGAGGATCTCTAAG-3'
	HEC2 D-R	5'-TTCTTGAGAAACTTAACGTAATGGATAG -3'
HEC3	HEC3 A-F	5'-AAGAGAGAAGGAGATAATTAAAGGGATT-3'
	HEC3 A-R	5'-GACTTGAATTTAGGGTATATCGAGAAAG-3'
	HEC3 B-F	5'-ATATATACATATAAGCATCGCCTCAAGC-3'

	HEC3 B-R	5’-GTTCCAAGTGTAATTTTGGAAGAGAGAT-3’
	HEC3 C-F	5'-CTTCTCATTTCCCTCCTCTCTCTTCTTC -3'
	HEC3 C-R	5'-TTACGGCGTTTGGGTTTCTTGACGGT -3'
PIF1	PIF1 A-F	5'-AAAATGATGCATATCTCTCTCTCTACAA -3'
	PIF1 A-R	5'-TTACGGCGTTTGGGTTTCTTGACGGT -3'
	PIF1 B-F	5'-ATGATTTCTGCTCAGATCTTCTCTTCT -3'
	PIF1 B-R	5'-AGATTCACCACCTCTACCGTTATTAAA -3'
GAI	GAI B-F	5'-GGACCCGTTTTACACGTG-3'
	GAI B-R	5'-TATGTACTTAACGCCGTCGC-3'
	GAI D-F	5'-GAAGACGATCTTTCTCAACTCG-3'
	GAI D-R	5'-CACCGGGAATAGCTTTAAGATC-3'
RGA	RGA B-F	5'-CAGACTCGGTCCCTACCGTTT -3'
	RGA B-R	5'-GCCGTCATTAACGGCCTCTTTCT -3'
	RGA D-F	5'-TATGAATGATGATTGAAGTGGTAGTAGC -3'
	RGA D-R	5'-CTATGAGTTTCGATTAGATTAGGTCTGA -3'
HFR1	HFR1 P2-F	5'-GATACCATTTTCTCGGACAAAGCTGAAA -3'
	HFR1 P2-R	5'-AACTATTAGGGTTTACGATACAAATCAT -3'
	HFR1 P3-F	5'-CGATATATGCTACTATGACGTAGTTTTG -3'
	HFR1 P3-R	5'-CAACAAACATTGTAATGAAAATATTG -3'
	HFR1 qRT-F	5'-TACCACCGTTTACTAATATTTCATTCC -3'
	HFR1 qRT-R	5'-AAAAATCCAAGAAACTTGGGAAATAAG -3'
	HFR1 1stEXON-F	5'-CGTCGTATCCAGGTCTTAAGTAGTGAT -3'
	HFR1 1stEXON-R	5'-TTACTCATCTTCTCGTCTCTTCTTCTTC -3'

3.4 Results

3.4.1. HDA9 negatively regulates the phyB- dependent promotion of seed germination.

Posttranslational histone deacetylation has been implicated to play a role in germination through pharmacological and genetic studies (Tanaka et al., 2008; van Zanten et al., 2014). For the roles of RPD3 Class I HDACs in germination, reported were only HDA6 and HDA19 to redundantly repress embryonic properties and roles of other HDACs remain to be discovered. It prompted me to explore the role of HDA9 in germination process.

To examine the role of *HDA9* during seed germination, I first performed the germination assay using wt, *hda9-1*, and the complemented line *HDA9 hda9-1* (Kang et al., 2015) under constant white light (Fig. 1a). In order to avoid the possible complexity caused by the difference in seed viability and vigor, seeds were harvested from wild-type (wt) Col and *hda9-1* plants grown side by side under 16 h light /8 h dark condition and dried for more than 2 weeks at room temperature. Germination efficiency was measured by counting the number of seeds with emerging radicles on the seed surface. As shown in Fig. 1a, the germination efficiency of *hda9-1* was rapidly increased compared to wt at 44 hours (hr) after planting, and reached to 100% after 70 hr. Accelerated germination phenotype of *hda9-1* was rescued by the introduction of the genomic *HDA9* fragment (*HDA9g hda9-1*), indicating the mutant phenotype was indeed caused by

the loss of HDA9 function.

Because phyB plays key role in regulating seed germination under red or white light condition (Poppe and Schafer, 1997; Oh et al., 2004), it was questioned whether early germination caused by *hda9* is phyB-dependent. In order to address this, the germination efficiency was assessed after 5min red light pulse (Rp) following 5min far-red light (Fp; 1.8 μmol/m^2s) exposure. Seeds were imbibed in dark for 1hr (Fig. 1b-e) before light treatments. As shown in Fig. 1b, wt, *hda9-1*, and *HDA9g hda9-1* seeds similarly showed very poor germination after given only Far-red light pulse, indicating that phyB in all genotypes was inactivated by this treatment. When red-light pulse was given after far-red light pulse which converts phyB to its active form, the germination of all genotypes seeds were observed and reached to 100 % at 5 days after planting (DAP). Interestingly the germination of *hda9-1* more rapidly occurred compared to either wt or *HDA9g hda9-1*, showing ~93% germination efficiency at 2DAP while wt and *HDA9g hda9-1*, 53 and 57%, respectively (Fig. 1c and e).

To more confirm that accelerated germination of *hda9-1* seeds is phyB-dependent, I irradiated the seeds with Fp at the end of sequential applications of Fp and Rp to inactive phyB. This prevented the germination of *hda9-1* seeds, together with wt and *HDA9g hda9-1* seeds (Fig. 1d), which supports that the effect of the *hda9-1* mutation on seed germination requires phyB activity.

Different intensities or prolonged red light is known to affect germination efficiency (Oh et al., 2006). I examined the germination efficiency of wt, *hda9-1*

and*HDA9g hda9-1*using low fluence Rp (10 μmol/m^2s) of different duration. Seeds were irradiated with first, Fp for 5 min and then with Rp for 5 sec, 1min, 2 hr and 20 hr and kept in the dark for 5 days. *hda9-1* seeds showed higher germination efficiency than wt and *HDA9g hda9-1* when a 5- sec Rp and, to less extent, a 1-min Rp were given, whereas after longer than 2 hr red-light treatment, *hda9-1* showed a comparable level of germination to that of either wt or *HDA9g hda9-1* (Fig. 2).

Together, these results indicate that HDA9 is likely to be involved in the negative regulation of phyB-dependent seed germination.

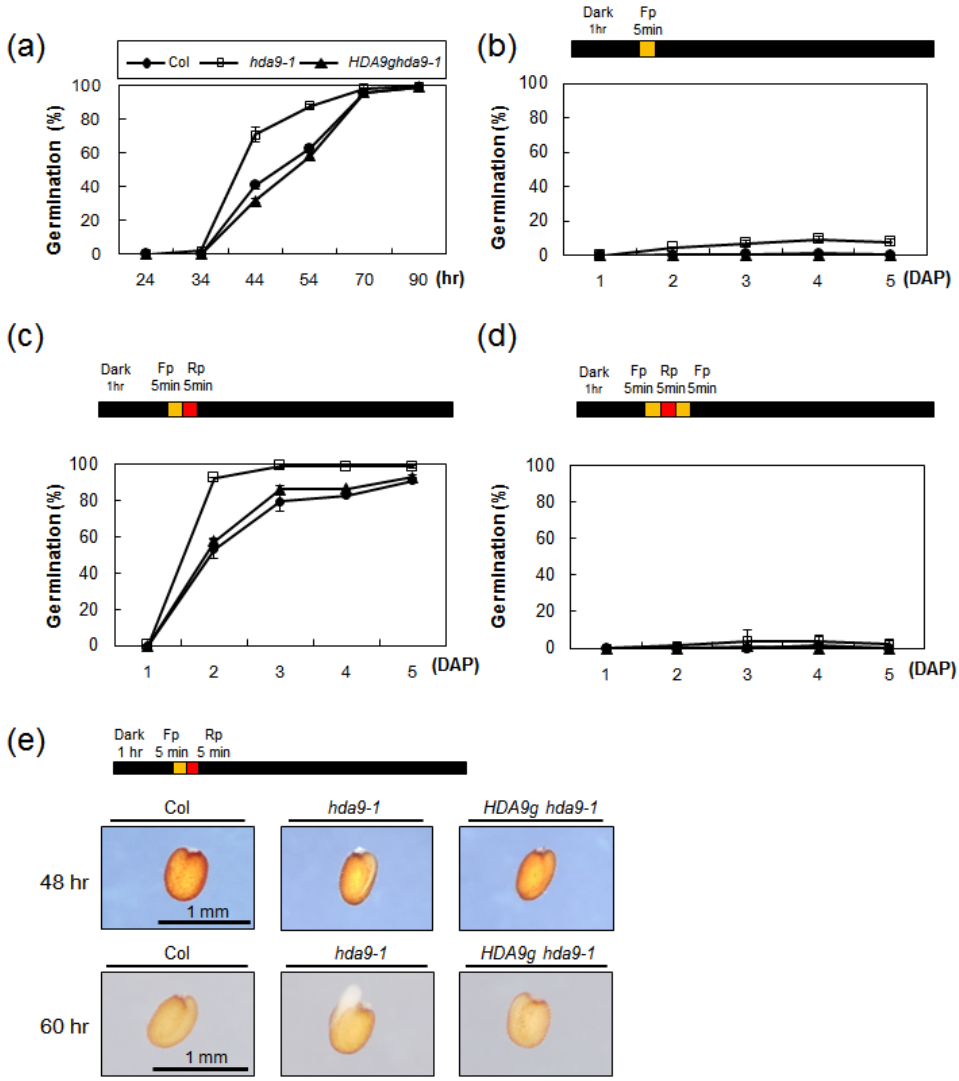

Fig. 1 phyB- dependent enhanced seed germination of *hda9-1*.

(a) Seed germination assay of Col (circle), *hda9-1* (square), and *hda9-1* transformed with a genomic copy of *HDA9 (HDA9g hda9-1)* (triangle) under constant white light condition. Germination was scored at indicated hours. (b-d) phyB- dependent germination assay. Seeds were imbibed for 1 hr in the dark. The

light treatment regime is indicated in the diagram at the top. The intensity for Fp is 1.8 μmol/m^2s or Rp is 40 μmol/m^2s. Light treated seeds were kept in the dark for 5 additional days (black box). Germinated seeds were counted every 24 hr after light treatment. Fp denotes far-red pulse and Rp indicate red pulse. Error bars represent standard errors (SE) from three independent biological replicates. (b) Seeds were exposed to Fp for 5 min and further incubated in the dark for indicated days to see the phyB off effect. (c) Seeds were exposed to Fp for 5 min and immediately exposed to Rp. Light treated seeds were further incubated in the dark for indicated days. (d) To disrupt phyB-dependent activity, seeds exposed to Fp and Rp for 5 min each as indicated in (c) were further exposed to 5 min of Fp. (e) Early germination phenotype of *hda9-1*.Seeds were imbibed for 1 hr in the dark and immediately exposed to Fp or Rp. Light treated seeds were further incubated in the dark for 48 hrs (upper panel) or 60 hrs (lower panel). Germinating seeds were photographed using optical microscope. Scale bars represent 1 mm.

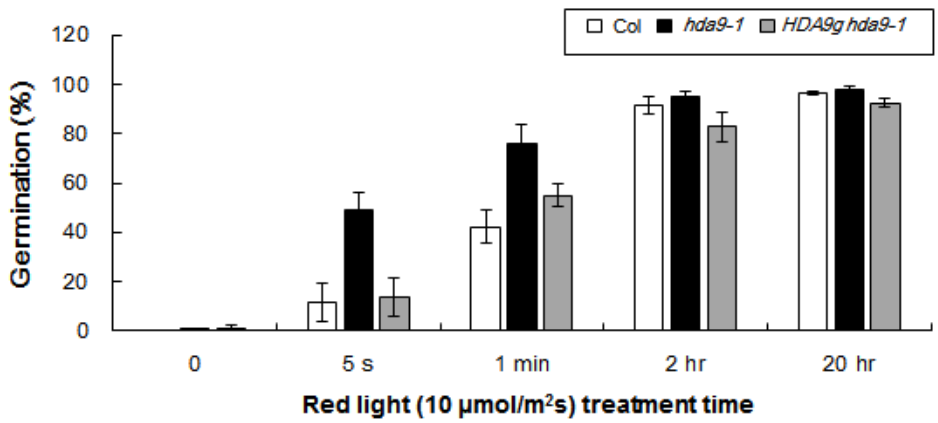

Fig. 2 Enhanced seed germination of *hda9-1* under low flux red-light.

Germination of Col (white), *hda9-1* (black), and *HDA9g hda9-1* (gray) seeds counted under various period in Rp after 5 min of Fp. Seeds were exposed to low intensity Rp (10 µmol/m^2s) for the indicated period after 5 min Fp treatment. Light treated seeds were kept in dark for 5 additional days. Results shown are the percentage of germinated seeds (number of emerging radicles divided by total sowed seeds) scored 5 days after light treatment. Error bars indicate standard errors of three independent biological replicates.

3.4.2. Expression of HDA9 is not affected by red light.

The role of HDA9 in phyB-dependent seed germination led me to ask whether HDA9 expression is red-light dependent. So, I investigated and compared the spatial expression patterns of *HDA9* using HDA9:GUS fusion protein in Fp- or Rp-treated embryos. HDA9:GUS expression was detected in the entire region of the embryos and its strength was not influenced by an exposure to either Fp or Rp (Fig. 3a). In addition, I performed immunoblot assay using Fp- or Rp- treated *HDA9:HA hda9-1* transgenic seeds (Kang et al., 2015) to study whether HDA9 protein level changes by red-light. HDA9:HA protein level was not significantly different between two light treatments (Fig. 3b), which is in line with the result of HDA9:GUS expression (Fig. 3a). Hence, I concluded that HDA9 protein level is not affected by red light.

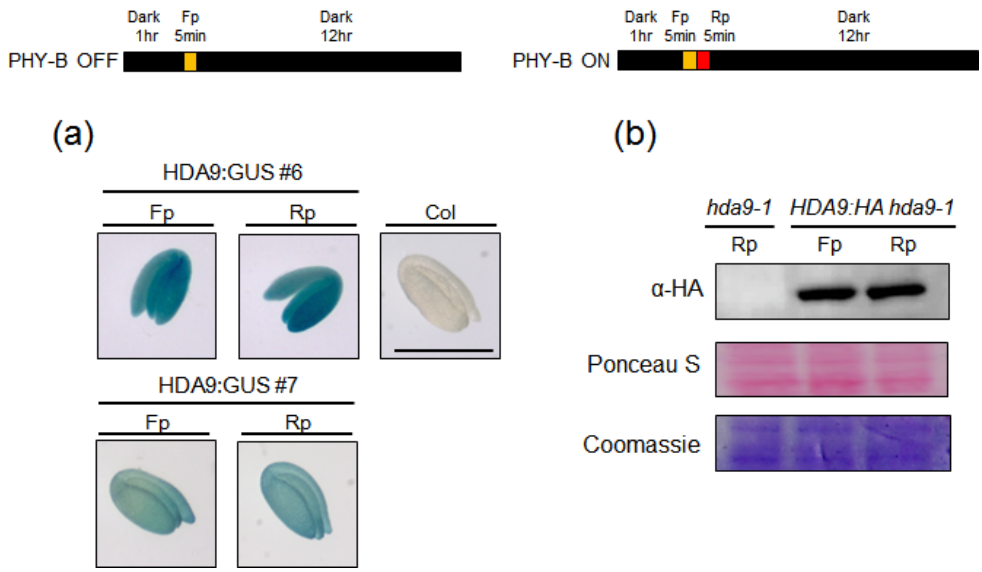

Fig. 3 HDA9 protein level is not affected by red light.

(a) Histochemical GUS staining of HDA9:GUS embryos. Seeds were incubated for 12 hr in the dark after 5 min of Fp (1.8 μmol/m^2s) or Rp (40 μmol/m^2s). Embryos of two independent HDA9:GUS transgenic lines (#6, upper panel and line #7, lower panel) were GUS stained for 2 hr 30 min with X-Gluc solution and photographed using optical microscope. Scale bar represent 1mm. (b) HDA9:HA protein level in Fp and Rp. Total HDA9:HA protein was extracted from Fp or Rp treated seeds. Anti-HA antibody was used to detect HDA9:HA protein. Ponceau S staining for Rubisco protein and Coomassie staining were performed as loading control.

3.4.3. Expression of *HECATEs*, positive regulators in seed germination, is increased by the *hda9-1* mutation.

Next, I questioned how *HDA9* regulates seed germination. Because the most well-known role of HDACs is to regulate transcription of genes and HDA9 was also previously found to be involved in the negative regulation of *AGL19* transcription (Kang et al., 2015), it is plausible that HDA9 plays a role in the transcriptional regulation of germination-related gene expression. bHLH transcription factors PIF1, HFR1, HEC1 and HEC2 were reported to function in phytochrome signaling and seed germination (Oh et al., 2004; Shi et al., 2012; Zhu PhD thesis, 2012). Therefore, I tested whether the *hda9-1* mutation affects mRNA levels of these genes. Total RNA was extracted from Fp- or Rp- treated seeds and the transcript levels of *HEC1, HEC2,* and *HEC3* (Figure 4a), *HFR1* and *PIF1* were determined by quantitative real-time reverse transcription polymerase chain reaction analysis (RT-qPCR; Figure 4b and5 a). Noticeably, *HEC1, HEC2,* and *HEC3* mRNA levels were significantly increased by Rp treatment while HFR1 and PIF1 were not. Moreover, the increase in *HECs* expression was much higher in *hda9-1* (R *hda9-1*) seeds compared to wt (R Col). The increased *HECs* expression by *hda9-1* mutation was restored to wt level in *HDA9g hda9-1* seeds. Interestingly, *HEC1* and *HEC2* transcript levels were also slightly higher in *hda9-1* (F *hda9-1*) than wt seeds (F Col) treated with a Fp. I also examined the protein levels of HECs in wt and *hda9-1* using *HEC1p::HEC1:GUS (HEC1:GUS*; Gremski et al., 2007*). HEC1:GUS* was introduced into *hda9-1* background by crossing. *HEC1:GUS* staining was detected in the entire region of the embryo and stronger in *hda9-1* mutant (Fig. 4c).

Immunoblot assay performed with anti-GUS using nuclear extracts from imbibed seeds identified a positive signal in either wt or *hda9-1* background at ~90 kD that was similar to the size of HEC1:GUS (Fig. 4c and 4d). Intensity of the signal was stronger in *hda9-1* than in wt, indicating more HEC1 protein is present in *hda9-1* than in wt. These results point out that HDA9 might control germination by negatively regulating the transcription of the positive regulator of germination HECs.

In addition to bHLH proteins, several transcription factors are reported to regulate light-dependent seed germination. Among them, *SOMNUS* (*SOM*) and *SPATULA* (*SPT*) are known to act as repressors during light dependent seed germination, while *JMJ20* and *JMJ22* are reported to be involved in the promotion of seed germination. So, I also examined the changes in transcript levels of *SOM*, *SPT*, *JMJ20*, and *JMJ22* together with *PIF1* (Oh et al., 2004; Penfield et al., 2005; Kim et al., 2008; Cho et al., 2012). However, I found no significant difference in the transcript levels of these genes between wt and *hda9-1* after both F and R-treatment (Fig. 5a).

Two phytohormones, ABA and GA antagonistically control seed germination through complicated signaling crosstalk. I further analyzed the mRNA levels of GA- and ABA metabolic genes in wt and *hda9-1* seeds that were irradiated with Rp or Fp and then incubated in dark for 12 hrs. Expression levels of GA biosynthetic genes (*GA3ox1*, *GA3ox2*, and *GA2ox2*) were not significantly different between wt and *hda9-1* in all conditions (Fig. 5b). Overall expression of

ABA anabolic genes such as *ABA-deficient (ABA1)* and *9-cis-epoxycarotenoid dioxygenases (NCED6)* and an ABA catabolic gene, *CYP707A2* were slightly decreased in *hda9-1* compared to wt in all conditions with the exception of the *NCED6* expression in F-treated seeds being largely reduced by the *hda9* mutation (Fig. 5b). However, Both decreases in the expressions of ABA anabolic genes and ABA catabolic genes, when combined together are not likely responsible for the early germination phenotypes of *hda9*.

3.4.4. *HECATE* expressions were enhanced in seed germination.

In order to confirm the promoting role in seed germination of HECs and compare it with the effect of the *hda9* mutation, I assessed the seed germination efficiency of *35S::HEC2* along with *hda9-1* after a red or a far-red light pulse was given. I could not perform the seed germination assay for *HEC1* and *HEC3* overexpression plants because of their fertility defects (Gremski et al., 2007). Notably, unlike *hda9-1*, *35S::HEC2* transgenic line showed enhanced seed germination irrespective of light regimes (Fig. 4e). On the other hand, the germination efficiency of *35S::HEC2* and *hda9-1* after Rp was similarly enhanced after 2 DAP, higher than wt. Considered together with light-dependent induction of *HEC* expression, these results indicates that HECs act as positively regulators in the phyB-dependent seed germination and the amount of HECs might be not limiting factor in this process.

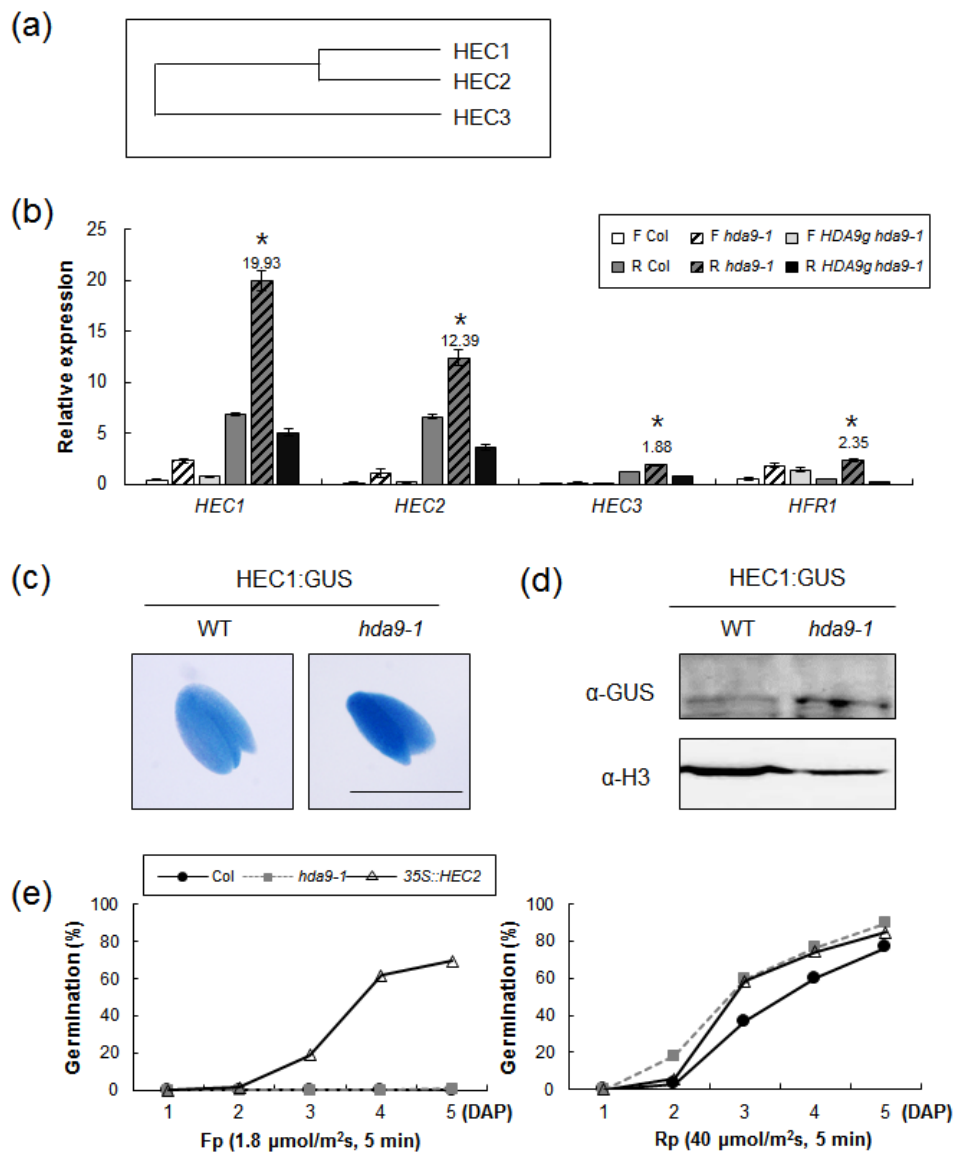

Fig. 4 The *hda9-1* mutation causes increased expression of *HEC* genes at both transcript and protein levels.

(a) Phylogenetic analysis of HECATE proteins using neighbor-joining (NJ) method. The amino acid sequences of Arabidopsis HECATE proteins were aligned using

CLUSTAL W. (b) Transcript level of *HEC1*, *HEC2*, *HEC3*, and *HFR1* analyzed by quantitative real-time reverse transcription polymerase chain reaction (RT-qPCR). The level of F Col was set to 1 after normalization by *UBQ11*. Seeds were exposed to 1.8 μmol/m^2s of Fp for 5 min and 40 μmol/m^2s of Rp for 5 min. Asterisks indicate statistically significant differences ($P<0.05$). Error bars represent standard error of three independent biological replicates. (c) HEC1:GUS expression level is enhanced in *hda9-1*. Histochemical expression patterns of HEC1:GUS in WT (left panel) and *hda9-1* embryos (right panel). All the seeds were homozygous for HEC1:GUS. Seeds were incubated for 12 hr in the dark after 5 min of Rp (40 μmol/m^2s). Light treated seeds were fixed by acetone and dissected. Embryos were stained for 36 hr with X-Gluc solution and photographed using optical microscope. Scale bar represent 1mm. (d) HEC1:GUS protein level is increased by *hda9-1* mutation. Nuclear enriched proteins were extracted from HEC1:GUS in WT and *hda9-1* seeds using Honda buffer. Seeds were treated with 5 min of Rp (40 μmol/m^2s) and incubated in the dark for 12 hr before harvesting. For immunoblot analysis, HEC1 protein was detected with anti-GUS antibody (1:1000) using Chemi-doc (Fusion solo). Histone H3 was detected using anti-H3 (1:10000) as nuclear protein control. (e) Germination efficiency of Col (circle), *hda9-1* (square), and *35S:HEC2* (triangle). Seeds were exposed to 5 min of Fp (1.8 μmol/m^2s) and 5 min of Rp (40 μmol/m^2s). Light treated seeds were incubated in the dark and germinated seeds were counted at indicated days.

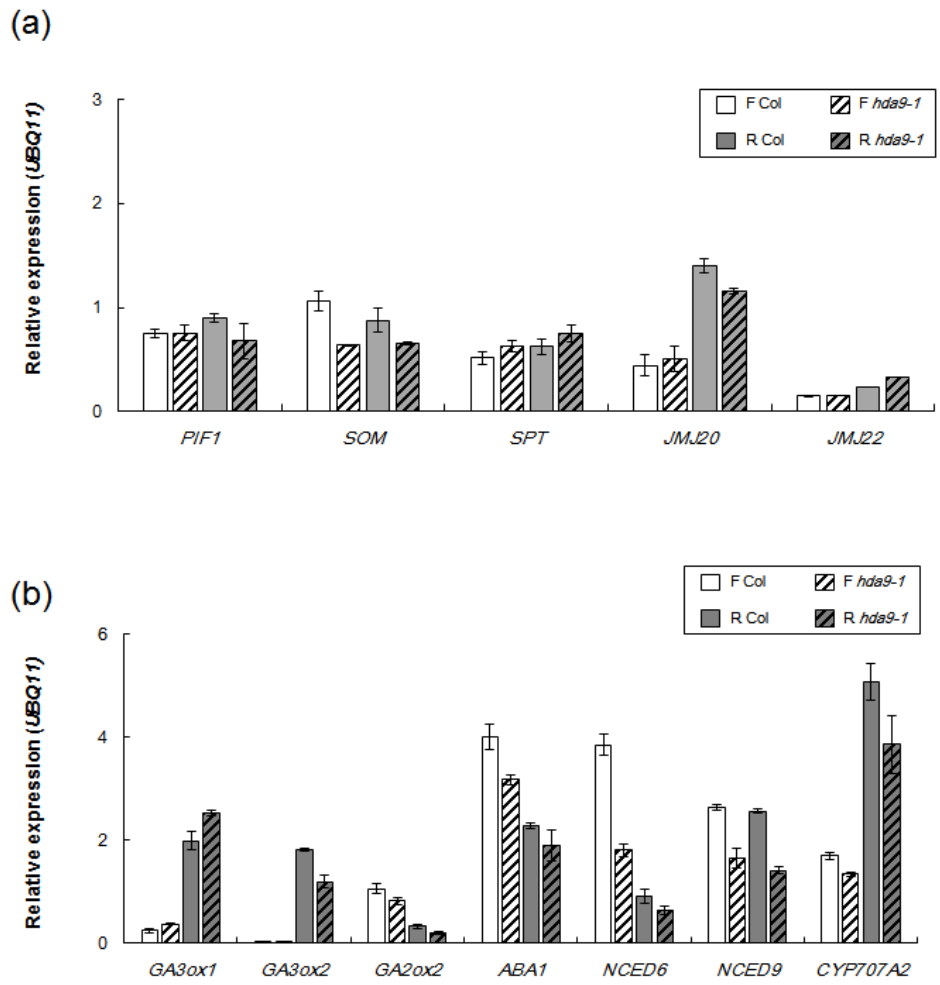

Fig. 5 Expression of germination-related genes in wt and *hda9-1*.

(a) Transcript level of *PIF1, SOM, SPT, JMJ20, JMJ22* under red light condition. Seeds were imbibed for 1 hr in the dark and irradiated with 1.8 μmol/m^2s of Fp for 5 min followed with 40 μmol/m^2s of Rp for 5 min. Then, seeds were kept in the dark for 12 hr before total RNA extraction. Transcript levels were analyzed by RT-qPCR. *UBQ11* was used as an internal control. Error bars represent standard error of three independent biological replicates. (b) Transcript level of GA biosynthetic

genes and ABA metabolism and signaling genes examined by RT-qPCR. Dry seeds were imbibed for 1 hr in the dark and irradiated with 1.8 μmol/m^2s of Fp for 5 min followed with 40 μmol/m^2s of Rp for 5 min. Then, seeds were kept in the dark for 12 hr and harvested for total RNA extraction. *UBQ11* was used as internal control. Error bars represent standard error of three independent biological replicates.

3.4.5. HDA9 directly represses *HECs* transcription through histone deacetylation.

I performed chromatin immuno-precipitation (ChIP) experiment to test whether *HDA9* represses the transcription of *HECs* by changing their chromatin environment through histone deacetylation (Fig. 6b-d). ChIP assay using anti acetylated histone H3 (H3Ac) antibody showed that H3Ac level was gradually increased in region within *HEC1* (B and C region), *HEC2* (B region) and *HEC3* (C region) in wt after Rp treatment. These results indicate that the transcriptional activation of *HECs* requires histone acetylation under Rp condition. Furthermore, in accordance to the increased transcript level of *HECs* in *hda9-1*, the H3Ac level in R-treated *hda9-1* was much higher in promoters and transcribed regions within *HEC1* (regions A, B, and C), *HEC2* (regions A, B, and D) and *HEC3* (regions A, B, and C) compared to R-treated wt (Fig. 6a and 6b). Therefore, the increased *HECs* transcription in *hda9-1* might be a consequence of hyperacetylated H3 in *HECs* chromatin.

Next, I examined the RNA polymerase II (RNA pol II) occupancy to see whether hyperacetylation of *HECs* was related to RNA pol II mediated transcription. In wt, there was no noticeable change in the RNA pol II occupancy in regions of *HECs* chromatin in Rp compared to Fp-treated condition. On the other hand, RNA pol II occupancy within *HEC1* (regions A, B and C), *HEC2* (regions A, B and D) and *HEC3* (regions A, B and C) chromatin was increased in Rp-treated *hda9-1* (Fig. 6a and 6c). Thus, hyperacetylation by *hda9-1* mutation in Rp

condition might increase the accessibility of RNA pol II to the *HECs* chromatin.

I further performed the ChIP assay with anti-HA using *HDA9:HA hda9-1* transgenic seeds to address whether HDA9 play a direct role in the transcriptional regulation of *HEC*s chromatin. ChIP-qPCR analysis clearly showed the association of HDA9:HA with the promoter, transcription start site and gene body (regions A, B, and C) of *HEC1* chromatin under Rp condition (Figure 6d). In addition, HDA9:HA strongly bound to the region near the transcription start sites of *HEC2* (regions A, B, and C) and *HEC3* (region A), but not *PIF1* (Fig. 6a and 6d). These results indicate that HDA9 directly bind to the *HECs* chromatin, which is consistent with the increases of H3Ac level and RNA pol II occupancy at *HECs* loci in *hda9-1*compared to wt. Together, these results suggest that HDA9 has a direct role in maintaining the proper transcriptional activity of *HECs* through histone deacetylation.

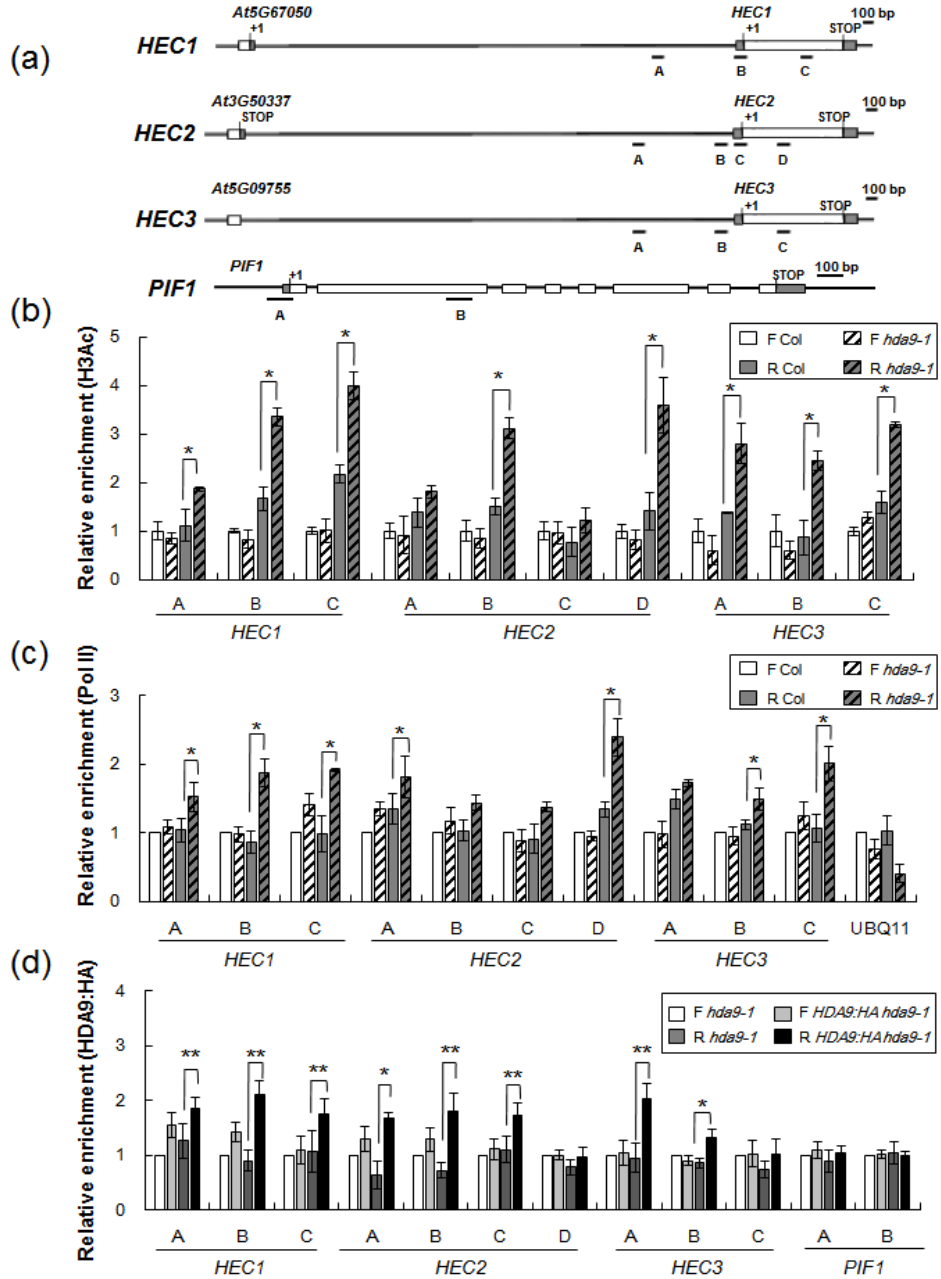

Fig. 6 HDA9 directly affects *HEC* transcription via histone deacetylation.

(a) Schematics representing the genomic structures of *HEC1*, *HEC2*, *HEC3*, and

PIF1. Gray boxes represent 5' and 3' untranslated regions and white boxes indicate exons. Introns are represented as solid lines and the transcription start site is indicated as +1. Regions amplified in chromatin immunoprecipitation followed by qPCR (ChIP-qPCR) are shown for each gene. (b) H3Ac level in *HEC1*, *HEC2*, and *HEC3* chromatin analyzed by ChIP-qPCR. Col and *hda9-1* seeds were incubated for 12 hr in the dark after 5 min treatment of Fp (1.8μmol/m^2s) or 5 min of Rp (40 μmol/m^2s). H3Ac level was increased by red light around the promoters and gene bodies of *HEC1*, *HEC2*, and *HEC3* chromatin. The H3Ac level of R *hda9-1* was higher than R Col. Levels of F Col were set to 1 after normalization by *UBQ11*. Asterisks indicate statistically significant differences ($P<0.05$). (c) RNA polymerase II occupancy within *HEC1*, *HEC2*, and *HEC3* chromatin examined by ChIP-qPCR. Samples were prepared as in (b). The F Col level was set to 1 after normalization to the corresponding input. *UBQ11* was used as internal control. Asterisks indicate statistically significant differences ($P<0.05$). (d) HDA9:HA enrichment using anti-HA antibody analyzed by ChIP-qPCR. HDA9:HA *hda9-1* and *hda9-1* seeds were incubated for 12 hr in the dark after 5 min of Fp (1.8 μmol/m^2s) or 5 min of Rp (40 μmol/m^2s). The amount of immunoprecipitated chromatin was normalized to the corresponding input and compared with untagged lines. The regions of *PIF1* were used as nonspecific control. Shown are the means± SE of three biological replicates. Asterisks indicate statistically significant differences (* $P<0.05$, ** $P<0.01$).

3.4.6. HDA9 acts as an upstream regulator of *HECs.*

In order to the increased HECs levels indeed cause the early germination of the *hda9* mutant, I analyzed the phyB-dependent germination of *hda9-1* in the absence of HECs. *hec1 hec2 RNAi* double mutant displayed reduced germination efficiency compared with wt (Fig. 7) which *35S::HEC2* showed clearly enhanced germination (Fig. 4e), demonstrating the positive role of HECs in seed germination. Remarkably, the promoting effects of the *hda9* mutation greatly disappeared in *hec1 hec2 RNAi hda9-1* ; the triple mutant seeds displayed similar germination efficiency as the *hec1 hec2 RNAi* seeds (Fig. 7), indicating the early germination of *hda9* is in great part attributed to HECs. I observed the slight increase of germination efficiency in *hec1 hec2 RNAi hda9-1* compared to *hec1 hec2 RNAi*. This slightly early germination of *hec1 hec2 RNAi hda9-1* might be due to the enhanced expression of *HEC3* or other unknown factors by *hda9-1* mutation.

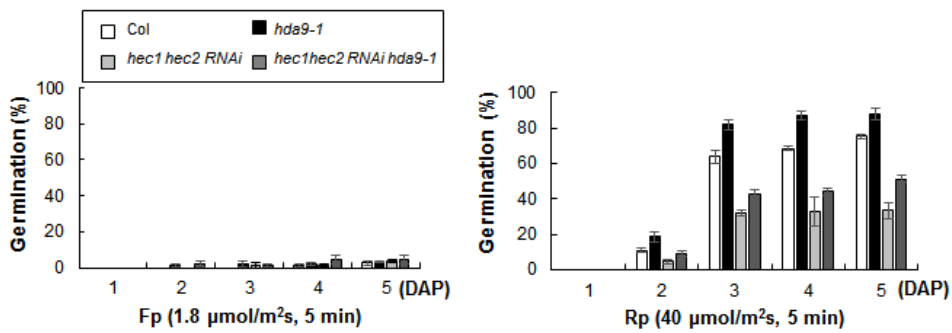

Fig. 7 HECs are required for the enhanced germination of *hda9-1*.

hec mutations are epistatic to the *hda9-1* mutation under red light. Germination efficiencies were observed in Col (white), *hda9-1* (black), *hec1hec2 RNAi* (light gray), and *hec1 hec2 RNAi hda9-1* (dark gray). Germinated seeds were counted every 24 hr after dark incubation following light treatment (Fp; left or Rp; right). Values are the means ± SE of three independent biological replicates.

3.4.7. *GAI* and *RGA* mRNAs are reduced by the *hda9* mutation under red light regime.

Previously, it was reported that HEC2 blocks DNA binding activity of PIF1 and regulate the expression of GAI and RGA in a way opposite to PIF1. So, I examined in *wt* and *hda9-1* seeds the expressions of *PIF1* and *PIF1* target genes (*SOM*, *GAI*, and *RGA*) after the application of a Rp (40 or 10 μmol/m^2s) followed by a Fp or of a Fp only. When only a Fp was given, the transcript levels of all the examined genes were reduced in *hda9-1* compared to wt with the exception of *PIF1* of which expression was not significantly decreased in the mutant (Figure 8a and b). Yet, germination of Fp-treated *hda9-1* was indistinguishable from Fp-treated wt (Fig. 1b), indicating that the extent of reduction in the expression of *SOM*, *GAI* and *RGA* in *hda9-1* is not enough to overcome the strong influence of germination-repressing factors such as PIF1 in Fp-treated seeds. Irradiation with a Rp resulted in the decreases in *SOM*, *GAI*, *RGA*, and to lesser extent, *PIF1* (Figure 8a and b). This was more noticeable with higher-fluence rate red light. After a pulse of both high- and low- fluence red light was applied, the mRNA levels of *GAI* and *RGA* but not of *SOM* were reduced more in *hda9-1* than in wt. Small difference in *SOM* transcript level between wt and *hda9-1* was detectable after a pulse of low- fluence light only (Figure 8b). Then, I performed ChIP assay using HDA9:HA in order to test possibility that HDA9 directly regulate the transcription of *GAI* and *RGA*. There was no detectable association of HDA9:HA with either *GAI*- or *RGA* chromatin regions analyzed (Fig. 8c and 8d). Combined together, these results suggest that *HDA9* affects the mRNA levels of *GAI* and *RGA* that are the target

genes of the germination repressor *PIF1*, probably by regulating the transcription of HEC1, a negative regulator of *PIF1* activity.

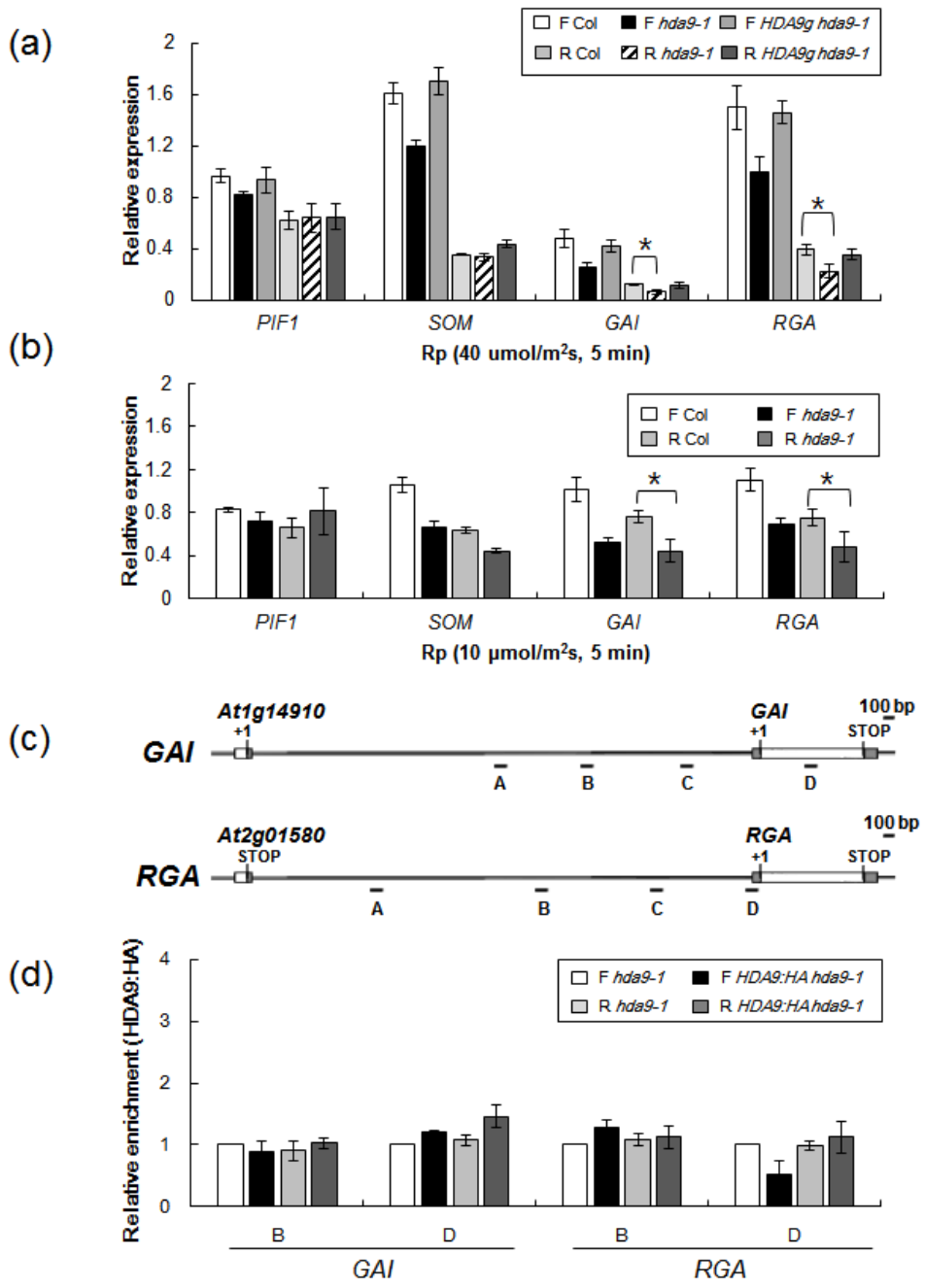
(a)
F Col
F hda9-1
F HDA9g hda9-1
R Col
R hda9-1
R HDA9g hda9-1
Relative expression
2
1.6
1.2
0.8
0.4
0
*
*
PIF1
SOM
GAI
RGA
Rp (40 umol/m²s, 5 min)
(b)
F Col
F hda9-1
R Col
R hda9-1
Relative expression
2
1.6
1.2
0.8
0.4
0
*
*
PIF1
SOM
GAI
RGA
Rp (10 μmol/m²s, 5 min)
(c)
At1g14910
+1
GAI
+1
100 bp
STOP
GAI
A
B
C
D
At2g01580
STOP
RGA
+1
100 bp
STOP
RGA
A
B
C
D
(d)
F hda9-1
F HDA9:HA hda9-1
R hda9-1
R HDA9:HA hda9-1
Relative enrichment (HDA9:HA)
4
3
2
1
0
B
D
B
D
GAI
RGA

Fig. 8 Transcript levels of *GAI* and *RGA* are reduced by the *hda9-1* mutation under red light regime.

(a) *GAI* and *RGA* transcript levels are decreased in R *hda9-1*. Transcript level of *PIF1* and its direct target genes, *SOM*, *GAI*, and *RGA* quantified by RT-qPCR. Seeds were exposed to 5 min of Fp (1.8 μmol/m^2s) or 5 min of Rp (40 μmol/m^2s). The level of F Col was set 1 after internal normalization by *UBQ11*. Shown are the means of three independent biological replicates and error bars represent SE. Asterisks indicate statistically significant difference (P <0.05). (b) *GAI* and *RGA* transcript levels are decreased in low-intensity R *hda9-1*. The transcript levels of *PIF1*, *SOM*, *GAI*, and *RGA* under low quantity of red light (10 μmol/m^2s) were analyzed by RT-qPCR. The level of F Col was set to 1 after internal normalization by *UBQ11*. Values are the means ± SE of three independent biological replicates. Asterisks indicate statistically significant differences (P <0.05). (c) Schematics of the genomic structures of *GAI* and *RGA*. Gray boxes represent 5' and 3' untranslated regions and white boxes represent exons. Introns are indicated as solid lines, +1 represent transcription start site. Regions amplified in ChIP-qPCR are shown for each gene. (d) HDA9:HA does not directly bind to *GAI* or *RGA* chromatin. HDA9:HA *hda9-1* and *hda9-1* seeds were incubated for 12 hr in the dark after 5 min of Fp (1.8 μmol/m^2s) or 5 min of Rp (40 μmol/m^2s). The amount of immunoprecipitated chromatin was normalized to the corresponding input and compared with the untagged line. Values are the means ± SE of three independent biological replicates.

3.4.8. The *pif1* mutation is epistatic to the *hda9* mutation.

As an initial attempt to test the hypothetical regulatory pathway consisting of HDA9-HEC1-PIF1-PIF1 targets in the phyB-dependent germination process, I analyzed the effect of *pif1-2* mutation on the early germination of *hda9-1* by assessing the germination efficiency of *hda9-1 pif1-2*. *pif1-2* mutant showed extremely enhanced germination after both Fp and Rp as previously reported (Oh et al., 2004). Germination efficiency of *pif1-2 hda9-1* double mutant was similar to that of *pif1-2* single mutant without any additive effect of *pif1-2* and *hda9-1* after both Fp and Rp (Fig. 9). This result that *pif1-2* mutation is epistatic to *hda9-1* mutation supports the above hypothesis.

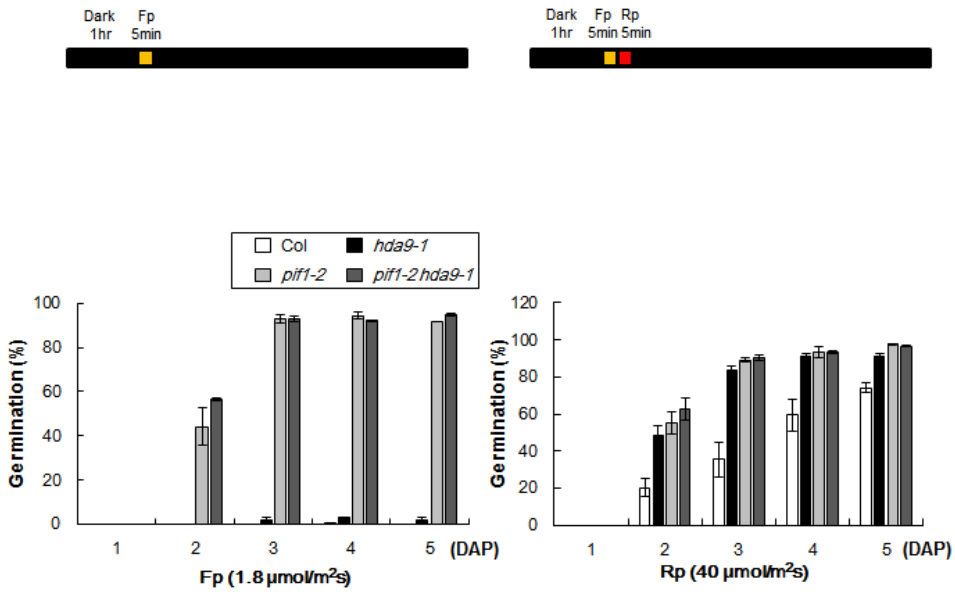

Fig. 9 The *pif1-2* mutation is epistatic to the *hda9-1* mutation in seed germination.

Germination percentages of Col (white), *hda9-1* (black), *pif1-2* (light gray), and *pif1-2 hda9-1* (dark gray) seeds exposed to 5 min of Fp (1.8 μmol/m^2s; left) or 5 min of Rp (40 μmol/m^2s; right). Light treated homozygous seeds were kept in the dark and germinated seeds were counted every 24 hr. Error bars represent standard error from three independent biological replicates.

3.4.9. HDA9 targeting to *HFR1* is less clear.

Recently it was reported that HFR1 forms a heterodimer with PIF1 and inhibit the transcription activity of PIF1 on targets genes (Shi et al., 2013). Interestingly, I observed the increase of *HFR1* transcript level *hda9-1* after a red light pulse following a far-red light pulse (Fig. 4b). So, I investigated whether HDA9 also regulate the transcription of *HFR1* through histone deacetylation. I found that H3Ac levels in the regions of promoter (P2), transcription start site (P3) and gene body (E1) of *HFR1* were higher in *hda9-1* than in wt after subsequent Rp the but not after Fp pulse only (Fig. 10a and 10b). Next, I performed the ChIP assay with anti-RNA pol II antibody using imbibed seeds to investigate the accessibility of RNA pol II to *HFR1* chromatin. Although H3Ac level at HFR1 was elevated by *hda9-1* mutation, RNA pol II occupancy in *hda9-1* was indistinguishable from that in wt irrespective of light regimes (Fig. 10c). I further examined whether HDA9 directly binds to *HFR1* by ChIP assay with anti-HA antibody using *HDA9:HA* seeds and found no significant binding of HDA9:HA to the analyzed regions of *HFR1* chromatin (Fig. 10d). These results indicate that *HDA9* indirectly regulate the transcription of *HFR1*.

In addition, I analyzed the germination efficiency of *hfr1-201*, *hda9-1*, wt Col, and *hfr1-201 hda9-1* double mutants after different duration of red-light (10 μmol/m^2s) exposure. *hfr1-201* showed poor germination compared to other genotypes after up to 2 hrs of red-light exposure. However, the germination efficiency of *hfr1-201 hda9-1* was better than *hfr1-201* single mutant and was

moreover, in fact comparable to that of *hda9-1* (Fig. 10e). These results strongly suggest that HFR1 is not required for HDA9-medaited regulation of germination.

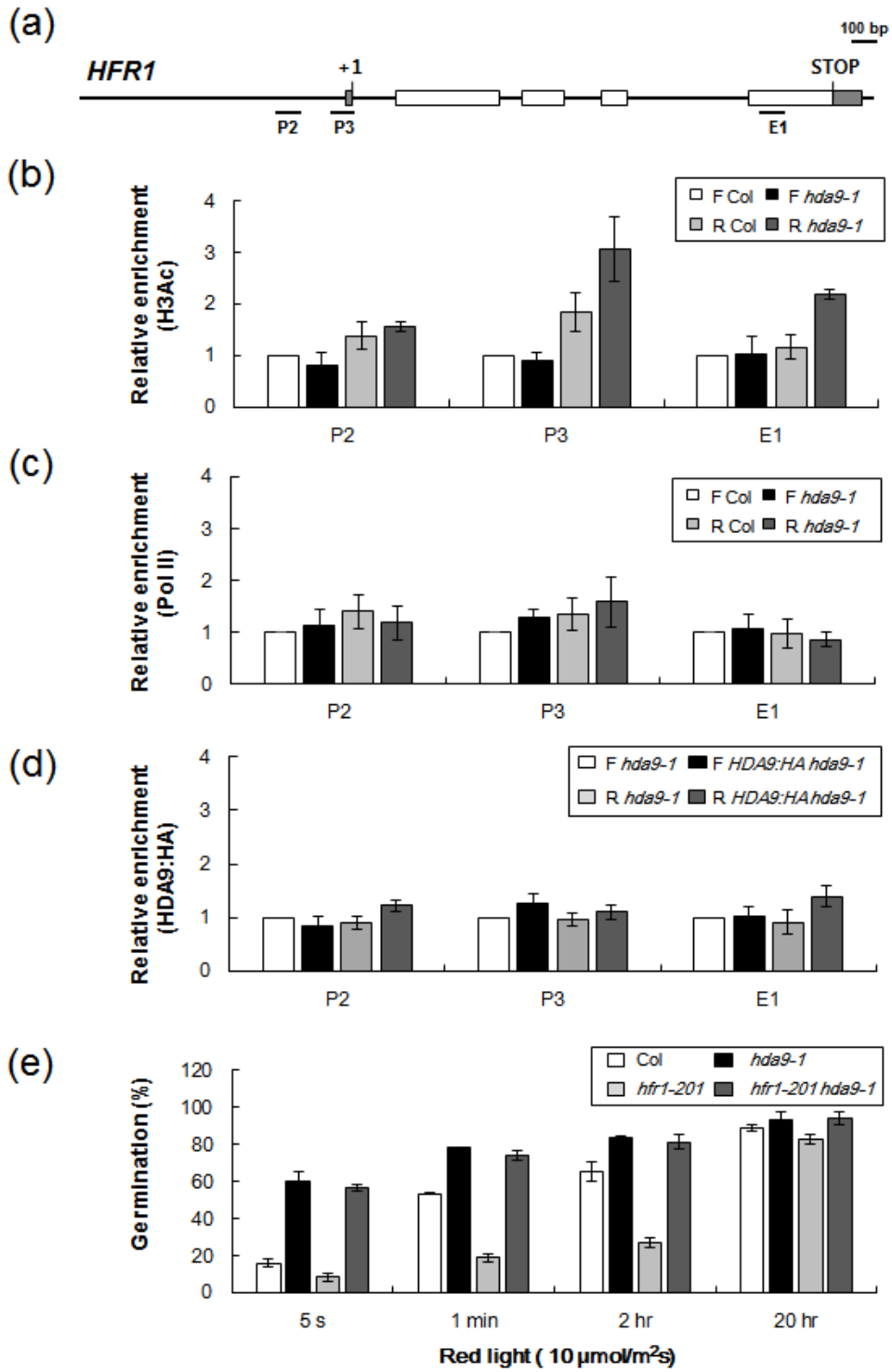

Fig. 10 Contribution of HFR1 in the enhanced seed germination of *hda9-1* is

not obvious.

(a) Schematic of the *HFR1*genomic structure. Gray boxes represent 5' and 3' untranslated regions and white boxes represent exons. Introns are indicated as solid lines, +1 designates transcription start site. Underlines indicate regions amplified in chromatin immunoprecipitation followed by qPCR. (b) H3Ac level at the *HFR1* locus is increased by red light. The increase of H3Ac by red light at the *HFR1* locus was more pronounced in R *hda9-1* than R Col. H3Ac level at the *HFR1* chromatin was analyzed by ChIP-qPCR. Level of F Col was set to 1 after normalization by *UBQ11*. Seeds were exposed to 5 min of Fp (1.8 μmol/m^2s) and 5 min of Rp (40 μmol/m^2s). Values are the means± SE of three independent biological replicates. (c) RNA polymerase II occupancy at the *HFR1* locus is not substantially increased in *hda9-1*. RNA polymerase II occupancy within *HFR1* chromatin was analyzed by ChIP-qPCR. The sample of F Col was set 1 after normalization to the corresponding input. Values are the means± SE of three independent biological replicates. (d) *HDA9* targeting to *HFR1* is less clear. The enrichment of HDA9:HA within the *HFR1* chromatin using anti-HA antibody was analyzed by ChIP-qPCR. The amount of immunoprecipitated chromatin was normalized to the corresponding input and compared with untagged lines. Values are the means± SE of three independent biological replicates. (e) Germination efficiencies of Col, *hda9-1, hfr1-201* and *hfr1-201 hda9-1* seeds. Seeds were exposed to low intensity Rp (10 μmol/m^2s) for the indicated time period after 5 min Fp treatment. Light treated seeds were kept in the dark for 5 additional days. Results shown are the percentage of germinated seeds scored 5 days after light

treatment. Error bars indicate standard errors from three independent biological replicates**.**

3.4.10. Proposed working model of HDA9-HEC-PIF1 regulatory module controlling the phyB-dependent seed germination.

From all the results above, I propose a working model for the functions of HDA9-HEC-PIF1 module in the regulation of the phyB-dependent seed germination (Fig. 11). When seeds are subjected to red light, most phytochromes are converted to the biologically active Pfr form and then moves into the nucleus. In the nucleus, phyB (Pfr) interacts with PIF1, which induces rapid degradation of PIF1 through the 26S proteasome pathway leading to the release of seeds germination from the restraint by PIF1. phyB (Pfr) also causes the expression of *HECs*. HECs form heterodimers with residual PIF1 from the degradation, which sequesters PIF1 and blocks its transcriptional activity toward the target genes such as *RGA* and *GAI*, ensuring the promotion of germination. HDA9 plays a role in restricting hyper-acetylation in the *HECs* chromatin during transcription which may cause the increase of transcriptional activity of *HECs* chromatin and the following illegitimate seed germination. Consequently, the HDA9-HECs-PIF1 module plays a role in fine-tuning the expression of PIF1 target genes such as *GAI* and *RGA*, two DELLA genes involved in the inhibition of the accumulation of GA, which allow the proper timing of germination under environmental conditions subjected to seeds.

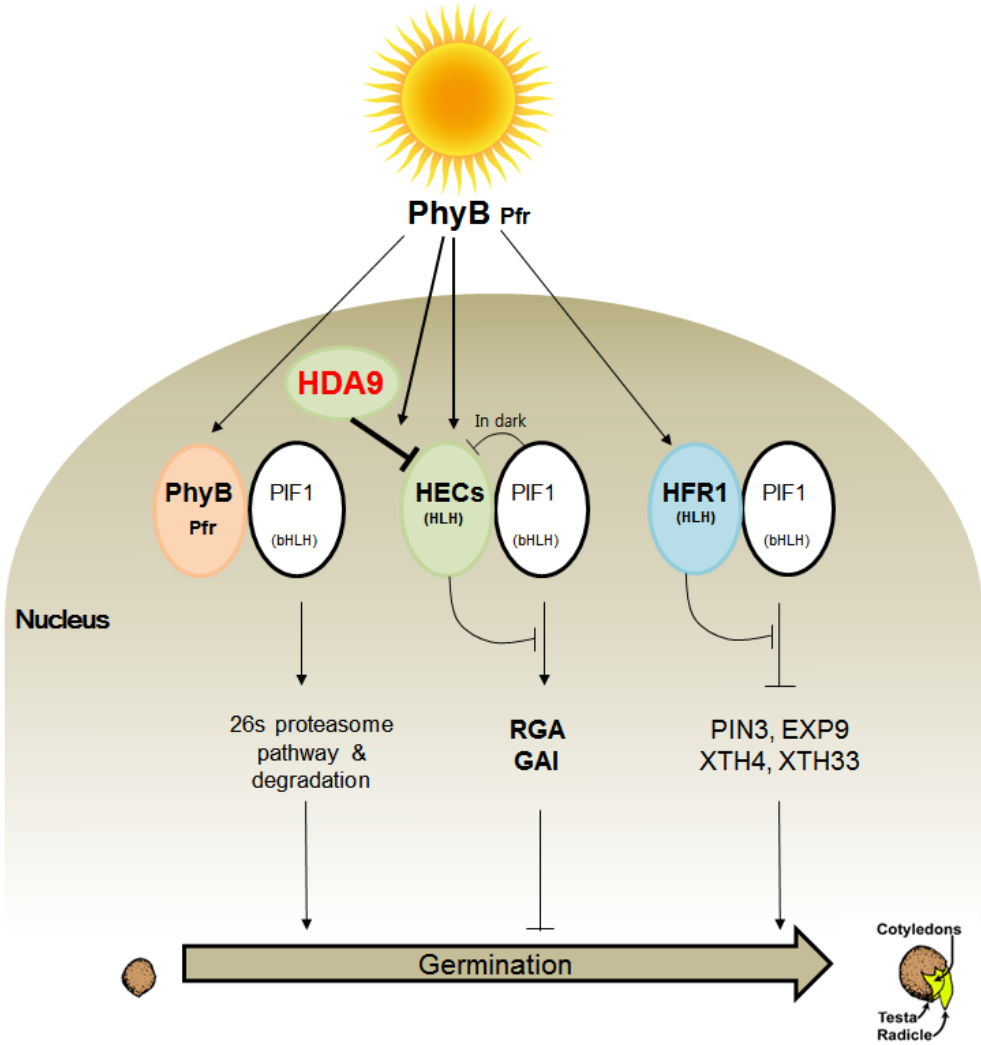

Fig. 11 Proposed working model of *HDA9-HECs-PIF1* module in phyB-dependent seed germination.

Upon exposure to red light, phyB perceives the red light and phyB Pfr form becomes activated. The activated phyB Pfr form translocate into the nucleus, where it interacts with PIF1. Interaction of PIF1 with phyB Pfr form triggers the proteolytic degradation of PIF1 via the 26S proteasome (left). In addition to phyB,

PIF1 also interact with HECs. The expression of *HECs* is induced under red light and HECs protein interacts with PIF1 to remove residual PIF1 activity. The expression of *HECs* is regulated at the transcriptional level by HDA9. HDA9 directly binds to the *HECs* chromatin and sequesters its hyperactivation via histone deacetylation. The loss of PIF1 activity through its binding with HDA9-HECs leads to the down regulation of PIF1 target genes such as *RGA* and *GAI* leading to the inhibition of illegitimate germination (middle). Under low light condition, the level of HFR1 protein is increased and prevents PIF1 to further inhibit the suppression of seed germination. This allows seeds to rapidly respond to low light initiated seed germination without delay (right). However, the relationship of HFR1 and HDA9 in the control of PIF1 is yet unclear.

3.4.11. HECs are involved in controlling the light- dependent inhibition of hypocotyl elongation by HDA9.

It was also reported that HECs positively regulate the inhibition of hypocotyl elongation (Zhu PhD thesis, 2012). Since the *hda9-1* mutation causes less elongated petioles and hypocotyls (Kang et al., 2015; unpublished data), I tested if the functional relationship between HDA9 and HECs observed in the phyB-dependent seed germination also exists in the light-mediated inhibition of hypocotyl elongation. In order to do that, *hda9-1*, *hec1hec2 RNAi*, and *hec1hec2 RNAi hda9-1* seedlings were grown in constant darkness (DD; left panel) or constant red light condition (Rc; 10 μmol/m^2s; right panel) and their hypocotyl lengths were measured and compared. As shown in Fig. 12, the hypocotyl lengths of wt, *hda9-1*, *hec1hec2 RNAi*, and *hec1hec2 RNAi hda9-1* were comparable to that of wt in DD. Under Rc, in contrast, *hda9-1* displayed shorter hypocotyls than wt, *hec1hec2 RNAi* and *hec1hec2 RNAi hda9-1*. As previous reports by Zhu PhD thesis, 2012, the hypocotyl length *hec1hec2 RNAi* was slightly longer than wt under our light condition. However, surprisingly, the short hypocotyl phenotype of *hda9-1* was masked in *hec1hec2 RNAi* background as shown by the similar hypocotyl lengths of *hec1hec2 RNAi hda9-1* and wt. Together, these results suggest that HDA9 requires HECs in controlling the phyB-dependent inhibition of hypocotyl elongation as well as seed germination (Fig. 12).

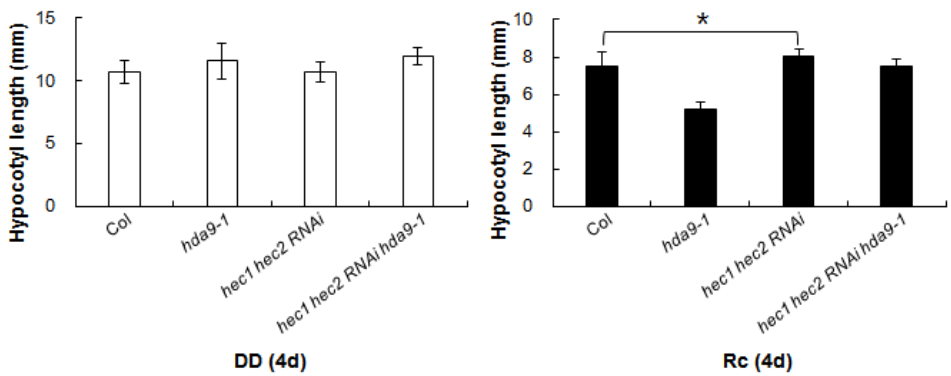

Fig.12 HECs are required for the short-hypocotyl phenotype of *hda9-1*.

Hypocotyl elongations of wild type Col, *hda9-1*, *hec1hec2 RNAi*, *hec1hec2 RNAi hda9-1*. Seedlings were grown for 4 days under constant dark (DD; left panel) or 40 μmol/m^2s of constant red light condition (Rc; right panel). Hypocotyl length was measured using ImageJ software. At least 20 individual seedlings were used for hypocotyl measurement. Bars indicate standard deviation of averages. Asterisks indicate statistically significant differences (*P <0.0005).

3.5 Discussion

Histone deacetylases have shown to be key players in differentiation and development of multicellular organisms. I and others previously reported an Arabidopsis RPD3/HDA1 class I histone deacetylases, HDA9 functions in repressing floral transition under unfavorable day-length condition. In this study I find an additional biological role of HDA9. HDA9 plays a role in germination, one of dramatic developmental transition during plant life cycle. Germination-relate gene expression studies, ChIP analyses for H3Ac levels and HDA9 binding and genetic studies for epistasis all pointed out that HDA9 controls the light-induced germination through repressing the expressions of HECs, positive regulators of light-induced germination.

Although the target genes and underlying mechanisms of HDA9-mediated regulation of flowering and germination are different, there appear some aspects in common between two events. HDA9 deacetylates chromatin of target genes (AGL19 for flowering and HECs for germination) when they are actively transcribed. This was supported by the ChIP results which show in both cases the increase in H3Ac level, the differences in H3Ac levels between wt and the mutant and HDA9 binding were more significant under the conditions that activate the expression of target genes. Thus the role of HDA9 in transcription, unlike the conventional idea of HDACs is to modulate the transcription activity of target chromatin by resetting the landscape of chromatin during active transcription. Similarly it was reported that Arabidopsis homologs of a component of Sin3-HDAC complex are recruited to *FT* chromatin only at the end of day when *FT* is

actively transcribed to dampen the *FT* expression level (Gu et al., 2013). My works suggest that above function of HDA9 in transcription act as a tool to fine-tune the timing of critical developmental transitions such as germination and flowering. Timing of germination and flowering are both exquisitely regulated by environmental stimuli. If the responses of plants to environmental stimuli are abnormal, either hyper-sensitive or hypo-sensitive, it would lead to improper timing of transitions which must be damaging to plants. The function of HDA9 to prevent hyper-activation of target gene expression in response to environmental stimuli would also prevent illegitimately early initiation of the downstream events and subsequent developmental transition. Although my work demonstrated that the recruitment of HDA9 to the *HECs* chromatin is light- dependent, its underlying mechanism of this remains unanswered. One possibility would be the light dependent expression of HDA9 in seeds. However the analyses of *HDA9* protein level in seeds either kept in dark or exposed to light (Fig. 3) showed that that is not the case. Another possibility would be that a red-light specific transcription factor(s) recruits HDA9 to the *HEC* chromatin. One of such candidates is LONG HYPOCOTYL 5 (HY5), a bZIP transcription factor which is known to directly bind to and activate the expression of the light induced genes (Chattopadhyay S., 1998). However, *HEC* transcript level was not changed by *hy5* mutation under red light (data not shown), indicating that the recruitment of HDA9 to *HECs* chromatin is not likely caused by *HY5*. It is also conceivable that HDA9 might be recruited via a component of the HDA9-containing complex that recognize the histone marks produced during transcription such as H3K4- and H3K36 methylation.

Previously it was reported that Eaf3/Rpd3C deacetylase complex can recognize H3K36 methylation mark and remove histone acetylation immediately subsequent to Pol II transcription, thus maintaining a repressive chromatin structure. Although the role of such deacetylation was known to prevent unwanted intragenic transcription initiation or cryptic transcription in yeast, it has not been clearly demonstrated in multicellular organisms. Therefore, it would be possible that HDA9 is recruited to actively transcribed chromatin in similar way but it role in the regulation of transcription is different from that in yeast. Further studies are required to decipher the molecular mechanism by which HDA9 is recruited to *HEC* chromatin in the light-dependent manner.

According to previous studies (Oh et al., 2008), PIF1 regulates gene transcription either positively or negatively depending on the target in seeds. Interestingly, a gene ChIP study (Oh et al., 2008) showed that some of light-induced genes (dark-repressed genes) are PIF1-repressed genes and I found HEC1 in the list of the genes belong to that category. My preliminary data showed that *HEC* mRNA levels were significantly increased by *pif1-2* mutation under far-red light and PIF1 protein was directly associated with *HEC* chromatin (data not shown). Thus, light promotes germination by removing PIF1 via two modes: degradation of PIF1 by activation of phyB and inhibition of PIF1 activity by increasing the level of its antagonistic interacting partners HECs. Thus, this HECs-PIF1 inhibitory circuit might serve as a safety mechanism to ensure germination by light and HDA9 refine it to prevent the start of germination by low fluence or short irradiation of light by regulating HECs levels.

References

Adamczyk BJ, Lehti-Shiu MD, Fernandez DE. 2007. The MADS domain factors AGL15 and AGL18 act redundantly as repressors of the floral transition in Arabidopsis. *Plant Journal* **50:** 1007-1019.

Adrian, J., Farrona, S., Reimer, J.J., Albani, M.C., Coupland, G. and Turck, F. 2010. cis-Regulatory elements and chromatin state coordinately control temporal and spatial expression of FLOWERING LOCUS T in Arabidopsis. *The Plant cell* **22:** 1425-1440.

Alexandre CM, Hennig L. 2008. FLC or not FLC: the other side of vernalization. *J Exp Bot* **59:**1127-1135

Amasino R. 2010. Seasonal and developmental timing of flowering. *Plant Journal* **61:** 1001-1013.

Aufsatz W, Mette MF, van der Winden J, Matzke M, Matzke AJM. 2002. HDA6, a putative histone deacetylase needed to enhance DNA methylation induced by double-standard RNA. *EMBO Journal* **21:** 6832-6841.

Aukerman MJ, Sakai H. 2003. Regulation of flowering time and floral organ identity by a MicroRNA and its APETALA2-like target genes. *Plant Cell* **15:** 2730-2741.

Benhamed M, Bertrand C, Servet C, Zhou DX. 2006. Arabidopsis GCN5, HD1, and TAF1/HAF2 interact to regulate histone acetylation required for light-

responsive gene expression. *Plant Cell* **18:** 2893-2903.

Blázquez MA, Weigel D. 2000. Integration of floral inductive signals in Arabidopsis. *Nature* **404:** 889-892.

Carey, B.W., Finley, L.W., Cross, J.R., Allis, C.D. and Thompson, C.B. 2015. Intracellular alpha-ketoglutarate maintains the pluripotency of embryonic stem cells. Nature **518:** 413-416.

Castillejo C, Pelaz S. 2008. The balance between CONSTANS and TEMPRANILLO activities determines *FT* expression to trigger flowering. *Current Biology* **18:** 1338-1343.

Chattopadhyay S, Ang LH, Puente P, Deng XW, Wei N. 1998. Arabidopsis bZIP protein HY5 directly interacts with light-responsive promoters in mediating light control of gene expression. *Plant Cell* **10:** 673-683.

Chen, H., Zhang, J., Neff, M.M., Hong, S.W., Zhang, H., Deng, X.W. and Xiong, L. 2008. Integration of light and abscisic acid signaling during seed germination and early seedling development. *Proceedings of the National Academy of Sciences of the United States of America* **105:** 4495-4500.

Cho, J.N., Ryu, J.Y., Jeong, Y.M., Park, J., Song, J.J., Amasino, R.M., Noh, B. and Noh, Y.S. 2012. Control of seed germination by light-induced histone arginine demethylation activity. *Developmental cell* **22:** 736-748.

Choi SM, Song HR, Han SK, Han M, Kim CY, Park J, Lee YH, Jeon JS, Noh

YS, Noh B. 2012. HDA19 is required for the repression of salicylic acid biosynthesis and salicylic acid-mediated defense responses in Arabidopsis. *Plant Journal* **71:** 135-146.

Cigliano, R.A., Cremona, G., Paparo, R., Termolino, P., Perrella, G., Gutzat, R., Consiglio, M.F. and Conicella, C. 2013. Histone deacetylase AtHDA7 is required for female gametophyte and embryo development in Arabidopsis. *Plant physiology* **163:** 431-440.

Clough SJ, Bent AF. 1998. Floral dip: a Simplified method for Agrobacterium-mediated transformation of *Arabidopsis thaliana*. *Plant Journal* **16:** 735-743.

Costas, C., de la Paz Sanchez, M., Stroud, H., Yu, Y., Oliveros, J.C., Feng, S., Benguria, A., Lopez-Vidriero, I., Zhang, X., Solano, R., Jacobsen, S.E. and Gutierrez, C. 2011. Genome-wide mapping of Arabidopsis thaliana origins of DNA replication and their associated epigenetic marks. *Nature structural & molecular biology* **18:** 395-400.

Cunliffe VT. 2008. Eloquent silence: developmental functions of Class I histone deacetylases. *Current Opinion in Genetics & Development* **18:** 404-410.

Dechaine, J.M., Gardner, G. and Weinig, C. 2009. Phytochromes differentially regulate seed germination responses to light quality and temperature cues during seed maturation. *Plant, cell & environment* **32:** 1297-1309.

Earley K, Lawrence RJ, Pontes O, Reuther R, Enciso A, Silva M, Neves N,

Gross M, Viegas W, Pikaard CS. 2006. Erasure of histone acetylation by Arabidopsis HDA6 mediates large-scale gene silencing in nucleolar dominance. *Genes & Development* **20:** 1283-1293.

Earley KW, Pontvianne F, Wierzbicki AT, Blevins T, Tucker S, Costa-Nunes P, Pontes O, Pikaard CS. 2010. Mechanisms of HDA6-mediated rRNA gene silencing: suppression of intergenic Pol II transcription and differential effects on maintenance versus siRNA-directed cytosine methylation. *Genes & Development* **24:** 1119-1132.

Fairchild CD, Schumaker MA, Quail PH. 2000. HFR1 encodes an atypical bHLH protein that acts in phytochrome A signal transduction. *Genes Dev* **14:** 2377-91.

Fong PM, Tian L, Chen J. 2006. *Arabidopsis thaliana* histone deaetylase 1 (AtHD1) is localized in euchromatic regions and demonstrates histone deacetylase activity in vitro. *Cell Research* **16:** 479-488.

Finch-Savage, W.E. and Leubner-Metzger, G. 2006. Seed dormancy and the control of germination. *The New phytologist* **171:** 501-523.

Gabriele, S., Rizza, A., Martone, J., Circelli, P., Costantino, P. and Vittorioso, P. 2010. The Dof protein DAG1 mediates PIL5 activity on seed germination by negatively regulating GA biosynthetic gene AtGA3ox1. *The Plant journal : for cell and molecular biology* **61:** 312-323.

Graeber, K., Linkies, A., Steinbrecher, T., Mummenhoff, K., Tarkowska, D.,

Tureckova, V., Ignatz, M., Sperber, K., Voegele, A., de Jong, H., Urbanova, T., Strnad, M. and Leubner-Metzger, G. 2014. DELAY OF GERMINATION 1 mediates a conserved coat-dormancy mechanism for the temperature- and gibberellin-dependent control of seed germination. *Proceedings of the National Academy of Sciences of the United States of America* **111:** E3571-3580.

Gremski K, Ditta G, Yanofsky MF.2007. The HECATE genes regulate female reproductive tract development in Arabidopsis thaliana. *Development* **134:** 3593-601

Grozinger CM, Schreiber SL. 2000. Regulation of histone deacetylase 4 and 5 and transcriptional activity by 14-3-3-dependent cellular localization. *Proceedings of the National Academy of Sciences, USA* **97:** 7835-7840.

Gu X, Jiang D, Wang Y, Bachmair A, He Y. 2009. Repression of the floral transition via histone H2B monoubiquitination. *Plant Journal* **57:** 522-533.

Gu X, Le C, Wang Y, Li Z, Jiang D, Wang Y, He Y. 2013. *Arabidopsis* FLC clade members form flowering-repressor complexes coordinating responses to endogenous and environmental cues. *Nature Communications* **4:** 1947.

Gu, X., Wang, Y. and He, Y. 2013. Photoperiodic regulation of flowering time through periodic histone deacetylation of the florigen gene FT. *PLoS biology* **11:** e1001649.

Gremski K, Ditta G, Yanofsky MF. 2007. HECATE genes regulate female reproductive tract development in Arabidopsis thaliana. *Development* **20:** 3593-601

Han, C. and Yang, P. 2015. Studies on the molecular mechanisms of seed germination. *Proteomics* **10:** 1671-1679

Han SK, Song JD, Noh YS, Noh B. 2007. Role of plant CBP/p300-like genes in the regulation of flowering time. *Plant Journal* **49:** 103-114.

Hayakawa T, Nakayama J. **2011.** Physiological roles of Class I HDAC complex and histone demethylases. *Journal of Biomedicine and Biotechnology* **2011:** 1-10.

He Y, Michaels SD, Amasino RM. 2003. Regulation of flowering time by histone acetylation in Arabidopsis. *Science* **302:** 1751-1754.

He Y. 2012. Chromatin regulation of flowering. *Trends Plant Sci* **17:** 556-562

Helliwell CA, Wood CC, Robertson M, Peacock WJ, Dennis ES. 2006. The Arabidopsis FLC protein interacts directly in vivo with *SOC1* and *FT* chromatin and is a part of a high-molecular-weight protein complex. *Plant Journal* **46:** 183-192.

Hollender C, Liu Z. 2008. Histone deacetylase genes in Arabidopsis development. *Journal of Integrative Plant Biology* **50:** 875-885.

Holdsworth, M.J., Bentsink, L. and Soppe, W.J. 2008. Molecular networks regulating Arabidopsis seed maturation, after-ripening, dormancy and

germination. *The New phytologist* **179:** 33-54.

Hu, Y. and Yu, D. 2014. BRASSINOSTEROID INSENSITIVE2 interacts with ABSCISIC ACID INSENSITIVE5 to mediate the antagonism of brassinosteroids to abscisic acid during seed germination in Arabidopsis. *The Plant cell* **26:** 4394-4408.

Jeong JH, Song HR, Ko JH, Jeong YM, Kwon YE, Seol JH, Amasino RM, Noh B, Noh YS. 2009. Repression of FLOWERING LOCUS T chromatin by functionally redundant histone H3 lysine 4 demethylases in Arabidopsis. *PLoS One* **25:** e8033

Jung JH, Seo YH, Seo PJ, Reyes JL, Yun J, Chua NH, Park CM. 2007. The GIGANTEA-regulated microRNA172 mediates photoperiodic flowering independent of CONSTANS in Arabidopsis. *Plant Cell* **19:** 2736-2748.

Jung, J.H., Park, J.H., Lee, S., To, T.K., Kim, J.M., Seki, M. and Park, C.M. 2013. The cold signaling attenuator HIGH EXPRESSION OF OSMOTICALLY RESPONSIVE GENE1 activates FLOWERING LOCUS C transcription via chromatin remodeling under short-term cold stress in Arabidopsis. *The Plant cell* **25:** 4378-4390.

Kang MJ, Jin HS, Noh YS, Noh B. 2015. Repression of flowering under a noninductive photoperiod by the HDA9-AGL19-FT module in Arabidopsis. *New Phytol* **206:** 281-294.

Kang, H., Oh, E., Choi, G. and Lee, D. 2010. Genome-wide DNA-binding

specificity of PIL5, an Arabidopsis basic Helix-Loop-Helix (bHLH) transcription factor. *International journal of data mining and bioinformatics* **4:** 588-599.

Kaufmann K, Muiño JM, Østerås M, Farinelli L, Krajewski P, Angenent GC. 2010. Chromatin immunoprecipitation (ChIP) of plant transcription factors followed by sequencing (ChIP-SEQ) or hybridization to whole genome arrays (ChIP-CHIP). *Nature Protocol* **5:** 457-472.

Kendall, S. 2012. Temp regulation of seed dormancy and germination in arabidopsis.

Kim, D.H., Yamaguchi, S., Lim, S., Oh, E., Park, J., Hanada, A., Kamiya, Y. and Choi, G. 2008. SOMNUS, a CCCH-type zinc finger protein in Arabidopsis, negatively regulates light-dependent seed germination downstream of PIL5. *The Plant cell* **20:** 1260-1277.

Kim, D.H. and Sung, S. 2010. The Plant Homeo Domain finger protein, VIN3-LIKE 2, is necessary for photoperiod-mediated epigenetic regulation of the floral repressor, MAF5. *Proceedings of the National Academy of Sciences of the United States of America* **107:** 17029-17034.

Kim, D.H. and Sung, S. 2013. Coordination of the vernalization response through a VIN3 and FLC gene family regulatory network in Arabidopsis. *Plan cell* **25:** 454-469.

Kim DH, Sung S. 2014. Genetic and Epigenetic Mechanisms Underlying

Vernalization. *Arabidopsis Book* **12:** e0171.

Kim JY, Oh JE, Noh YS, Noh B. 2015. Epigenetic control of juvenile-to-adult phase transition by the Arabidopsis SAGA-like complex. *Plant J* **83:** 537-545

Kim W, Latrasse D, Servet C, Zhou DX. 2013. Arabidopsis histone deacetylase HDA9 regulates flowering time through repression of AGL19. *Biochemical and Biophysical Research Communications* **432:** 394–398.

Kim KC, Lai Z, Fan B, Chen Z. 2008. *Arabidopsis* WRKY38 and WRKY62 transcription factors interact with histone deacetylase 19 in basal defense. *Plant Cell* **20:** 2357-2371.

Kim SY, Zhu T, Sung ZR. 2010. Epigenetic regulation of gene programs by EMF1 and EMF2 in Arabidopsis. *Plant Physiology* **152:** 516–528.

Kinkema M, Fan W, Dong X. 2000. Nuclear localization of NPR1 is required for activation of *PR* gene expression. *Plant Cell* **12:** 2339-2350.

Koornneef M, Alonso-Blanco C, Peeters AJM, Soppe W. 1998. Genetic control of flowering time in Arabidopsis. *Annual Review of Plant Physiology and Plant Molecular Biology* **49:** 345-370.

Koornneef M, Vrles HB, Hanhart C, Soppe W, Peeters T. 1994. The phenotype of some late-flowering mutants is enhanced by a locus on chromosome 5 that is not effective in the Landsberg erecta wild-type. *Plant Journal* **6:**

911–919.

Kurdistani SK, Robyr D, Tavazoie S, Grunstein M. 2002. Genome-wide binding map of the histone deacetylase Rpd3 in yeast. *Nature Genetics* **31:** 248-254.

Lee I, Michaels SD, Amasino RM. 1994. The late-flowering phenotype of *FRIGIDA* and mutations in *LUMINIDEPENDENS* is suppressed in the Landsberg *erecta* strain of Arabidopsis. *Plant Journal* **6:** 903-909.

Lee, N., Kang, H., Lee, D. and Choi, G. 2014. A histone methyltransferase inhibits seed germination by increasing PIF1 mRNA expression in imbibed seeds. *The Plant journal : for cell and molecular biology* **78:** 282-293.

Liu, P.P., Koizuka, N., Martin, R.C. and Nonogaki, H. 2005. The BME3 (Blue Micropylar End 3) GATA zinc finger transcription factor is a positive regulator of Arabidopsis seed germination. *The Plant journal : for cell and molecular biology* **44:** 960-971.

Liu X, Yu CW, Duan J, Luo M, Wang K, Tian G, Cui Y, Wu K. 2012. HDA6 directly interacts with DNA methyltransferase MET1 and maintains transposable element silencing in Arabidopsis. *Plant Physiology* **158:** 119-129.

Liu, X., Chen, C.Y., Wang, K.C., Luo, M., Tai, R., Yuan, L., Zhao, M., Yang, S., Tian, G., Cui, Y., Hsieh, H.L. and Wu, K. 2013. PHYTOCHROME INTERACTING FACTOR3 associates with the histone deacetylase

HDA15 in repression of chlorophyll biosynthesis and photosynthesis in etiolated Arabidopsis seedlings. *The Plant cell* **25:** 1258-1273.

Livak KJ, Schmittgen TD. 2001. Analysis of relative gene expression data using real-time quantitative PCR and the $2^{-\Delta\Delta CT}$ method. *Methods* **25:** 402-408.

Liu X, Yang S, Zhao M, Luo M, Yu CW, Chen CY, Tai R, Wu K. 2014. Transcriptional repression by histone deacetylases in plants. *Mol Plant* **7:**764-72.

Long JA, Ohno C, Simth ZR, Meyerowitz EM. 2006. TOPLESS regulates apical embryonic fate in Arabidopsis. *Science* **312:** 1520-1523.

Lu, X., Wontakal, S.N., Kavi, H., Kim, B.J., Guzzardo, P.M., Emelyanov, A.V., Xu, N., Hannon, G.J., Zavadil, J., Fyodorov, D.V. and Skoultchi, A.I. 2013. Drosophila H1 regulates the genetic activity of heterochromatin by recruitment of Su(var)3-9. *Science* **340:** 78-81.

Michaels SD, Amasino RM. 2001. Loss of FLOWERING LOCUS C activity eliminates the late flowering of *FRIGIDIA* and autonomous pathway mutants but not responsiveness to vernalization. *Plant Cell* **13:** 935-941.

Michales SD, Ditta G, Gustafson-Brown C, Pelaz S, Yanofsky M, Amasino R. 2003. AGL24 acts as a promoter of flowering in Arabidopsis and is positively regulates by vernalization. *Plant Journal* **33:** 867-874.

Molitor, A.M., Bu, Z., Yu, Y. and Shen, W.H. 2014. Arabidopsis AL PHD-PRC1

complexes promote seed germination through H3K4me3-to-H3K27me3 chromatin state switch in repression of seed developmental genes. *PLoS genetics* **10:** e1004091.

Moon J, Suh SS, Lee H, Choi KR, Hong CB, Paek NC, Kim SG, Lee I. 2003. The *SOC1* MADS-box gene integrates vernalization and gibberellin signals for flowering in Arabidopsis. *Plant Journal* **35:** 613-623.

Morris, K., Linkies, A., Muller, K., Oracz, K., Wang, X., Lynn, J.R., Leubner-Metzger, G. and Finch-Savage, W.E. 2011. Regulation of seed germination in the close Arabidopsis relative Lepidium sativum: a global tissue-specific transcript analysis. *Plant physiology* **155:** 1851-1870.

Nakabayashi, K., Bartsch, M., Xiang, Y., Miatton, E., Pellengahr, S., Yano, R., Seo, M. and Soppe, W.J. 2012. The time required for dormancy release in Arabidopsis is determined by DELAY OF GERMINATION1 protein levels in freshly harvested seeds. *The Plant cell* **24:** 2826-2838.

Nelson, D.C., Flematti, G.R., Ghisalberti, E.L., Dixon, K.W. and Smith, S.M. 2012. Regulation of seed germination and seedling growth by chemical signals from burning vegetation. *Annual review of plant biology* **63:** 107-130.

Noh B, Lee SH, Kim HJ, Yi G, Shin EA, Lee M, Jung KJ, Doyle MR, Amasino RM, Noh YS. 2004. Divergent roles of a pair of homologous jumonji/zinc-finger-class transcription factor proteins in the regulation of Arabidopsis flowering time. *Plant Cell* **16:** 2601-2613.

Noh B, Murphy AS, Spalding EP. 2001. *Multidrug resistance*-like genes of Arabidospis required for auxin transport and auxin-mediated development. *Plant Cell* **13:** 2441-2454.

Ogawa, M. 2003. Gibberellin Biosynthesis and Response during Arabidopsis Seed Germination. *The Plant Cell Online* **15:** 1591-1604.

Oh, E., Kang, H., Yamaguchi, S., Park, J., Lee, D., Kamiya, Y. and Choi, G. 2009. Genome-wide analysis of genes targeted by PHYTOCHROME INTERACTING FACTOR 3-LIKE5 during seed germination in Arabidopsis. *The Plant cell* **21**, 403-419.

Oh, E., Kim, J., Park, E., Kim, J.I., Kang, C. and Choi, G. 2004. PIL5, a phytochrome-interacting basic helix-loop-helix protein, is a key negative regulator of seed germination in Arabidopsis thaliana. *The Plant cell* **16**, 3045-3058.

Oh, E., Yamaguchi, S., Kamiya, Y., Bae, G., Chung, W.I. and Choi, G. 2006. Light activates the degradation of PIL5 protein to promote seed germination through gibberellin in Arabidopsis. *The Plant journal : for cell and molecular biology* **47**, 124-139.

Oh, E., Yamaguchi, S., Hu, J., Yusuke, J., Jung, B., Paik, I., Lee, H.S., Sun, T.P., Kamiya, Y. and Choi, G. 2007. PIL5, a phytochrome-interacting bHLH protein, regulates gibberellin responsiveness by binding directly to the GAI and RGA promoters in Arabidopsis seeds. *The Plant cell* **19:**1192-1208.

Pandey R, Muller A, Napoli CA, Selinger DA, Pikarrd CS, Richard EJ, Bender J, Mount DW, Jorgensen A. 2002. Analysis of histone acetyltransferase and histone deacetylase families of *Arabidopsis thaliana* suggests functional diversification of chromatin modification among multicellular eukaryotes. *Nucleic Acids Research* **30:** 5036-5055.

Park DH, Somers DE, Kim YS, Choy YH, Lim HK, Soh MS, Kim HJ, Kay SA, Nam HG. 1999. Control of circadian rhythms and photoperiodic flowering by the Arabidopsis *GIGANTEA* gene. *Science* **285:** 1579-1582.

Park, S.J., Kwak, K.J., Oh, T.R., Kim, Y.O. and Kang, H. 2009. Cold shock domain proteins affect seed germination and growth of Arabidopsis thaliana under abiotic stress conditions. *Plant & cell physiology* **50:** 869-878.

Penfield, S., Josse, E.M., Kannangara, R., Gilday, A.D., Halliday, K.J. and Graham, I.A. 2005. Cold and light control seed germination through the bHLH transcription factor SPATULA. *Current biology : CB* **15:** 1998-2006.

Perales M, Màs P. 2007. A functional link between rhythmic changes in chromatin structure and the Arabidopsis biological clock. *Plant Cell* **19:** 2111-2123.

Probst AV, Fagard M, Proux F, Mourrain P, Boutet S, Earley K, Lawrence RJ, Pikkard CS, Murfett J, Furner I, Vaucheret H, Scheid OM. 2004. Arabidopsis histone deacetylase HDA6 is required for maintenance of

transcriptional silencing and determines nuclear organization of rDNA repeats. *Plant Cell* **16:** 1021-1034.

Ramsey, S.A., Knijnenburg, T.A., Kennedy, K.A., Zak, D.E., Gilchrist, M., Gold, E.S., Johnson, C.D., Lampano, A.E., Litvak, V., Navarro, G., Stolyar, T., Aderem, A. and Shmulevich, I. 2010. Genome-wide histone acetylation data improve prediction of mammalian transcription factor binding sites. *Bioinformatics* **26:** 2071-2075.

Ratcliffe OJ, Kumimoto RW, Wong BJ, Riechmann JL. 2003. Analysis of the Arabidopsis *MADS AFFECTING FLOWERING* gene family: *MAF2* prevents vernnalization by short periods of cold. *Plant Cell* **15:** 1159-1169.

Rashid, A. and Deyholos, M.K. 2011. PELPK1 (At5g09530) contains a unique pentapeptide repeat and is a positive regulator of germination in Arabidopsis thaliana. *Plant cell reports* **30:** 1735-1745.

Rincon-Arano, H., Halow, J., Delrow, J.J., Parkhurst, S.M. and Groudine, M. 2012. UpSET recruits HDAC complexes and restricts chromatin accessibility and acetylation at promoter regions. *Cell* **151:** 1214-1228.

Rivera, C., Gurard-Levin, Z.A., Almouzni, G. and Loyola, A. 2014. Histone lysine methylation and chromatin replication. *Biochimica et biophysica acta* **1839:** 1433-1439.

Robin J. Probert. 2012 The Role of Temperature in the Regulation of Seed

Dormancy and Germination *Seeds: The Ecology of Regeneration in Plant Communities* **2:** 261-292

Sanchez Mde, L., Caro, E., Desvoyes, B., Ramirez-Parra, E. and Gutierrez, C. 2008. Chromatin dynamics during the plant cell cycle. *Seminars in cell & developmental biology* **19:** 537-546.

Santopolo, S., Boccaccini, A., Lorrai, R., Ruta, V., Capauto, D., Minutello, E., Serino, G., Costantino, P. and Vittorioso, P. 2015. DOF AFFECTING GERMINATION 2 is a positive regulator of light-mediated seed germination and is repressed by DOF AFFECTING GERMINATION 1. *BMC plant biology* **15:** 72.

Sassone-Corsi, P. 2013. Physiology. When metabolism and epigenetics converge. *Science* **339:** 148-150.

Schmid M, Uhlenhaut NH, Godard F, Demar M, Bressan R, Weigel D, Lohmann JU. 2003. Dissection of floral induction pathways using global expression analysis. *Development* **130:** 6001-6012.

Schönrock N, Bouveret R, Leroy O, Borghi L, Kohler C, Gruissem W, Hennig L. 2006. Plycomb-group proteins repress the floral activator *AGL19* in the *FLC*-independent vernalization pathway. *Genes & Development* **20:** 1667-1678.

Schuster C, Gaillochet C, Lohmann JU. 2015. Arabidopsis HECATE genes function in phytohormone control during gynoecium development.

Development **142:** 3343-3350

Servet, C., Conde e Silva, N. and Zhou, D.X. 2010. Histone acetyltransferase AtGCN5/HAG1 is a versatile regulator of developmental and inducible gene expression in Arabidopsis. *Mol Plant* **3:** 670-677.

Seo, M., Hanada, A., Kuwahara, A., Endo, A., Okamoto, M., Yamauchi, Y., North, H., Marion-Poll, A., Sun, T.P., Koshiba, T., et al. 2006. Regulation of hormone metabolism in Arabidopsis seeds: phytochrome regulation of abscisic acid metabolism and abscisic acid regulation of gibberellin metabolism. *Plant J* **48:** 354–366.

Seo, M., Nambara, E., Choi, G., and Yamaguchi, S. 2009. Interaction of light and hormone signals in germinating seeds. *Plant Mol. Biol* **69:** 463–472.

Sharma, V.M., Tomar, R.S., Dempsey, A.E. and Reese, J.C. 2007. Histone deacetylases RPD3 and HOS2 regulate the transcriptional activation of DNA damage-inducible genes. *Molecular and cellular biology* **27:** 3199-3210.

Shi, H., Wang, X., Mo, X., Tang, C., Zhong, S. and Deng, X.W. 2015. Arabidopsis DET1 degrades HFR1 but stabilizes PIF1 to precisely regulate seed germination. *Proceedings of the National Academy of Sciences of the United States of America* **112:** 3817-3822.

Shi, H., Zhong, S., Mo, X., Liu, N., Nezames, C.D. and Deng, X.W. 2013. HFR1 sequesters PIF1 to govern the transcriptional network underlying light-

initiated seed germination in Arabidopsis. *The Plant cell* **25:** 3770-3784.

Silva-Correia, J., Freitas, S., Tavares, R.M., Lino-Neto, T. and Azevedo, H. 2014. Phenotypic analysis of the Arabidopsis heat stress response during germination and early seedling development. *Plant methods* **10:** 7.

Shinomura, T., Nagatani, A., Chory, J., and Furuya, M. 1994. The induction of seed germination in Arabidopsis thaliana is regulated principally by phytochrome B and secondarily by phytochrome A. *Plant Physiol* **104:** 363–371.

Suzuki, Y., Kawazu, T., and Koyama, H. 2004. RNA isolation from siliques, dry seeds, and other tissues of Arabidopsis thaliana. *Biotechniques* **37:** 542.

Soh MS, Kim YM, Han SJ, Song PS. 2000. REP1, a basic helix-loop-helix protein, is required for a branch pathway of phytochrome A signaling in arabidopsis. *Plant Cell* **12:** 2061-2074.

Song, C.P. and Galbraith, D.W. 2006. AtSAP18, an orthologue of human SAP18, is involved in the regulation of salt stress and mediates transcriptional repression in Arabidopsis. *Plant molecular biology* **60:** 241-257.

Stamm, P. 2012. Insights into the molecular mech of RGL2 mediated inhibition of seed germination in arabidopsis. *BMC plant biology* **12:**179

Sung S, Schmitz RJ, Amasino RM. 2006. A PHD finger domain involved in both the verrnalization and photoperiod pathways in Arabidopsis. *Genes & Development* **20:** 3244-3248.

Sutendra, G., Kinnaird, A., Dromparis, P., Paulin, R., Stenson, T.H., Haromy, A., Hashimoto, K., Zhang, N., Flaim, E. and Michelakis, E.D. 2014. A nuclear pyruvate dehydrogenase complex is important for the generation of acetyl-CoA and histone acetylation. *Cell* **158:** 84-97.

Takada S, Goto K. 2003. TERMINAL FLOWER 2, a HETEROCHROMATIN PROTEION1-Like protein of Arabidopsis, counteracts the activation of *FLOWERING LOCUS T* by CONSTANTS in the vascular tissues of leaves to regulate flowering time. *Plant Cell* **15:** 2856-2865.

Tanaka M, Kikuchi A, Kamada H. 2008. The Arabidopsis histone deacetylases HDA6 and HDA19 contribute to the repression of embryonic properties after germination. *Plant Physiology* **146:** 149-161.

Tai HH, Tai GC, Beardmore T. 2005. Dynamic histone acetylation of late embryonic genes during seed germination. *Plant Mol Biol* **59:** 909-925.

Tian L, Chen ZL. 2001. Blocking histone deacetylation in Arabidopsis induces pleiotropic effects on plant gene regulation and development. *Proceedings of the National Academy of Sciences, USA* **98:** 200-205.

Tian L, Fong MP, Wang JJ, Wei NE, Jianf J, Doerge RW, Chen ZJ. 2005. Reversible histone acetylation and deacetylation mediate genome0wide, promoter-dependent and locus-specific changes in gene expression during plant development. *Genetics* **169:** 337-345.

Tian L, Wang J, Fong MP, Chen M, Cao H, Gelvin SB, Chen ZJ. 2003.

Genetic control of developmental changes induced by disruption of Arabidopsis histone deacetylase 1 (AtHD1) expression. *Genetics* **165:** 399-409.

Toyomasu, T., Kawaide, H., Mitsuhashi, W., Inoue, Y., and Kamiya, Y. 1998. Phytochrome regulates gibberellin biosynthesis during germination of photoblastic lettuce seeds. *Plant Physiol* **118:** 1517–1523.

To TK, Kim JM, Matsui A, Kurihara Y, Morosawa T, Ishida J, Tanaka M, Endo T, Kakutani T, Toyoda T, Kimura H, Yokoyama S, Shinozaki K, Seki M. 2011. Arabidopsis HDA6 regulates locus-directed heterochromatin silencing in cooperation with MET1. *PLoS Genetics* **7:** e1002055.

Torii KU, Mitsukawa N, Oosummi T, Matsuura Y, Yokoyamma R, Whittier RF, Komeda Y. 1996. The Arabidopsis *ERECTA* gene encodes a putative receptor protein kinase with extracellular kinase leucine-rich repeats. *Plant Cell* **8:** 735-746.

Turck F, Fornara F, Coupland G. 2008. Regulation and identity of florigen: FLOWERING LOCUS T moves center stage. *Annual Review of Plant Biology* **59:** 573-594.

van Dijk, K., Ding, Y., Malkaram, S., Riethoven, J.J., Liu, R., Yang, J., Laczko, P., Chen, H., Xia, Y., Ladunga, I., Avramova, Z. and Fromm, M. 2010. Dynamic changes in genome-wide histone H3 lysine 4 methylation patterns in response to dehydration stress in Arabidopsis thaliana. *BMC plant biology* **10:** 238.

van Zanten M, Zöll C, Wang Z, Philipp C, Carles A, Li Y, Kornet NG, Liu Y, Soppe WJ. 2014. HISTONE DEACETYLASE 9 represses seedling traits in Arabidopsis thaliana dry seeds. *Plant Journal* **80:** 475–488

Verdel A, Curtet S, Brocard MP, Rousseaux S, Lemercier C, Yoshida M, Khochbin S. 2000. Active maintenance of mHDA2/mHDA6 histone-deacetylase in the cytoplasm. *Current Biology* **10:** 747-749.

Villedieu-Percheron, E., Lachia, M., Jung, P.M., Screpanti, C., Fonne-Pfister, R., Wendeborn, S., Zurwerra, D. and De Mesmaeker, A. 2014. Chemicals inducing seed germination and early seedling development. *Chimia* **68:** 654-663.

Wang JW, Czech B, Weigel D. 2009a. miR156-regulated SPL transcription factors define an endogenous flowering pathway in *Arabidopsis thaliana*. *Cell* **138:** 738-749.

Wang, Y., Gu, X., Yuan, W., Schmitz, R.J. and He, Y. 2014. Photoperiodic control of the floral transition through a distinct polycomb repressive complex. *Developmental cell* **28:** 727-736

Wang Z, Cao H, Chen F, Liu Y. 2014. The roles of histone acetylation in seed performance and plant development. *Plant Physiol Biochem* **84:**125-33

Wang Z, Zang C, Cui K, Schones DE, Barski A, Peng W, Zhao K. 2009b. Genome-wide mapping of HATs and HDACs reveals distinct functions in

active and inactive genes. *Cell* **138:** 1019-1031.

Wang Z, Cao H, Sun Y, Li X, Chen F, Carles A, Li Y, Ding M, Zhang C, Deng X, Soppe WJ, Liu YX. 2013. Arabidopsis paired amphipathic helix proteins SNL1 and SNL2 redundantly regulate primary seed dormancy via abscisic acid-ethylene antagonism mediated by histone deacetylation. *Plant Cell* **25:**149-166.

Weitbrecht, K., Muller, K. and Leubner-Metzger, G. 2011. First off the mark: early seed germination. *Journal of experimental botany* **62:** 3289-3309.

Wu K, Zhang L, Zhou C, Yu CW, Chaikam V. 2008. HDA6 is required for jasmonate response, senescence and flowering in Arabidopsis. *Journal of Experimental Botany* **59:** 225-234.

Xu CR, Liu C, Wang YL, Li LC, Chen WQ, Xu ZH, Bai SN. 2005. Histone acetylation affects expression of cellular patterning genes in the Arabidopsis root epidermis. *Proceedings of the National Academy of Sciences, USA* **102:** 14469-14474.

Yamaguchi, S., Smith, M.W., Brown, R.G., Kamiya, Y., and Sun, T. 1998. Phytochrome regulation and differential expression of gibberellin 3betahydroxylase genes in germinating Arabidopsis seeds. *Plant Cell* **10:** 2115–2126.

Yamauchi, Y., Takeda-Kamiya, N., Hanada, A., Ogawa, M., Kuwahara, A., Seo, M., Kamiya, Y., and Yamaguchi, S. 2007. Contribution of gibberellin

deactivation by AtGA2ox2 to the suppression of germination of dark-imbibed Arabidopsis thaliana seeds. *Plant Cell Physiol* **48:** 555–561.

Yang KY, Kim YM, Lee S, Song PS, Soh MS. 2003. Overexpression of a mutant basic helix-loop-helix protein HFR1, HFR1-deltaN105, activates a branch pathway of light signaling in Arabidopsis. *Plant Physiol* **133:**1630-1642

Yang, X.J. and Seto, E. 2007. HATs and HDACs: from structure, function and regulation to novel strategies for therapy and prevention. *Oncogene* **26:** 5310-5318.

Yang XJ, Seto, E. 2008. The Rpd3/Hda1 family of lysine deacetylases: from bacteria and yeast to mice and men. *Nature Reviews Molecular Cell Biology* **9:** 206-218.

Yang, Y. and Karlson, D. 2013. AtCSP1 regulates germination timing promoted by low temperature. *FEBS letters* **587:** 2186-2192.

Yano, R., Takebayashi, Y., Nambara, E., Kamiya, Y. and Seo, M. 2013. Combining association mapping and transcriptomics identify HD2B histone deacetylase as a genetic factor associated with seed dormancy in Arabidopsis thaliana. *The Plant journal : for cell and molecular biology* **74:** 815-828.

Yelagandula, R., Stroud, H., Holec, S., Zhou, K., Feng, S., Zhong, X., Muthurajan, U.M., Nie, X., Kawashima, T., Groth, M., Luger, K., Jacobsen, S.E. and Berger, F. 2014. The histone variant H2A.W defines

heterochromatin and promotes chromatin condensation in Arabidopsis. *Cell* **158:** 98-109.

Yoo SK, Wu X, Lee JS, Ahn JH. 2011. AGAMOUS-LIKE 6 is a floral promoter that negatively regulates the *FLC/MAF* clade genes and positively regulates *FT* in Arabidopsis. *Plant Journal* **65:** 62-76.

Yoo SK, Chung KS, Kim J, Lee JH, Hong SM, Yoo SJ, Yoo SY, Lee JS, Ahn JH. 2005. CONSTANS activates *SUPPRESSOR OF OVEREXPRESSION OF CONSTANS 1* through *FLOWERING LOCUS T* to promote flowering in Arabidopsis. *Plant Physiology* **139:** 770-778.

Yu CW, Liu X, Luo M, Chen C, Lin X, Tian G, Lu Q, Cui Y, Wu K. 2011. HISTONE DEACETYLASE6 interacts with FLOWERING LOCUS D and regulates flowering in Arabidopsis. *Plant Physiology* **156:** 172-184.

Yu H, Xu Y, Tan EL, Kumar PP. 2002. AGAMOUS-LIKE 24, a dosage-dependent mediator of the flowering signals. *Proceedings of the National Academy of Sciences, USA* **99:** 16336-16341.

Zografos BR, Sung S. 2012. Vernalization-mediated chromatin changes. *J Exp Bot* 63:4343-4348.

Zhou C, Zhang L, Duan J, Miki B, Wu K. 2005. HISTONE DEACETYLASE 19 is involved in jasmonic acid and ethylene signaling of pathogen response in Arabidopsis. *Plant Cell* **17:** 1196-1204.

Zhou, J., Wang, X., He, K., Charron, J.B., Elling, A.A. and Deng, X.W. 2010.

Genome-wide profiling of histone H3 lysine 9 acetylation and dimethylation in Arabidopsis reveals correlation between multiple histone marks and gene expression. *Plant molecular biology* **72:** 585-595.

Zhu L. 2012. The HECATE proteins promote photomorphogenesis by negatively regulating the function of PIF1 in Arabidopsis, *PhD Thesis*

Zhou, Y., Tan, B., Luo, M., Li, Y., Liu, C., Chen, C., Yu, C.W., Yang, S., Dong, S., Ruan, J., Yuan, L., Zhang, Z., Zhao, L., Li, C., Chen, H., Cui, Y., Wu, K. and Huang, S. 2013. HISTONE DEACETYLASE19 interacts with HSL1 and participates in the repression of seed maturation genes in Arabidopsis seedlings. *The Plant cell* **25:** 134-148.

국문 초록

히스톤 아세틸화와 탈아세틸화는 유전자 발현을 결정하는 중요한 변형 중 하나이다. 최근 연구들에서 히스톤 탈아세틸화는 유전자 발현 억제뿐만 아니라, 아세틸화와 함께 유전자 발현 활성에도 밀접한 연관이 있다는 것이 보고되었다. 하지만 식물의 발달과정에서 유전자 발현 활성 조절에 필요한 히스톤 탈아세틸화 효소에 대해서는 현재까지 충분히 연구되어 있지 않다. 따라서 본 연구는 모델식물인 애기장대에서 유전자 발현활성의 균형을 유지하는데 HDA9이 필요하다는 것에 연구의 초점을 두었다.

식물에서 HAT과 HDAC 효소에 의한 히스톤 변형은 외부 환경에 반응하여 종자발아 및 개화시기 조절 등의 발달과정에 영향을 준다. 식물이 영양생장에서 생식생장으로 전이되는 과정은 성공적인 생식을 위해 중요하며, 이는 주요 유전자의 히스톤 변형을 동반한다. 본 연구에서는 단일 조건 특이적인 *hda9* 돌연변이체의 조기개화 현상이 광주기 의존적 개화 촉진 인자인 *AGL19* 과발현을 동반함을 확인하였다. 나아가 HDA9은 히스톤 탈아세틸화를 통해 단일 조건과 춘화 처리 신호에 의해 과발현될 *AGL19* 전사활성을 억제하고, 이어 개화 호르몬인 *FT* 전사활성에 영향을 주어 조기 개화를 제한함을 증명하였다.

개화뿐만 아니라, 종자가 주어진 환경에서 발아시기를 최적화 하는 일은 생존과 생장을 위한 중요한 과정 중 하나이다. 본 연구에서는 종자 발아 촉진 인자인 *HEC*가 적색광에 의해 유도되고, 과발현될 *HEC*를 HDA9이

히스톤 탈아세틸화를 통해 억제함을 확인하였다. 따라서, 적절한 *HEC* 전사활성을 유지하는데 히스톤 탈아세틸화가 필요함을 증명하였다. 더 나아가 HDA9-HEC-PIF1 모듈을 통해 HDA9이 비정상적인 종자발아 현상을 지연시킨다는 것을 규명하였다.

본 연구는 개화와 종자발아 등 식물의 발달과정에서 HDA9이 외부 환경요인에 의해 과발현될 AGL19, HEC 등의 전사활성의 균형을 유지시키기 위해 국부적으로 과활성화될 수 있는 염색질을 에피유전학적으로 재프로그래밍함에 중요한 인자임을 증명하였다. 이러한 HDA9 기능은 기존에 알려진 히스톤 탈아세틸화 효소들의 역할과 구분되는 독특한 것이며, 향후 애기장대의 발달 연구에 있어서 히스톤 탈아세틸화 효소들의 보다 다양한 기능이 규명될 가능성을 시사한다.

주요어: 히스톤 탈아세틸화, HDA9, AGL19, 개화시기, HEC, 종자발아

학 번: 2008-30102

이학박사학위논문

애기장대 히스톤 탈아세틸화 효소 HDA9의 개화 및 발아 관련 기능에 대한 연구

A Study on the Role of Histone Deacetylase HDA9 in Arabidopsis Flowering and Germination

2016년 2월

서울대학교 대학원

생명과학부

강 민 정

Abstract

A Study on the Role of Histone Deacetylase HDA9 in Arabidopsis Flowering and Germination

Min-Jeong Kang

Department of Biological Sciences

The Graduate School

Seoul National University

Posttranslational acetylation of histones is reversibly regulated by histone deacetylases (HDACs). Despite the evident significances of HDACs in Arabidopsis development, the biological roles and underlying molecular mechanisms of many HDACs are yet to be elucidated. In this study, I revealed the biological role of the RPD3/HDA1-class histone deacetylase HDA9 in resetting histone acetylation levels during active transcription to maintain proper transcription activity in two major phase transition of plants; seed germination and flowering.

Loss-of-function in *HDA9* flowered early under non-inductive short-day

(SD) condition and showed increased expression of the floral integrator, *FT* and floral activator, *AGL19*. The *hda9* mutation increased histone H3 acetylation and RNA polymerase II occupancy at *AGL19* chromatin but not *FT* during active transcription. In addition, HDA9 directly targeted *AGL19*, and *AGL19* expression was higher in SD than LD condition. The *agl19* mutation is epistatic to the *hda9* mutation, masking the early flowering and increased *FT* expression of *hda9*. Taken together, my data indicates that HDA9 prevents precocious flowering in SD by curbing the hyper-activation of *AGL19*, an upstream activator of *FT*, through resetting local chromatin environment.

Epigenetic regulation network through HAT and HDAC is known to play crucial roles in seed development. Timing of seed germination is controlled by various environmental factors in order to initiate a successful new life cycle under favorable environment. Light is the most critical environmental factor to promote seed germination. Light-induced germination process involves the perception of light mainly by phytochrome B (phyB) and degradation of the germination repressor PHYTOCHROME INTERACTING FACTOR (PIF1) resulted from its interaction with phyB.

Through this study, I found out that HDA9 adds a new layer of regulation for phyB-dependent germination process. Loss-of-*HDA9* activity caused rapid germination after red-light pulse treatment and under continuous white light. The expressin of *HECs*, previously known repressors of PIF1 transcription activity was also increased in the *hda9* mutant. Epistatic analysis between the *hda9* mutant and

hec1hec2 RNAi showed that rapid seed germination of the *hda9* mutant was caused by the increased *HECs* expression. Histone H3 acetylation level and RNA polymerase II occupancy at *HECs* were more elevated in *hda9-1* than in wt after red light pulse but not after far-red light pulse. The direct association of HDA9 with *HECs* chromatin was also observed after red light pulse but not after far-red light pulse. Furthermore, HDA9 also affect the expression of *GA-INSENSITIVE (GAI)* and *REPRESSOR OF GA1-3 (RGA/RGA1),* downstream target genes of *PIF1*. Taken together, my results indicate that HDA9 plays a role in the prevention of the hyper light-sensitive germination by inhibiting the hyper-activation of *HECs* transcription by light through deacetylating *HEC* chromatin during active transcription. Thus, HDA9 acts as a fine-tuning mechanism of phyB-dependent germination ensuring the beginning of germination under proper light condition.

In conclusion, throughout my research, I focused on the identification of the novel roles of HDA9 during seed germination and flowering. The role of HDA9 in transcription, unlike the conventional idea of HDACs is to modulate the transcription activity of target chromatin (*AGL19* and *HECs*) by resetting the landscape of chromatin during active transcription.

Key words: histone deacetylation, histone deacetylase (HDA9), HECATE (HEC), seed germination, AGAMOUS-LIKE 19 (AGL19), flowering.

Student Number: 2008-30102

Contents

List of tables

Chapter II.

Chapter III.

List of figures

Chapter I. General introduction

Chapter II.

Chapter III.

Abbreviations

AGL19	AGAMOUS-LIKE 19
bP	base pair
ChIP	chromatin immunoprecipitation
DAP	days after planting
DNA	deoxyribonucleic acid
FLC	FLOWERING LOCUS C
FT	FLOWERING LOCUS T
Fp	far-red light pulse
GAI	GA-INSENSITIVE
GUS	β-glucuronidase
HA	hemagglutinin
HDAC	Histone deacetylation
HDA9	Histone deacetylase 9
HEC	HECATE
K	lysine
kD	kilodalton
LD	long day
LN	leaf number

MS	Murashige-skoog
mRNA	messenger ribonucleic acid
N	nuclear protein
NN	nonnuclear protein
NV	nonvernalization
PAGE	polyacrylamide gel
PCR	polymerase chain reaction
phyB	phytochrome B
PIF1	PHTOCHROME INTERACTING FACTOR 1
qPCR	quantitative polymerase chain reaction
RAM	root apical meristem
RGA	REPRESSOR OF GA1-3
Rp	red light pulse
RT	reverse-transcription
SAM	shoot apical meristem
SD	short day
SDS	sodium dodecyl sulfate
S.E	standard error
UTR	untranslated region
V	vernalization

General introduction

1. Epigenetics and gene regulation

Multicellular eukaryotes are composed of structurally distinctive and membrane-enclosed organelles. They have developed well-organized systems for the regulation of gene expression. Eukaryotic organs and tissues are affected by differential gene expression during development. Gene-expression control in eukaryotes begins with an access to DNA before transcription initiation. The DNA accessibility is related with epigenetics, which allows stable differential gene expressions without changes in DNA sequence. These epigenetically regulated expression patterns are heritable through mitotic and/or meiotic cell divisions.

Hitherto, three main mechanisms are acknowledged underlying epigenetic gene regulations: histone modification, DNA methylation, and ATP-dependent chromatin remodeling. In addition, small or long non-coding RNAs are recently ascertained to affect chromatin structure and transcription control via RNA interference (RNAi) pathways (Holoch and Moazed, 2015). Moreover, crosstalks between these mechanisms also exist. Occurrence of one mechanism may promote another to arise in cooperative manner or may also be disrupted by another due to antagonistic effects between them. Therefore, multiple epigenetic mechanisms provide a higher level of complexity and more fine-tuned control for the regulation of gene expression.

1.1 Histone modification

Chromatin modification exerts critical roles in cell proliferation, differentiation, cell-cycle regulation, and cell function in all eukaryotes. Generally, 147 base pairs (bp) of DNA wraps around a compact histone octamer, which is assembled by two H2A-H2B histone heterodimers and two H3-H4 histone heterodimers, forming 'beads-on-a-string'-like structure. The histone octamer and the surrounding DNA make interactions through the core histone fold and its N-terminal tails. Indeed, N-terminal tails of each histone proteins are exposed to the outer surface of histone octamer in such way that many chemical modifications can frequently occur on those tails and thus easily modulate the transcription of the adjacent DNA (Strahl and Allis, 2000; Zhang and Reinbag, 2001; Berger, 2002).

The compaction of chromatin changes depending on the stage of cell cycle, and its conformational change alters the accessibility of RNA polymerase and transcription regulatory proteins to the DNA strand. Chromatin loosening during interphase allows RNA and DNA polymerases to approach for transcription and replication. Genes within the relaxed state of chromatin, called euchromatin, are actively transcribed and associated with RNA polymerases. On the other hand, heterochromatin, more condensed state of chromatin, is responsible for repression of gene expression during the remaining of cell cycles and serves to protect chromosome integrity.

Histone modification has been widely studied, and different types of histone modification mechanisms have been examined. Covalent histone posttranslational modifications, including acetylation, methylation, phosphorylation, sumoylation,

ubiquitination, and ADP-ribosylation, play critical roles in epigenetic control of transcription. Among them, acetylation and methylation are the most profoundly studied histone modifications. The first one will be further discussed in detail in the following sections. Briefly, histone methylation can either increase or decrease transcription activity depending on which lysine or arginine on the N-terminal tails of the histones is modified. Histone phosphorylation is associated with chromatin compaction during mitosis and meiosis. Histone ubiquitination is a covalent modification on lysine residues, and its function is determined upon the substrate specificity or the degree of ubiquitination. Sumoylation also involves a covalent attachment of small ubiquitin-like modifier to lysine residues and is responsible for the repression of its target gene. ADP-ribosyltransferases catalyze mono- and poly-ADP ribosylation at glutamate and arginine residues, and this type of posttranslational modification occurs reversibly in various cellular processes (Bannister and Kouzarides, 2011).

1.1.1 Histone acetylation

It has been demonstrated that histone acetylation is associated with transcriptional activation in various cellular processes such as chromatin dynamics, cell cycle progression, DNA repair, and many others. This type of modification is catalyzed by histone acetyltransferases (HATs), which are also known as transcriptional co-activators. These enzymes neutralize the positive charge on the lysine residues at N-terminal tails of histone proteins by transferring an acetyl group from acetyl-coenzyme A (acetyl-CoA) to the NH_3^+ of the amino group on

the histone tails. Neutralization of the lysine residues leads to a weaker binding between the core histone proteins and the negatively charged DNA, and this allows the chromatin to be in an open conformation. Moreover, transferred acetyl group can be recognized by a reader module, such as bromodomain, of other proteins that finally allow additional loosening of chromatin. As a result, RNA polymerase and transcription factors are prone to access the euchromatin region. Generating binding sites for protein-protein interaction ensues in gene activation located on the chromatin. Indeed, expression of transcribed gene is correlated with enriched HATs on the gene locus. Several studies have demonstrated that HATs are preferentially associated with promoters or exonic regions of target genes. In addition, from studies on genome-wide distribution maps, it is revealed that recruitment of HATs and RNA polymerase II binding are positively correlated each other, supporting the idea that histone acetylation serves as an important positive regulator of its target gene expression (Barski et al., 2007; Shahbazian and Grunstein, 2007; Wang et al., 2009).

HATs are classified into two families depending on their subcellular localizations: type-A in the nucleus and type-B in the cytoplasm. Type-A HATs are diverse and function within context. They often recognize acetylated lysine residues with their conserved bromodomain. According to their structural features and functional roles, type-A HATs are subdivided into separate groups of the cAMP Responsive Element-Binding Protein (CREB)-Binding Protein (CBP)/p300 family, the MOZ, Ybf2/Sas3, Sas2, and Tip60 (MYST) family, the GCN5-Related N-terminal Acetyltransferase (GNAT) family, the TATA-Binding Protein-

Associated Factor $(TAF)_{II}250$ family, and the mammalian-specific nuclear hormone-related HAT family, ACTR/AIB1 and SRC1 (Neuwald and Landsman, 1997: Goodman and Smolik, 2000; Sterner and Berger, 2000; Roth et al., 2001; Kalkhoven, 2004; Hodawadekar and Marmorstein, 2007; Lee and Workman, 2007). Type-B HATs, on the other hand, acetylate free histones prior to their assembly into nucleosomes (Hodawadekar and Marmorstein, 2007; Yang and Seto, 2007; Bannister and Kouzarides, 2011). They function on newly synthesized histone H3 and histone H4, while type-A members act on H2A, H2B, H3 and H4. Moreover, they share higher amino-acid sequence similarity than type-A HATs (Parthun, 2007; Bannister and Kouzarides, 2011).

In Arabidopsis, 12 genes are identified to encode HATs, and they are classified into four groups as summarized in Fig.1-1(a) (Pandey et al., 2002; Liu et al., 2012). Moreover, N-terminal lysine residues of histone H3 (K9, K14, K18, K23, and K27) and H4 (K5, K8, K12, K16, and K20) are well conserved as acetylation or de-acetylation sites in Arabidopsis (Servet et al., 2010). Five proteins, named as HACs in Arabidopsis, are members of CBP/P300 family: HAC1, HAC2, HAC4, HAC5, and HAC12. In plant, there are more number of this type of HATs than animals which usually possess only one or two homologs. MYST-family members are called as HAM1/HAG4 and HAM2/HAG5. HAG1/GCN5, HAG2, and HAG3/ELP3 belong to the GNAT family. Moreover, two of the TATA-binding protein-associated factor (TAFII 250)-family members are renamed as HAF1 and HAF2/TAF1 in Arabidopsis. The classification of Arabidopsis HATs are summarized in Fig1-1(a).

HATs play critical roles in many cellular processes in Arabidopsis. Among the CBP/p300-family members, HAC1 functions in flowering-time control (Deng et al., 2007; Han et al., 2007) and immune response (Singh et al., 2014). In addition, HAC1 and HAC5 are involved in the ethylene-signaling pathway (Li et al., 2014). In the TAFII family, HAF2 is required to integrate light response such as in chlorophyll accumulation (Bertrand et al., 2005; Renhamed et al., 2006). The GNAT/MYST family, the most extensively studied group of HATs, function in developmental processes, cell differentiation, leaf or floral organogenesis, and meristem function (Servet et al., 2010). Moreover, HAG1/GCN5 mutations result in various pleiotropic defects during developmental process. The role of HAG1/GCN5 is well characterized in root and shoot development, flower development, micro RNA (miRNA) production, light signaling and response, and low-temperature response (Bertrand et al., 2003; Renhamed et al., 2006; Earley et al., 2007; Servet et al., 2010; Wang et al., 2014; Kim et al., 2015). HAG2 is necessary for DNA replication and cell cycle progression (Ramirez-Parra et al., 2003; Vandepoele et al., 2005). HAG3 is involved in ABA response, oxidative stress, cell-cycle progression, immune responses, and leaf patterning (Nelissen et al., 2005; Chen et al., 2006; Zhou et al., 2009; Defraia et al., 2010; Xu et al., 2012). In short, histone acetylation is one of the most important posttranslational modification that affect transcription activities in various developmental aspects and environmental responses.

1.1.2 Histone deacetylation

Conformation change of chromatin via histone acetylation is reversible by histone deacetylases (HDACs), which have an opposite role against HATs. They remove the acetyl group from N-acetyl lysine residues in both histone and non-histone proteins. Histone deacetylation turns neutralized histone tail back into positively charged one and tight binding between the histone tail and the DNA backbone is reestablished, resulting in heterochromatin state of the modulated chromatin. The compacted chromatin structure prevents access of transcription factors and RNA polymerases to the target DNA, and thus transcription repression occurs (Cress and Seto, 2000; Yang and Seto, 2003).

HDACs, also known as transcriptional co-repressors, are traditionally considered to be recruited to mainly repressed genes replacing HATs. However, based on recent findings, it has been revealed that HDAC-enrichment patterns are more dynamic than anticipated through transient bindings of HATs and HDACs and via crosstalk with other types of histone modifications. Three association models of HDAC-binding mechanisms were established through genome-wide studies (Wang et al., 2009). First, as a contradiction to the traditional hypothesis, HDACs are more enriched on active genes rather than repressed ones. HDACs are recruited on active genes to maintain a suitable level of histone acetylation. After transcription activation followed by acetylation, chromatin status is normally required to be reset. Then, HDACs are recruited and function on those genes to reset their acetylation levels. Moreover, excessive acetylation of histones in

transcribed regions may result in cryptic initiation of transcription due to the destabilized chromatin status. Hence, it is a requisite for active genes to be controlled by HDACs for their adequate acetylation levels. In addition, both HATs and HDACs are detected at the highest levels on actively transcribed genes. In other words, the binding patterns of HDACs are positively correlated with transcription, RNA polymerase II occupancy, and histone acetylation levels. Second, HDACs are associated with poised genes, which are primed by histone H3 lysine 4 (H3K4) methylation or histone H2A.Z variant. H3K4 methylation or H2A.Z priming prepares yet-to-be expressed genes for activation by modulating the chromatin architecture to facilitate acetylation. HATs then transiently bind on the chromatin regions, transfer acetyl groups and potentiate future activation upon activation signals. Simultaneously and dynamically, HDACs function to reduce acetylation to keep the primed gene unexpressed until signaling. Low level distribution patterns of both HATs and HDACs on primed genes were observed genome-widely (Wang et al., 2009). In short, transient acetylation and deacetylation occur concurrently and sporadically to poise silent genes adept for further activation. Third, HDACs are recruited on silent genes with unexpectedly low frequency at undetectable levels. Unlike silenced but primed genes, neither histone acetylation nor deacetylation activities were detected on these repressive non-primed genes. It is clear that enriched level of histone H3 lysine 27 (H3K27) trimethylation, generated by the Polycomb Group (PcG) complex, is related with the gene silencing. However, it is not evident that HATs or HACs function on those genes for transcriptional regulation. Therefore, depending on target genes and

their chromatin status, role of HDACs may vary.

HDACs can be classified into 4 different classes, from I to IV, based on sequence similarity among them (Yang and Seto, 2007). Depending on species, entitlement can be differed. Fig1-1(b) shows the phylogenetic trees of Arabidopsis HDACs, illustrating the similarity of HDAC domains using neighbor-joining algorithm. In Arabidopsis, 18 HDAC proteins are categorized into three large groups. 12 of the Arabidopsis 18 HDACs belong to the yeast Reduced Potassium Deficiency (RPD3/HDA1) superfamily, which are named as HDAs in Arabidopsis. Other 4 belong to the plant-specific Histone Deacetylase 2 (HD2) family, known as HD-tuins (HDT), and the other 2 belong to the yeast Silent Information Regulator 2 (SIR2) family and are termed as SiRTuin 1 (SRT). Then, RPD3/HDA1 superfamily of plant HDACs is further divided into three subclades, Class I, II, and III, based on their homology to yeast HDAC proteins. Arabidopsis Class I HDAC proteins are most closely related to the yeast RPD3 family, and Arabidopsis Class II to the yeast HDA1 family. Class III members share no sequence homology with yeast HDACs. (Rundlett et al., 1996; Grozinger et al., 1999; Gao et al., 2002; Pandey et al., 2002). In Arabidopsis, 6 HDA proteins belong to Class I: HDA6, HDA7, HDA9, HDA10, HDA17, and HDA19. This class of the RPD3/HDA1 includes most of identified Arabidopsis HDA proteins. Of the 6 Class I proteins, HDA6 and HDA19 are most profoundly investigated for their function and mechanism. HDA6 functions in the acceleration of flowering, repression of embryonic trait, and light-induced chromatin compaction (Tanaka M et al., 2008; Snoek LB et al., 2009; Yu CW et al., 2011). HDA19 is involved in light-mediated hypocotyl elongation,

repression of salicylic acid (SA) biosynthesis and SA-dependent defense response (Benhamed et al., 2006; Choi et al., 2012). Moreover, HDA9, HDA10, and HDA17 are proposed to be involved in disease resistance because the intergenic sequence between *HDA9* and *HDA10* genes and *HDA17* gene is annotated as 'disease-resistance-like' gene in the Genebank database. Yet, Class I members, other than HDA6 and HDA19, are not extensively characterized for their function and mechanism. In the Chapter II and III of this thesis, I will demonstrate the mechanism and biological role of HDA9 in photoperiodic flowering and seed germination in detail. Class II proteins include the following three HDACs that contain subcellular localization signals: HDA5, HDA15, and HDA18. Among them, HDA5 and HDA18 possess putative nuclear export signals and may be shuttled between nucleus and cytoplasm (Grozinger and Schreiber, 2000; Verdel et al., 2000). HDA15 encompasses a RanBP zinc-finger domain which was shown to function in nucleocytoplasmic transport and nuclear envelope localization (Vetter et al., 1999). HDA2 is a sole member of Class III and has an incomplete HDAC domain. Class III proteins contain sequences similar to bacterial acetoin utilization proteins and cyanobacteria glutamine syntheses, suggesting that class III HDACs may have a novel function derived from bacterial origin (Pandey et al., 2002). Moreover, the Arabidopsis genome encodes plant-specific HDAC proteins which are categorized as the HD2 superfamily: HDT1, HDT2, HDT3, and HDT4 (Danql et al., 2001; Pandey et al., 2002; Wu et al., 2003). Two members of this family, HDT1 and HDT3, have antagonistic effects in seed development (Wu et al., 2000; Colville et al., 2011). In addition, there are two members (SRT1 and SRT2) in the

SRT superfamily which are NAD-dependent HDACs. These HDACs were identified to have a distinctive NAD-dependent ADP-ribosyltransferase activity in addition to the HDAC activity (Frye, 1999; Imai et al., 2000). Arabidopsis SRT2, a homolog of yeast Sir2, functions as a negative regulator in basal defense by suppressing SA biosynthesis (Wang et al., 2010).

It is clear that identified HDACs play critical roles in the regulation of various biological processes in Arabidopsis, including seed germination, development, and defense against diverse pathogen infections. As briefly mentioned above, HDA6 and HDA19 are the most studied HDACs in Arabidopsis. HDA6 acts as a global repressor in jasmonate (JA) signaling, senescence, embryonic-fate suppression, transgene and transposon silencing, RNA-directed DNA methylation, and flowering (Aufsatz et al., 2002; Probst et al., 2004; Tanaka et al., 2008; Hollender and Liu, 2008; Wu et al., 2008; Earley et al., 2010; To et al., 2011; Yu et al., 2011; Liu et al., 2012). The closest homolog of HDA6, HDA19, also functions as a global repressor during embryonic and flower development, immune response, JA and ethylene response, and light signaling (Tian et al., 2003; Zhou et al., 2005; Benhamed et al., 2006; Long et al., 2006; Kim et al., 2008; Hollender and Liu., 2008; Choi et al., 2012). Loss of *HDA19* also results in developmental abnormalities (Tanaka et al., 2008). HDA7, another member of the Class I RPD3/HDA1 Superfamily, is required for female-gametophyte development and embryogenesis (Cigliano RA et al., 2013). Moreover, an alteration of *HDA7* expression may lead to delay in post-germination and later developmental growth (Ciqliano et al., 2013). HDA5, belonging to the Class II

RPD3/HDA1 Superfamily, is involved in flowering regulation by repressing *FLOWERING LOCUS C (FLC)* and *MADS AFFECTING FLOWERING 1 (MAF1)/ FLOWERING LOCUS M (FLM)* expression (Luo M et al., 2015). Moreover, HDA5 and HDA6 form a complex with FLOWERING LOCUS D (FLD) and FVE to control flowering and gene expression (Luo et al., 2015). It is now more and more evident that multiple HDAC complexes are involved in higher level regulation of target gene expression. HDA15, belonging to the Class II of RPD3/HDA1 Superfamily of Arabidopsis, is involved in repression of chlorophyll biosynthesis and photosynthesis in etiolated seedlings (Liu X et al., 2013). Furthermore, a proper HDA15 activity requires PIF3 recruitment on their co-target genes for chlorophyll biosynthesis and photosynthesis in the dark (Liu et al., 2013). Deciphering an HDAC complex, formed not only by HDAC-multiplex but also with transcription factors or other proteins, provides deeper understanding of epigenetic regulatory mechanisms of histone deacetylation.

In my dissertation, I will specifically focus on the understanding of the biological roles and the mechanism of HDA9. Throughout my research, HDA9 has been anticipated to play pivotal roles in various biological responses from seed germination to flowering regulation upon environmental signals through epigenetic mechanisms on its target genes. As depicted in the phylogenetic tree (Fig.1), HDA9 shares high sequence similarity with HDA10 and HDA17, which might represent endoduplication and rearrangement of an important gene during evolution. Therefore, the purpose of this study is to elucidate biochemical function of HDA9 and to find its target genes underlying plasticity of plants upon external

signals.

1.2 DNA methylation

DNA methylation occurs when a methyl group ($-CH_3$) is covalently added to the cytosine bases of DNA and, without alteration of DNA sequence, forms 5-methylcytosine. It arises in both prokaryotes and eukaryotes. Bacterial DNA methylation differentiates genomic DNA from invading phage DNA. The foreign phage DNA is then fragmented by the host restriction enzymes so that the intruding DNA cannot be replicated (Chinnusamy and Zhu, 2009). DNA methylation is a well-conserved epigenetic mechanism in most eukaryotes, from fungi to animals and plants. Moreover, transposons, other repetitive elements, and DNA in centromeric, peri-centromeric, and some genic regions are highly methylated intendedly for inactivation of the methylated DNA loci within the genome.

In mammals, most DNA methylation occurs exclusively in CG context while non-CG methylation is observed only in embryonic stem cells. Moreover, *de novo* DNA methylation is established by DNA methyltransferase 3 (DNMT3) during the development of germ cells whereas methylated DNA pattern is maintained via DNA methyltransferase 1 (DNMT1) during replication (Zhao and Chen, 2014). Unlike animals, DNA methylation *in planta* occurs in all possible cytosine contexts, such as CG, CHG, and CHH (where H is A, C, or T) (Pikaard and Scheid, 2014). Although animals and plants share common features of dynamic regulation mechanism of DNA methylation and demethylation, there are more evidences that

DNA methylation is elaborated involving RNA interference (RNAi) pathway in plants.

De novo DNA methylation in Arabidopsis is mediated by the RNA-directed DNA methylation (RdDM) pathway. Small RNAs generated via RNAi pathway, such as 24-nucleotide (nt) small-interfering RNAs (siRNAs), or long non-coding RNAs (lncRNAs) may guide the DNA methylation to occur.

At RdDM target loci, single-stranded RNAs are transcribed and converted into double-stranded RNAs (dsRNAs). DICER-LIKE 3 (DCL3) then generates primary 24-nt siRNAs by cleaving the long dsRNA precursors, and HUA ENHANCER 1 (HEN1) assists maturation of the siRNAs. The mature siRNAs are loaded onto ARGONAUTE 4 (AGO4) (Law and Jacobsen, 2010). Next, via the sequence complementarity between the AGO4-bound siRNA and the scaffold RNA transcribed from an intergenic non-coding region, the RdDM effector complex, including DOMAINS REARRANGED METHYLTRANSFERASE 2 (DRM2), is recruited to RdDM target genes establishing *de novo* DNA methylation (He et al., 2011; Zhao and Chen, 2014).

To maintain DNA methylation patterns after replication, the nascent strand of hemimethylated double-stranded DNA becomes the target of metyltransferases. Maintenance of DNA methylation in plants is carried out via three distinctive pathways using different methyltransferases subject to cytosine sequence contexts (Law and Jacobsen, 2010). First, DNA methylation in CG context is the most frequently observed modification in plant genome as in animals (Chan et al., 2005).

DNA METHYLTRANSFERASE 1 (MET1), which is the ortholog of mammalian DNMT1, governs the maintenance CG methylation. Furthermore, it is recently revealed that VARIANTION IN METHYLATION/ORTHRUS (VIM/ORTH) family proteins and DECREASE IN DNA METHYLATION 1 (DDM1) are also required for this mechanism (Law and Jacobsen, 2010; Zhao and Chen, 2014). Next, the maintenance CHG methylation is implemented by a plant-specific DNA methyltransferase, CHROMOMETHYLASE 3 (CMT3), involving dimethylated histone H3 lysine 9 (H3K9me2) (Cao et al., 2003). In Arabidopsis, H3K9me2 is enriched by a histone methyltransferase, KRYPTONITE (KYP), and its homologs SU(VAR)3-9 HOMOLOG 5 (SUVH5) and SUVH6. Then, CMT3 is guided by H3K9me2 at target loci (Law and Jacobsen, 2010; Zhao and Chen, 2014). Occasionally, in CHG methylation, another DNA methyltransferase, DRM2, is also involved through the RdDM pathway (Stroud et al., 2013). Lastly, asymmetric CHH methylation is predominantly sustained by DDM1 and CMT2 in cooperation with the RdDM pathway (Zemach et al., 2013). DDM1 is required for DNA methylation on linker histone H1. CMT2 preferentially binds to enriched H3K9me2, just like its homolog CMT3. In other words, CMT2 and CMT3 methylate CHG sites in a redundant manner. However, CMT2 is only functional on large transposable elements (TEs) at heterochromatin region unlike CMT3 that also function on protein-coding genes (Stroud et al., 2014).

1.3 ATP-dependent chromatin remodeling

Another eminent epigenetic regulation occurs via ATP-dependent chromatin remodeling mechanism. It uses an energy derived from ATP hydrolysis to alter histone-DNA interactions by sliding, ejecting, or restructuring the nucleosome. In this manner, the accessibility of transcription factors or the recruitment of transcription machinery to the genomic region in chromatin is controlled (Cairns, 2005; Ho and Crabtree, 2010; Zhao et al., 2015).

There are four classes of ATP-dependent chromatin remodelers in eukaryotes: SWItching defective/Sucrose Non-Fermenting (SWI/SNF), Imitation SWI (ISWI), Chromodomain (CHD), and INO80 groups (Eisen et al., 1995; Vignali et al., 2000; Varga-Weisz, 2001; Jerzmanowski, 2007). In addition to their catalytic ATPase domains, these remodelers have unique structures that allow specific association with their targets within the biological context. They act in diverse processes and associate with other types of epigenetic modification mechanism.

First, SWI/SNF is the most characterized group among the ATP-dependent chromatin remodelers. Members of this family consist of a highly conserved ATPase subunit, which includes a helicase-SANT (HSA), a post-HSA, and a bromodomain within the structure. When actin or actin-related proteins (ARPs) are associated with the HSA domain and acetylated target loci is recognized by their c-terminal bromodomain, the ATPase activity is modulated. Second, the ATPase subunit of ISWI family has a SANT (ySWI3, yADA2, hNCoR, and hTFIIIB) or SLIDE (SANT-like ISWI) domain at the C-terminus of the catalytic ATPase domain. The C-terminal module is able to interact with a DNA-binding histone-

fold motif, plant homeodomain (PHD), or bromodomain of other proteins. This group of chromatin remodeler binds to an unmodified histone tail and DNA and provides an optimized space to promote chromatin assembly and repression of transcription. Third, CHD family includes two tandem chromodomains at the N-terminus of its ATPase domain. The tandemly arranged chromodomain binds to methylated lysine or forms a complex with deacetylases and methyl CG-binding domain (MBD) proteins. CHD remodelers promote or repress transcription by sliding or ejecting nucleosomes. Last, INO80 remodelers include more than 10 subunits. The prominent feature of this family is that its ATPase domain is split by a long insertion, to which ARPs and AAA-ATPases can bind. This group of remodelers functions by either sliding nucleosome along the DNA or exchanging histones with their variants to promote transcriptional activation or DNA repair.

Arabidopsis genome also encodes a number of characterized ATPase chromatin remodelers. PHOTOPERIOD-INDEPENDENT EARLY FLOWERING 1 (PIE1) is most homologous to SWR1, a member of INO80 class remodeler, although it harbors SANT domain which is normally found in ISWI family members (Noh and Amasino, 2003). As an SWR1 complex, PIE1 plays a key role in repression of floral transition and in ambient temperature response through interaction with ACTIN-RELATED PROTEIN 6 (ARP6) (Noh and Amasino, 2003; Kumar and Wigge, 2010). SPLAYED (SYP) and BRAHMA (BRM) are identified as possible SWI/SNF ATPase remodelers associated with developmental processes in Arabidopsis (Wagner and Meyerowitz, 2002; Bezhani et al., 2007). Loss of SYP and BRM exhibits pleiotropic developmental defects such as slow growth,

dwarfism, abnormal separation of cotyledons, and reduced apical dominance (Wagner and Meyerowitz, 2002; Hurtado et al., 2006; Kwon et al., 2006). DECREASE IN DNA METHYLATION (DDM1) also belongs to the SWI/SNF family and causes DNA methylation (Shaked et al., 2006). BUSHY (BSH) is a plant-specific ATPase that is involved in control of auxin response (Brzeski et al., 1999). Moreover, PICKLE (PKL), a CHD3 group remodeler, represses expression of seed-associated genes during germination and regulates the post-embryonic transition via histone H3 lysine 27 methylation (Jerzmanowski, 2007; Zhang et al., 2008). Concisely, plant chromatin-remodeling factors perform important functions in epigenetic control of plant growth and development.

1.4 RNA interference (RNAi)

Only recently, a highly complex and diverse network of noncoding RNAs (ncRNAs) has been revealed. Large-scale and genome-wide analyses have indicated that only 1~2% of the genome can actually encode proteins, although approximately 90% of eukaryotic genomes are transcribed. This implies that a large portion of the eukaryotic genome produces unexpected RNAs that do not have protein-coding potential and are thus called ncRNAs.

NcRNAs are classified into either housekeeping or regulatory ncRNAs. Housekeeping ncRNAs are constitutively expressed, which include transfer RNAs (tRNAs), ribosomal RNAs (rRNAs), small nuclear RNAs (snRNAs), and small nucleolar RNAs (snoRNAs). Regulatory ncRNA can be further divided into two

groups according to the size of transcripts, short ncRNAs and long noncoding RNAs (lncRNAs).

Short ncRNAs are less than 200 nucleotides comprising micro RNAs (miRNAs), small interfering RNAs (siRNAs), and piwi-interacting RNAs (piRNAs). Among short ncRNAs, miRNA and siRNA are extensively investigated. MiRNAs are derived from short hairpins, whereas siRNAs are derived from longer regions of double strand RNAs. However, both miRNAs and siRNAs are about 22 nt long as they are cleaved by an endoribonuclease, DICER. These small ncRNAs are loaded onto AGO or RNA-induced silencing complex (RISC) (Ramachandran and Chen, 2009). RISC then binds to the target messenger RNAs (mRNAs) through partial base paring with the loaded small ncRNAs. These bindings negatively regulate target-gene expression via mRNA degradation or repression of translation (Guo et al., 2014). On the other hand, long non-protein coding transcripts are termed as lncRNAs (Heo et al., 2013; Cao, 2014; Shafiq et al., 2015). LncRNAs were initially thought to be non-functional junk transcripts. However, their significances have been emerged and it is now considered that many lncRNAs actually function as key regulators of transcription and translation in various biological pathways, for instances, genomic imprinting, nuclear organization, alternative splicing, and chromatin regulation. More and more lncRNAs have been identified through different approaches in plants and yet their exact functions are still abstruse.

In Arabidopsis, best-known lncRNAs are COLD INDUCED LONG

ANTISENSE INTRAGENIC RNA (COOLAIR) (Swiezewski et al., 2009) and COLD ASSISTED INTRONIC ncRNA (COLDAIR) (Heo and Sung, 2011). Both COOLAIR and COLDAIR were found based on analogy from human HOX TRANSCRIPT ANTISENSE RNA (HOTAIR) (Rinn et al., 2007). These plant lncRNAs are involved in the repression of *FLC* expression during vernalization. COOLAIR is transcribed from the 3-end heterochromatic region of *FLC* in an antisense direction compared to *FLC* mRNA. COOLAIR lncRNA transcript covers the whole *FLC* gene locus, which is 7 kb long, and can be alternatively spliced and polyadenylated (Swiezewski et al., 2009). On the hand, COLDAIR lncRNA does not have any alternative isoforms and is transcribed from the first intron of *FLC*. 5'-end of COLDAIR is capped but not polyadenylated unlike COOLAIR. Although they originate differently, both COOLAIR and COLDAIR function in *FLC* repression during vernalization. Vernalization intervenes the epigenetic regulation of *FLC* through decreased histone H3 lysine 36 trimethylation (H3K36me3) and increased histone H3 lysine 27 trimethylation (H3K27me3) by recruiting the PLANT HOMEODOMAIN (PHD) protein, VERNALIZATION INSENSITIVE 3 (VIN3) and POLYCOMB REPRESSVIE COMPLEX 2 (PRC2) (Sung and Amasino, 2004; Song et al., 2012). During this process, COLDAIR transcription is increased after COOLAIR induction but before the elevation of *VIN3* transcription. COLDAIR physically interacts with PRC2 complex to promote H3K27me3 accumulation during vernalization. It is considered that COLDAIR functions as a scaffold RNA to recruit the PRC2 complex and to epigenetically repress *FLC* expression during vernalization.

Moreover, a 236-nt lncRNA called HIDDEN TREASURE1 (HID1) was newly identified through transcriptome analysis (Wang et al., 2014). HID1 is characterized to be involved in both transcriptional and post-transcriptional regulation of photomorphogenesis-related gene expression. Transcription level of HID1 itself is not regulated by light. However, it promotes photomorphogenic response through the repression of PHYTOCHROME-INTERACTING FACTOR (PIF3) activity under continuous red light. PIF3 is a well-known transcription factor that triggers hypocotyl elongation. HID1, as the first identified lncRNA to be involved in the control of light-mediated plant development, is still required to be clarified for its precise function and mechanism.

Further studies connecting the posttranslational regulatory networks of histones and DNA to ncRNA-based transcriptional regulation will bring better understandings of cellular processes and developments in eukaryotes. Ultimately, studies in epigenetics will enlighten the fine regulatory mechanisms underlying gene expression as a whole.

2. Photoperiod regulates floral transition

Transition from vegetative to reproductive phase is very crucial process for reproductive success in higher plants. Arabidopsis has been well characterized for decades with regard to the genetic and molecular mechanisms of flowering. Floral transition in Arabidopsis is controlled by environmental stimuli (including

photoperiod, circadian rhythm, and vernalization) gibberellin (GA) pathway, and by internal cues including developmental and autonomous signals. Signals from these pathways are finely tuned by other mechanisms.

2.1 Photoperiod and circadian rhythm

Photoperiod and circadian rhythm are crucial factors for seasonal plant growth and flowering. Higher plants, animals, and fungi have their own endogenous biological clocks, and they can auto-regulate through their negative-feedback loops. In Arabidopsis, the central oscillator depends on multiple interconnected loops to generate biological rhythm. These multiple loops comprise three feedback loops, two morning MYB transcription factors, and an evening-phased pseudo response regulator. The morning-expressed MYB transcription factors include CIRCADIAN CLOCK ASSOCIATED 1 (CCA1) and LATE ELONGATED HYPOCOTYL (LHY) (Schaffer et al., 1998; Wang and Tobin, 1998; Makino et al., 2000). The evening-phased PSEUDO RESPONSE REGULATOR (PRR), TIMING OF CAB2 EXPRESSION1 (TOC1), is a member of the PRR family (Nagel and Kay, 2012; McClung et al., 2013). Light activates transcript levels of *LHY* and *CCA1*, and represses *TOC1* expression in the morning. LHY and CCA1 proteins inhibit *TOC1* transcription through binding with the evening element in the *TOC1* promoter (Schaffer et al., 1998; Wang and Tobin, 1998; Green and Tobin, 1999, 2002; Alabadi et al., 2001, 2002). At night, TOC1 protein up-regulates the transcription of *LHY1* and *CCA1* (Alabadi et al., 2001 and 2002; Pruneda-Paz et al., 2009). In addition, *TOC1* is repressed by TOC1 protein

itself, forming a second loop (Locke et al., 2005). LHY and CCA1 function as positive regulators of three *TOC1* relatives (*PRR5*, *PRR7*, and *PRR9*), and this forms the third loop (Farre´ et al., 2005; Harmer and Kay, 2005; Mizuno and Nakamichi, 2005).

Moreover, GIGANTA (GI), EARLY FLOWERING 3 (ELF3), ELF4, and LUX are also required for *LHY* and *CCA1* expression (Park et al., 1999; Doyle et al., 2002; Mizoguchi et al., 2002; Hazen et al., 2005). ELF3, ELF4, and LUX act together in a transcription complex called EVENING COMPLEX (EC) (Hicks et al., 2001; Doyle et al., 2002; Dixon et al., 2011; Helfer et al., 2011; Nusinow et al., 2011; Herrero et al., 2012).

The connection between the circadian clock and photoperiod (day length) has been developed into the external coincidence model. The photoperiodic response is controlled by light at certain times of the day (Bünning, 1936; Pittindrigh and Minis, 1964). Arabidopsis behaves as a facultative long-day plant because its flowering is accelerated during long days (16 hr light and 8 hr dark photoperiod). The output of photoperiod depends on *CONSTANS* (*CO*) gene. The circadian clock regulates *CO* mRNA expression in late afternoon, and then CO protein is accumulated and stabilized. Stabilized CO protein can bind directly to a *cis*-element (CCAAT box) in the distal promoter of *FLOWERING LOCUS T* (*FT*) (Wenkel et al., 2006; Kumimoto et al., 2008 and 2010). Hence, light promotes *FT* expression in the phloem companion cells at the end of the day, and FT protein is translocated to the shoot apical meristem and facilitates flowering (Michaels, 2009; Amasino and Michaels, 2010; Pruneda-Paz and Kay, 2010). Whereas, at night, CO

protein is degraded by 26S proteasome. Thus, the mobile FT protein is considered a florigen. FT forms a complex with FD, a bZIP transcription factor, in the shoot apical meristem. The FT–FD module initiates flowering by activating a floral integrator, *SUPPRESSOR OF OVEREXPRESSION OF CONSTANS 1* (*SOC1*; Michaels, 2009).

Although CO-mediated regulation accounts for most of the activation of *FT*, CO-independent mechanisms function in parallel (Liu el al., 2008; Sawa and Kay, 2011; Iñigo et al., 2012; Kumar et al., 2012; Pin and Nilsson, 2012). *FT* expression is also controlled by various repressive signals: *FLOWERING LOCUS C* (*FLC*) and *SHORT VEGETATIVE PHASE* (*SVP*), two MADS-box proteins. They repress *FT* expression by directly binding to the CArG motifs in the promoter and intron of *FT*. *FLC* directly represses transcription of floral integrators, *SOC1* and *FT*, which combine the signals from several pathways to promote flowering (Borner et al., 2000; Lee et al., 2000; Michaels and Amasino, 2001; Helliwell et al., 2006; Schörock et al., 2006). Another negative transcriptional regulator of *FT* is *TEMPRANILLO 1* (*TEM1*), a RAV-like AP2 domain-containing protein that directly interacts with the 5'UTR of *FT* chromatin (Castillejo and Pelaz, 2008). In addition, miR172-targeted AP2-like transcription factors, including *TARGET OF EAT 1* (*TOE1*), *TOE2*, *SCHLAFMÜTZE* (*SMZ)*, and *SCH ARCHZAPFEN (SNZ)*, negatively affect *FT* expression in an age-dependent manner and reduce miR156 but increase miR172 expression levels (Jung et al., 2007; Mathieu et al., 2009; Wu et al., 2009; Huijser and Schmid, 2011). It has been reported that *FT* transcription is also controlled by epigenetic mechanisms. Tri-methylation of H3K27

(H3K27me3) within *FT* chromatin, a representative repressive mark, is established by *CURLY LEAF* (*CLF*) of the polycomb repressive complex 2 (PRC2) (Coupland and Turck, 2008; Jiang et al., 2008; Pazhouhandeh et al., 2011). LIKE HETEROCHROMATIN PROTEIN 1 (LHP1), a component of the plant PRC1, is associated with the H3K27me3 within *FT* chromatin, leading to *FT* repression (Turck et al., 2007; Adrian et al., 2010). H3K4me3 in the *FT* promoter region is influenced by Jumonji (Jmj)-family histone demethylases, AtJmj4 and EARLY FLOWERING 6 (ELF6), which also lead to reduced *FT* transcription (Jeong et al., 2009).

2.2 Vernalization pathway

Winter-annual Arabidopsis accessions flower late without winter exposure and show accelerated flowering after prolonged exposure to low temperature. This process is called vernalization, and *FLC* is largely responsible for this process (Koornneef et al., 1994; Lee et al., 1994; Sanda and Amasino, 1996; Michaels and Amasino, 1999 and 2001, Sheldon et al., 1999, 2000 and 2002; Rouse et al., 2002). *FLC* encodes a MADS-box transcription factor. Its transcript and protein levels are high in winter-annual accessions, resulting in delayed flowering. However, *FLC* is repressed when plants are exposed to prolonged cold or by the autonomous pathway.

In Arabidopsis, vernalization results in mitotically stable repression of *FLC* chromatin through the PRC2 complex and long noncoding RNAs (Gendall et al., 2001; Levy et al., 2002; Sung and Amasino, 2004; Helliwell et al.,2011; Heo and

Sung, 2011).

Before cold exposure, *FLC* chromatin is at active state, with active histone marks, such as H3K4, H3K36, and H3Ac (Zografos and Sung, 2012). Many histone modifying complexes, including yeast RNA pol II Associated Factor 1 (PAF1) complex and COMPASS- complex are involved in *FLC* activation before cold (He et al., 2004; Tamada et al., 2009; Jiang et al., 2011; Kim et al., 2014).

During winter, the repression of *FLC* chromatin is initiated by VERNALIZATION INSENSITIVE 3 (VIN3), the plant homeodomain (PHD)- and fibronectin type III domain-containing protein. VIN3 and VIL1/VRN5 act together with PRC2 and enhance their activity (Kim and Sung, 2014). Among Arabidopsis PRC2 components, CURLY LEAF (CLF) and SWINGER (SWN), two homologs of E(z), and VRN2, the homolog of Su(z)12, are involved in the repression of FLC during vernalization (Chanvivattana et al., 2004). The enrichment of PRC2 to the *FLC* chromatin increases by vernalization. PRC2 contributes to the repression of FLC by mediating tri-methylation of H3K27 at *FLC* chromatin.

Components of another Polycomb group complex, PRC1 which include VIL1, LHP1, EMF1, AtBMI1A, AtBMI1B, and AtBMI1C also contributes to the repression of FLC. After cold, the components of the PRC1 complex such as LHP1, PRC2, and VIL1 act with the PRC2 complex for the stable silencing of the *FLC* chromatin.

Recently studies indicate that long noncoding RNAs (lncRNAs) also play a role in the epigenetic repression of *FLC*. One such lncRNA, *COOLAIR* is increased by cold exposure and its antisense transcript does not affect *FLC* repression during

vernalization (Helliwell et al.,2011). However, another lncRNA, COLDAIR physically interacts with the CLF and is required for establishing stable *FLC* repression through direct interaction with PRC2 during vernalization (Heo and Sung, 2011; Zografos and Sung, 2012).

MADS AFFECTING FLOWERING (MAF1~5) proteins are paralogs of FLC. Their genes are arranged in tandem clusters on Arabidopsis chromosome V. *MAF* genes have 53~98% nucleotide-sequence identities with *FLC* (Bodt et al., 2003; Raccliffe et al., 2003). Vernalization also represses *MAF1*, *MAF2*, and *MAF3* expression but not *MAF5*. *MAF4* is not strongly affected by vernalization either. MAF1/FLOWERING LOCUS M (FLM) acts as a floral repressor such that its repression by vernalization contributes to accelerated flowering (Sung et al., 2006). MAF1 has also been reported to be involved in the acceleration of flowering by elevated temperature (Werner et al., 2005; Li et al., 2006; Sung et al., 2006). MAF2, another floral repressor reacts to a relatively short cold period (Raccliffe et al., 2003). MAF3 has a redundant function with MAF1 in repressing *FT* expression and delaying flowering. It has also been reported that MAF1 acts redundantly with FLC, MAF2, and MAF4 in floral repression (Raccliffe et al., 2001 and 2003; Sheldon et al., 2009; Gu et al., 2012). Transcript levels of *MAF4* and *MAF5* are increased transiently by short-term cold, and these increases have roles in inhibiting precocious response to vernalization (Kim and Sung, 2013).

In addition to *FLC*, other genes of the MADS-box family also respond to the vernalization pathway (Alexander and Hennig, 2008). AGOMOUS-LIKE 19 (AGL19) belongs to the TM3 clade of the MADS-box family, and is highly similar

to SOC1. *AGL19* was originally characterized as a root-specific gene (Alvarez-Buylla et al., 2000). However, *AGL19* is also involved in flowering control through the vernalization pathway. Ectopically expressed *AGL19* promotes flowering under both LD and SD, suggesting that AGL19 acts as a floral activator (Schönrock et al., 2006). In the absence of cold, *AGL19* expression is maintained at very low levels by the PRC2 complex, which is composed of MSI1, CLF, FERTILISATION INDEPENDENT ENDOSPERM (FIE), and EMBRYONIC FLOWER 2 (EMF2). It has been reported that *AGL19* chromatin is associated with H3K27me3 but not with H3K9me2 (Schönrock et al., 2006). When the plant is exposed to prolonged cold, H3K27me3 level within *AGL19* chromatin is reduced by decreased PRC2 occupancy, and thus, *AGL19* is relieved from PRC2 repression and promotes flowering. Therefore, the vernalization pathway in Arabidopsis has two branches, FLC- dependent and FLC-independent. Both branches are dependent on the PRC2 complex. While *FLC* is repressed by VRN2-containing PRC2 after vernalization, *AGL19* is repressed by EMF2-containing PRC2 before vernalization. In sum, different polycomb group (PcG) proteins have been recruited to synchronize the vernalization response and to regulate the transition from developmental growth to reproductive growth (Alexandre and Hennig, 2008).

AGAMOUS LIKE 24 (AGL24) belongs to the MADS-box family and functions as an activator of floral transition (Yu et al., 2002; Bodt et al., 2003; Michaels et al., 2003). *AGL24* is regulated by multiple flowering pathways such as the photoperiod pathway, the autonomous pathway and vernalization (Yu et al., 2004; Liu et al., 2007 and 2008; Lee J et al., 2008).Previous studies have reported

that *AGL24* and *SOC1* affect expression of each other (Yu et al., 2002; Michaels et al., 2003). However, *AGL24* and *SOC1* are also regulated differently in several aspects during flowering. During vernalization, *AGL24* but not *SOC1* is controlled in a manner independent of *FLC* (Michaels et al., 2003). In the photoperiod pathway, *AGL24* is influenced by *CO* but not by *FT*, whereas *SOC1* is affected directly by *FT* and indirectly by *CO* (Lee et al., 2000; Samach et al., 2000; Hepworth et al., 2002). These results suggest that *AGL24* and *SOC1* may have an interdependent or independent effect on each other in the perception of flowering cues.

2.3 Autonomous pathway

The autonomous-pathway proteins are characterized as a combination of proteins that affect late flowering under the influence of photoperiod, the vernalization pathway, and even in summer-annual accessions that are defective in the functional allele of *FRI* (Koornneef et al., 1991; Simpson, 2004). When the autonomous-pathway genes are mutated, the resulting mutant plants flower later than wild-type plants in both LD and SD conditions (Simpson, 2004). This occurs because the components of the autonomous pathway inhibit the accumulation of FLC, the major floral repressor. Therefore, the autonomous pathway can promote flowering independent of day length.

The autonomous-pathway proteins include FCA, FY, FLOWERING LATE KH MOTIF (FLK), FPA, LUMININDEPENDENS (LD), FLOWERING LOCUS D (FLD), FVE, and RELATIVE OF EARLY FLOWERING 6 (REF6) (Michaels

and Amasino, 1996; Koorneef et al., 1998; Lim et al., 2004; Noh et al., 2004). FCA, FPA, and FLK encode RNA-binding proteins (Macknight et al., 1997; Schomburg et al., 2001; Lim et al., 2004). FCA has two RNA Recognition Motifs (RRMs) and a WW protein-interaction domain, whereas FPA has three RRMs (Macknight et al., 1997; Schomburg et al., 2001). FLK is a plant-specific protein that has three K-homology (KH)-type RNA-binding domains (Lim et al., 2004). FY is homologous to the *Saccharomyces cerevisiae* protein Rfs2p (polyadenylation factor 1 subunit 2), a component of RNA-processing factors and required for FCA to promote flowering (Simpson et al., 2003; Amasino and Michaels, 2010). FVE, FLD, and REF6 epigenetically regulate *FLC* expression. FVE is a plant homolog of the yeast protein MULTIPLE SUPPRESSOR OF IRA1 (MSI) and the mammalian retinoblastoma associated proteins RbAp46 and RbpA48. FVE is required for a protein complex repressing *FLC* transcription via histone deacetylation (Ausin et al., 2004). FLD and RFF6 have histone demethylase activities and play roles in histone demethylation within *FLC* chromatin. FLD is homologous to human LYSINE-SPECIFIC HISTONE DEMETHYLASE1 (LSD1), whereas REF6 is one of the plant Jumonji-family proteins (He et al., 2003; Noh et al., 2004). LD encodes a homeodomain-containing protein (Lee et al., 1994), although the mechanism how LD represses *FLC* expression is yet to be elucidated.

In sum, numerous studies indicate that the autonomous pathway represses *FLC* expression mainly through RNA processing or chromatin modifications (Kim et al., 2009; Michaels, 2009).

2.4 GA pathway

Gibberellic acid (GA), one of the phytohormones, has an effect on plant development and growth, including seed germination, stem elongation, floral development, and flowering. A GA biosynthesis mutant, *ga1-3*, did not promote flowering in SD, but promoted late flowering in LD (Wilson et al., 1992). This stronger effect of GA in SD is perhaps due to the photoperiod pathway masking the effect of loss of GA signaling under LD (Reeves and Coupland, 2001; Mouradov et al., 2002; Porri et al., 2012).

GA promotes the expression of *SOC1* (Bonhomme et al., 2000; Moon et al., 2003) and *LFY* (Blazquez et al., 1998) that are involved in flowering at the shoot apical meristem. In addition, GA upregulates the expression of miR159 and its target *MYB33* mRNA that encode the MYB transcription factor and regulate *LFY* expression (Gocal et al., 2001; Woodger et al., 2003; Achard et al., 2004). The *GATA NITRATE INDUCIBLE CARBON METABOLISM INVOLVED* (*GNC*) *and GNC LIKE* (*GNL*) genes are GATA transcription factors that inhibit flowering, and GA represses *GNC* and *GNL* expressions (Richter et al., 2010).

DELLA proteins, GIBBERELLIC ACID INSENSITIVE (GAI), REPRESSOR OF GA1-3 (RGA), and RGA-LIKE 1 (RGL1), have a negative role in GA signaling, and the GA signal mediates flowering primarily through degradation of these DELLA proteins (Dill and Sun., 2001; King et al., 2001; Mouradov et al., 2002; Cheng et al., 2004).

3. Light regulates seed germination

Higher plants such as Arabidopsis are well adapted to optimizing their survival and reproductive success through environmental and endogenous signals. Light is an important environmental signal that influences plant developmental processes differently at tissue- and organ-dependent levels.

Seed germination is a physiological process in which the radicle surrounded by the seed coat emerges after the absorption of water by dry seed (Bewley, 1997b; Baskin and Baskin 2004; Finch-Savage and Leubner-Metzger, 2006). Arabidopsis has two layers, an outer dead testa, also called the seed coat, and an inner layer with living endosperm cells, called the aleurone layer (Linkies et al., 2009; Morris et al., 2011). In Arabidopsis, seed germination takes place in two visible steps. The first step is the testa rupture, and one or several slits form at the seed surface (Debeaujon et al., 2000; Piskurewicz and Lopez-Molina, 2009). The second step is the endosperm rupture and the hypocotyl and radicle break through the micropylar endosperm layer (Morris et al., 2011). Seed germination is affected by numerous environmental factors, including water, temperature, oxygen, nutrients, and light. Among them, light is a crucial factor in plants with small seeds such as Arabidopsis and lettuce (Shinomura, 1997). These plant species use phytochrome, a photoreceptor, to sense light and ultimately initiate seed germination. The phytohormones, including GA and abscisic acid (ABA), are also involved in the seed germinating process. Endosperm rupture is antagonistically controlled by GA and ABA (Piskurewicz and Lopez-Molina, 2009). The mutual negative regulation between GA and ABA might contribute to an effective change in the balance of

GA and ABA hormones in response to an external signal (Toyomasu et al., 1998; Yamaguchi et al., 1998; Seo et al., 2006). Hence, phytochrome regulates endogenous GA and ABA levels to optimize seed germination.

3.1 Light regulates phytochrome signaling

Light signaling in plants begins with perception of light through a photoreceptor, which induces modulation of the transcriptional regulatory networks. Plants are well adapted in this regard and react to a combination of cues, including light quality, quantity, and duration. Light quality is recognized by different light receptors for specific light wavelengths (Jiao et al., 2007). Phytochromes (phys) absorb red (660 nm) and far-red light (730 nm) (Wang and Deng, 2002; Lau and Deng, 2010). Arabidopsis phytochromes are designated phyA to phyE (Fankhauser and Staiger, 2002; Quail, 2002). Cryptochromes (CRYs), including CRY1 and CRY2, are flavin-type blue-light receptors (Cashmore, 1997; Fankhauser and Staiger, 2002). Arabidopsis possesses two UV-A light photoreceptors, PHOT1 and PHOT2 (Briggs et al., 2001; Christie and Briggs, 2001; Fankhauser and Staiger, 2002).

Phytochrome holoproteins are assembled in the cytosol. During this process, apoproteins are conjugated with linear tetrapyrrole chromophores. Light causes conversion of phytochrome structure based on whether the phytochrome absorbs red light (Pfr) or far-red light (Pr), and these forms determine biological activation and inactivation, respectively. Phytochrome is composed of two domains, N-terminal chromophore-binding photo sensory domain and C-terminal regulatory

domain. The C-terminal domain interacts with phytochrome-interacting factors (PIFs) (Wang and Deng, 2002; Lau and Deng, 2010). Conformation change of phytochrome is a reversible process that occurs upon absorbing red or far-red light. The Pfr form translocates into the cell nucleus where it binds to PIFs, and then regulates physiological processes (Sakamoto and Nagatani, 1996; Nagatani, 2004; Kircher et al., 1999, 2002; Frankin and Quail, 2009). There are five phytochromes (phyA to phyE) in Arabidopsis. Of the five phytochromes, phyA is a light-labile protein that belongs to the photo-irreversible 'type I phytochrome'. phyA reacts to very low fluence responses (VLFRs) and far-red high irradiance response (FR-HIR). The activated Pfr form of phyA is responsible for far-red light reception, and it is rapidly degraded upon light illumination. phyA influences diverse plant growth and developmental processes, such as seed germination and seedling de-etiolation.

phyB, a 'type II phytochrome', is involved in low fluence responses (LFRs). phyB is a light-stable protein and senses the red light necessary for seed germination. phyB, phyD, and phyE show different expression patterns, but their functions partially overlap each other.

3.2 Phytochrome-interacting factors (PIFs)

PIF, a bHLH transcription factor, has been known as a negative regulator of photomorphogeneis. The structure of the bHLH protein is comprised of the N-terminal DNA-binding basic domain (b) and the C-terminal dimerization region (HLH). The DNA-binding region possesses 15 amino acids with high numbers of basic residues, and the HLH region contains two alpha helices of a variable loop

that homo- or hetero-dimerizes with other bHLH proteins via their *cis*-acting regulatory motifs (Ortiz et al., 2003). These *cis*-acting regulatory elements have a conserved E-box (5'-CANNTG-3') and G-box (5'-CACGTG-3'). There are 15 PIF proteins in Arabidopsis, and each PIF has distinct or redundant biological function during plant development. Of the PIF family, PIF3 is the first characterized bHLH transcription factor that favorably binds to the Pfr form of phyA and phyB. In addition, PIF3 negatively controls phyB-mediated inhibition of hypocotyl elongation, cotyledon opening, and anthocyanin accumulation (Kim et al., 2003). PIF4 is the negative regulator of phyB-mediated inhibition of hypocotyl elongation and cotyledon opening (Huq and Quail, 2002). PIF1, also known as PHTYOCHROME INTERACTING FACTOR 3-LIKE 5 (PIL5), plays a negative role in seed germination, inhibition of hypocotyl elongation, negative hypocotyl gravitropism in the dark, and chlorophyll accumulation in the light (Huq et al., 2004; Oh et al., 2004).

HECATE (HEC) protein belongs to the HLH subfamily. HECATE lacks the basic DNA-binding region of the bHLH proteins, and therefore is referred to as HLH protein (Benezra et al., 1990). There are three *HECATE* genes (*HEC1*, *HEC2*, and *HEC3*) in Arabidopsis, and they function redundantly in the processes of germination and floral development. Because of the lack of a DNA-binding motif, these proteins are only able to interact with other bHLH proteins. The heterodimerization between HLH and bHLH proteins inhibits the DNA-binding activity of bHLH proteins. Accordingly, HLH proteins are considered to have a dominant negative effect on bHLH proteins. Mutation in *HEC* genes has resulted in

phenotypes defective in transmitting tract and stigma development. The dimerization between HEC and other bHLH proteins might be involved in gynoecium development (Gremski et al., 2007). A recent study showed that HEC proteins interact with PIF1 in the light and remove residual PIF1 which was not degraded by the 26S proteasome pathway, and then subsequently promote photo-morphogenesis (Zhu PhD thesis, 2012).

LONG HYPOCTYL IN FAR-RED 1 (HFR1) also belongs to the HLH subfamily and cannot bind directly to the DNA (Fairchild et al., 2000). HFR1 protein functions as a positive regulator in phyA-mediated inhibition of hypocotyl elongation and negative gravitropism (Fairchild et al., 2000; Fankhauser and Chory, 2000; Soh et al., 2000). HFR1 accumulates in the light but not in the dark, and is targeted by the E3 ubiquitin ligase, CONSTITUTIVE PHOTOMORPHOGENESIS 1 (COP1). HFR1 was reported to sequester PIF1 transcriptional activity by forming a heterodimer with PIF1, blocking PIF1 from binding to DNA. The light–HFR1–PIF1 module regulates PIF1-target genes, including *PIF3*, *EXP9*, *XTH4*, and *XTH33*, that mediate cell-wall loosening and cell-cycle initiation, (Shi et al., 2013). In addition, an overexpression of N-terminus truncated HFR1 resulted in constitutive germination in the dark (Yang et al., 2003).

3.3 Phytochrome modulates PIF1 during seed germination

PIFs can bind directly with activated phytochrome (with a stronger preference to phyB than phyA). In seed germination, PIF1 preferentially binds with Pfr form of phyB (also Pfr phyA), and the phyB–PIF1 interaction leads to

degradation of PIF1 through the 26S proteasome pathway (Oh et al., 2004, 2006). Previous data indicated that the *pif1* mutant seeds produce a constitutive germination phenotype in both inductive red light and non-inductive far-red light conditions. Conversely, constitutive *PIF1* expressors require much higher red light irradiation than wild type to initiate seed germination. PIF1 also regulates the increasing expression of ABA anabolic genes (*ABA1*, *NCED6*, and *NCED9*) and a GA catabolic gene (*GA2ox2*), whereas it represses an ABA catabolic gene (*CYP707A2*) and GA anabolic genes (*GA3ox1* and *GA3ox2*). As a result, seed germination is affected by increasing ABA and decreasing GA levels. PIF1 also activates the transcription of *RGA* and *GAI*, DELLA protein-encoding genes. A chromatin immunoprecipitation assay has shown that PIF1 binds directly to the promoters within *RGA* and *GAI* chromatin via G-box motifs (CACGTG). However, it does not bind to the promoters of other GA and ABA metabolic genes (Oh et al., 2007). Therefore, *RGA* and *GAI* may be the target genes of PIF1. It has also been reported that SOMNUS (SOM) regulates GA and ABA metabolic genes at the downstream of PIF1. *SOM* encodes a CCCH-type zinc finger protein (Kim et al., 2008).

3.4 Light regulates GA pathway during seed germination

Seed germination is determined by a balance between ABA and GA levels. Increased endogenous ABA levels inhibit seed germination. Previous studies have reported that GA functions in promoting seed germination, because GA-deficient mutants (*ga1-3* and *ga2-1*) were shown to be defective in seed germination

(Koornneef and van der Veen, 1980). In addition, treatment with GA inhibitors, paclrobutrazol or uniconazole, produced a phenotype with reduced seed germination (Nambara et al., 1991; Jacobsen and Olszewski, 1993; Ogawa et al., 2003). GA catabolism and anabolism influence seed germination through the alteration of endogenous GA levels. GA1 (the amount of which is usually ~10% that of GA4) and GA4 (the major bioactive GA in Arabidopsis), the precursors of GA biosynthesis, increase the bioactive GA level and promote seed germination. Bioactive GA1 and GA4 are produced in later steps during GA metabolism. Their productions are catalyzed by GA 3-oxidase (GA3ox) and GA 20-oxidase (GA20ox). These catalytic enzymes belong to 2-oxoglutarate-dependent dioxygenases (2ODDs), a family of the small multigene proteins. The 2ODDs are known as primary targets in the regulation of bioactive GA (Yamaguchi, 2008; Seo et al., 2009). GA 2-oxidase (GA2ox) was identified as a GA deactivation enzyme, and is a member of the 2ODDs (Yamaguchi, 2008; Seo et al., 2009). The transcript levels of endogenous *GA3ox* are increased after exposure to red light, whereas those of *GA2ox* are decreased. *GA3ox1* expression is induced sharply, peaks at 12 hr after light pulse, and then decreases rapidly. However, *GA3ox2* expression is gradually increased and peaks at 36 hr after light pulse. *GA3ox1* and *GA3ox2* transcript levels increase more with a pulse of red light than with far-red light. However, GA deactivating gene, *GA2ox2*, is increased at 12 hr after exposure to far-red light pulse. Therefore, bioactive GA levels are antagonistically regulated by GA3ox and GA2ox (Seo et al., 2009).

3.5 Light regulates ABA pathway

ABA, a phytohormone, regulates various environmental processes such as drought, cold, and conditions of high salinity (Leung and Giraudat, 1998). ABA controls light-dependent seed germination and maintains seed dormancy (Koornneef et al., 2002). Red-light activated phyB Pfr leads to repressed ABA levels, and subsequently it triggers seed germination. Alternatively, phyB Pr with far red light increases ABA levels and prohibits seed germination (Seo et al., 2006). Previous studies have shown that ABA inhibits GA biosynthetic genes (*GA3ox1* and *GA3ox2*) in imbibed seeds (Seo et al., 2006). Consistent with the changes in ABA levels, the transcript levels of ABA metabolic genes, *ZEAXANTHIN EPOXIDASE* (*ZEP)/ABA DEFICIENT 1(ABA1), 9-CIS EPOXYCAROTENOID DIOXYGENASE 6* (*NCED6*), and (*NCED9*), are decreased by red light, whereas the transcript levels of *ABSCISIC ACID 8'-HYDROXYLASE 2* (*CYO707A2)*, a gene encoding an ABA-deactivating enzyme, is increased (Seo et al., 2006; Oh et al., 2007; Sawada et al., 2008; Seo et al., 2009). Therefore, ABA levels in imbibed seeds are regulated in a manner opposite to GA levels (Seo et al., 2006).For these reasons, plant must carefully monitor to survive for their optimized seed germination through interaction with various environmental signals.

(a)

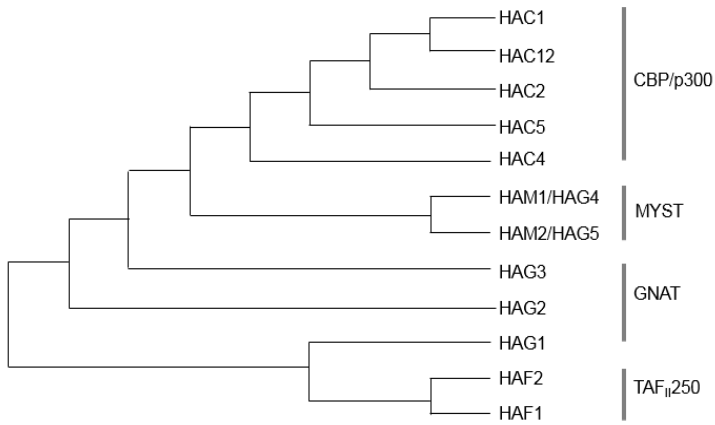

(b)

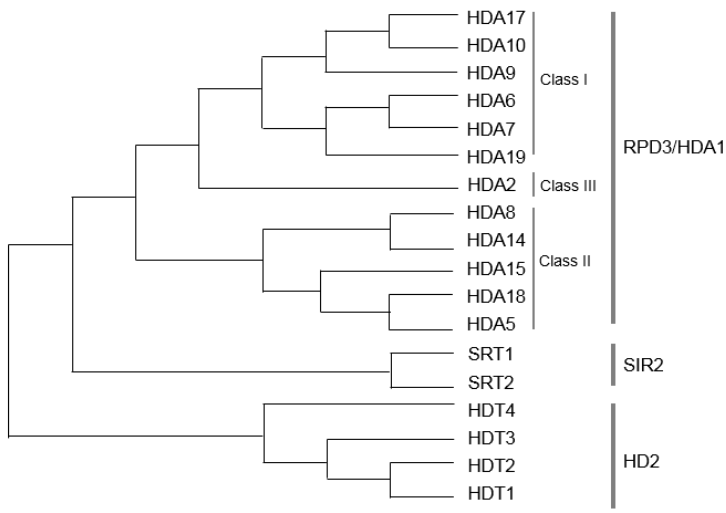

Figure 1-1. Phylogenetic tree for Arabidopsis HATs and HDACs.

The phylogenetic trees was generated using MEGA software (version 6.06) and displayed as neighbor-joining (NJ) tree. Arabidopsis HAT (a) and HDAC (b) amino-acid sequences were aligned with ClustalW.

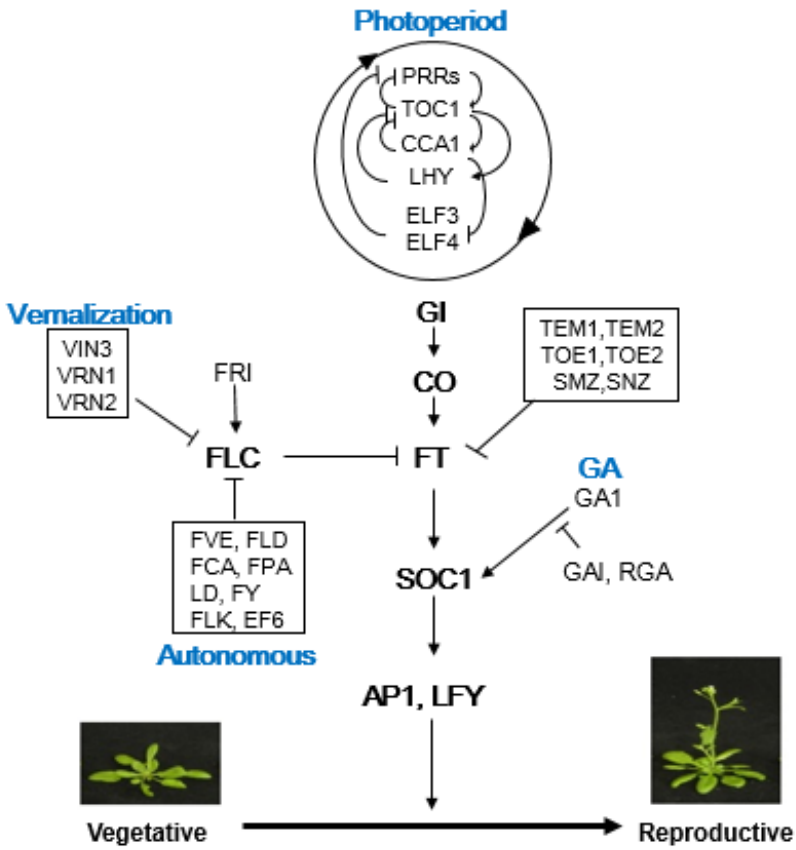

Figure 1-2. Flowering pathways in Arabidopsis

Chapter II.

Repression of flowering in non-inductive photoperiod by the *HDA9-AGL19-FT* module in Arabidopsis

---

This Chapter was published as ″Kang MJ, Jin HS, Noh YS, Noh B (2015) Repression of flowering in non-inductive photoperiod by the HDA9-AGL19-FT module in Arabidopsis. *New Phytol* **206:** 281-294″

2.1 Abstract

Posttranslational acetylation of histones is reversibly regulated by histone deacetylases (HDACs). Despite the evident significances of HDACs in Arabidopsis development, the biological roles and underlying molecular mechanisms of many HDACs are yet to be elucidated.

By reverse-genetic approach, I isolated an *hda9* mutant and performed phenotypic analyses on it. In order to address the role of HDA9 in flowering, genetic, molecular, and biochemical approaches were employed.

hda9 flowered early in non-inductive short days (SD) and had increased expression of the floral integrator *FLOWERING LOCUS T* (*FT*) and the floral activator *AGAMOUS-LIKE 19* (*AGL19*) compared to wild type. The *hda9* mutation increased histone acetylation and RNA polymerase II occupancy at *AGL19* but not at *FT* during active transcription, and HDA9 protein directly targeted *AGL19*. *AGL19* expression was higher in SD than in inductive long days, and an *AGL19* overexpression caused a strong upregulation of *FT*. A genetic analysis showed that an *agl19* mutation is epistatic to the *hda9* mutation, masking both the early flowering and the increased *FT* expression of *hda9*.

Taken together, my data indicate that HDA9 prevents precocious flowering in SD by curbing the hyper-activation of *AGL19*, an upstream activator of *FT*, through resetting local chromatin environment.

2.2 Introduction

Histone acetylation has been implicated in transcriptional activation. The addition of acetyl groups on lysine residues at the histone N-terminal tails by histone acetyltransferases (HATs) decreases the affinity of DNA to histones by increasing negative charges on histones, thereby relaxing the chromatin structure to be more accessible to transcription factors. The histone-tail acetylation also creates binding surfaces for other chromatin modifiers or transcription cofactors positively regulating transcription. Histone deacetylases (HDACs) remove acetyl groups from histone lysine residues, which results in the opposite effects to HATs on chromatin structure and transcription. In fact, HDACs have been found in various types of transcription repressor complexes in yeasts and higher eukaryotes (Cunliffe, 2008; Yang and Seto, 2008). Interestingly, genome-wide association studies in yeast and human have shown the presence of HDACs together with HATs in active as well as in inactive genes (Kurdistani *et al*., 2002; Wang *et al*., 2009b), suggesting the role of HDACs in controlling transcription that is beyond the traditional paradigm.

Arabidopsis has 12 putative HDACs belonging to the RPD3/HDA1 superfamily that is divided into four subgroups, namely Class I through III and an outlier group (Pandey *et al*., 2002). Genetic or pharmacological ablation of the HDAC function has shown that HDACs play diverse and important roles in many aspects of development and physiology in Arabidopsis. Antisense or T-DNA insertional knockout mutants of *HDA19*, a Class I *HDAC*, show multiple defects in

growth and development and altered responses to exogenous stimuli, such as light and pathogens, accompanied by deregulation of genes (Tian *et al*., 2003; Zhou *et al*., 2005; Benhamed *et al*., 2006; Long *et al*., 2006; Kim *et al*., 2008; Tanaka *et al*., 2008; Choi *et al*., 2012), reflecting the role of HDA19 as a global repressor (Tian *et al*., 2005). HDA6, the closest homolog of HDA19, plays key roles in the silencing of transgenes, transposable elements, and rRNA genes in association with RNA-directed DNA methylation (RdDM; Aufsatz *et al*., 2002; Probst *et al*., 2004; Earley *et al*., 2010) or RdDM-independent DNA methylation (To *et al*., 2011; Liu *et al*., 2012). Studies using *hda6* mutants have revealed that HDA6 has roles in flowering (Wu *et al*., 2008; Yu *et al*., 2011), embryonic-to-postembryonic transition (Tanaka *et al*., 2008), and senescence (Wu *et al*., 2008). Pharmacological studies employing trichostatin A (TSA), an inhibitor of the RPD3/HDA1 family of HDACs, have also revealed the importance of HDACs in directing the expression of root epidermal cell-patterning genes (Xu *et al*., 2005) and in controlling the rhythmic expression of the circadian clock gene, *TOC1* (Perales and Màs, 2007).

Flowering is controlled by environmental cues, such as photoperiod and temperature, and by developmental signals. In facultative long-day (LD) plants including Arabidopsis, inductive LD promotes rapid flowering, whereas non-inductive short-day (SD) represses the floral promotion activity and thus results in delayed flowering (Koornneef *et al*., 1998). There have been extensive studies on the signaling and mechanism of LD-induced floral promotion (Turck *et al*., 2008; reviewed in Amasino, 2010); however, the signaling and mechanistic detail of

floral repression and default flowering in SD are poorly understood. Gibberellic acid (GA) is known to allow default flowering in SD through activating *SUPPRESSOR OF OVEREXPRESSION OF CONSTANS 1* (*SOC1*) and *LEAFY* (*LFY*), two of the downstream floral activators (Blázquez and Weigel, 2000; Moon *et al*., 2003). VIN3-LIKE 1 (VIL1) and VIL2 have been reported to repress *FLOWERING LOCUS M* (*FLM*) and *MADS AFFECTING FLOWERING 5* (*MAF5*), two of the *FLOWERING LOCUS C* (*FLC*)-clade floral repressors, respectively in SD, leading to the promotion of floral transition (Sung *et al*., 2006; Kim and Sung, 2010). Lately, the micro RNA156 (miR156)-*SQUAMOSA PROMOTER BINDING PROTEIN LIKEs* (*SPLs*) regulatory module for vegetative phase transition has also been shown to play an important role in age-dependent flowering, especially under non-inductive SD conditions (Wang *et al*., 2009a).

Although there is evidence that indicates the significance of HDACs in the development and physiology of Arabidopsis, the biological roles and underlying molecular mechanisms of many HDACs have not yet been studied. Here, I report the *in vivo* roles of HDA9, a member of the RPD3/HDA1 family Class I HDACs. Loss of *HDA9* affects the development of several organs and caused early flowering in SD. Recently, an SD-specific early flowering of *hda9* mutants with increased *AGAMOUS-LIKE 19* (*AGL19*) expression and histone acetylation at the *AGL19* locus was reported (Kim et al., 2013). However, several important questions including whether *AGL19* is a direct target of HDA9, whether the increased expression of *AGL19* is a direct cause for the early flowering of *hda9*,

and how the loss of HDA9 activity results in SD-specific early flowering remain unanswered. Moreover, the pathway for which *AGL19* acts as a floral activator has not been elucidated. I demonstrate that HDA9 prevents precocious flowering in SD and during vernalization by directly targeting *AGL19* and repressing its expression during active transcription through histone deacetylation. Derepression of *AGL19* caused by the *hda9* mutation in turn induces the expression of *FLOWERING LOCUS T* (*FT*), which results in early flowering. I also show that *AGL19* expression is upregulated by SD photoperiod as well as by vernalization (Schönrock *et al*., 2006). These results indicate that the role of HDA9 in preventing the overstimulation of *AGL19* transcription by the inductive signals together with the photoperiod-dependent expression of *AGL19* are the basis of the SD-specific early flowering of *hda9*. My results suggest that the biochemical role of HDA9 might be to reset histone acetylation levels during active transcription to attain proper transcription activity and controlled gene expression.

2.3 Materials and Methods

2.3.1 Plant materials and growth conditions

The following T-DNA insertion mutants were obtained from the SALK collection (http://signal.salk.edu/): *hda9-1*, SALK_007123; *maf4*, SALK_028506; *maf5-1*, CS876411; and *maf5-2*, SALK_054770. The following mutants and transgenic plants were previously described as written in the text: *flc-3*, *fld-3*, *ld-1*, *FRI*, *hac1-1*, *ref6-3*; *co-101*, *ft-10*, *gi-2*, *agl19-1*, and *FT::GUS* plants. All the transgenic and mutant plants used in this study are in the Columbia (Col) background. All the plants were grown at 22℃ under 100 μmol m^{-2} s^{-1} of cool white fluorescent light with a 16 hours light/8 hours dark (LD) or an 8 hours light/16 hours dark (SD) photoperiod.

2.3.2 Histochemical β-glucuronidase (GUS) assay

For *HDA9:GUS*, a 3.9-kb genomic fragment of *HDA9* containing 0.9 kb promoter and the entire coding region was generated by polymerase chain reaction (PCR) using HDA9-GUS-F and HDA9-GUS-R as primers (Table S2). After restriction digestion with *Xho*I-*Sma*I, the PCR product was ligated to the *Sal*I-*Sma*I digested pPZP211G (Noh *et al*., 2001). *HDA9:GUS* was introduced into wt by the floral dip method (Clough and Bent, 1998) via *Agrobacterium tumefaciens* strain ABI, and

transformants were selected on MS media containing 50 μg ml^{-1} kanamycin. Histochemical GUS staining was performed as previously described (Noh *et al*., 2004). The GUS expression patterns in Fig. 2b,c were observed using a light microscope (Carl Zeiss Axioskop 40). *FT::GUS* from wt was introgressed into *hda9-1* through crossing, and the *hda9-1* mutants carrying *FT::GUS* (+/+) were selected. FT::GUS expression in wt and *hda9-1* was then compared.

2.3.3 Subcellular localization study

Nuclear fractionation was performed as previously described (Kinkema *et al*., 2000). Protein samples were quantified using a protein assay kit (Bio-Rad), subjected to SDS-PAGE, and transferred to nitrocellulose membranes (Millipore). For the detection of proteins, α-HA (Abcam ab9110), α-H3 (Abcam ab1791), and α-tubulin (Sigma-Aldrich T9026) were used at 1:3,000, 1:10,000, and 1:4,000, respectively.

2.3.4 HDA9 complementation construct and HDA9:HA

For the complementation construct (*HDA9g*), a 3.9 kb genomic fragment was amplified by PCR using HDA9-GUS-F and HDA9G-R (Table S2) as primers and cloned into the pPZP221-rbcsT which contains the transcriptional terminator of Arabidopsis *rbcS*. For the construction of *HDA9:HA*, a 3.9 kb *HDA9* genomic

fragment amplified using HDA9 gateway-F and HDA9 gateway-R as primers (Table S2) was cloned into the pENTR/SD/D-TOPO entry vector (Invitrogen) and then integrated into the pEarleyGate 301 destination vector (Earley *et al*., 2006) through recombination. The complementation construct and *HDA9:HA* were introduced into *hda9-1* as described for *HDA9:GUS*, and transformants were selected on MS media containing 100 μg ml^{-1} gentamycin (Sigma-Aldrich) or 25 μg ml^{-1} glufosinate ammonium (Sigma-Aldrich), respectively.

2.3.5 Flowering time analysis

Flowering times were measured as the means ± S.D. of the number of rosette and cauline leaves produced from the primary meristems at bolting. At least 15 plants were scored for each genotype and treatment. For vernalization treatment, plants were grown for 14 days (d) in SD and vernalized at 4℃ under SD conditions for 30 d. Vernalized samples were harvested immediately after the cold treatment.

2.3.6 RT-PCR and RT-qPCR analyses

Total RNA was isolated from plant tissues using TRI Reagent (Sigma-Aldrich) according to the manufacturer′s instructions. 4 μg of total RNA was reverse transcribed using MMLV Reverse Transcriptase (Fermentas) and the resulting first

strand was used as template for semi-quantitative PCR or quantitative real-time PCR (qPCR). The sequences of primers used for reverse transcription followed by PCR (RT-PCR) or qPCR (RT-qPCR) are provided in Table S3 or Table S4, respectively. qPCR was performed in 96-well blocks using an Applied Biosystems 7300 real-time PCR system (http://www.appliedbiosystems.com/) and SYBR Green I master mix (Kappa Biosystems). Absolute quantification was performed by generating standard curves using serial dilutions of a mixture of all cDNA samples to be analyzed. Normalization was to *Ubiquitin 10* (*UBQ10*). All the RT-qPCR results were presented as means ± S.E. of three biological replicates performed in triplicate.

2.3.7 ChIP assay

Chromatin immunoprecipitation (ChIP) was performed as previously described (Han *et al*., 2007; Kaufmann *et al*., 2010). Antibodies used for ChIP were α-H3Ac (Millipore 06-599), α-H3 (Abcam ab1791), α-RNA Pol II (Covance MMS-126R), and α-HA (Abcam ab9110). The α-H3Ac recognizes acetylated lysine 9 and 14 of H3, and the α-RNA Pol II recognizes both initiating and elongating forms of Pol II. The amount of immunoprecipitated chromatin was determined by qPCR (ChIP-qPCR) using primer pairs listed in Table S5, and the relative amounts of amplified

products were evaluated according to the $2^{\Delta\Delta CT}$ method (Livak and Schmittgen, 2001).

Table 2-1. Oligonucleotides used for genotyping

Gene	Name	Sequence
T-DNA border	SALK LB1.3	5'-ATTTTGCCGATTTCGGAAC-3'
	SAIL LB3	5'-TAGCATCTGAATTTCATAACCAATCTCGATACA-3'
HDA9	HDA9-F1	5'-GAAATGGCTAGATGTAAGTTTTGTGTCT-3'
	HDA9-R1	5'-TCGCCTGTCCCTGGAAAGAACTTATC-3'
AGL19	AGL19-1F	5'-TCACACCCTCTTCCCAAAATCTCGCC-3'
	AGL19-1R	5'-GGTGTCAAACTCATCTTTCTTACAAAC-3'
MAF4	MAF4-F	5'-GTTATTGGGTCTCATGGGCCAAAGAAACTG-3'
	MAF4-R	5'-GTTAACCAATAGTTTTTGCACTTCTCTAAC-3'
MAF5	MAF5-1F	5'-GGCGCCATCATACATAAGCTA -3'
	MAF5-1R	5'-TCTCCACAATAATAGGGCCCT-3'
	MAF5-2F	5'-AATTTGGCAACTACCATGCA-3'
	MAF5-2R	5'-TTGAATTGTTAGTTGTTCCGCTT-3'
HAC1	HAC1-3F	5'-ATGCAGAAGACCGTCATGCAGGTTC-3'
	HAC1-4R	5'-TTTTTAATCGAGCAAGGGACCGTGC-3'
REF6	T29H11-1	5'-CCTCCATGTTACATTGGTATGCTGCACATT-3'
	T29H11-2	5'-CAAATGTCTGATCCGCACAAGGGAATTATC-3'
FLD	FLD-3-1	5'-ACGGATCCATCAAATTTGTTCCCGAATTAC-3'
	FLD-3-2	5'-CTGAAGCTCCCACTGCAACATTAGAGTAAG-3'
LD	ld-1 MSEIF	5'-GCTGCGTAGCTTTCATCAATGCCA-3'
	ld-1 MSEIR	5'-GAATATCTTCCTGTTACGACACG-3'

FRI	FRI UJ26-F	5'-AGATTTGCTGGATTTGATAAGG-3'
	FRI UJ26-R	5'-GAAATTCACCGAGTGAGAACAGA-3'
GI	pGI2-1F	5'-CCACTAGTTGTAGCTTTGCTCAGAC-3'
	pGI2-1R	5'-ATGACTATTCGGAGCAATGGGCT-3'
CO	Constas R KO-F	5'-AGCTCCCACACCATCAAACTTACTACATC-3'
	Constas A-R	5'-AGTCCATACTCGAGTTGTAATCCAC-3'
FT	JH2295	5'-TAAGCTCAATGATATTCCCGTACA-3'
	JH2296	5'-CAGGTTCAAAACAAGCCAAGA-3'
	JH2297	5'-CCCATTTGACGTGAATGTAGACAC-3'
FLC	pFLC33	5'-CTCATGTATCTATCATGGTCGCAG-3'
	pFLC24	5'-CGTATCGTAGGGGAGGAAAGATAG-3'

Table 2-2. Oligonucleotides used for *HDA9g*, *HDA9:GUS*, and *HDA9:HA* constructs

Construct	Name	Sequence
HDA9:GUS	HDA9-GUS-F	5'-AGCTCGAGGGTCATCATTTCTCTCAACATTGTT-3'
	HDA9-GUS-R	5'-CAACCCGGGGATGACGCATCGTTATCGTTGTCTC-3'
HDA9:HA	HDA9 gateway-F	5'-CACCGGTCATCATTTCTCTCAACATTGT-3'
	HDA9 gateway-R	5'-TGACGCATCGTTATCGTTGTCTCC-3'
HDA9g	HDA9-GUS-F	5'-AGCTCGAGGGTCATCATTTCTCTCAACATTGTT-3'
	HDA9 GUS-R	5'-CCCGGGTTATGACGCATC GTTATCGTTGTCT-3'

Table 2-3. Oligonucleotides used for RT-PCR analysis

Gene	Name	Sequence
UBQ10	UBQ-F	5′-GATCTTTGCCGGAAAACAATTGGAGGATGGT-3′
	UBQ-R	5′-CGACTTGTCATTAGAAAGAAAGAGATAACAGG-3′
HDA9N	HDA9F	5'-GAGATGCGTTCCAAGGACAA-3'
	HDA9R-1	5'-GCCGGCGTAAAGTTGACAAAAT-3'
HDA9F	HDA9F	5'-GAGATGCGTTCCAAGGACAA-3'
	HDA9R-2	5'-TTATGACGCATCGTTATCGTTGTCT -3'
FT	FT-F	5'-GCTACAACTGGAACAACCTTTGGCAAT-3'
	FT-R	5'-TATAGGCATCATCACCGTTCGTTACTC-3'
TEM1	TEM1-F	5'-GCGTGTTGTTTCGGTATCACTA-3'
	TEM1-R	5'-ATTCAGAGAACGGCGTCGA-3'
TEM2	TEM2-F	5'-TTCCTCAGCCTAACGGAAGAT-3'
	TEM2-R	5'-TCCTTGACGAATCGACTCCAT-3'
TOE1	TOE1-F	5'-ACTCAGTACGGTGGTGACTC-3'
	TOE1-R	5'-CGAGGATCCATAAGGAAGAGG-3'
TOE2	TOE2-F	5'-CACTTTCTATCGGAGGACAG-3'

	TOE2-R	5'-CTTCCACATACGGAATTGTT-3'
TOE3	TOE3-F	5'-GTTACGTTTTACCGACGAAC-3'
	TOE3-R	5'-TGCTTGCAATATCAGACTTG-3'
SMZ	SMZ-F	5'-AATGGTGAAGAAGAGCAGAA-3'
	SMZ-R	5'-CTTTCCGATGATGATGAAAT-3'
SNZ	SNZ-F	5'-TTTGGAATCCTTAAACGAAA-3'
	SNZ-R	5'-TATCTCATTGCATTTTGCTG-3'
AGL15	AGL15-F	5'-TTATCTAGATGGGTCGTGGAAAAATCGAG-3'
	AGL15-R	5'-TTAGCGGCCGCAGAGAACCTTTGTCTTTTGGCTTC -3'
AGL18	AGL18-F	5'-ATGGGGAGAGGAAGGATTGAGATTAAGAA -3'
	AGL18-R	5'-TCAATCAGAAGCCACTTGACTCCCAGAGT -3'
AGL19	AGL19-F	5'-ATGGTGAGGGGCAAAACGGAGATG-3'
	AGL19-R	5'-TCCAGATGTTTCGTCTCTCGCTTGC-3'
AGL24	AGL24-F	5'-TCCATCGAAGTCAACTCTGCTGGATC-3'
	AGL24-R	5'-GTCTTCATGCAAGTAACATCAAC-3'
MAF4	MAF4-F	5'-ATTAGGTCAGAAGAATTAGTCGGAGAAAAC-3'
	MAF4-R	5'-CTTGGATGACTTTTCCGTAGCAGGGGGAAG-3'

MAF5	MAF5-F	5'-GGGGATTAGATGTGTCGGAAGAGTGAAG-3'
	MAF5-R	5'-GATCCTGTCTTCCAAGGTAACACAAAGG-3'

Table 2-4. Oligonucleotides used for RT-qPCR analyses

Gene	Name	Sequence
UBQ10	qUBQ-F	5′-GGCCTTGTATAATCCCTGATGAATAAG-3′
	qUBQ-R	5′-AAAGAGATAACAGGAACGGAAACATAGT-3′
CO	qCO-F	5'-AAACCCATTTGCACAACAG-3'
	qCO-R	5'-GAGCAAGGGTTCAACACGAT-3'
FT	qFT-F	5'-CCATTGGTTGGTGACTGATATCC-3'
	qFT-R	5'-TTGCCAAAGGTTGTTCCAGTT-3'
FLC	qFLC-F	5'-AGCAAGCTTGTGGGATCAAATGTC-3'
	qFLC-R	5'-TGGCTCTAGTCACGGAGAGGGC-3'
SOC1	qSOC1-F	5'-TCGAGCAAGAAAGACTCAAGTG-3'
	qSOC1-R	5'-TTGACCAAACTTCGCTTTCA-3'
SPL3	qSPL3-F	5′-CTTAGCTGGACACAACGAGAGAAGGC-3′
	qSPL3-R	5′-GAGAAACAGACAGAGACACAGAGGA-3′
SPL4	qSPL4-F	5′-GTAGCATCAATCGTGGTGGC-3′
	qSPL4-R	5′-CTTCGCTCATTGTGTCCAGC-3′
SPL5	qSPL5-F	5′-CCAGACTCAAGAAAGAAACAGGGTAGACAG-3′
	qSPL5-R	5′-TCCGTGTAGGATTTAATACCATGACC-3′

SPL9	qSPL9-F	5′-CAAGGTTCAGTTGGTGGAGGA-3′
	qSPL9-R	5′-TGAAGAAGCTCGCCATGTATTG-3′
SPL15	qSPL15-F	5′-TTGGGAGATCCTACTGCGTGGTCAACC-3′
	qSPL15-R	5′-AGCCATTGTAACCTTATCGGAGAATGAG-3′
MAF1	qMAF1-F	5'-TCACCTTAAACTCAAAGCCTGATTC-3'
	qMAF1-R	5'-CAAACTCTGATCTTGTCTCCGAAG-3'
MAF2	qMAF2-F	5'-CATTGTGGGTCTCCGGTGATTAG-3'
	qMAF2-R	5'-GATGAGACCATTGCGTCGTTTG-3'
MAF3	qMAF3-F	5'-TATCTTCCTCGCGCCAATG-3'
	qMAF3-R	5'-AGCACAAGAACTCTGATATTTGTCTAC-3'
MAF4	qMAF4-F	5'-GCTTCTCAAGTAACCACCATCAC-3'
	qMAF4-R	5'-CTTGGATGACTTTTCCGTAGCAG-3'
MAF5	qMAF5-F	5'-CATGGATTGTGCTAGAAAACAACTG-3'
	qMAF5-R	5'-GCTTCACTCTTCCGACACATCTAATC-3'
AGL6	qAGL6-F	5'-TTTCCGGTAGAGCCTTCTCA-3'
	qAGL6-R	5'-CCCAACCTTGGACGAAATTA-3'
AGL19	qAGL19-F	5'-TCAGCAAGCGAGAGACGAAACATC-3'
	qAGL19-R	5'-TGCATCAATGCCTTCTCCAAGCAA-3'
AGL24	qAGL24-F	5'-TCTCCGGCTTGAGAATTGTAACCTC-3'
	qAGL24-R	5'-TCCAGCCGCTGCAACTCTTC-3'

AGL15	qAGL15-F	5'-CTGCAGGGCAAGGGCTTGAA TCCT-3'
	qAGL15-R	5'-TGCTCGTTGTTCCTTGAGGCGTG-3'
AGL18	qAGL18-F	5'-ATGGGGAGAGGAAGGATTGAGATTAAGAA -3'
	qAGL18-R	5'-GATGATAAGAGCAACCTCGGCGTC-3'
VIN3	qVIN3-F	5'-ATCTTGCTTGAATCTCTTCTACTCT-3'
	qVIN3-R	5'-ATTGGGAGTGATGATCTTGATGGTA-3'

Table 2-5. Oligonucleotides used for ChIP assays

Locus	Name	Sequence
UBQ10	ChIP-F	5′-TTGCCAATTTTCAGCTCCAC-3′
	ChIP-R	5′-TGACTCGTCGACAACCACAA-3′
ACTIN2/7	ChIP-F	5′-GATCCGTTCGCTTGATTTTGC-3′
	ChIP-F	5′-ACAAGCACGGATCGAATCACA-3′
AGL19-A	AGL19-AF	5'-CCATTGATAGATTTTGGATATTAGATAA-3'
	AGL19-AR	5'-CAGGTGTCGCACGCTAGGAGAGGACCACA-3'
AGL19-B	AGL19-BF	5'-GTTACTGTTTTATTTGTGCGAAGGT-3'
	AGL19-BR	5'-TTCCACAGAAGAAGCAGAACTTTAT-3'
AGL19-C	AGL19-CF	5'-GTATCCATTTTTGTGTCGAAGTCTTTT-3'
	AGL19-CR	5'-TCGGACAAAATAAGTAGTTAGGACACAC-3'
AGL19-D	AGL19-DF	5'-CTATCCGTAGCCATAAGAGAAAATG-3'
	AGL19-DR	5'-AAGCCCTAGATTTATGATGAAGGAG-3'
AGL19-E	AGL19-EF	5'-TTTCTTTCTTTCTCTCCCCTCCTTCAT-3'
	AGL19-ER	5'-ATCTATCTTCTATAAGTGAGTGGAGAGT-3'
AGL19-I	AGL19-IF	5'-TCTTCCCAAAATCTCGCCTA-3'
	AGL19-IR	5'-CAACCACAAACAGAAGATGGAA-3'
AGL19-II	AGL19-IIF	5'-AAACGGAGATGAAGAGGATAGAGAAC-3'
	AGL19-IIR	5'-CATAGAGTTTGGATCTTGGAGAGAAG-3'
AGL19-III	AGL19-IIIF	5'-GCCATCCATTTTTTCGCTGTA-3'
	AGL19-IIIR	5'-GCCTAGCAGTAGCACTGGTGT-3'

AGL19-IV	AGL19-IVF	5'-TTTTGAGCAAACTCAAGAGAGG-3'
	AGL19-IVR	5'-GGACACGCTCAAATCGAAAT-3'
AGL19-V	AGL19-VF	5'-GGAATGGGAACAGCAACAAT-3'
	AGL19-VR	5'-GGAGGTCCAATGAACAAACC-3'
SOC1-1	SOC1-1F	5'-TATATCGGGAGGAGGACCACAC-3'
	SOC1-1R	5'-ATCCATACAGATTTTCGGACCT-3'
SOC1-2	SOC1-2F	5'-TCTCGTACCTATATGCCCCCACT-3'
	SOC1-2R	5'-TTTATCTGTTGGGATGGAAAGA-3'
SOC1-3	SOC1-3F	5'-GCAAAAGAAGTAGCTTTCCTCG-3'
	SOC1-3R	5'-AGCAGAGAGAGAAGAGACGAGTG-3'
SOC1-4	SOC1-4F	5'-GGATGCAACCTCCTTTCATGAG-3'
	SOC1-4R	5'-ATATGGGTTTGGTTTCATTTGG-3'
SOC1-5	SOC1-5F	5'-ATCACATCTCTTTGACGTTTGCTT-3'
	SOC1-5R	5'-GCCCTAATTTTGCAGAAACCAA-3'
SOC1-6	SOC1-6F	5'-TGTTTCAGACATTTGGTCCATTTG-3'
	SOC1-6R	5'-AGTCTTGTACTTTTTCCCCCTATTTTAG-3'
FT2	FT2-F	5'-TCTGATTTGGGGTTCAAAA -3'
	FT2-R	5'-TCGAACTGATTCCGATTGAA-3'
FT3	FT3-F	5'-GGCCAACATTAGAAGAAGATTCC-3'
	FT3-R	5'-TCTTGACATGGAGCGAAAGA -3'
FT7	FT7-F	5'-CTGCGACTGCGACCTATTTT-3'
	FT7-R	5'-GCCACTGTTCTACACGTCCA-3'

cArG VII	cArG VII-F	5'-GGTGGAGAAGACCTCAGGAA -3'
	cArG VII-R	5'-GTGGGGCATTTTTAACCAAG-3'

2.4 Results

2.4.1 Isolation of an *hda9* mutant

The amino acid sequence alignment of HDA9 (At3g44680) and other Arabidopsis Rpd3/HDA1 Class I HDACs (HDA6, HDA7, and HDA19) showed that the HDAC domain of HDA9 is highly similar to that of other HDACs, but its C-terminal region is quite divergent and varies in length compared with that of others (Fig. 1a). Interestingly, the C-terminal region of HDA9 (277 - 426) is nearly identical to the entire regions of HDA10 and HDA17, which belong to the outlier group (Fig. S1b; Pandey *et al*., 2002; Hollender and Liu, 2008). However, HDA10 and HDA17 possess partial HDAC domains and are thus unlikely to be functionally redundant with HDA9 (Fig. 1b). These structural features suggest that HDA9 might possess a unique role in Arabidopsis.

To address the biological role of HDA9 and determine if it is distinct from the roles of the well-characterized HDA6 and HDA19, I first isolated a mutant carrying a T-DNA insertion in the fourth exon of *HDA9* from the SALK collection and named it *hda9-1* (Fig. 2a). This mutant allele was also reported by Kim *et al.* (2013). RT-PCR analyses showed that the full-length *HDA9* transcript is not expressed at a detectable level, although a truncated transcript upstream of the T-DNA insertion site in *hda9-1* is expressed at a reduced level (Fig. 2b). Thus, *hda9-1* is believed to be a null allele.

The *hda9-1* mutants showed a normal morphology in most organs in contrast to *hda19* mutants, which display severely distorted morphological

phenotypes in many organs (Tian and Chen, 2001; Tian *et al*., 2003; Long *et al*., 2006). Nonetheless, subtle morphological differences between wild type (wt) and *hda9-1* were observed in a few organs. At the fully-developed stage, *hda9-1* flowers did not open as fully as wt flowers, and the petals and sepals were less tightly attached to the receptacles in *hda9-1* than in wt (Fig. 2c). In addition, the tips of the *hda9-1* siliques were wide and blunt, whereas those of the wt siliques were tapered and acute (Fig. 2d). The *hda9-1* silique phenotype was similar to that of *erecta* (*er*) mutants (Torii *et al*., 1996). However, unlike *er* mutation, the *hda9-1* mutation did not affect silique length (Fig. 2, 3). In addition, the size of adult *hda9-1*, especially when grown in SD, was smaller than wt mainly because of less elongated petioles and leaves (Figs. 2e,f, 3b). All the *hda9-1* phenotypes described above were restored to wt phenotypes when a genomic copy of *HDA9* was introduced into the *hda9* mutant plants (Fig. 2c,d,f), demonstrating that these phenotypes are indeed caused by the loss of *HDA9* function. Because the *hda9-1* phenotypes described here have not been reported for either *hda6* or *hda19*, it is likely that HDA9 has a distinct *in planta* role.

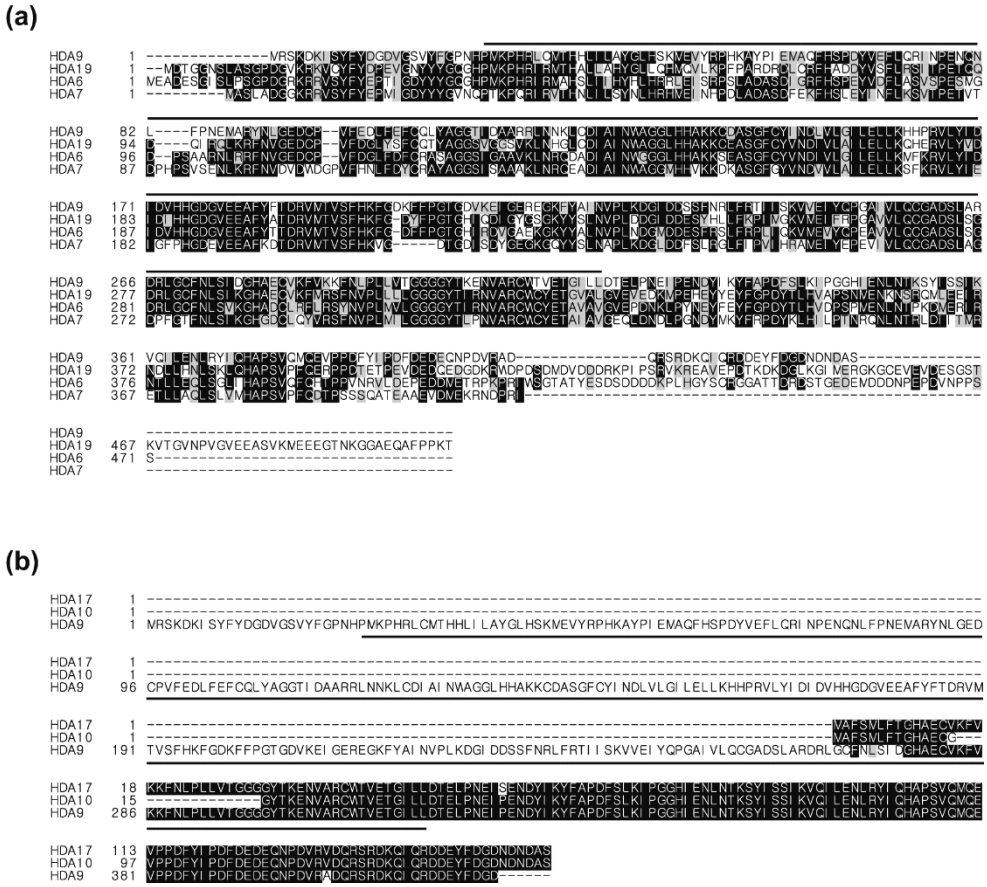

Fig. 1 Sequence comparison between Arabidopsis Class I HDAC proteins.

(a) Multiple sequence alignment of HDA9 (At3g44680), HDA19 (At4g38130), HDA6 (At5g63110), and HDA7 (At5g35600) generated using ClustalW. The numerals indicate amino acid positions, and HDAC domains are marked with solid lines (a,b). (b) Multiple sequence alignment of HDA17 (At3g44490), HDA10 (At3g44660), and HDA9 generated using ClustalW.

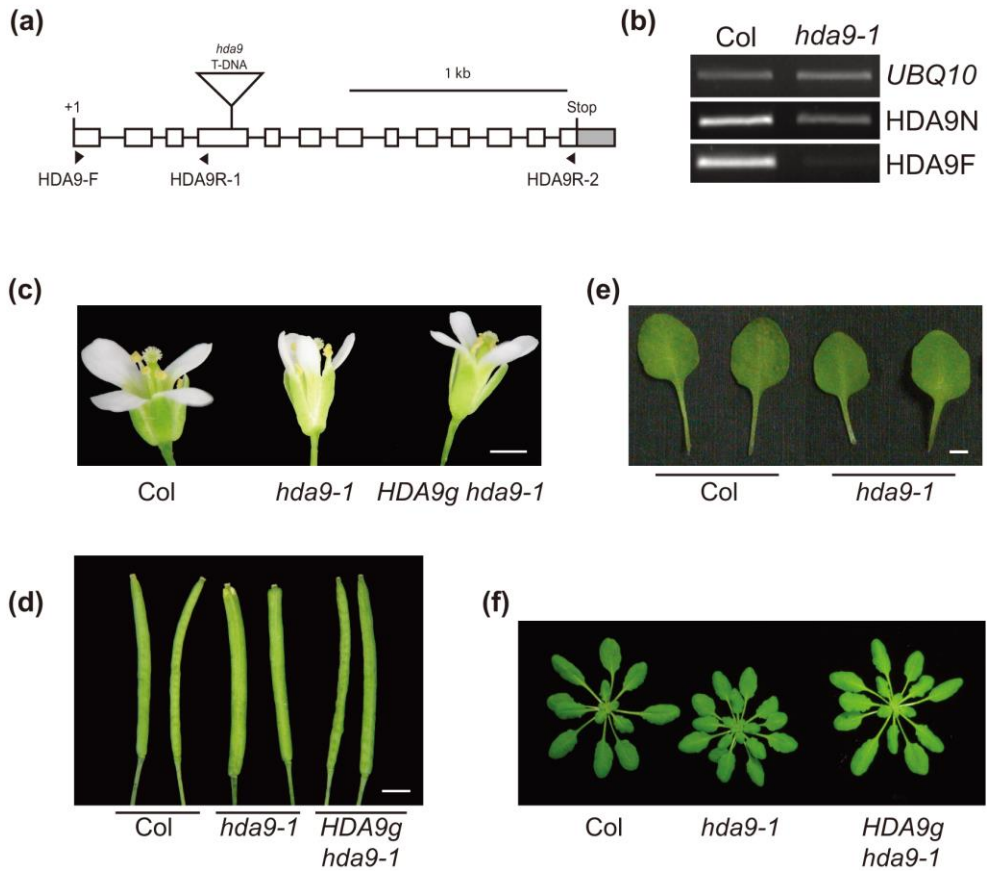

Fig. 2 Phenotype of *hda9-1* mutant

(a) Schematic illustration of the gene structure of *HDA9* and a T-DNA insertion in *hda9-1*. Exons and the 3′ untranslated region (UTR) are represented with white

boxes and a gray box, respectively. Introns are indicated as solid lines. ′+1′ refers to the transcription start site. The T-DNA insertion position in *hda9-1* is marked with a triangle. Arrows indicate the primers used for RT-PCR in (b). (b) RT-PCR analysis of a 5′ (HDA9N) and the full-length (HDA9F) *HDA9* transcript expression in wild type (Col) and *hda9-1*. HDA9-F/HDA9-R1 and HDA9-F/HDA9-R2 primer pairs (a; Table S3) were used for HDA9N and HDA9F, respectively. *UBQ10* was used as an expression control. (c, d) Flower (c) and silique (d) phenotype of wt, *hda9-1*, and *hda9-1* transformed with a genomic copy of *HDA9* (*HDA9g hda9-1*). Scale bars represent 1 mm. (e) Representative 5th and 6th rosette leaves with petioles of wt and *hda9-1* plants grown for 45 d in SD. Scale bars represent 5 mm. (f) Rosette development in wt, *hda9-1*, and *HDA9g hda9-1*. Shown are plants grown for 45 d in SD.

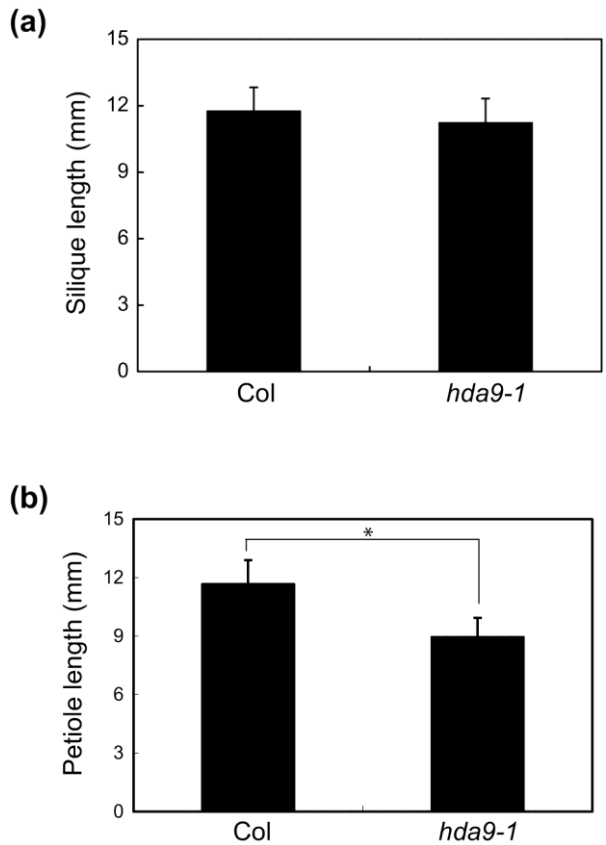

Fig. 3 Effect of the *hda9-1* mutation on silique and petiole lengths.

(a) Length of the 5th and 6th siliques from the primary inflorescence tips. At least fifteen wt or *hda9-1* plants were used for scoring, and values are the means±s.d. (a,b). Length was measured from digital images using UTHSCSA Image Tool (a,b). (b) Length of the petioles of the 5th and 6th rosette leaves. Asterisk denotes a statistically significant difference (P<0.001).

2.4.2 Spatial expression pattern and nuclear localization of HDA9

Because the expression pattern of *HDA9* has not been reported previously, we generated transgenic plants harboring the native promoter and genomic coding region of *HDA9* translationally fused to *GUS* (*HDA9:GUS*), and performed histochemical analyses to study the spatial expression pattern of *HDA9*. GUS staining was observed in the cotyledons, hypocotyls, and roots of the seedlings (Fig. 4a). The shoot apexes, leaf primordial, and root tips were the organs most strongly stained (Fig. 4b,c). In older developmental stages, GUS staining was detected in the entire rosette leaves, including the trichomes and petioles (Fig. 4d), floral organs such as the stigmas, anthers, filaments, pollens, and the siliques (Fig. 4e,f). The nearly ubiquitous spatial expression pattern of *HDA9* studied with the *HDA9:GUS* plants was confirmed by RT-qPCR using RNAs obtained from various tissues (Fig. 4g) and by analysis of the expression profile of *HDA9* exploiting publicly available microarray datasets (Fig. 5).

As shown in Fig. 4c, HDA9:GUS expression was dispersed but not restricted to any particular subcellular compartment. However, it was not clear whether this subcellular GUS-staining pattern reflects the real subcellular localization of the HDA9 protein because *HDA9:GUS* was not able to complement *hda9-1*. Therefore, I generated transgenic *hda9-1* plants expressing the HDA9 protein with a C-terminal HA tag (HDA9:HA) from the native *HDA9* promoter. Unlike *HDA9:GUS*, *HDA9:HA* was able to fully rescue the *hda9-1* mutant phenotypes (Fig. 6), indicating that HDA9:HA is functionally equivalent to HDA9.

To determine the subcellular localization of HDA9:HA, non-nuclear and nuclear proteins were fractionated from the *HDA9:HA hda9-1* plants and used for immunoblot analysis using an anti-HA antibody. A ~55 kilo-dalton protein corresponding to HDA9:HA was detected in the nuclear but not in the non-nuclear fraction (Fig. 4h). Thus, HDA9 seems to be localized predominantly in the nuclei like HDA6 and HDA19 (Earley *et al*., 2006; Fong *et al*., 2006; Long *et al*., 2006; Wu *et al*., 2008).

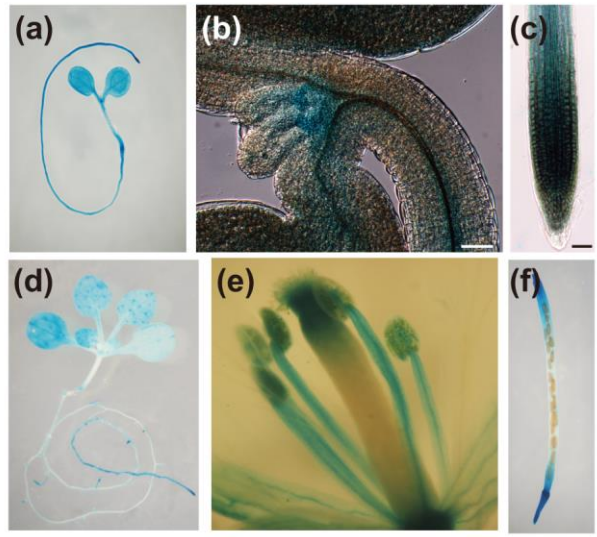
(a)
(b)
(c)
(d)
(e)
(f)

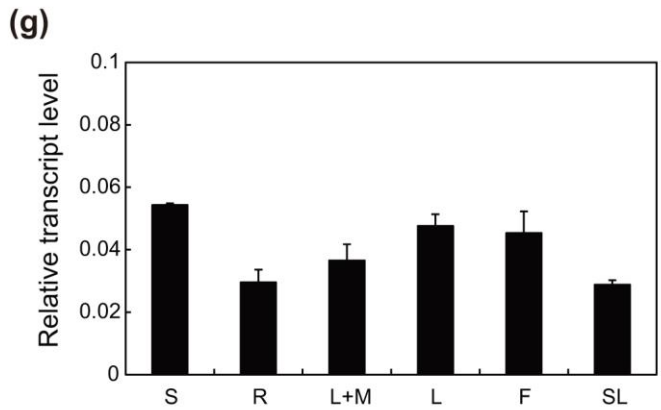
(g)
Relative transcript level
0.1
0.08
0.06
0.04
0.02
0
S
R
L+M
L
F
SL

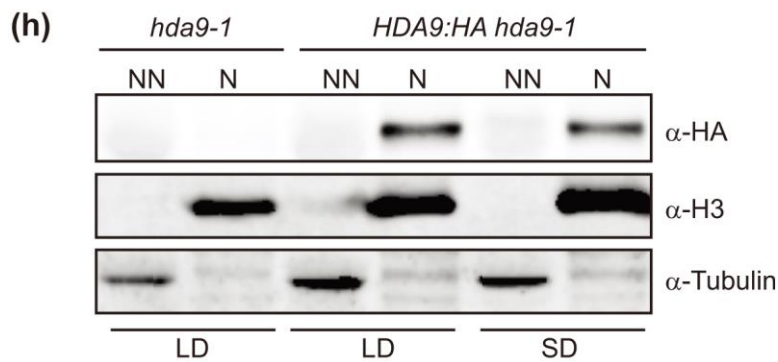
(h)
hda9-1
HDA9:HA hda9-1
NN
N
NN
N
NN
N
α-HA
α-H3
α-Tubulin
LD
LD
SD

Fig. 4 Expression pattern of *HDA9*.

(a-f) Histochemical GUS staining of *HDA9:GUS*-containing transgenic Arabidopsis. (a) 4 d-old seedling grown in SD. (b) Magnified shoot-apex of the seedling shown in (a). Scale bars represent 50 μm (b, c). (c) Primary root tip of 6 d-old seedling grown in SD. (d) 16 d-old whole seedling grown in SD. (e, f) Open flower (e) and silique (f) of LD-grown plant. (g) mRNA expression of *HDA9* in various tissues as studied by RT-qPCR. RNA was isolated from 10 d-old seedlings (S), roots (R), entire shoots including the shoot apical meristems (L+M), rosette leaves (L), flowers (F), and siliques (SL). *UBQ10* was used as an expression control. (h) Nuclear localization of HDA9. Nuclear (N) and nonnuclear (NN) proteins were extracted from *hda9-1* and *HDA9:HA*-containing *hda9-1* transgenic seedlings grown for 10 d in LD or for 14 d in SD and subjected to immunoblot analysis with anti-HA antibody. Histone H3 and tubulin were detected as nuclear and nonnuclear protein controls, respectively.

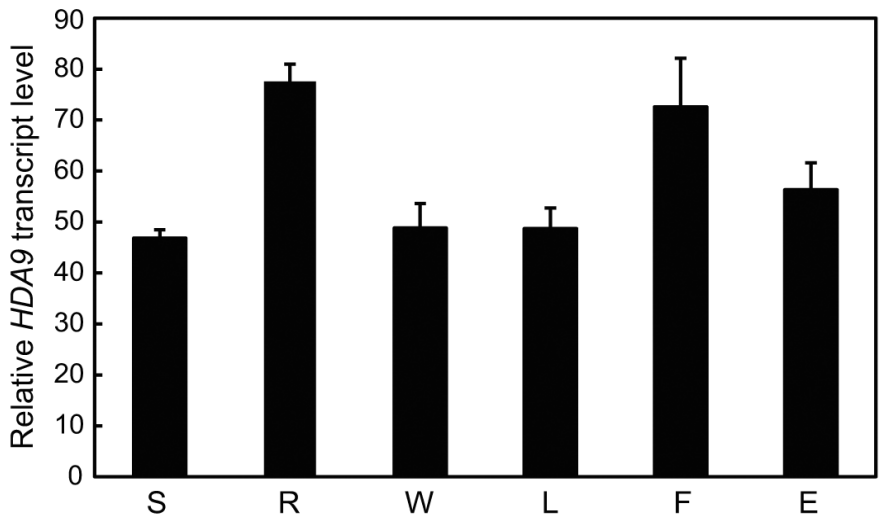

Fig. 5 Predicted spatial expression profile of *HDA9*.

Transcript levels of HDA9 in various tissues were obtained from publicly obtained microarray dataset http://www.arabidopsis.org/servlets/Search?action=new_search&type=expression). S, seedlings; R, roots; W, whole plants; L, leaves; F, flowers; E, embryos.

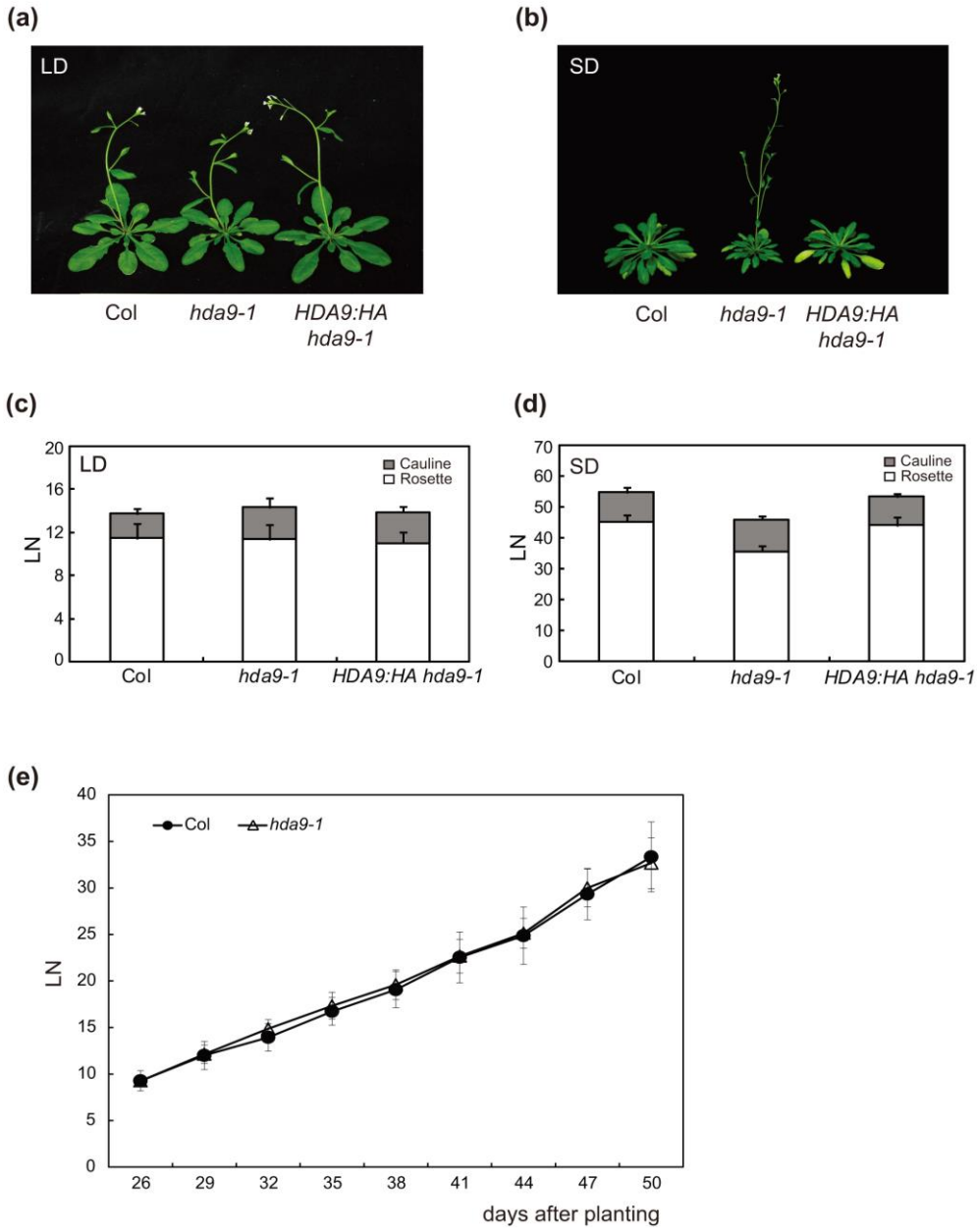
(a)
LD
Col
hda9-1
HDA9:HA hda9-1
(b)
SD
Col
hda9-1
HDA9:HA hda9-1
(c)
LD
Cauline
Rosette
LN
0
4
8
12
16
20
Col
hda9-1
HDA9:HA
hda9-1
(d)
SD
Cauline
Rosette
LN
0
10
20
30
40
50
60
70
Col
hda9-1
HDA9:HA
hda9-1
(e)
Col
hda9-1
LN
0
5
10
15
20
25
30
35
40
26
29
32
35
38
41
44
47
50
days after planting

Fig. 6 Complementation of the early-flowering phenotype of *hda9-1* by *HDA9:HA*.

(a,b) wt, *hda9-1*, and a representative complementation line of *hda9-1* harboring *HDA9:HA* (*HDA9:HA hda9-1*). Pictures were taken when plants were 28-day old in LD (a) or 84-day old in SD (b). (c,d) Flowering time of wt, *hda9-1*, and *HDA9:HA hda9-1* plants in LD (c) or SD (d) as determined by LN. (e) Leaf initiation rate of wt and *hda9-1* plants in SD. At least 15 individual plants per genotype were used for leaf number counting at indicated time until the appearance of primary inflorescence. Values are the means±s.d.

2.4.3 The *hda9-1* mutation causes early flowering in SD

The *hda9-1* mutants displayed another remarkable phenotype: an early flowering in non-inductive SD as evidenced by smaller number of rosette leaves at the onset of flowering (Fig. 7a,b) without change in leaf initiation rate (Fig. 6e). The early-flowering phenotype of *hda9-1* was rescued by the introduction of a genomic *HDA9* fragment (*HDA9g*; Fig. 7a,b) and by *HDA9:HA* (Fig. 6b,d). However, the early-flowering phenotype of *hda9-1* was not obvious in inductive LD (Figs. 6a,c, 7c,d).

I then analyzed the genetic interactions between *hda9-1* and mutations in the autonomous pathway, the photoperiod pathway, and the floral integrator group. The *hda9-1* mutation caused partial suppression of the late-flowering phenotypes of the autonomous-pathway mutants *hac1-1* (Han *et al*., 2007), *relative of early flowering 6-3* (*ref6-3*; Noh *et al*., 2004), *flowering locus d-3* (*fld-3*; He *et al*., 2003), *luminidependens-1* (*ld-1*; Lee *et al*., 1994), and *FRIGIDA* (*FRI*; Koornneef *et al*., 1994; Lee *et al*., 1994)-containing Col in LD (Fig. 7e) and to a greater extent in SD (Fig. 7f). The late-flowering phenotypes of the photoperiod-pathway mutants were also suppressed by *hda9-1* but not as effectively as those of the autonomous-pathway mutants: the *gigantea-2* (*gi-2*; Park *et al*., 1999) *hda9-1* and *constans-101* (*co-101*; Takada and Goto, 2003) *hda9-1* double mutants flowered slightly earlier than the *gi-2* and *co-101* single mutants, respectively (Fig. 7g,h). Notably, the *hda9-1* mutation was not capable of accelerating the floral transition of a floral integrator mutant, *flowering locus t-10* (*ft-10*; Yoo *et al*., 2005), both in LD and SD

(Fig. 7g,h), indicating that *FT* acts downstream of *HDA9*. These results indicate that *HDA9* negatively regulates flowering in parallel with the autonomous and photoperiod pathways and acts upstream of *FT*.

The day-length-dependent effect of the *hda9-1* mutation on flowering (Fig. 7a-d) raised a possibility of day-length dependent *HDA9* expression or nuclear-cytoplasmic shuttling of HDA9 protein as the mammal Class II HDACs (Grozinger *et al*., 2000; Verdel *et al*., 2000). However, HDA9:HA protein was accumulated to comparable levels in LD- and SD-grown plants and predominantly localized to nuclei in both photoperiodic conditions (Fig. 4h), excluding those possibilities.

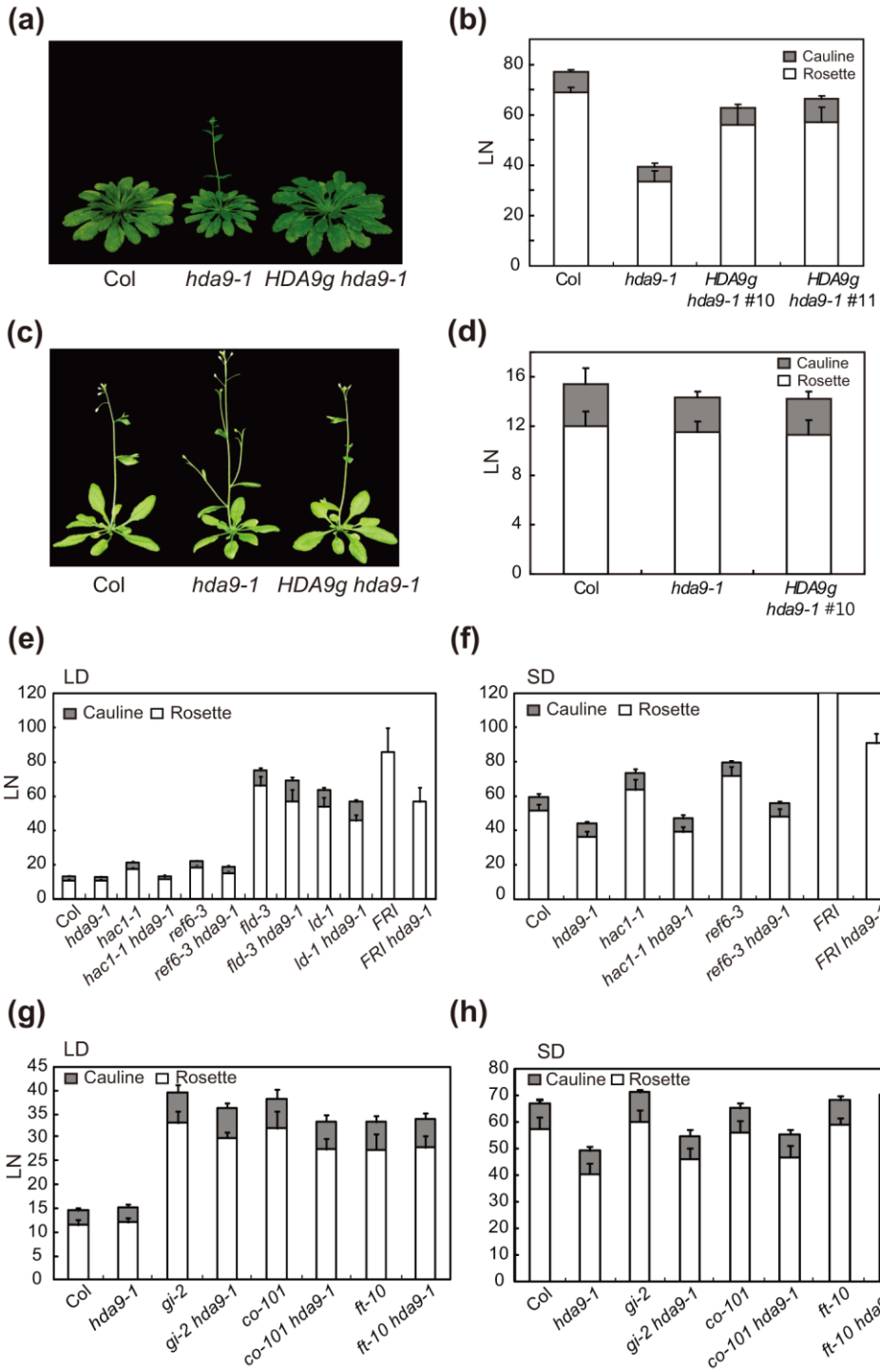
(a)
Col
hda9-1
HDA9g hda9-1
(b)
Cauline
Rosette
LN
Col
hda9-1
HDA9g hda9-1 #10
HDA9g hda9-1 #11
(c)
Col
hda9-1
HDA9g hda9-1
(d)
Cauline
Rosette
LN
Col
hda9-1
HDA9g hda9-1 #10
(e)
LD
Cauline
Rosette
LN
Col
hda9-1
hac1-1
hac1-1 hda9-1
ref6-3
ref6-3 hda9-1
fld-3
fld-3 hda9-1
ld-1
ld-1 hda9-1
FRI
FRI hda9-1
(f)
SD
Cauline
Rosette
Col
hda9-1
hac1-1
hac1-1 hda9-1
ref6-3
ref6-3 hda9-1
FRI
FRI hda9-1
(g)
LD
Cauline
Rosette
LN
Col
hda9-1
gi-2
gi-2 hda9-1
co-101
co-101 hda9-1
ft-10
ft-10 hda9-1
(h)
SD
Cauline
Rosette
Col
hda9-1
gi-2
gi-2 hda9-1
co-101
co-101 hda9-1
ft-10
ft-10 hda9-1

Fig. 7 The *hda9-1* mutation causes early flowering.

(a) Wt, *hda9-1*, and *HDA9g hda9-1* plants grown for 85 d in SD. (b) Flowering time of wt, *hda9-1*, and two independent *HDA9g hda9-1* transgenic lines in SD. Flowering times were determined as the numbers of rosette and cauline leaves formed at bolting (LN). (c) Wt, *hda9-1*, and *HDA9g hda9-1* plants grown for 25 d in LD. (d) Flowering time of wt, *hda9-1*, and an *HDA9g hda9-1* transgenic line in LD as determined by LN. (e-h) Double mutant analyses of *hda9-1* with various late flowering mutants of the autonomous (e, f) or photoperiod pathway (g, h). Flowering time was measured either in LD (e, g) or SD (f, h) by scoring LN. The *FRI* plants grown in SD (f) did not flower at the time of measurement and produced more than 130 rosette leaves.

2.4.4 Loss of *HDA9* affects the expression of *FLC*, *MAF4*, *MAF5*, and *FT*

Because HDA9 localizes to the nuclei and many Rpd3/HDA1 Class I HDACs in yeast, fly, and human are present within various transcriptional repressor complexes (reviewed in Hayakawa and Nakayama, 2010), I questioned whether the *hda9-1* mutation affects the expression of key flowering genes at their mRNA level: *CO*, a key floral promoter in the photoperiod pathway; *FLC*, a central floral repressor in the autonomous and vernalization pathways, and its five paralogs (*MAF1* through *MAF5*); and the floral integrators *FT* and *SOC1*. Under both LD and SD conditions, *FLC* mRNA levels were slightly reduced in *hda9-1*, whereas *CO* mRNA levels in wt and *hda9-1* were comparable (Fig. 8a,b). Downregulation of *MAF4* and *MAF5* mRNAs by *hda9-1* was also observed in SD (Fig. 8b). Consistent with the early-flowering phenotype of *hda9-1*, *FT* and, to a much lesser extent, *SOC1* mRNA levels were higher in *hda9-1* than in wt (Fig. 8a,b).

Because the genetic analysis positioned *FT* downstream of *HDA9*, I further examined the effect of *hda9-1* mutation on the spatial expression of *FT* using *FT::GUS* (Takada and Goto, 2003). In LD, GUS staining was detected mainly in the vascular tissues of the distal parts of both wt and *hda9-1* rosette leaves with similar staining intensity (Fig. 8c). In SD, GUS staining was detected in the primary veins and petioles of both wt and *hda9-1* leaves; however, a stronger intensity was observed in *hda9-1* than in wt, which indicates that *HDA9* affects the expression level but not the expression domain of *FT*. Collectively, these results show that *HDA9* is required for the full expression of *FLC*, *MAF4*, and, *MAF5*, and

for the negative regulation of *FT*.

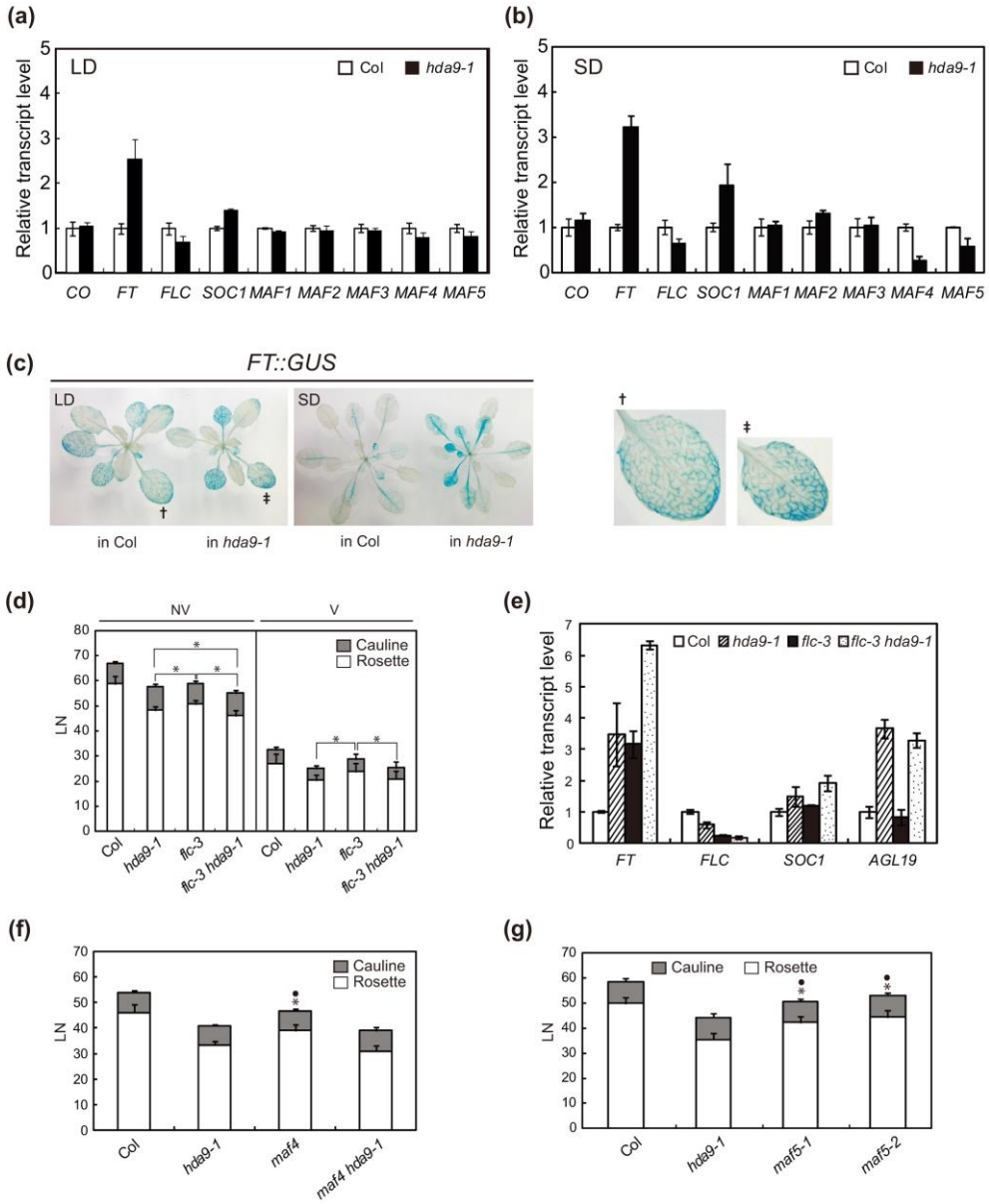

Fig. 8 The *hda9-1* mutation affects *FT* expression.

(a, b) RT-qPCR analyses of the transcript levels of various flowering genes in wt and *hda9-1* seedlings grown for 2 weeks in LD (a) or 4 weeks in SD (b). Wt levels

were set to 1 after normalization by *UBQ10*. Values are the means ± S.E. of three biological replicates. (c) Histochemical GUS staining of wt and *hda9-1* plants harboring *FT::GUS*. Plants were grown for 21 d in LD or for 45 d in SD before staining. All the plants were homozygous for *FT::GUS*. Right panel: 300% digital magnification of the marked leaves on the left to show vascular expression of FT::GUS. (d) Flowering time of *hda9-1*, *flc-3*, and *flc-3 hda9-1* without (NV) or with (V) vernalization as determined by LN. Vernalization was performed as described in the Materials and Methods, and the plants were subsequently grown in SD until bolting. Asterisks indicate statistically significant differences between the two comparisons marked by brackets ($P \leq 0.01$). (e) Additive effect of *flc-3* and *hda9-1* on *FT* expression. Plants were grown for 21 d in SD before being harvested for RNA extraction. Transcript levels of *FT*, *FLC*, *SOC1*, and *AGL19* were determined by RT-qPCR, and wt levels were set to 1 after normalization by *UBQ10*. Values are the means ± S.E. of three biological replicates. (f) Flowering time of *hda9-1*, *maf4*, and *maf4 hda9-1* in SD as determined by LN. Closed circles or asterisks indicate statistically significant differences from Col or *hda9-1*, respectively ($P < 0.001$; f, g). (g) Flowering time of *hda9-1* and *maf5* mutants in SD as determined by LN.

2.4.5 HDA9 controls flowering mostly independently of *FLC, MAF4,* and *MAF5*

FLC directly binds to the *FT* and *SOC1* promoters and represses the transcription of *FT* and *SOC1* (Helliwell *et al*., 2006). It is therefore possible that the upregulation of *FT* and *SOC1* in *hda9-1* might be the result of the reduced *FLC* expression. To test this possibility, I compared the flowering times of *hda9-1*, *flc-3* (an *FLC* null mutant; Michaels and Amasino, 2001), and the *flc-3 hda9-1* double mutants in SD. The flowering time of *hda9-1* was similar to that of *flc-3* (Fig. 8d), although a substantial amount of *FLC* transcript was present in *hda9-1* (Fig. 8b). Moreover, compared to both single mutants, the *flc-3 hda9-1* double mutant flowered slightly earlier and had a higher level of *FT* transcript (Fig. 8d,e). *SOC1* expression in *flc-3 hda9-1* compared to either of the single mutant was not increased as substantially as *FT* (Fig. 8e). These results indicate that the reduced *FLC* expression alone is not sufficient to cause the early flowering of *hda9-1*.

Similar to *FLC*, *MAF4* and *MAF5* have also been implicated in floral repression (Ratcliffe *et al*., 2003; Gu *et al*., 2008). Thus, to examine whether the decreased expression of *MAF4* and *MAF5* contributes to the accelerated flowering of *hda9-1*, T-DNA insertion mutants of *MAF4* and *MAF5* (Fig. 9) were isolated from the SALK collection, and their flowering time was analyzed. Both *maf4* and *maf5* flowered slightly earlier than wt but significantly later than *hda9-1* in SD (Fig. 8f,g). In addition, the *maf4 hda9-1* double mutants flowered slightly earlier than the *maf4* or the *hda9-1* single mutants (Fig. 8f). Moreover, *flc-3 hda9-1*

flowered earlier than *flc-3* even after vernalization (Fig. 8d), which should have decreased the expression of *MAF4* (Ratcliffe *et al*., 2003). Thus, although the decreased expression of *MAF4* and *MAF5* might contribute to the early flowering of *hda9-1*, it does not seem to fully account for the flowering behavior observed in *hda9-1*. In sum, these results suggest that HDA9 controls flowering time mostly independently of *FLC*, *MAF4*, and *MAF5*.

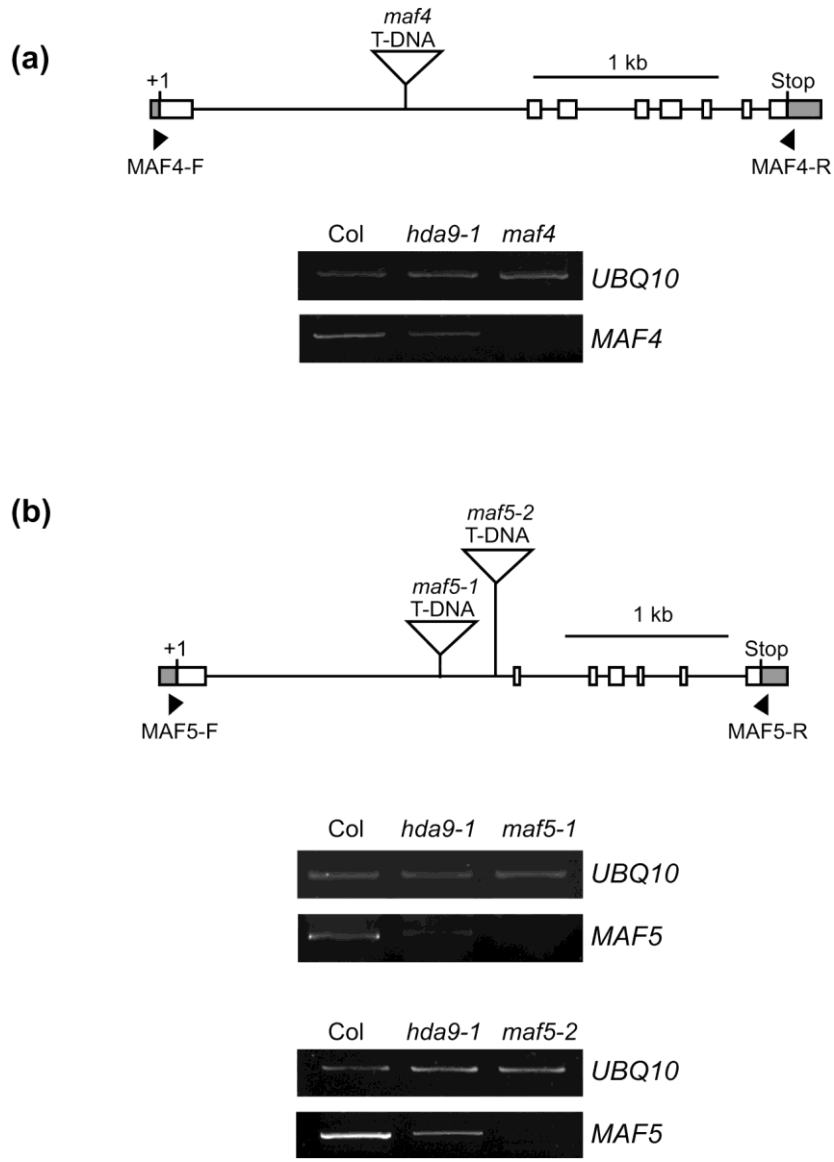

Fig. 9 T-DNA insertion mutants for *MAF4* and *MAF5*.

(a) Schematic gene structure of *MAF4* and its expression in the *maf4* mutants. The position of T-DNA insertion in *maf4* is marked with a triangle. White and gray boxes represent exons and UTRs, respectively, while introns are indicated as solid lines (a,b). *MAF4* mRNA expression in wt, *hda9-1*, and *maf4* was examined by RT-

PCR using MAF4-F and MAF4-R (supplementary material Table S3) as primers. *UBQ10* was used as an expression control (a,b). (b) Schematic gene structure of *MAF5* and its expression in the *maf5-1* and *maf5-2* mutants. The positions of T-DNA insertions in *maf5-1* and *maf5-2* are marked with triangles. *MAF5* mRNA expression in wt, *hda9-1*, *maf5-1*, and *maf5-2* was examined by RT-PCR using MAF5-F and MAF5-R (supplementary material Table S3) as primers.

2.4.6 The expression of *AGL19*, a floral activator, is increased in *hda9-1*

A number of MADS- and AP2-domain transcription factors that affect flowering in an *FLC*-independent manner have been identified (Yu *et al*., 2002; Aukerman and Sakai, 2003; Michales *et al*., 2003; Schmid *et al*., 2003; Schönrock *et al*., 2006; Adamczyk *et al*., 2007; Jung *et al*., 2007; Castillejo *et al*., 2008; Yoo *et al*., 2011). In addition, it was lately shown that SPL transcription factors promote flowering independently of *FLC* (Wang *et al*., 2009a). To study whether HDA9 affects flowering by regulating these factors, I compared their expression levels in wt and *hda9-1*. All the genes examined, with the exception of *AGL19*, were expressed at similar levels in wt and *hda9-1* (Figs. 10a, 11). Interestingly, in both LD and SD, the transcript level of *AGL19* was substantially higher in *hda9-1* than in wt (Figs. 10a, 11). The upregulation of *AGL19* is not thought to be related to the reduced *FLC* expression in *hda9-1* because the expression of *AGL19* was not affected by *flc-3* (Fig. 8e). I found that the transcript level of *AGL19*, similar to *FT*, was greatly elevated in 5-week-old plants compared with 1-week-old seedlings (Fig. 10b,c), consistently with previous report on the age-dependent induction of *AGL19* (Schönrock *et al*., 2006). Interestingly, the effect of the *hda9-1* mutation on the *AGL19* expression was barely detectable in young seedlings, although it became obvious in 5-week-old plants (Fig. 10b).

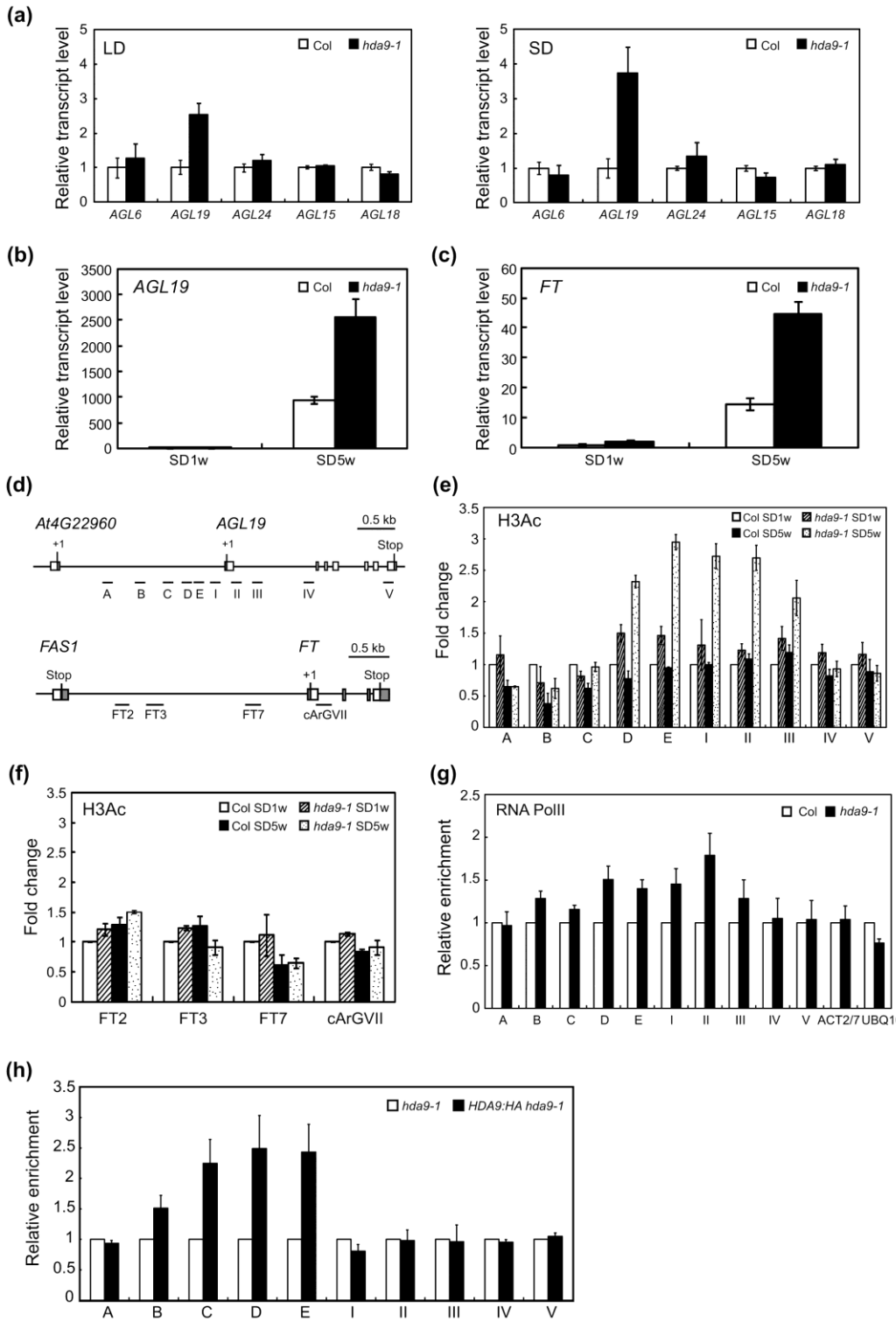

Fig. 10 HDA9 directly controls *AGL19* transcription through histone deacetylation.

(a) RT-qPCR analyses of the transcript levels of several *AGL* genes, which have floral regulatory roles, in wt and *hda9-1* seedlings grown for 2 weeks in LD (left) or for 4 weeks in SD (right). Wt levels were set to 1 after normalization by *UBQ10*, and values are the means ± S.E. of three biological replicates (a-c, h). (b, c) Transcript levels of *AGL19* (b) or *FT* (c) in 1- (SD1w) or 5-week (SD5w)-old wt and *hda9-1* plants grown in SD as determined by RT-qPCR. (d) Schematics of the genomic structures of *AGL19* and *FT*. Gray boxes represent 5′ and 3′ UTRs, and white boxes are exons. Solid lines indicate promoters, introns, or intergenic regions. ′+1′s refer to the transcription start sites. Regions amplified by primers used for ChIP (e-g) are shown for each gene. (e, f) ChIP-qPCR analyses of *AGL19* (e) and *FT* (f) chromatin using an anti-H3Ac antibody. Plants as grown in (b, c) were used for ChIP. Shown are the means ± S.E. of three biological replicates. SD1w wt levels were set to 1 after normalization by input and the internal control *UBQ10*. (g) ChIP-qPCR analyses of *AGL19* chromatin with an anti-PolII antibody. Plants grown for 5 weeks in SD were used for ChIP. Shown are the means ± S.E. of three biological replicates. Wt levels were set to 1 after normalization by input. *Actin 2/7* (*ACT2/7*) and *UBQ10* were used as internal controls. (h) ChIP-qPCR analyses of HDA9:HA enrichment at the *AGL19* locus using an anti-HA antibody. *HDA9:HA hda9-1* and *hda9-1* plants grown for 5 weeks in SD were used for ChIP. The amount of immunoprecipitated chromatin was normalized to the

corresponding input and compared with untagged plants. Shown are the means ± S.E. of three biological replicates.

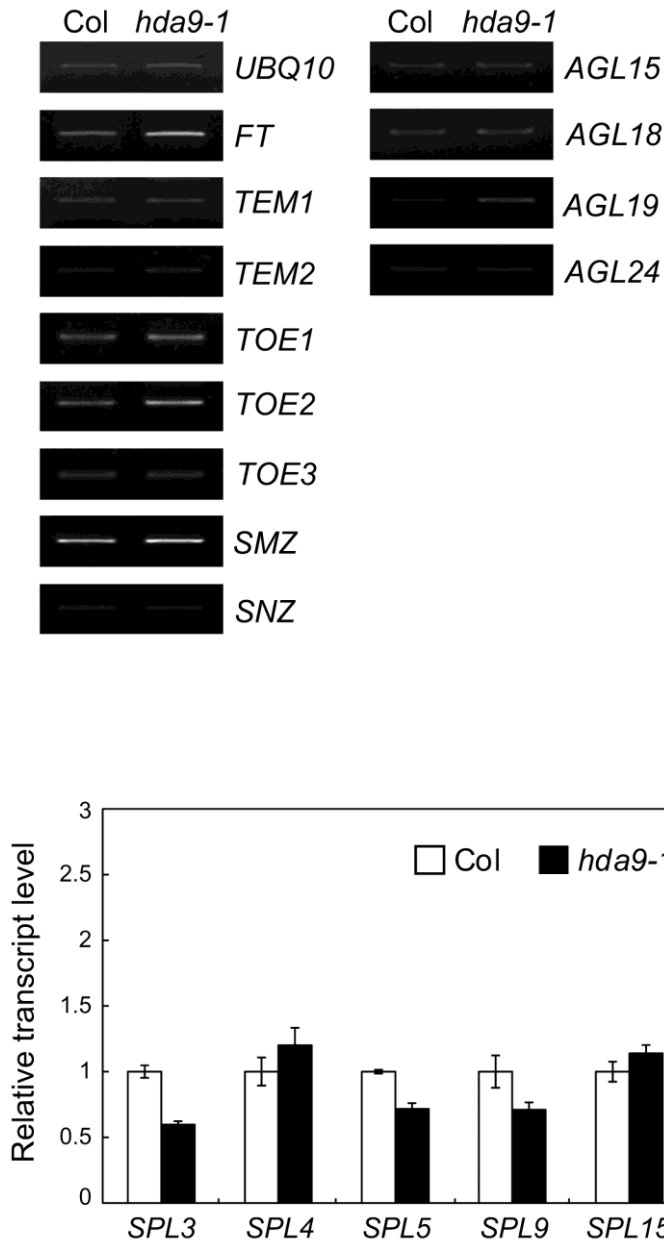

Fig. 11 Expression of genes encoding *FT* regulators and SPL-family transcription factors in *hda9-1*.

Plants were grown for 3 weeks in SD, harvested at zeitgeber 8, and used for RT-

PCR (upper panel) or RT-qPCR (lower panel) analysis. *UBQ10* was used as an expression control in the upper panel. In the lower panel, wt levels were set to 1 after normalization by *UBQ10*, and values are the means±s.e. of three biological replicates. The sequences of primers used to study the expression of each gene are in supplementary material Tables S3, S4.

2.4.7 HDA9 directly represses *AGL19* transcription through histone deacetylation

The increased expression of *AGL19*, *FT*, and *SOC1* by the loss of *HDA9* led us to test whether HDA9 directly represses the transcription of these genes by deacetylating histones within *AGL19* or *FT* chromatin. ChIP studies using anti-acetylated histone H3 (H3Ac) antibody showed that H3Ac levels at the *AGL19* locus were comparable between wt and *hda9-1* in 1-week-old seedlings (Fig. 10d,e). However, H3Ac levels around the transcription start site of *AGL19* (regions D, E, I, II, and III) were clearly increased in 5-week-old *hda9-1* but not in wt plants compared to the levels observed in 1-week-old seedlings (Fig. 10d,e). In contrast to *AGL19*, there was no clear difference in H3Ac levels at *FT* and *SOC1* loci between wt and *hda9-1* at both the seedling and mature stages (Figs. 10d,f, 12a,b). Given the fact that the transcript levels of both *AGL19* and *FT* were developmentally increased and upregulated by the loss of *HDA9* (Fig. 10b,c), these results suggest that the hyperacetylation of histones within *AGL19* chromatin in *hda9-1* is not merely a consequence of the increased *AGL19* transcription. Instead, it might be resulted from decreased HDAC activity caused by the loss of *HDA9*.

To study whether the increased *AGL19* mRNA levels and the hyperacetylation of histones within *AGL19* chromatin in *hda9-1* are related with increased transcriptional activity, I compared RNA Polymerase II (PolII) occupancies at *AGL19* in wt and *hda9-1* through ChIP assays using an anti-PolII antibody. The PolII occupancy at *AGL19* was higher in *hda9-1* than in wt; in

addition, the occupancy pattern was closely correlated with that of H3Ac (Fig. 10g). The PolII occupancy in the regions around the transcription start site (I, II, and III) but not in the elongation or termination regions (IV and V), was clearly higher in *hda9-1* than in wt. These results suggest that the histone hyperacetylation in the promoter and 5′ transcribed regions of *AGL19* might increase the accessibility of these regions to PolII, which in turn accelerates transcription.

Finally, in order to address whether HDA9 plays a direct role in the transcriptional regulation of *AGL19*, I performed ChIP assays using *HDA9:HA hda9-1* plants (Fig. 6). HDA9:HA protein was clearly enriched within *AGL19* (Fig. 10h) but not within *SOC1* chromatin (Fig. 12c), consistent with the effect of the *hda9-1* mutation on H3Ac levels at these loci (Figs. 10e, 12b). HDA9:HA enrichment was most obvious in regions upstream of the transcription start site of *AGL19*. Thus, HDA9 has a direct role in controlling and maintaining the transcription activity of *AGL19* at proper level by resetting the local chromatin environment through dynamic histone deacetylation.

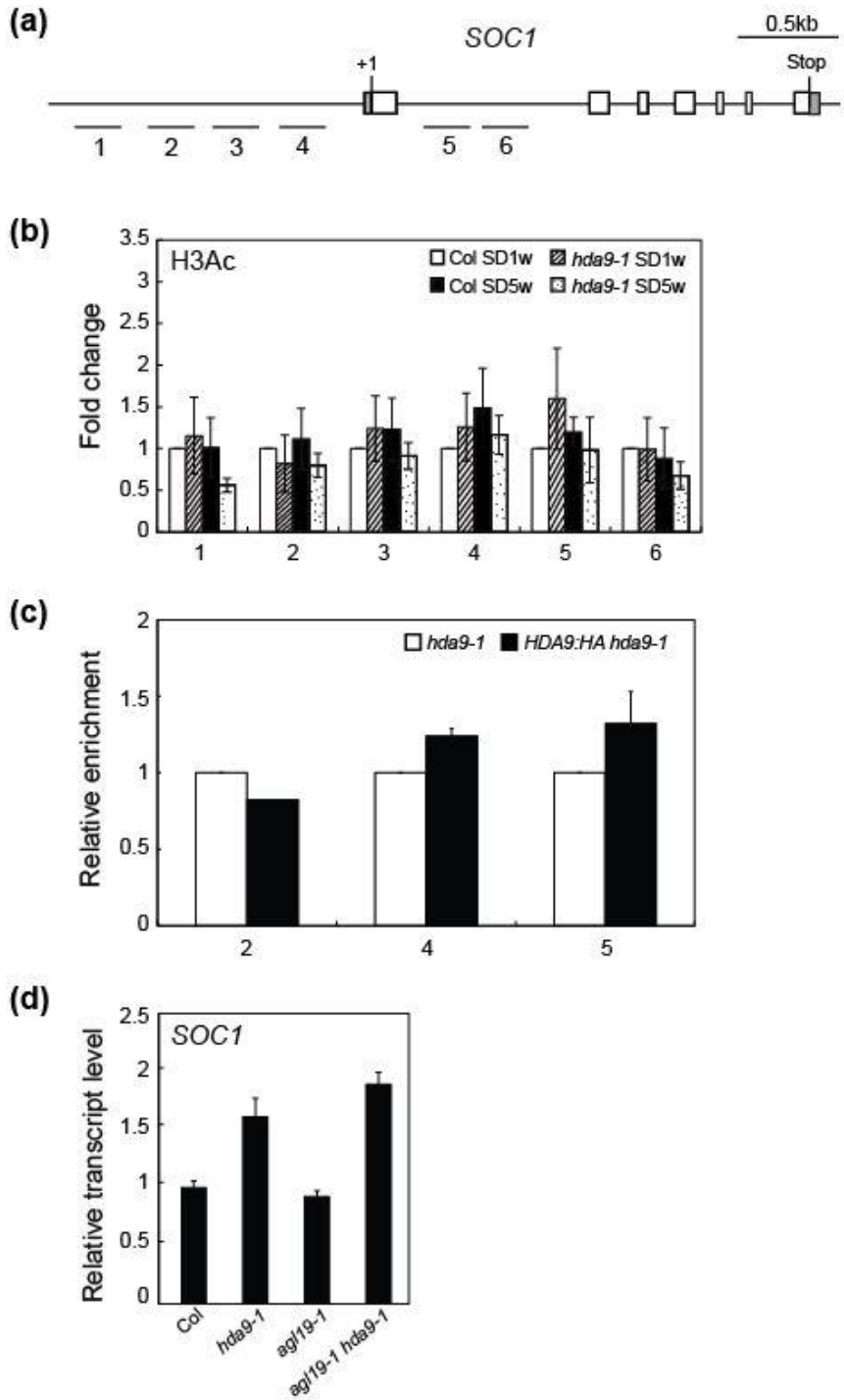
(a)
SOC1
0.5kb
+1
Stop
1
2
3
4
5
6
(b)
H3Ac
Col SD1w
hda9-1 SD1w
Col SD5w
hda9-1 SD5w
Fold change
3.5
3
2.5
2
1.5
1
0.5
0
1
2
3
4
5
6
(c)
hda9-1
HDA9:HA hda9-1
Relative enrichment
2
1.5
1
0.5
0
2
4
5
(d)
SOC1
Relative transcript level
2.5
2
1.5
1
0.5
0
Col
hda9-1
agl19-1
agl19-1 hda9-1

Fig. 12 *SOC1* is not a direct target of HDA9.

(a) Schematic of the genomic structure of *SOC1*. Gray boxes represent 5′ and 3′ UTRs, and white boxes are exons. Solid lines indicate promoters, introns, or intergenic regions. Lines with numbers indicate regions tested for ChIP-qPCR (b,c). (b) ChIP-qPCR analyses of *SOC1* chromatin with an anti-H3Ac antibody. Shown are the means±s.e. of three biological replicates performed in triplicate. Plants used for ChIP were grown as described in Fig. 5b,c. SD1w wt levels were set to 1 after normalization by input and the internal control *UBQ10*. (c) ChIP-qPCR analyses of HDA9:HA enrichment at the *SOC1* locus using an anti-HA antibody. ChIP samples used for Fig. 5H were also used here. Normalization was performed as in Fig. 5H. Shown are the means±s.e. of three biological replicates performed in triplicate. (d) RT-qPCR analyses of *SOC1* transcript levels in wt, *hda9-1*, *agl19-1*, and *agl19-1 hda9*. Plants grown for 5 weeks in SD were used for RNA extraction. Wt level was set to 1 after normalization by *UBQ10*, and values are the means±s.e. of three biological replicates.

2.4.8 HDA9 controls *FT* expression and flowering through *AGL19*

The correlation between the transcript and H3Ac levels of *AGL19* but not of *FT* and *SOC1* (Figs. 8b, 10b-f, 12b), led us to question whether the upregulation of *FT*/*SOC1* and the accelerated floral transition in *hda9-1* are caused by the increased *AGL19* expression. We thus measured the mRNA levels of *FT* and *SOC1* in wt, *hda9-1*, *agl19-1*, and transgenic plants overexpressing *AGL19* (*AGL19OE*; Schönrock *et al*., 2006). *FT* mRNA level was greatly increased when *AGL19* was overexpressed and was not largely affected by *agl19-1* (Schönrock *et al*., 2006; Fig. 13a). However, the mRNA levels of *FLC* and *SOC1* were barely affected by differential *AGL19* expression (Fig. 13a), indicating that the upregulation of *FT* in *AGL19OE* is independent of *FLC*. These results suggest that the repressive effect of *HDA9* on *FT* might be, at least in part, through the inhibition of *AGL19* transcription. Therefore, I analyzed the effect of the *agl19* mutation on the early flowering of *hda9-1* by measuring the flowering time of the *agl19-1 hda9-1* double mutants. *agl19-1 hda9-1* flowered at a similar time as wt but significantly later than the *hda9-1* single mutants (Fig. 13b), clearly demonstrating that *AGL19* is required for the early flowering of *hda9-1*. Furthermore, the increased expression of *FT* in *hda9-1* was strongly suppressed by the *agl19-1* mutation (Fig. 13c). By contrast, the upregulated *SOC1* expression in *hda9-1* was not suppressed by the *agl19-1* mutation (Fig. 12d). Thus, I concluded that HDA9 prevents precocious flowering in SD mostly by inhibiting *AGL19* upregulation, which otherwise would in turn activate *FT*.

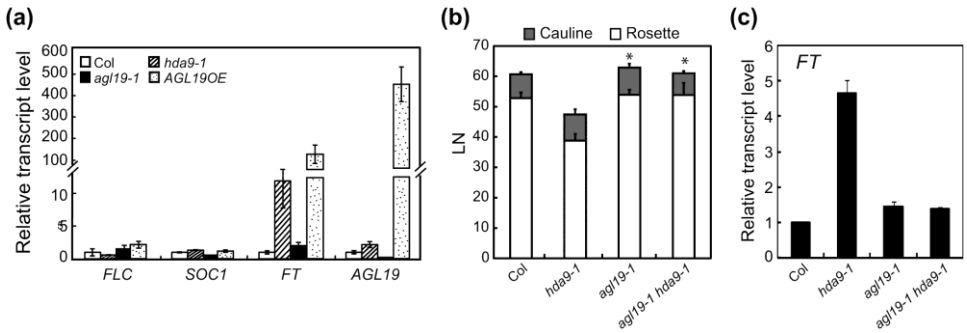

Fig. 13 HDA9 affects *FT* expression and flowering through *AGL19*.

(a) RT-qPCR analyses of the transcript levels of *FLC*, *SOC1*, *FT*, and *AGL19* in *hda9-1*, *agl19-1*, and *AGL19OE* plants. Plants grown for 3 weeks in SD were used for RNA extraction. (b) Flowering time of *hda9-1*, *agl19-1*, and *agl19-1 hda9-1* mutant plants in SD as determined by LN. Asterisks denote statistically significant differences from *hda9-1* ($P < 0.001$). (c) *FT* transcript levels as determined by RT-qPCR in *hda9-1*, *agl19-1*, and *agl19-1 hda9-1* mutant plants grown for 13 weeks in SD. Wt level was set to 1 after normalization by *UBQ10*, and values are the means ± S.E. of three technical replicates.

2.4.9 Loss of *HDA9* increases the levels of *AGL19* mRNA and H3Ac at *AGL19* in vernalized seedlings

Previous work showed that *AGL19* mRNA expression is induced by vernalization (Schönrock *et al*., 2006). Therefore, I examined the effect of the *hda9-1* mutation on the vernalization-induced *AGL19* expression (Fig. 14a). In non-vernalized seedlings, *AGL19* mRNA level was low and similar between wt and *hda9-1*. However, after 4 weeks of vernalization, it was increased in wt and, notably to a greater extent, in *hda9-1*. The hyperinduction of the vernalization-mediated *AGL19* expression by the *hda9-1* mutation might account for the accelerated floral transitions of *hda9-1* and *flc-3 hda9-1* compared to *flc-3* (Fig. 8d). I then studied H3Ac levels at *AGL19* in wt and *hda9-1* seedlings before and after vernalization (Fig. 14b). There was no detectable difference in H3Ac levels at *AGL19* between non-vernalized wt and *hda9-1* seedlings. However, an evident increase in H3Ac levels at *AGL19*, especially in regions around the transcription start site, was detected in *hda9-1* but not in wt after vernalization. Thus, the results in Fig. 14 indicate that HDA9 also prevents the hyper-activation of *AGL19* transcription during vernalization through a dynamic histone deacetylation.

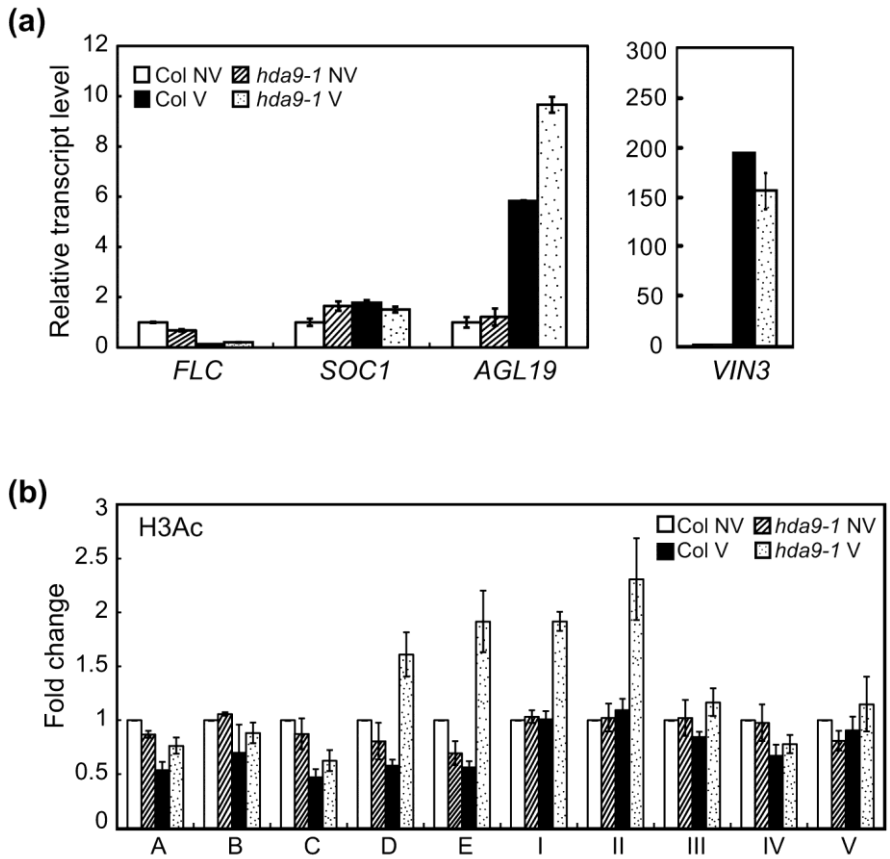

Fig. 14 Hyperacetylation of histones within *AGL19* chromatin by the *hda9-1* mutation in vernalized seedlings.

(a) RT-qPCR analyses of the transcript levels of *FLC*, *SOC1*, *AGL19*, and *VIN3* in wt and *hda9-1* seedlings vernalized for 30 d (V) or not vernalized (NV). NV wt levels were set to 1 after normalization by *UBQ10*. Values are the means ± S.E. of three biological replicates. (b) ChIP-qPCR analyses of *AGL19* chromatin using an anti-H3Ac antibody. Plants were grown as described in (a). NV wt levels were set to 1 after normalization by input and the internal control *UBQ10*. Shown are the

means ± S.E. of three biological replicates.

2.4.10 *AGL19* is differentially expressed in different photoperiods

We then questioned whether the regulation of *AGL19* by HDA9 is relevant to the photoperiod-dependent early-flowering phenotype of *hda9-1*. Interestingly, *AGL19* mRNA levels were ~10-fold higher in 5-week-old SD-grown plants than in 4-week-old LD-grown plants regardless of the *HDA9* genotype (Fig. 15a). This difference in *AGL19* expression is unlikely to be due to the age difference between the LD- and SD- grown plants because the 4-week-old LD-grown plants were rather developmentally more progressed than the 5-week-old SD-grown plants (Fig. 15a). Thus, *AGL19* might be expressed only in SD-grown *hda9-1* plants to the level required for the activation of *FT* and precocious flowering, and this might be the cause for the SD-specific early flowering of *hda9-1*.

Notably, *AGL19* expression was not as much affected by the loss of *CO* or *GI* under LD condition as by SD (Fig. 15b). The *AGL19* mRNA level in 3-week-old LD-grown *gi-2* or *co-101* mutants was moderately higher than that in 3-week-old LD-grown wt but substantially lower than that in 4-week-old SD-grown wt. Thus, unlike *FT* (Fig. 15b), the photoperiodic regulation of *AGL19* is largely independent of the GI-CO pathway. This result is in agreement with my observations that the suppressive effect of the *hda9-1* mutation on the late flowering of *co-101* or *gi-2* in LD (Fig. 7g) was weaker than its effect in SD (Fig.

7h). Taken together, these results suggest that the repressive role of HDA9 in *AGL19* expression together with the photoperiod-dependent expression of *AGL19* might underlie the SD-specific early flowering of the *hda9-1* mutants.

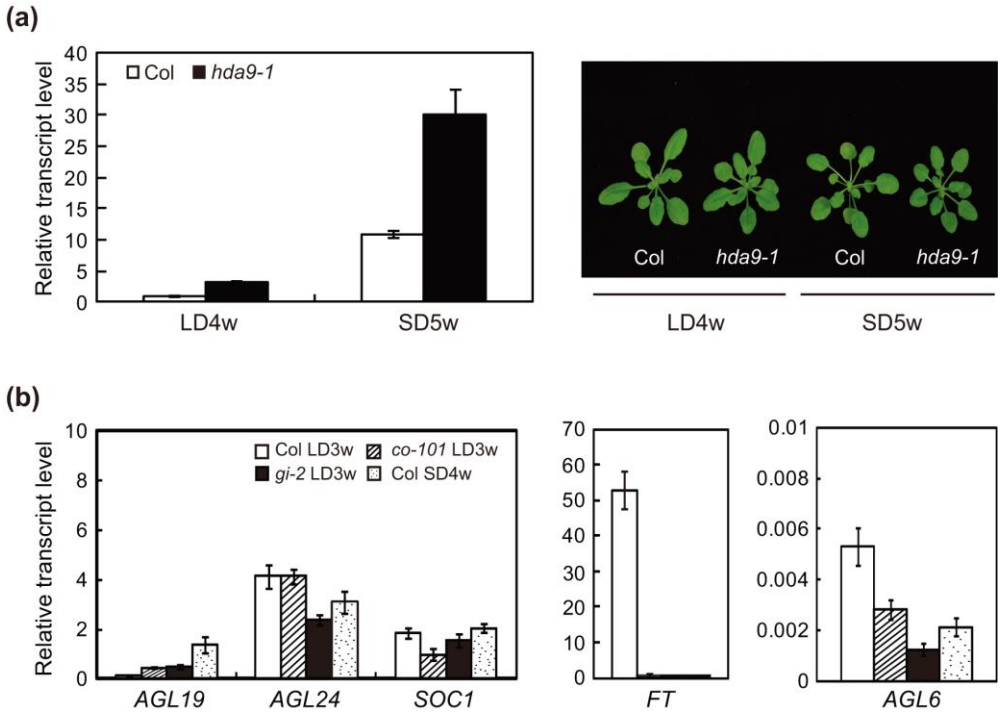

Fig. 15 Photoperiod-dependent expression of *AGL19*.

(a) RT-qPCR analyses of *AGL19* transcript levels in wt and *hda9-1* plants grown for 4 weeks in LD (LD4w) or for 5 weeks in SD (SD5w). The picture on the right shows representative wt and *hda9-1* plants. LD4w wt level was set to 1 after normalization by *UBQ10*. The values are the means ± S.E. of three biological replicates. (b) RT-qPCR analyses of the transcript levels of *AGL19*, *AGL24*, *SOC1*, *FT*, and *AGL6* in wt, *co-101*, and *gi-2* plants grown for 3 weeks in LD (LD3w) or for 4 weeks in SD (SD4w). Transcript levels of each gene were normalized by *UBQ10*, and values are the means ± S.E. of three biological replicates.

2.5 Discussion

Arabidopsis has a higher number of HDACs than other multicellular eukaryotes; however, to date, the biological roles of individual Arabidopsis HDACs, with the exception of HDA6 and HDA19, are mostly unknown. In this study, I show that HDA9, an Arabidopsis RPD3/HDA1 family Class I HDAC, plays distinct roles in plant development. The loss of *HDA9* causes several morphological alterations in a limited number of organs (Fig. 2), none of which are observed in the *hda6* or *hda19* mutants. These observations suggest that the *in planta* function of HDA9 might be localized and not global and that this function does not overlap with the functions of HDA6 or HDA19. It would be interesting to know how HDA9 and its phylogenetically close members, HDA6 and HDA19, perform distinct biological roles despite their conserved HDAC activity. The specificity of these HDACs might lie in their participation in different multi-protein complexes. Studies on animal and yeast HDACs have shown that most Class I HDACs perform their functions within a variety of multi-protein complexes, each of which has different target range (Cunliffe, 2008; reviewed in Yang and Seto, 2008). Although, to my knowledge, no HDAC complex has yet been biochemically purified from Arabidopsis, Arabidopsis HDACs are also likely to interact with different proteins or complexes, which might lead to different biological effects. Therefore, biochemical purification of HDA9-containing complexes will provide a better understanding of the action mechanisms of HDA9 and insights into its target

specificity.

My study using *hda9-1* revealed that HDA9 is involved in the control of flowering time, especially under non-inductive SD conditions. Floral repression in SD is as important as floral promotion in LD for the reproductive success of a facultative LD plant, such as Arabidopsis. Precocious flowering of a number of loss-of-function mutants in SD suggests that the repressive mechanisms to attenuate floral competence as well as the lack of floral promoter activity of the CO-FT pathway contribute to the repression of flowering in Arabidopsis under SD conditions. Our data indicate that HDA9 contributes to this floral repression mainly by negatively regulating the expression *AGL19*, an *FT* activator (Figs. 10, 13). *AGL19* appears to be responsible for the SD-specific early flowering of *hda9-1* as well. *AGL19* expression is higher in SD than LD (Fig. 15a), and its low level of expression in *hda9-1* under LD conditions may not be sufficient to effectively activate *FT* (Fig. 15b). Thus, in addition to strong CO activity, the low level of *AGL19* expression might be responsible for the normal flowering behavior of the *hda9-1* mutants in LD. The role of *AGL19* in promoting floral transition in wt is likely redundant or its expression level in wt is not sufficient for effective *FT* activation because its loss-of-function mutants displayed a normal flowering behavior without reduced *FT* expression (Fig. 13b,c). In either case, ensuring the proper expression of *AGL19* during the developmental time course is crucial for the prevention of precocious flowering in non-inductive SD. In sum, the control of *AGL19* expression by HDA9 adds a new layer to the mechanisms that prevent precocious flowering in SD.

Conventionally, the role of HDACs has been thought to be associated with inactive genes. However, the *hda9-1* mutation-induced increase of H3Ac levels at *AGL19* was clearly observed only at times when *AGL19* was actively expressed, such as in the adult stages or after vernalization (Figs. 10e, 14b). Thus, the role of HDA9 at *AGL19* is distinct from the conventional corepressor role of HDACs. Interestingly, a recent genome-wide mapping of HDACs in human CD4+ cells showed that HDACs associate more with transcriptionally active genes than with inactive genes (Wang *et al*., 2009b), which suggests a novel role of HDACs during transcription. Increased H3Ac levels at *AGL19* in *hda9-1* but not in wt during development in SD (Fig. 10e) implies that acetyl groups may be dynamically added to the histone tails and reversibly removed by HDA9 during the transcription of *AGL19*. This HDA9 function might be important in the prevention of hyperactive transcription by resetting the chromatin state. This postulate is supported by the *hda9-1* mutation-induced increased PolII occupancy, which is correlated with increased H3Ac levels in regions surrounding the *AGL19* transcription start site (Fig. 10g). Histone hyper-acetylation in these regions might cause hyperactive transcription at premature developmental stages. It will be of interest in the future to determine whether HDA9 has a similar role in the control of other genes during their transcription.

Chapter III.

HDA 9 plays a negative role in light-induced seed germination

3.1 Abstract

Timing of seed germination is controlled by various environmental factors in order to initiate a successful new life cycle under favorable environment. Light is the most critical environmental factor to promote seed germination. Light-induced germination process involves the perception of light mainly by phytochrome B (phyB) and then degradation of the germination repressor PHYTOCHROME INTERACTING FACTOR (PIF1) resulted from its interaction with phyB. In this study, I found the RPD3/HDA1-class histone deacetylase HDA9 is involved in a new layer of regulation for phyB-dependent germination process.

Loss-of-HDA9 activity caused rapid germination after a red-light pulse treatment as well as under continuous white light and had the increased expression of *HECs*, previously known repressors of PIF1 transcription activity. Epistatic analysis between the *hda9* mutant and *hec1hec2 RNAi* showed that rapid seed germination of the *hda9* mutant was caused by the increased *HECs* expression. Histone H3 acetylation level and RNA polymerase II occupancy at *HECs* were more elevated in *hda9-1* than in wt after red light pulse but not after far-red light pulse. The direct association of HDA9 with *HECs* chromatin was also observed after red light pulse but not after far-red light pulse. Furthermore, I found that mRNA levels of *GA-INSENSITIVE (GAI)* and *REPRESSOR OF GA1-3 (RGA/RGA1)* regulated positively by *PIF1* were decreased by the *hda9* mutation.

Taken together, my results indicate that HDA9 plays a role in the prevention of the hyper light-sensitive germination by inhibiting the hyper-

activation of HECs transcription by light through deacetylating HEC chromatin during active transcription. Thus, HDA9 acts as a fine-tuning mechanism of phyB-dependent germination ensuring the beginning of germination under proper light condition.

3.2 Introduction

Seed germination is a critical process to initiate a new life cycle of seed plants. Optimal timing of seed germination under favorable environmental condition is profoundly important since once seeds germinates, they have no other choice but to grow and reproduce in that environment. Indeed, seed germination is controlled by multiple environmental factors including light, oxygen, water, nutrient, and temperature as well as endogenous factors. In most seed plant species, light is one of the critical factors which affects seed germination. Among the various wavelengths of light, red and far-red wavelengths control the seed germination through phytochrome signaling (Shinomura et al., 1994; Oh et al., 2007). Among the identified phytochromes, phyB is known as a major phytochrome that is involved in the low influence response (LFR) and recognizes red light (R) to promote seed germination (Shinomura et al., 1994; Oh et al., 2007). Although the role of phyB in light-induced seed germination has long been known in plant biology, until recently the details of phyB downstream regulatory networks in seed germination have been mostly unknown. Recent studies showed that in seeds exposed to red light, phyB, converted to its active form, translocated into the nucleus. In nucleus, phyB interacts with PIF1 (Shen et al., 2005, 2008), also known as PIL5 (Oh et al., 2004). PIF1 is one of various basic helix-loop-helix (bHLH) transcription factor and is known to play a negative role in seed germination (Oh et al., 2004; Bae and Choi, 2008). Interaction of PIF1 with phyB (Pfr) causes PIF1 phosphorylation and rapid degradation through the ubiquitin/26S proteasome pathway (Oh et al., 2006). This event results in the decrease of the amount of PIF1

protein which is highly accumulated in seeds kept in dark and the diminution of PIF1-mediated repression of germination.

Recently, in addition to light-dependent degradation of PIF1, fine-tuning mechanisms of PIF1 activity by PIF1- interacting proteins have been reported. According to Zhu PhD thesis (2012), the closely related bHLH proteins HECATE 1 (HEC1) and HEC2 that are previously well known regulators of transmitting tract and stigma development (Gremski et al., 2007) also positively regulate germination and several aspects of photomorphogenesis. Zhu PhD thesis, (2012) demonstrated that HEC1 and HEC2 protein directly interacts with PIF1 and it reduces the DNA binding ability of PIF1, placing HECs as new positively acting components in phyB signaling (Zhu PhD thesis, 2012). Another HLH transcription factor, LONG HYPOCOTYL IN FAR-RED (HFR1) is also reported to heterodimerize with PIF1 and prevents the binding of PIF1 to its target genes related to germination (Shi et al., 2013).

Like other developmental transition in plants, transition to seed germination involves rapid changes in gene expression. Lately it has been reported that posttranslational modifications of histones functions in the transcriptional regulation of genes for appropriate light-induced germination. Histone arginine demethylase activity catalyzed by Jumonji C (JMJ) 20 and JMJ22 is required for the phyB-dependent seed germination while histone lysine methyltranseferase, EARLY FLOWERING IN SHORT DAYS (EFS) negatively regulates seed germination in the dark. Other histone mehyltransferases involved in repressive

chromatin states are also identified in seed germination. PHD-domain protein interacts with the Polycomb repressive complex 1 (PRC1), and this PHD-PRC1 complex promotes seed germination via changing the chromatin state (Cho et al., 2012; Lee et al., 2014; Molitor et al., 2014). Among diverse histone modifications, histone acetylation has been linked to the active transcription. Histone acetylases (HDACs) remove acetyl groups from histones which form the transcriptionally incompetent chromatin landscape. It was reported that two Arabidopsis HD2 family histone deacetylases HD2a and HD2C represses and enhance germination, respectively (Colville et al., 2011). The components of HDAC complex SIN3-LIKE1 (SNL1) and SNL2, together with HDAC19 modulate the transcription of genes involved in the ethylene and abscisic acid (ABA) pathways, consequently affecting seed dormancy and ABA sensitivity of germination (Wang et al., 2013). HISTONE DEACETYLATION COMPLEX1 (HDC1) was identified as a putative component of HDAC complexs and demonstrated to interact with the RPD3/HDA1 class I histone deacetylases HDA6 and HDA19. Studies using HDC1 overexpression and mutant lines showed that HDC1 plays a role in determining the ABA sensitivity of seed germination (Perrella et al., 2013). In addition, pharmacological prevention of histone deacetylases (Class I and Class II HDACs) with trichostatin (TSA) treatment delayed germination (Tanaka et al., 2008). Furthermore, recent study using the loss of function mutants of RPD3/HDA1 family class I HDA9 suggested that these HDA9 plays a role in seed dormancy and germination. Unlike the mutation in either HDA6 or HDA19 that affects germination only in the presence of ABA, the *hda9* mutation causes faster

germination in the absence of ABA (van Zanten et al., 2014). Although the accumulated evidences support the role of HDACs in the regulation of germination, the underlying molecular mechanisms by which each HDAC regulates seed germination remains to be elucidated.

Here, I report that HDA9, a member of RPD3/HDA1 family Class I HDACs plays a repressive role in the regulation of light-induced germination. I demonstrated HDA9 prevents phyB-dependent germination by directly targeting to *HECs* (*HEC1, HEC2, and HEC3*) and repressing their expression through histone deacetylation during active transcription induced by light. I further show that derepression of HECs by the hda9 mutation through blocking the transcriptional activity of PIF1 changes the expression of germination related PIF1 target genes. Thus HDA9 controls the light sensitivity of phyB-dependent germination and subsequently its speed through preventing the hyperactivation of HECs transcription by light which attenuates the blocking of PIF1 transcription activity by HECs.

3.3 Material and methods

3.3.1 Plant materials and growth conditions

The *hda9-1* mutant, *HDA9:HA hda9-1* line and *hfr1-201 (rep1)* mutant allele were previously described as written in Kang et al., 2014 and Soh et al., 2000. *hec1/3/hec2 RNAI* +/- and *HEC1p:HEC1:GUS* transgenic lines were provided by Martin F. Yanofsky. *35s:HEC2 GFP*, *35s:TAP:PIF1 pif1-2*, and *pPIF1:TAP:PIF1* lines were provided by Enamul Huq. *pif1-2* (SALK_072677), T-DNA insertion mutant was obtained from the SALK collection (http://signal.salk.edu/) and genotyped by using gene-specific primers (Table 1).

Seeds were sterilized with 75% EtOH containing 0.08% TritonX-100, washed with 95% EtOH, and plated on 1/2 Murashige-Skoog (MS) growth media containing 0.8% phyto-agar without sucrose (1/2MS-Suc).

For the germination assay, gene expression and ChIP experiments seeds were harvested from plants grown side by side in the same tray and shelf. Plants were grown at 22 ℃ under 100 umol/m^2s in long day condition (16 hr light/ 8 hr dark). Seeds were dried for at least 2 weeks at room temperature.

3.3.2 Light treatment and seed germination assay

For phyB-dependent germination assay, seeds were imbibed for 1hr at 22 ℃ in the dark to induce germination. Imbibed seeds were exposed to 1.8 μmol /m^2s of Fp for 5 min to inactivate phyB. Seeds were further exposed to 40 μmol /m^2s of Rp for 5 min to activate phyB. Then, seeds were kept in the dark at 22 ℃ for 4 additional

days.

For low light intensity germination assay, seeds were irradiated with 10 μmol /m^2s of Rp for 5 min instead of Rp 40 μmol /m^2s following the same procedure as phyB-dependent germination assay.

Germinated seeds were scored by counting the emergence of the radicles at the indicated time. At least 80-100 seeds of each genotype were used for the germination assay. Experiments were performed as triplicates for statistical analyses.

3.3.3 Histochemical β-glucuronidase (GUS) assay

For GUS assay, dry seeds were imbibed for 1hr in the dark, treated with Fp for 5 min or Rp for 5 min and further incubated for 12 in the dark hr at 22 ℃. Seeds were fixed by acetone on ice for 30 min in the dark and washed three times with KPO_4 buffer. The fixed seeds were dissected using forceps, and the extracted embryos were stained with X-Gluc solution for 2hr 30 min (HDA9:GUS) or overnight (HEC:GUS) at 37˚C. The stained embryos were photographed using AxioVison under optical microscope (Carl Zeiss, Germany). To observe HEC1:GUS expression in the wt and *hda9-1* background, HEC1:GUS was introgressed into *hda9-1* by crossing, and the *hda9-1* mutants carrying HEC1:GUS (+/+) were selected. HEC1:GUS expression between wt and *hda9-1* were then compared.

3.3.4 RNA extraction and RT-qPCR analysis

Total RNA was extracted from light treated seeds as previously described (Ling Meng and Lewis Feldman, 2010) with minor modifications. The RNA pellet was treated with RNase-Free DNase I set (Qiagen) to remove genomic DNA. Then, RNA was purified by using Qiagen RNeasy Plant mini kit (Qiagen). 3 ug of total RNA was reverse transcribed using MMLV Reverse Transcriptase (Fermentas, USA). The RT-qPCR analysis was performed with Rotor-Gene Q (Qiagen) using the SYBR Green Fast qPCR master mix (Kappa Biosystems). Absolute quantification was performed by generating standard curves using serial dilutions of mixture of all cDNA samples to be analyzed. *UBQ11* was used as a normalized control of the expression data. All RT-qPCR results were performed as means±SE of duplicate technical repeats and biological triplicates. Primers used for RT-qPCR analysis are listed in Table 2.

3.3.5 Protein extraction and western blot

Total 50 mg of light treated seed was ground in liquid nitrogen and resuspended in extraction buffer (4% SDS, 200mM dithiothreitol (DTT), 20% glycerol, 100mM Tris-HCl (pH 6.8)). The mixture was boiled for 10 min and then centrifuged at 13,000 rpm for 5 min at room temperature. The supernatant was resuspended in an equal volume of 2x SDS sample buffer (4% SDS, 200mM dithiothreitol (DTT), 20% glycerol, 100mM Tris-HCl (pH 6.8) and 0.02% bromophenol blue).

Nuclear protein was extracted by using Honda buffer as previously described (Xia et al., 1997 and Kinkema et al., 2000). Seeds were homogenized in liquid nitrogen and resuspended in Honda buffer (2.5% Ficoll 400, 5% dextran T40,

0.4M sucrose, 25mM Tris-HCl (pH 7.4), 10mM $MgCl_2$, 10 mM b-mercaptoethanol, and a proteinase inhibitor cocktail) and then filtered through miracloth (Milipore, 485855-1R). Triton X-100 was added to a final concentration of 0.5%, and the mixture was incubated on ice for 15 min. Then, the solution was centrifuged at 1500 g for 5 min and the pellet was washed with Honda buffer containing 0.1% Triton X-100. The pellet was resuspended gently in 1 mL of Honda buffer using a brush, and the resuspended fraction was transferred to a new tube. This nuclear-enriched preparation was centrifuged at 1000 rpm (or 100*g*) for 1 min to pellet starch and cell debris. The supernatant was centrifuged subsequently at 4000 rpm for 5 min at 4˚c to pellet the nuclei. Next, the nuclear enriched mixture was boiled for 10 min and then centrifuged at 13,000 rpm for 5 min at room temperature. The supernatant was resuspended in an equal volume of 2x SDS sample buffer.

Protein extracts were equally loaded on 8% or 15% polyacrylamide gel. Total or nuclear protein samples were subjected to sodium dodecyl sulfate-polyacrylamide gel (SDS-PAGE) and transferred to nitrocellulose membrane (Millipore). After blocking the membrane with blocking solution containing 10% non-fat milk in 1x TBS-T, the membrane was incubated with primary antibody (α – HA, Abcam ab9110; α –GUS, Life technologies A5790; α -H3, Abcam ab1791 at 1:4000, 1:1000, 1:10000, 1:5000 respectively) overnight. Following, the membrane was washed three times for 15 min with 1x TBS-T at room temperature. Then the membrane was incubated with horseradish peroxidase (HRP)- linked secondary antibody (α-Rabbit, Vector, PI-1000) in 10% non-fat milk in 1x TBS-T. Next, the membrane was washed three times for 15 min with 1x TBS-T and detected using

Lumi Femto ECL kit (Dogen). For protein visualization, proteins were stained with coomassie blue (0.1% coomassie brilliant blue R-250, 50% methanol and 10% glacial acetic acid) and ponceau S (0.1% (w/v) Ponceau S in 5% (v/v) acetic acid).

3.3.6 Chromatin immunoprecipitation (ChIP) assay

Light treated seeds (roughly 300ul dry seed) were cross-linked in 1% formaldehyde solution for 30 min with vacuum and quenched for 10 min by adding 0.2M glycine. Cross-linked seeds were washed three times with distilled water. Samples were quickly frozen in liquid nitrogen. The nuclei was isolated by using lysis buffer (50mM HEPES, 150mM NaCl, 1mM EDTA, 1% Triton X-100, 0.1% Sodium deoxycholate, 1mM PMSF, and protease inhibitor and 0.1% SDS) and the chromatin was sheared using ultra sonicator (Fisher scientific). Chromatin was pre-cleared to remove cell debris with salmon sperm DNA/Protein-A beads (50% slurry; Upstate 16-157). After overnight immunoprecipitation with the corresponding antibody, the antibody-protein/DNA complexes were isolated using salmon sperm DNA/Protein-A beads. After washing the chromatin mixture for five times with wash buffers (low salt, high salt, LiCl and TE x2) at 4 ℃, the immune-complex was eluted from beads using elution buffer (1% SDS and 0.1 M $NaHCO_3$). Finally the ChIPed DNA was purified using a PCR purification kit (Qiagen) after reverse crosslinking and treatment of proteinase K. Antibodies for ChIP assay were α-H3Ac (Millipore, 06-599), α -RNA PolII (Covance, MMS-126R), and α -HA (Abcam, ab9110). α-H3Ac recognizes acetylated lysine 9 and 14 of Histone 3. α -RNA PolII recognizes both initiating and elongating forms of PolII. The amount of

immunoprecipitated DNA was determined by qPCR using primer sets listed in Table 3. The relative amounts of ChIPed DNA were evaluated using the $2^{-\Delta\Delta ct}$ method (Livak and Schmittgen, 2001).

Table 3-1. Oligonucleotides used for genotyping.

Gene	Name	Sequence
SALK LB1.3		5'-ATTTTGCCGATTTCGGAAC-3'
HEC1	ghec1 oKG156	5'- ACCACAACAACACTTACCCTTTTC -3'
	ghec1oKG157	5'- GTTCC A CACCCTTTCATAACCACT -3'
	ghec1 GABI-KAT	5'- CCCATTTGGACGTGAATGTAGACAC -3'
HEC3	ghec3 C-X1	5'- GTGCTATTTCGTGAAGAGACAAGAGA -3'
	ghec3 C-X4	5'- TCCTAACAAACCCTTAT TTC GTATCCA -3'
	ghec3JMLB2	5'- TTGGGTGATGGTTCACGTAGTGGG -3'
PIL5	gPIL5 F	5'- ATGATTATGTCAACAACCATAATTCTTC -3'
	gPIL5 R	5'- CTTTCATTCTCTCATTGATCCTATCTC -3'
HFR1	gHFR1 F	5'- GCTACAAAGTTAACATTC -3'
	gHFR1 R	5'- CTCTTTAACTAACATGTAAGTA -3'
phyB	gphyB F	5’-GTGGAAGAAGCTCGACCAGGCTTG-3’
	gphyB R	5’-GCAAAACTCTTGCGTCTGTG-3’
	dCAPS	5’-GTGGAAGAAGCTCGACCAGGCTTTG-3’

Table 3-2. Oligonucleotides used for RT and RT-qPCR analyses.

Gene	Name	Sequence
UBQ10	UBQ-F	5’-GATCTTTGCCGGAAAACAATTGGAGGATGGT-3’
	UBQ-R	5’-CGACTTGTCATTAGAAAGAAAGAGATAACAGG-3’
UBQ11	qUBQ11-F	5’-GATCTTCGCCGGAAAGCAACTT-3’
	qUBQ11-R	5’-CCACGGAGACGGAGGACC-3’
PP2A	qPP2A-F	5’-TATCGGATGACGATTCTTCGTGCAG-3’
	qPP2A-R	5’-GCTTGGTCGACTATCGGAATGAGAG-3’
HFR1	qHFR1-F	5'-TACCACCGTTTACTAATATTTCATTCC-3'
	qHFR1-R	5'-AAAAATCCAAGAAACTTGGGAAATAAG-3'
HEC1	qHEC1-F	5'-ATTTCACTTGTAAGCTTTTCACCAG-3'
	qHEC1-R	5'-AGAGAAAAGGGTAAGTGTTGTTGTG-3'
HEC2	qHEC2-F	5'-CTTGGAAATGCACAGATTCTTAGAT-3'
	qHEC2-R	5'-TAATTAACCATCCCAAACATTATCG-3'
HEC3	qHEC3-F	5’-CTTCTCATTTCCCTCCTCTCTCTTCTTC-3’
	qHEC3-R	5’-CTTCTCATTTCCCTCCTCTCTCTTCTTC-3’
SPT	SPT-F	5’-AAGAAGCAGAGAGTGATGGG-3’
	SPT-R	5’-ACTACAGCTTCTCCTCCTTC-3’
PIF1	PIF1-F	5’-GATGTGGAATGATGCCAATGATG-3’
	PIF1-R	5’-GGAGACCGCGGAACTGCTGATATG-3’
PIF1	qPIF1-F	5’-ATGATTTCTGCTCAGATCTTCTCTTCT-3’
	qPIF1-R	5’-AGATTCACCACCTCTACCGTTATTAAA-3’
SOM	qSOM-F	5'-GCTCTTTCGCCTTCCACTCC-3'
	qSOM-R	5'-TCCTAGATCAGGGTCACCAC-3'
GA3OX1	qGA3ox1-F	5'-TCCCGGATTCTTACAAGTGGAC-3'
	qGA3ox1-R	5'-GCCGGAGGAGAAGGAGCA-3'

GA3OX2	qGA3ox2-F	5'-GACCCTCATGACAATTCTGTACC-3'
	qGA3ox2-R	5'-GTTAAAATGTGGAGCAAGTCACC-3'
GA2OX2	qGA2ox2-F	5’-AATAACACGGCGGGTCTTCAAATCT-3’
	qGA2ox2-R	5’-TCCTCGATCTCCTTGTATCGGCTAA-3’
GAI	qGAI-F	5'-GAAGACTATGATGATGAATGAAGAAGAC-3'
	qGAT-R	5'-TATAGTGAACAGTCTCAGTAGCGAGTT-3'
RGA	qRGA-F	5'-TACATCGACTTCGACGGGTA-3'
	qRGA-R	5'-GTTGTCGTCACCGTCGTTC-3'
ABA1	qABA1-F	5’- GATGCAGCCAAATATGGGTCAAGG-3’
	qABA1-R	5’- GCCATTGCATGGATAATAGCGACTC-3’
CYP707A2	qCYP707A2-F	5’-TGGTGGTTGCACTGGAAAGAGC-3’
	qCYP707A2-R	5’-TTGGCGAGTGGCGAAGAAGG-3’
NCED6	qNCED6-F	5’-ACCGGGTCGGATATAAATTGGGTTG-3’
	qNCED6-R	5’-CCCGGGTTGGTTCTCCTGATTC-3’
NCED9	qNCED9-F	5’-GCGGGCTATTTGGGTTAGTC-3’
	qNCED9-R	5’-CGGTAAATCGTCTTCGGACA-3’

Table 3-3. Oligonucleotides used for ChIP assays.

Locus	Name	Sequence
UBQ11	UBQ11-ChIP-F	5'-GGCCTTGTATAATCCCTGATGAATAAG -3'
	UBQ11-ChIP-R	5'-AAAGAGATAACAGGAACGGAAACATAGT-3'
PP2A	PP2A-ChIP-F	5'-GCCTTAAGCTCCGTTTCCTACTT-3'
	PP2A-ChIP-R	5'-CGGCTTTCATGATTCCCTCT-3'
HEC1	HEC1 A-F	5'-ACAAAACCAGTTGATAATCTTTTACTCC-3'
	HEC1 A-R	5'-TCCACCATTATTATTGTATTCATTTCAT-3'
	HEC1 B-F	5'-ATTTCACTTGTAAGCTTTTCACCAG-3'
	HEC1 B-R	5'-AGAGAAAAGGGTAAGTGTTGTTGTG-3'
	HEC1 C-F	5'-GCTAGGCATAGAAGGGAGAGAATAAG -3'
	HEC1 C-R	5'-TCTTTAAAAACTTCACATAATGAATTGC-3'
HEC2	HEC2 A-F	5'-CCATCCAGGTTAAAAGTTAAAATAAGAA-3'
	HEC2 A-R	5'-TTTGTTTATAATTGTTAATTACCCCACA-3'
	HEC2 B-F	5'-TAAAATAATAAGAATGGGTCACAAATG-3'
	HEC2 B-R	5'-AGTTATGTGCGAAATGTAAACTGTTACT-3'
	HEC2 C-F	5'-ATCTTCTTCTTCCTCCATACCTTATCTC -3'
	HEC2 C-R	5'-ATCATGTTCATTAGAATGTCGGAGTTAT-3'
	HEC2 D-F	5'-AAAGAGAAAGAACGTGAGGATCTCTAAG-3'
	HEC2 D-R	5'-TTCTTGAGAAACTTAACGTAATGGATAG -3'
HEC3	HEC3 A-F	5'-AAGAGAGAAGGAGATAATTAAAGGGATT-3'
	HEC3 A-R	5'-GACTTGAATTTAGGGTATATCGAGAAAG-3'
	HEC3 B-F	5'-ATATATACATATAAGCATCGCCTCAAGC-3'

	HEC3 B-R	5’-GTTCCAAGTGTAATTTTGGAAGAGAGAT-3’
	HEC3 C-F	5'-CTTCTCATTTCCCTCCTCTCTCTTCTTC -3'
	HEC3 C-R	5'-TTACGGCGTTTGGGTTTCTTGACGGT -3'
PIF1	PIF1 A-F	5'-AAAATGATGCATATCTCTCTCTCTACAA -3'
	PIF1 A-R	5'-TTACGGCGTTTGGGTTTCTTGACGGT -3'
	PIF1 B-F	5'-ATGATTTCTGCTCAGATCTTCTCTTCT -3'
	PIF1 B-R	5'-AGATTCACCACCTCTACCGTTATTAAA -3'
GAI	GAI B-F	5'-GGACCCGTTTTACACGTG-3'
	GAI B-R	5'-TATGTACTTAACGCCGTCGC-3'
	GAI D-F	5'-GAAGACGATCTTTCTCAACTCG-3'
	GAI D-R	5'-CACCGGGAATAGCTTTAAGATC-3'
RGA	RGA B-F	5'-CAGACTCGGTCCCTACCGTTT -3'
	RGA B-R	5'-GCCGTCATTAACGGCCTCTTTCT -3'
	RGA D-F	5'-TATGAATGATGATTGAAGTGGTAGTAGC -3'
	RGA D-R	5'-CTATGAGTTTCGATTAGATTAGGTCTGA -3'
HFR1	HFR1 P2-F	5'-GATACCATTTTCTCGGACAAAGCTGAAA -3'
	HFR1 P2-R	5'-AACTATTAGGGTTTACGATACAAATCAT -3'
	HFR1 P3-F	5'-CGATATATGCTACTATGACGTAGTTTTG -3'
	HFR1 P3-R	5'-CAACAAACATTGTAATGAAAATATTG -3'
	HFR1 qRT-F	5'-TACCACCGTTTACTAATATTTCATTCC -3'
	HFR1 qRT-R	5'-AAAAATCCAAGAAACTTGGGAAATAAG -3'
	HFR1 1stEXON-F	5'-CGTCGTATCCAGGTCTTAAGTAGTGAT -3'
	HFR1 1stEXON-R	5'-TTACTCATCTTCTCGTCTCTTCTTCTTC -3'

3.4 Results

3.4.1. HDA9 negatively regulates the phyB- dependent promotion of seed germination.

Posttranslational histone deacetylation has been implicated to play a role in germination through pharmacological and genetic studies (Tanaka et al., 2008; van Zanten et al., 2014). For the roles of RPD3 Class I HDACs in germination, reported were only HDA6 and HDA19 to redundantly repress embryonic properties and roles of other HDACs remain to be discovered. It prompted me to explore the role of HDA9 in germination process.

To examine the role of *HDA9* during seed germination, I first performed the germination assay using wt, *hda9-1*, and the complemented line *HDA9 hda9-1* (Kang et al., 2015) under constant white light (Fig. 1a). In order to avoid the possible complexity caused by the difference in seed viability and vigor, seeds were harvested from wild-type (wt) Col and *hda9-1* plants grown side by side under 16 h light /8 h dark condition and dried for more than 2 weeks at room temperature. Germination efficiency was measured by counting the number of seeds with emerging radicles on the seed surface. As shown in Fig. 1a, the germination efficiency of *hda9-1* was rapidly increased compared to wt at 44 hours (hr) after planting, and reached to 100% after 70 hr. Accelerated germination phenotype of *hda9-1* was rescued by the introduction of the genomic *HDA9* fragment (*HDA9g hda9-1*), indicating the mutant phenotype was indeed caused by

the loss of HDA9 function.

Because phyB plays key role in regulating seed germination under red or white light condition (Poppe and Schafer, 1997; Oh et al., 2004), it was questioned whether early germination caused by *hda9* is phyB-dependent. In order to address this, the germination efficiency was assessed after 5min red light pulse (Rp) following 5min far-red light (Fp; 1.8 μmol/m^2s) exposure. Seeds were imbibed in dark for 1hr (Fig. 1b-e) before light treatments. As shown in Fig. 1b, wt, *hda9-1*, and *HDA9g hda9-1* seeds similarly showed very poor germination after given only Far-red light pulse, indicating that phyB in all genotypes was inactivated by this treatment. When red-light pulse was given after far-red light pulse which converts phyB to its active form, the germination of all genotypes seeds were observed and reached to 100 % at 5 days after planting (DAP). Interestingly the germination of *hda9-1* more rapidly occurred compared to either wt or *HDA9g hda9-1*, showing ~93% germination efficiency at 2DAP while wt and *HDA9g hda9-1*, 53 and 57%, respectively (Fig. 1c and e).

To more confirm that accelerated germination of *hda9-1* seeds is phyB-dependent, I irradiated the seeds with Fp at the end of sequential applications of Fp and Rp to inactive phyB. This prevented the germination of *hda9-1* seeds, together with wt and *HDA9g hda9-1* seeds (Fig. 1d), which supports that the effect of the *hda9-1* mutation on seed germination requires phyB activity.

Different intensities or prolonged red light is known to affect germination efficiency (Oh et al., 2006). I examined the germination efficiency of wt, *hda9-1*

and*HDA9g hda9-1*using low fluence Rp (10 μmol/m^2s) of different duration. Seeds were irradiated with first, Fp for 5 min and then with Rp for 5 sec, 1min, 2 hr and 20 hr and kept in the dark for 5 days. *hda9-1* seeds showed higher germination efficiency than wt and *HDA9g hda9-1* when a 5- sec Rp and, to less extent, a 1-min Rp were given, whereas after longer than 2 hr red-light treatment, *hda9-1* showed a comparable level of germination to that of either wt or *HDA9g hda9-1* (Fig. 2).

Together, these results indicate that HDA9 is likely to be involved in the negative regulation of phyB-dependent seed germination.

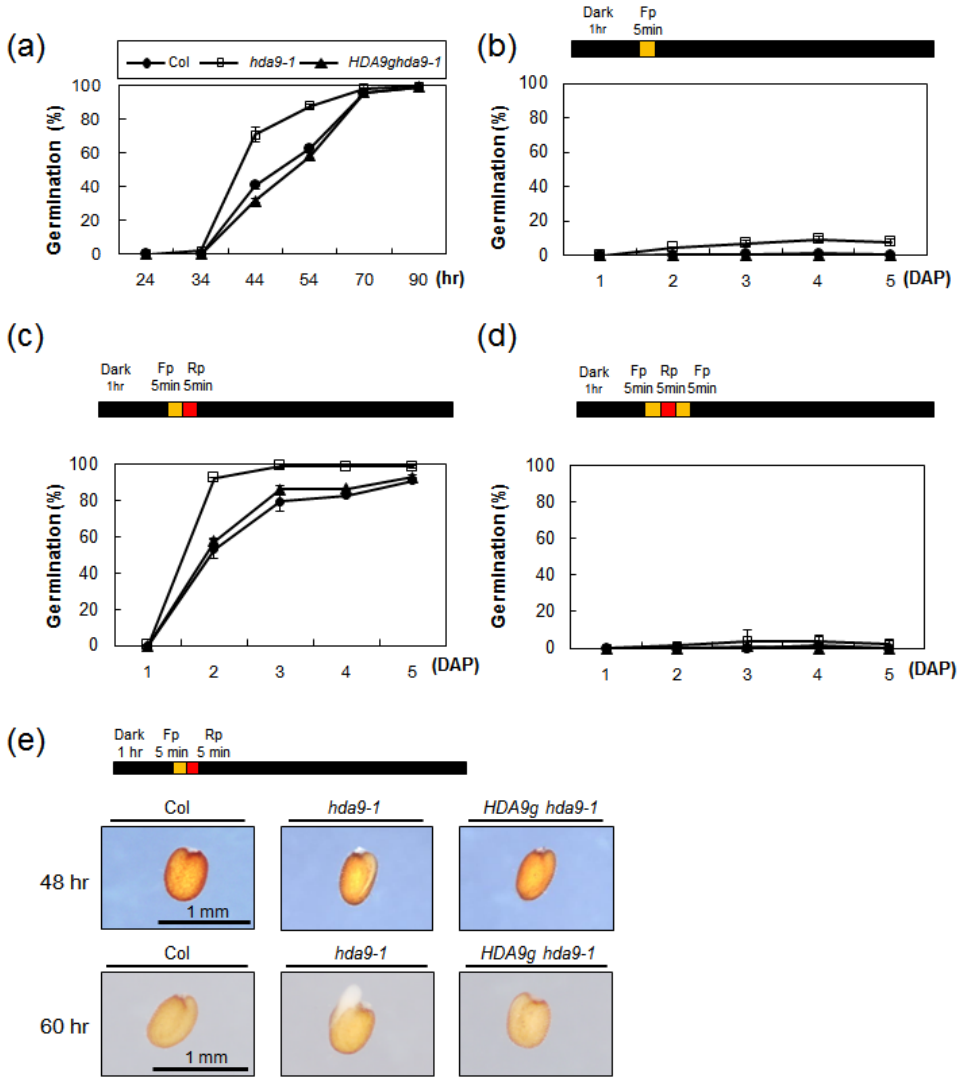

Fig. 1 phyB- dependent enhanced seed germination of *hda9-1*.

(a) Seed germination assay of Col (circle), *hda9-1* (square), and *hda9-1* transformed with a genomic copy of *HDA9 (HDA9g hda9-1)* (triangle) under constant white light condition. Germination was scored at indicated hours. (b-d) phyB- dependent germination assay. Seeds were imbibed for 1 hr in the dark. The

light treatment regime is indicated in the diagram at the top. The intensity for Fp is 1.8 μmol/m^2s or Rp is 40 μmol/m^2s. Light treated seeds were kept in the dark for 5 additional days (black box). Germinated seeds were counted every 24 hr after light treatment. Fp denotes far-red pulse and Rp indicate red pulse. Error bars represent standard errors (SE) from three independent biological replicates. (b) Seeds were exposed to Fp for 5 min and further incubated in the dark for indicated days to see the phyB off effect. (c) Seeds were exposed to Fp for 5 min and immediately exposed to Rp. Light treated seeds were further incubated in the dark for indicated days. (d) To disrupt phyB-dependent activity, seeds exposed to Fp and Rp for 5 min each as indicated in (c) were further exposed to 5 min of Fp. (e) Early germination phenotype of *hda9-1*.Seeds were imbibed for 1 hr in the dark and immediately exposed to Fp or Rp. Light treated seeds were further incubated in the dark for 48 hrs (upper panel) or 60 hrs (lower panel). Germinating seeds were photographed using optical microscope. Scale bars represent 1 mm.

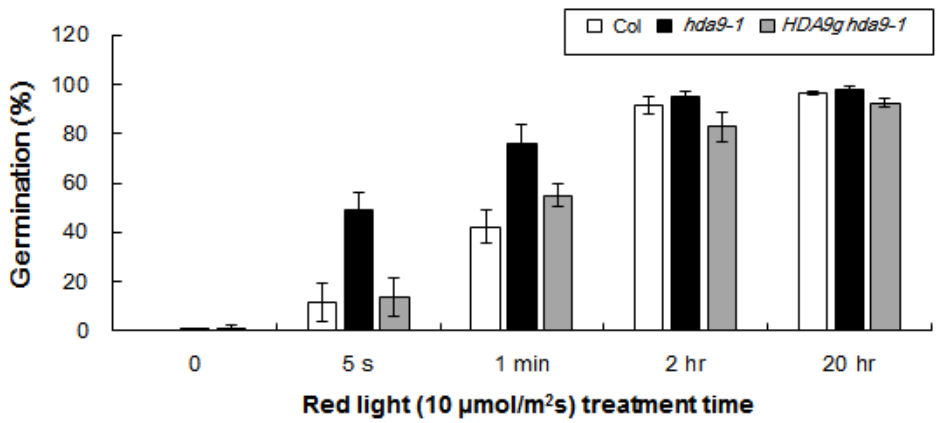

Fig. 2 Enhanced seed germination of *hda9-1* under low flux red-light.

Germination of Col (white), *hda9-1* (black), and *HDA9g hda9-1* (gray) seeds counted under various period in Rp after 5 min of Fp. Seeds were exposed to low intensity Rp (10 µmol/m^2s) for the indicated period after 5 min Fp treatment. Light treated seeds were kept in dark for 5 additional days. Results shown are the percentage of germinated seeds (number of emerging radicles divided by total sowed seeds) scored 5 days after light treatment. Error bars indicate standard errors of three independent biological replicates.

3.4.2. Expression of HDA9 is not affected by red light.

The role of HDA9 in phyB-dependent seed germination led me to ask whether HDA9 expression is red-light dependent. So, I investigated and compared the spatial expression patterns of *HDA9* using HDA9:GUS fusion protein in Fp- or Rp-treated embryos. HDA9:GUS expression was detected in the entire region of the embryos and its strength was not influenced by an exposure to either Fp or Rp (Fig. 3a). In addition, I performed immunoblot assay using Fp- or Rp- treated *HDA9:HA hda9-1* transgenic seeds (Kang et al., 2015) to study whether HDA9 protein level changes by red-light. HDA9:HA protein level was not significantly different between two light treatments (Fig. 3b), which is in line with the result of HDA9:GUS expression (Fig. 3a). Hence, I concluded that HDA9 protein level is not affected by red light.

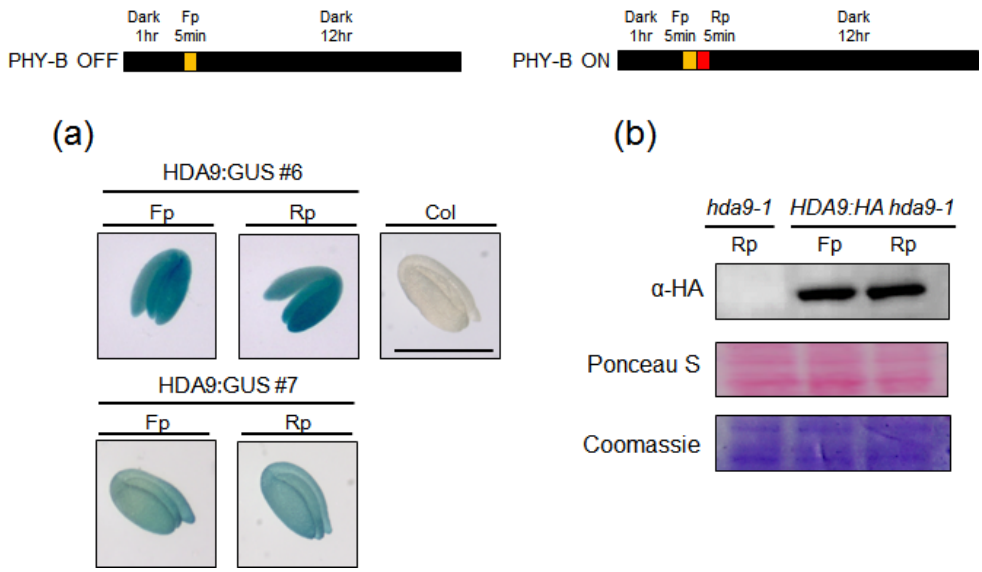

Fig. 3 HDA9 protein level is not affected by red light.

(a) Histochemical GUS staining of HDA9:GUS embryos. Seeds were incubated for 12 hr in the dark after 5 min of Fp (1.8 μmol/m^2s) or Rp (40 μmol/m^2s). Embryos of two independent HDA9:GUS transgenic lines (#6, upper panel and line #7, lower panel) were GUS stained for 2 hr 30 min with X-Gluc solution and photographed using optical microscope. Scale bar represent 1mm. (b) HDA9:HA protein level in Fp and Rp. Total HDA9:HA protein was extracted from Fp or Rp treated seeds. Anti-HA antibody was used to detect HDA9:HA protein. Ponceau S staining for Rubisco protein and Coomassie staining were performed as loading control.

3.4.3. Expression of *HECATEs*, positive regulators in seed germination, is increased by the *hda9-1* mutation.

Next, I questioned how *HDA9* regulates seed germination. Because the most well-known role of HDACs is to regulate transcription of genes and HDA9 was also previously found to be involved in the negative regulation of *AGL19* transcription (Kang et al., 2015), it is plausible that HDA9 plays a role in the transcriptional regulation of germination-related gene expression. bHLH transcription factors PIF1, HFR1, HEC1 and HEC2 were reported to function in phytochrome signaling and seed germination (Oh et al., 2004; Shi et al., 2012; Zhu PhD thesis, 2012). Therefore, I tested whether the *hda9-1* mutation affects mRNA levels of these genes. Total RNA was extracted from Fp- or Rp- treated seeds and the transcript levels of *HEC1, HEC2,* and *HEC3* (Figure 4a), *HFR1* and *PIF1* were determined by quantitative real-time reverse transcription polymerase chain reaction analysis (RT-qPCR; Figure 4b and5 a). Noticeably, *HEC1, HEC2,* and *HEC3* mRNA levels were significantly increased by Rp treatment while HFR1 and PIF1 were not. Moreover, the increase in *HECs* expression was much higher in *hda9-1* (R *hda9-1*) seeds compared to wt (R Col). The increased *HECs* expression by *hda9-1* mutation was restored to wt level in *HDA9g hda9-1* seeds. Interestingly, *HEC1* and *HEC2* transcript levels were also slightly higher in *hda9-1* (F *hda9-1*) than wt seeds (F Col) treated with a Fp. I also examined the protein levels of HECs in wt and *hda9-1* using *HEC1p::HEC1:GUS (HEC1:GUS*; Gremski et al., 2007*). HEC1:GUS* was introduced into *hda9-1* background by crossing. *HEC1:GUS* staining was detected in the entire region of the embryo and stronger in *hda9-1* mutant (Fig. 4c).

Immunoblot assay performed with anti-GUS using nuclear extracts from imbibed seeds identified a positive signal in either wt or *hda9-1* background at ~90 kD that was similar to the size of HEC1:GUS (Fig. 4c and 4d). Intensity of the signal was stronger in *hda9-1* than in wt, indicating more HEC1 protein is present in *hda9-1* than in wt. These results point out that HDA9 might control germination by negatively regulating the transcription of the positive regulator of germination HECs.

In addition to bHLH proteins, several transcription factors are reported to regulate light-dependent seed germination. Among them, *SOMNUS* (*SOM*) and *SPATULA* (*SPT*) are known to act as repressors during light dependent seed germination, while *JMJ20* and *JMJ22* are reported to be involved in the promotion of seed germination. So, I also examined the changes in transcript levels of *SOM*, *SPT*, *JMJ20*, and *JMJ22* together with *PIF1* (Oh et al., 2004; Penfield et al., 2005; Kim et al., 2008; Cho et al., 2012). However, I found no significant difference in the transcript levels of these genes between wt and *hda9-1* after both F and R-treatment (Fig. 5a).

Two phytohormones, ABA and GA antagonistically control seed germination through complicated signaling crosstalk. I further analyzed the mRNA levels of GA- and ABA metabolic genes in wt and *hda9-1* seeds that were irradiated with Rp or Fp and then incubated in dark for 12 hrs. Expression levels of GA biosynthetic genes (*GA3ox1*, *GA3ox2*, and *GA2ox2*) were not significantly different between wt and *hda9-1* in all conditions (Fig. 5b). Overall expression of

ABA anabolic genes such as *ABA-deficient (ABA1)* and *9-cis-epoxycarotenoid dioxygenases (NCED6)* and an ABA catabolic gene, *CYP707A2* were slightly decreased in *hda9-1* compared to wt in all conditions with the exception of the *NCED6* expression in F-treated seeds being largely reduced by the *hda9* mutation (Fig. 5b). However, Both decreases in the expressions of ABA anabolic genes and ABA catabolic genes, when combined together are not likely responsible for the early germination phenotypes of *hda9*.

3.4.4. *HECATE* expressions were enhanced in seed germination.

In order to confirm the promoting role in seed germination of HECs and compare it with the effect of the *hda9* mutation, I assessed the seed germination efficiency of *35S::HEC2* along with *hda9-1* after a red or a far-red light pulse was given. I could not perform the seed germination assay for *HEC1* and *HEC3* overexpression plants because of their fertility defects (Gremski et al., 2007). Notably, unlike *hda9-1*, *35S::HEC2* transgenic line showed enhanced seed germination irrespective of light regimes (Fig. 4e). On the other hand, the germination efficiency of *35S::HEC2* and *hda9-1* after Rp was similarly enhanced after 2 DAP, higher than wt. Considered together with light-dependent induction of *HEC* expression, these results indicates that HECs act as positively regulators in the phyB-dependent seed germination and the amount of HECs might be not limiting factor in this process.

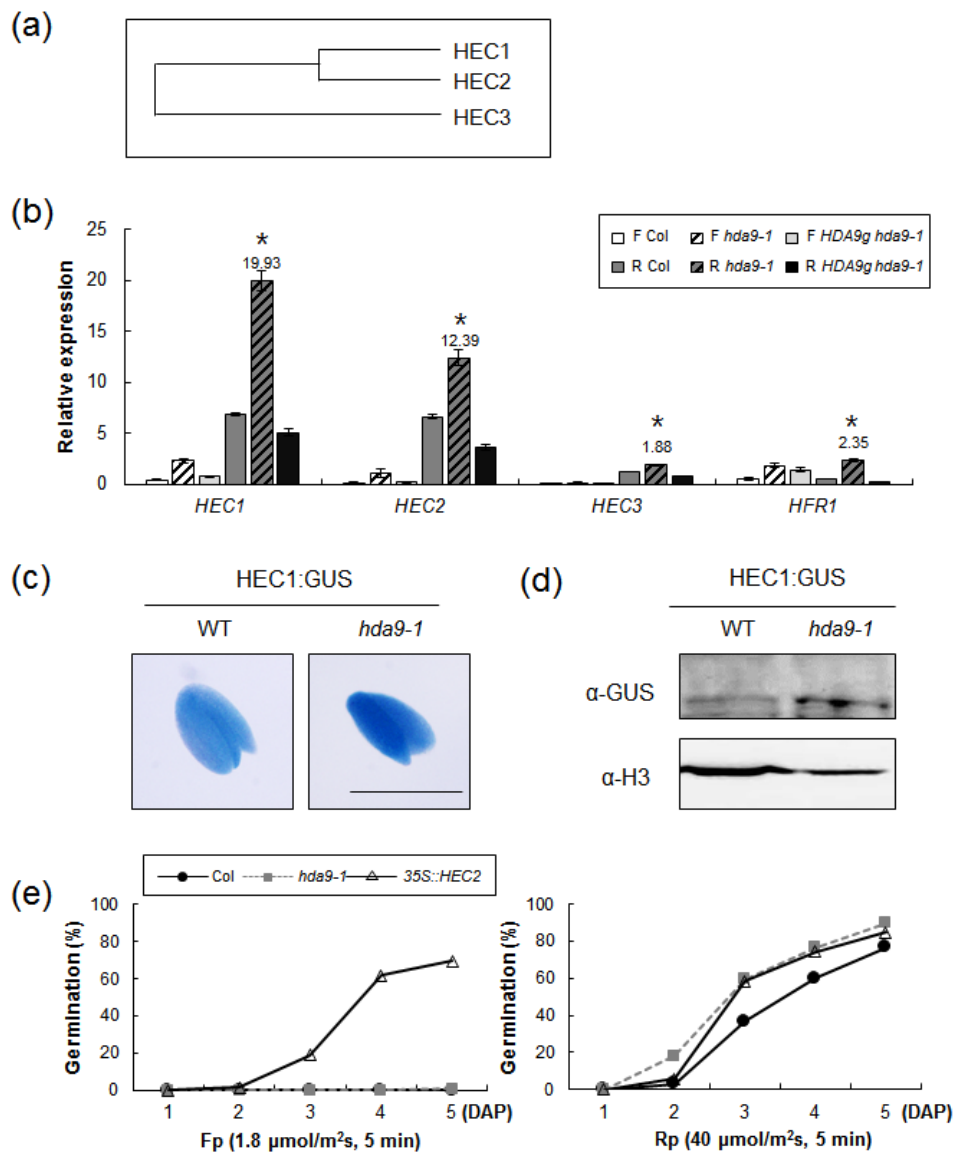

Fig. 4 The *hda9-1* mutation causes increased expression of *HEC* genes at both transcript and protein levels.

(a) Phylogenetic analysis of HECATE proteins using neighbor-joining (NJ) method. The amino acid sequences of Arabidopsis HECATE proteins were aligned using

CLUSTAL W. (b) Transcript level of *HEC1*, *HEC2*, *HEC3*, and *HFR1* analyzed by quantitative real-time reverse transcription polymerase chain reaction (RT-qPCR). The level of F Col was set to 1 after normalization by *UBQ11*. Seeds were exposed to 1.8 μmol/m^2s of Fp for 5 min and 40 μmol/m^2s of Rp for 5 min. Asterisks indicate statistically significant differences ($P<0.05$). Error bars represent standard error of three independent biological replicates. (c) HEC1:GUS expression level is enhanced in *hda9-1*. Histochemical expression patterns of HEC1:GUS in WT (left panel) and *hda9-1* embryos (right panel). All the seeds were homozygous for HEC1:GUS. Seeds were incubated for 12 hr in the dark after 5 min of Rp (40 μmol/m^2s). Light treated seeds were fixed by acetone and dissected. Embryos were stained for 36 hr with X-Gluc solution and photographed using optical microscope. Scale bar represent 1mm. (d) HEC1:GUS protein level is increased by *hda9-1* mutation. Nuclear enriched proteins were extracted from HEC1:GUS in WT and *hda9-1* seeds using Honda buffer. Seeds were treated with 5 min of Rp (40 μmol/m^2s) and incubated in the dark for 12 hr before harvesting. For immunoblot analysis, HEC1 protein was detected with anti-GUS antibody (1:1000) using Chemi-doc (Fusion solo). Histone H3 was detected using anti-H3 (1:10000) as nuclear protein control. (e) Germination efficiency of Col (circle), *hda9-1* (square), and *35S:HEC2* (triangle). Seeds were exposed to 5 min of Fp (1.8 μmol/m^2s) and 5 min of Rp (40 μmol/m^2s). Light treated seeds were incubated in the dark and germinated seeds were counted at indicated days.

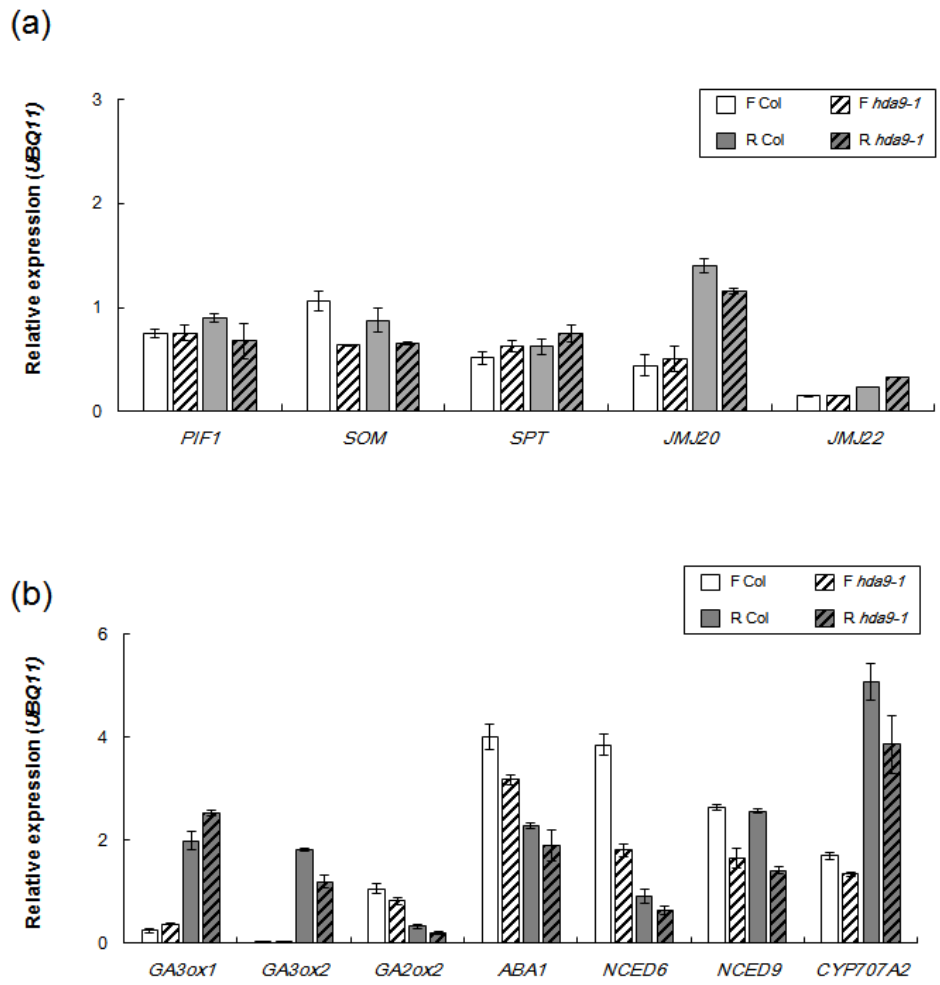

Fig. 5 Expression of germination-related genes in wt and *hda9-1*.

(a) Transcript level of *PIF1, SOM, SPT, JMJ20, JMJ22* under red light condition. Seeds were imbibed for 1 hr in the dark and irradiated with 1.8 μmol/m^2s of Fp for 5 min followed with 40 μmol/m^2s of Rp for 5 min. Then, seeds were kept in the dark for 12 hr before total RNA extraction. Transcript levels were analyzed by RT-qPCR. *UBQ11* was used as an internal control. Error bars represent standard error of three independent biological replicates. (b) Transcript level of GA biosynthetic

genes and ABA metabolism and signaling genes examined by RT-qPCR. Dry seeds were imbibed for 1 hr in the dark and irradiated with 1.8 μmol/m^2s of Fp for 5 min followed with 40 μmol/m^2s of Rp for 5 min. Then, seeds were kept in the dark for 12 hr and harvested for total RNA extraction. *UBQ11* was used as internal control. Error bars represent standard error of three independent biological replicates.

3.4.5. HDA9 directly represses *HECs* transcription through histone deacetylation.

I performed chromatin immuno-precipitation (ChIP) experiment to test whether *HDA9* represses the transcription of *HECs* by changing their chromatin environment through histone deacetylation (Fig. 6b-d). ChIP assay using anti acetylated histone H3 (H3Ac) antibody showed that H3Ac level was gradually increased in region within *HEC1* (B and C region), *HEC2* (B region) and *HEC3* (C region) in wt after Rp treatment. These results indicate that the transcriptional activation of *HECs* requires histone acetylation under Rp condition. Furthermore, in accordance to the increased transcript level of *HECs* in *hda9-1*, the H3Ac level in R-treated *hda9-1* was much higher in promoters and transcribed regions within *HEC1* (regions A, B, and C), *HEC2* (regions A, B, and D) and *HEC3* (regions A, B, and C) compared to R-treated wt (Fig. 6a and 6b). Therefore, the increased *HECs* transcription in *hda9-1* might be a consequence of hyperacetylated H3 in *HECs* chromatin.

Next, I examined the RNA polymerase II (RNA pol II) occupancy to see whether hyperacetylation of *HECs* was related to RNA pol II mediated transcription. In wt, there was no noticeable change in the RNA pol II occupancy in regions of *HECs* chromatin in Rp compared to Fp-treated condition. On the other hand, RNA pol II occupancy within *HEC1* (regions A, B and C), *HEC2* (regions A, B and D) and *HEC3* (regions A, B and C) chromatin was increased in Rp-treated *hda9-1* (Fig. 6a and 6c). Thus, hyperacetylation by *hda9-1* mutation in Rp

condition might increase the accessibility of RNA pol II to the *HECs* chromatin.

I further performed the ChIP assay with anti-HA using *HDA9:HA hda9-1* transgenic seeds to address whether HDA9 play a direct role in the transcriptional regulation of *HEC*s chromatin. ChIP-qPCR analysis clearly showed the association of HDA9:HA with the promoter, transcription start site and gene body (regions A, B, and C) of *HEC1* chromatin under Rp condition (Figure 6d). In addition, HDA9:HA strongly bound to the region near the transcription start sites of *HEC2* (regions A, B, and C) and *HEC3* (region A), but not *PIF1* (Fig. 6a and 6d). These results indicate that HDA9 directly bind to the *HECs* chromatin, which is consistent with the increases of H3Ac level and RNA pol II occupancy at *HECs* loci in *hda9-1*compared to wt. Together, these results suggest that HDA9 has a direct role in maintaining the proper transcriptional activity of *HECs* through histone deacetylation.

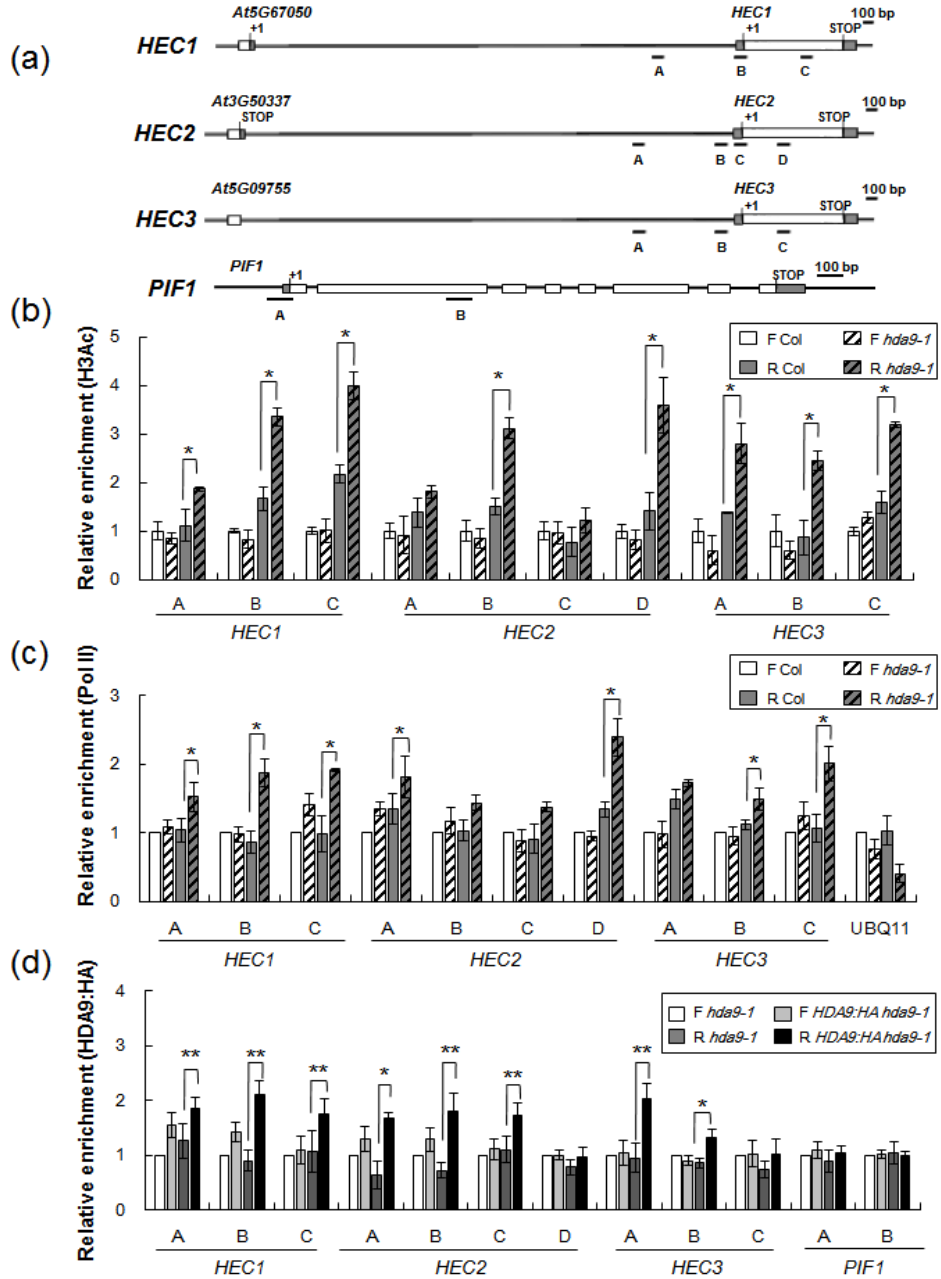

Fig. 6 HDA9 directly affects *HEC* transcription via histone deacetylation.

(a) Schematics representing the genomic structures of *HEC1*, *HEC2*, *HEC3*, and

PIF1. Gray boxes represent 5' and 3' untranslated regions and white boxes indicate exons. Introns are represented as solid lines and the transcription start site is indicated as +1. Regions amplified in chromatin immunoprecipitation followed by qPCR (ChIP-qPCR) are shown for each gene. (b) H3Ac level in *HEC1*, *HEC2*, and *HEC3* chromatin analyzed by ChIP-qPCR. Col and *hda9-1* seeds were incubated for 12 hr in the dark after 5 min treatment of Fp (1.8μmol/m^2s) or 5 min of Rp (40 μmol/m^2s). H3Ac level was increased by red light around the promoters and gene bodies of *HEC1*, *HEC2*, and *HEC3* chromatin. The H3Ac level of R *hda9-1* was higher than R Col. Levels of F Col were set to 1 after normalization by *UBQ11*. Asterisks indicate statistically significant differences ($P<0.05$). (c) RNA polymerase II occupancy within *HEC1*, *HEC2*, and *HEC3* chromatin examined by ChIP-qPCR. Samples were prepared as in (b). The F Col level was set to 1 after normalization to the corresponding input. *UBQ11* was used as internal control. Asterisks indicate statistically significant differences ($P<0.05$). (d) HDA9:HA enrichment using anti-HA antibody analyzed by ChIP-qPCR. HDA9:HA *hda9-1* and *hda9-1* seeds were incubated for 12 hr in the dark after 5 min of Fp (1.8 μmol/m^2s) or 5 min of Rp (40 μmol/m^2s). The amount of immunoprecipitated chromatin was normalized to the corresponding input and compared with untagged lines. The regions of *PIF1* were used as nonspecific control. Shown are the means± SE of three biological replicates. Asterisks indicate statistically significant differences (* $P<0.05$, ** $P<0.01$).

3.4.6. HDA9 acts as an upstream regulator of *HECs.*

In order to the increased HECs levels indeed cause the early germination of the *hda9* mutant, I analyzed the phyB-dependent germination of *hda9-1* in the absence of HECs. *hec1 hec2 RNAi* double mutant displayed reduced germination efficiency compared with wt (Fig. 7) which *35S::HEC2* showed clearly enhanced germination (Fig. 4e), demonstrating the positive role of HECs in seed germination. Remarkably, the promoting effects of the *hda9* mutation greatly disappeared in *hec1 hec2 RNAi hda9-1* ; the triple mutant seeds displayed similar germination efficiency as the *hec1 hec2 RNAi* seeds (Fig. 7), indicating the early germination of *hda9* is in great part attributed to HECs. I observed the slight increase of germination efficiency in *hec1 hec2 RNAi hda9-1* compared to *hec1 hec2 RNAi*. This slightly early germination of *hec1 hec2 RNAi hda9-1* might be due to the enhanced expression of *HEC3* or other unknown factors by *hda9-1* mutation.

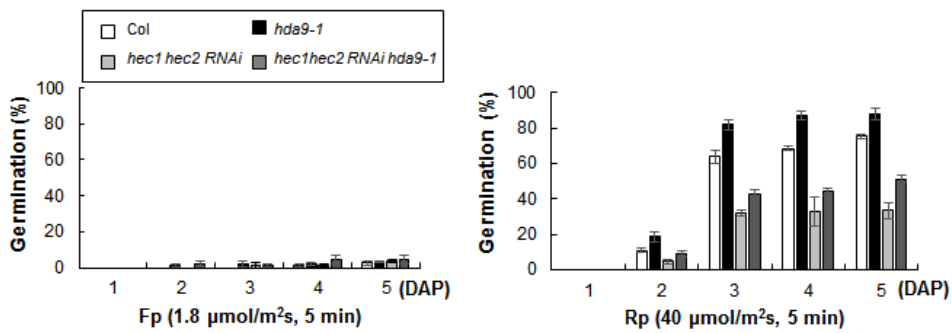

Fig. 7 HECs are required for the enhanced germination of *hda9-1*.

hec mutations are epistatic to the *hda9-1* mutation under red light. Germination efficiencies were observed in Col (white), *hda9-1* (black), *hec1hec2 RNAi* (light gray), and *hec1 hec2 RNAi hda9-1* (dark gray). Germinated seeds were counted every 24 hr after dark incubation following light treatment (Fp; left or Rp; right). Values are the means ± SE of three independent biological replicates.

3.4.7. *GAI* and *RGA* mRNAs are reduced by the *hda9* mutation under red light regime.

Previously, it was reported that HEC2 blocks DNA binding activity of PIF1 and regulate the expression of GAI and RGA in a way opposite to PIF1. So, I examined in *wt* and *hda9-1* seeds the expressions of *PIF1* and *PIF1* target genes (*SOM*, *GAI*, and *RGA*) after the application of a Rp (40 or 10 μmol/m^2s) followed by a Fp or of a Fp only. When only a Fp was given, the transcript levels of all the examined genes were reduced in *hda9-1* compared to wt with the exception of *PIF1* of which expression was not significantly decreased in the mutant (Figure 8a and b). Yet, germination of Fp-treated *hda9-1* was indistinguishable from Fp-treated wt (Fig. 1b), indicating that the extent of reduction in the expression of *SOM*, *GAI* and *RGA* in *hda9-1* is not enough to overcome the strong influence of germination-repressing factors such as PIF1 in Fp-treated seeds. Irradiation with a Rp resulted in the decreases in *SOM*, *GAI*, *RGA*, and to lesser extent, *PIF1* (Figure 8a and b). This was more noticeable with higher-fluence rate red light. After a pulse of both high- and low- fluence red light was applied, the mRNA levels of *GAI* and *RGA* but not of *SOM* were reduced more in *hda9-1* than in wt. Small difference in *SOM* transcript level between wt and *hda9-1* was detectable after a pulse of low- fluence light only (Figure 8b). Then, I performed ChIP assay using HDA9:HA in order to test possibility that HDA9 directly regulate the transcription of *GAI* and *RGA*. There was no detectable association of HDA9:HA with either *GAI*- or *RGA* chromatin regions analyzed (Fig. 8c and 8d). Combined together, these results suggest that *HDA9* affects the mRNA levels of *GAI* and *RGA* that are the target

genes of the germination repressor *PIF1*, probably by regulating the transcription of HEC1, a negative regulator of *PIF1* activity.

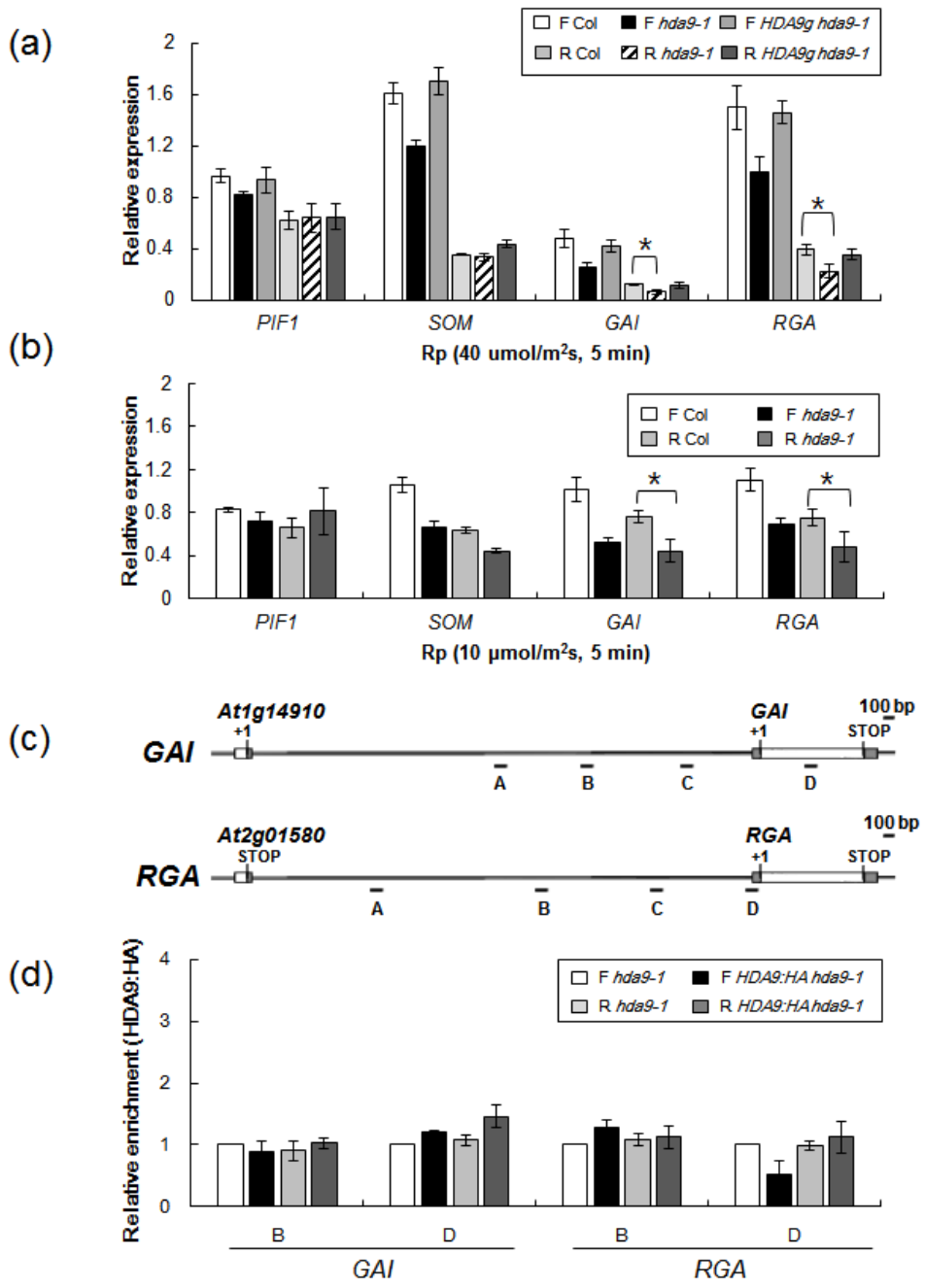
(a)
F Col
F hda9-1
F HDA9g hda9-1
R Col
R hda9-1
R HDA9g hda9-1
Relative expression
2
1.6
1.2
0.8
0.4
0
*
*
PIF1
SOM
GAI
RGA
Rp (40 umol/m²s, 5 min)
(b)
F Col
F hda9-1
R Col
R hda9-1
Relative expression
2
1.6
1.2
0.8
0.4
0
*
*
PIF1
SOM
GAI
RGA
Rp (10 μmol/m²s, 5 min)
(c)
At1g14910
+1
GAI
+1
100 bp
STOP
GAI
A
B
C
D
At2g01580
STOP
RGA
+1
100 bp
STOP
RGA
A
B
C
D
(d)
F hda9-1
F HDA9:HA hda9-1
R hda9-1
R HDA9:HA hda9-1
Relative enrichment (HDA9:HA)
4
3
2
1
0
B
D
B
D
GAI
RGA

Fig. 8 Transcript levels of *GAI* and *RGA* are reduced by the *hda9-1* mutation under red light regime.

(a) *GAI* and *RGA* transcript levels are decreased in R *hda9-1*. Transcript level of *PIF1* and its direct target genes, *SOM*, *GAI*, and *RGA* quantified by RT-qPCR. Seeds were exposed to 5 min of Fp (1.8 μmol/m^2s) or 5 min of Rp (40 μmol/m^2s). The level of F Col was set 1 after internal normalization by *UBQ11*. Shown are the means of three independent biological replicates and error bars represent SE. Asterisks indicate statistically significant difference (P <0.05). (b) *GAI* and *RGA* transcript levels are decreased in low-intensity R *hda9-1*. The transcript levels of *PIF1*, *SOM*, *GAI*, and *RGA* under low quantity of red light (10 μmol/m^2s) were analyzed by RT-qPCR. The level of F Col was set to 1 after internal normalization by *UBQ11*. Values are the means ± SE of three independent biological replicates. Asterisks indicate statistically significant differences (P <0.05). (c) Schematics of the genomic structures of *GAI* and *RGA*. Gray boxes represent 5' and 3' untranslated regions and white boxes represent exons. Introns are indicated as solid lines, +1 represent transcription start site. Regions amplified in ChIP-qPCR are shown for each gene. (d) HDA9:HA does not directly bind to *GAI* or *RGA* chromatin. HDA9:HA *hda9-1* and *hda9-1* seeds were incubated for 12 hr in the dark after 5 min of Fp (1.8 μmol/m^2s) or 5 min of Rp (40 μmol/m^2s). The amount of immunoprecipitated chromatin was normalized to the corresponding input and compared with the untagged line. Values are the means ± SE of three independent biological replicates.

3.4.8. The *pif1* mutation is epistatic to the *hda9* mutation.

As an initial attempt to test the hypothetical regulatory pathway consisting of HDA9-HEC1-PIF1-PIF1 targets in the phyB-dependent germination process, I analyzed the effect of *pif1-2* mutation on the early germination of *hda9-1* by assessing the germination efficiency of *hda9-1 pif1-2*. *pif1-2* mutant showed extremely enhanced germination after both Fp and Rp as previously reported (Oh et al., 2004). Germination efficiency of *pif1-2 hda9-1* double mutant was similar to that of *pif1-2* single mutant without any additive effect of *pif1-2* and *hda9-1* after both Fp and Rp (Fig. 9). This result that *pif1-2* mutation is epistatic to *hda9-1* mutation supports the above hypothesis.

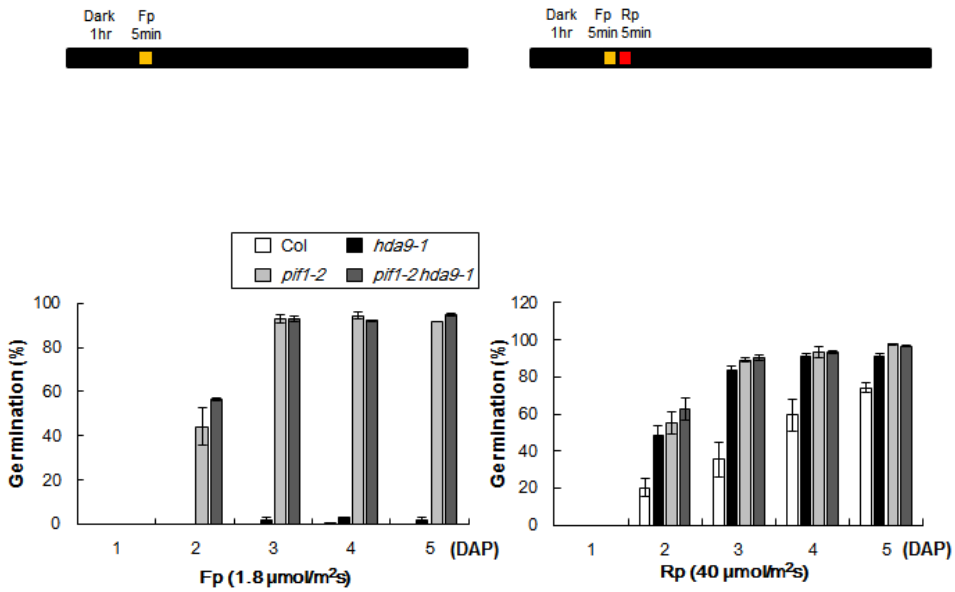

Fig. 9 The *pif1-2* mutation is epistatic to the *hda9-1* mutation in seed germination.

Germination percentages of Col (white), *hda9-1* (black), *pif1-2* (light gray), and *pif1-2 hda9-1* (dark gray) seeds exposed to 5 min of Fp (1.8 μmol/m^2s; left) or 5 min of Rp (40 μmol/m^2s; right). Light treated homozygous seeds were kept in the dark and germinated seeds were counted every 24 hr. Error bars represent standard error from three independent biological replicates.

3.4.9. HDA9 targeting to *HFR1* is less clear.

Recently it was reported that HFR1 forms a heterodimer with PIF1 and inhibit the transcription activity of PIF1 on targets genes (Shi et al., 2013). Interestingly, I observed the increase of *HFR1* transcript level *hda9-1* after a red light pulse following a far-red light pulse (Fig. 4b). So, I investigated whether HDA9 also regulate the transcription of *HFR1* through histone deacetylation. I found that H3Ac levels in the regions of promoter (P2), transcription start site (P3) and gene body (E1) of *HFR1* were higher in *hda9-1* than in wt after subsequent Rp the but not after Fp pulse only (Fig. 10a and 10b). Next, I performed the ChIP assay with anti-RNA pol II antibody using imbibed seeds to investigate the accessibility of RNA pol II to *HFR1* chromatin. Although H3Ac level at HFR1 was elevated by *hda9-1* mutation, RNA pol II occupancy in *hda9-1* was indistinguishable from that in wt irrespective of light regimes (Fig. 10c). I further examined whether HDA9 directly binds to *HFR1* by ChIP assay with anti-HA antibody using *HDA9:HA* seeds and found no significant binding of HDA9:HA to the analyzed regions of *HFR1* chromatin (Fig. 10d). These results indicate that *HDA9* indirectly regulate the transcription of *HFR1*.

In addition, I analyzed the germination efficiency of *hfr1-201*, *hda9-1*, wt Col, and *hfr1-201 hda9-1* double mutants after different duration of red-light (10 μmol/m^2s) exposure. *hfr1-201* showed poor germination compared to other genotypes after up to 2 hrs of red-light exposure. However, the germination efficiency of *hfr1-201 hda9-1* was better than *hfr1-201* single mutant and was

moreover, in fact comparable to that of *hda9-1* (Fig. 10e). These results strongly suggest that HFR1 is not required for HDA9-medaited regulation of germination.

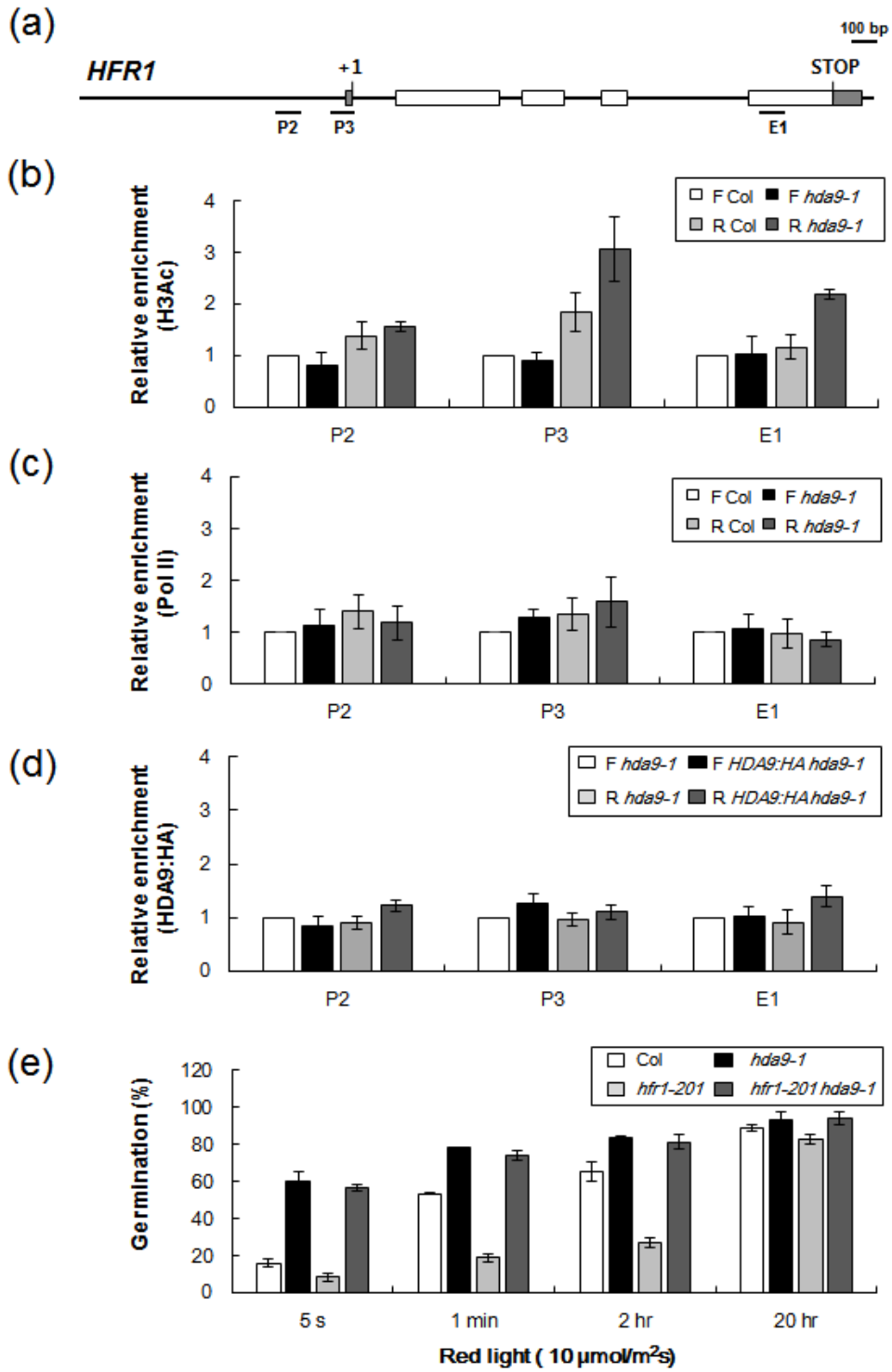

Fig. 10 Contribution of HFR1 in the enhanced seed germination of *hda9-1* is

not obvious.

(a) Schematic of the *HFR1*genomic structure. Gray boxes represent 5' and 3' untranslated regions and white boxes represent exons. Introns are indicated as solid lines, +1 designates transcription start site. Underlines indicate regions amplified in chromatin immunoprecipitation followed by qPCR. (b) H3Ac level at the *HFR1* locus is increased by red light. The increase of H3Ac by red light at the *HFR1* locus was more pronounced in R *hda9-1* than R Col. H3Ac level at the *HFR1* chromatin was analyzed by ChIP-qPCR. Level of F Col was set to 1 after normalization by *UBQ11*. Seeds were exposed to 5 min of Fp (1.8 μmol/m^2s) and 5 min of Rp (40 μmol/m^2s). Values are the means± SE of three independent biological replicates. (c) RNA polymerase II occupancy at the *HFR1* locus is not substantially increased in *hda9-1*. RNA polymerase II occupancy within *HFR1* chromatin was analyzed by ChIP-qPCR. The sample of F Col was set 1 after normalization to the corresponding input. Values are the means± SE of three independent biological replicates. (d) *HDA9* targeting to *HFR1* is less clear. The enrichment of HDA9:HA within the *HFR1* chromatin using anti-HA antibody was analyzed by ChIP-qPCR. The amount of immunoprecipitated chromatin was normalized to the corresponding input and compared with untagged lines. Values are the means± SE of three independent biological replicates. (e) Germination efficiencies of Col, *hda9-1, hfr1-201* and *hfr1-201 hda9-1* seeds. Seeds were exposed to low intensity Rp (10 μmol/m^2s) for the indicated time period after 5 min Fp treatment. Light treated seeds were kept in the dark for 5 additional days. Results shown are the percentage of germinated seeds scored 5 days after light

treatment. Error bars indicate standard errors from three independent biological replicates**.**

3.4.10. Proposed working model of HDA9-HEC-PIF1 regulatory module controlling the phyB-dependent seed germination.

From all the results above, I propose a working model for the functions of HDA9-HEC-PIF1 module in the regulation of the phyB-dependent seed germination (Fig. 11). When seeds are subjected to red light, most phytochromes are converted to the biologically active Pfr form and then moves into the nucleus. In the nucleus, phyB (Pfr) interacts with PIF1, which induces rapid degradation of PIF1 through the 26S proteasome pathway leading to the release of seeds germination from the restraint by PIF1. phyB (Pfr) also causes the expression of *HECs*. HECs form heterodimers with residual PIF1 from the degradation, which sequesters PIF1 and blocks its transcriptional activity toward the target genes such as *RGA* and *GAI*, ensuring the promotion of germination. HDA9 plays a role in restricting hyper-acetylation in the *HECs* chromatin during transcription which may cause the increase of transcriptional activity of *HECs* chromatin and the following illegitimate seed germination. Consequently, the HDA9-HECs-PIF1 module plays a role in fine-tuning the expression of PIF1 target genes such as *GAI* and *RGA*, two DELLA genes involved in the inhibition of the accumulation of GA, which allow the proper timing of germination under environmental conditions subjected to seeds.

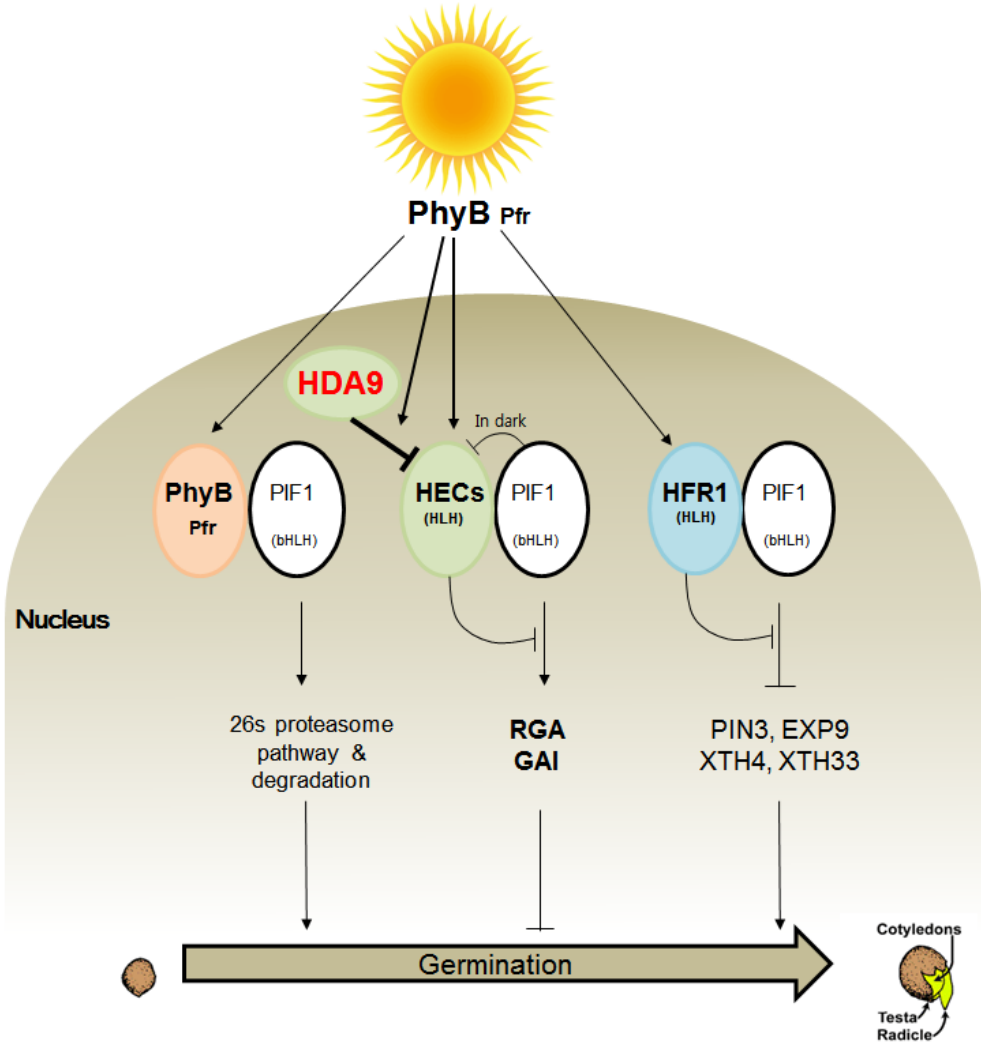

Fig. 11 Proposed working model of *HDA9-HECs-PIF1* module in phyB-dependent seed germination.

Upon exposure to red light, phyB perceives the red light and phyB Pfr form becomes activated. The activated phyB Pfr form translocate into the nucleus, where it interacts with PIF1. Interaction of PIF1 with phyB Pfr form triggers the proteolytic degradation of PIF1 via the 26S proteasome (left). In addition to phyB,

PIF1 also interact with HECs. The expression of *HECs* is induced under red light and HECs protein interacts with PIF1 to remove residual PIF1 activity. The expression of *HECs* is regulated at the transcriptional level by HDA9. HDA9 directly binds to the *HECs* chromatin and sequesters its hyperactivation via histone deacetylation. The loss of PIF1 activity through its binding with HDA9-HECs leads to the down regulation of PIF1 target genes such as *RGA* and *GAI* leading to the inhibition of illegitimate germination (middle). Under low light condition, the level of HFR1 protein is increased and prevents PIF1 to further inhibit the suppression of seed germination. This allows seeds to rapidly respond to low light initiated seed germination without delay (right). However, the relationship of HFR1 and HDA9 in the control of PIF1 is yet unclear.

3.4.11. HECs are involved in controlling the light- dependent inhibition of hypocotyl elongation by HDA9.

It was also reported that HECs positively regulate the inhibition of hypocotyl elongation (Zhu PhD thesis, 2012). Since the *hda9-1* mutation causes less elongated petioles and hypocotyls (Kang et al., 2015; unpublished data), I tested if the functional relationship between HDA9 and HECs observed in the phyB-dependent seed germination also exists in the light-mediated inhibition of hypocotyl elongation. In order to do that, *hda9-1*, *hec1hec2 RNAi*, and *hec1hec2 RNAi hda9-1* seedlings were grown in constant darkness (DD; left panel) or constant red light condition (Rc; 10 μmol/m^2s; right panel) and their hypocotyl lengths were measured and compared. As shown in Fig. 12, the hypocotyl lengths of wt, *hda9-1*, *hec1hec2 RNAi*, and *hec1hec2 RNAi hda9-1* were comparable to that of wt in DD. Under Rc, in contrast, *hda9-1* displayed shorter hypocotyls than wt, *hec1hec2 RNAi* and *hec1hec2 RNAi hda9-1*. As previous reports by Zhu PhD thesis, 2012, the hypocotyl length *hec1hec2 RNAi* was slightly longer than wt under our light condition. However, surprisingly, the short hypocotyl phenotype of *hda9-1* was masked in *hec1hec2 RNAi* background as shown by the similar hypocotyl lengths of *hec1hec2 RNAi hda9-1* and wt. Together, these results suggest that HDA9 requires HECs in controlling the phyB-dependent inhibition of hypocotyl elongation as well as seed germination (Fig. 12).

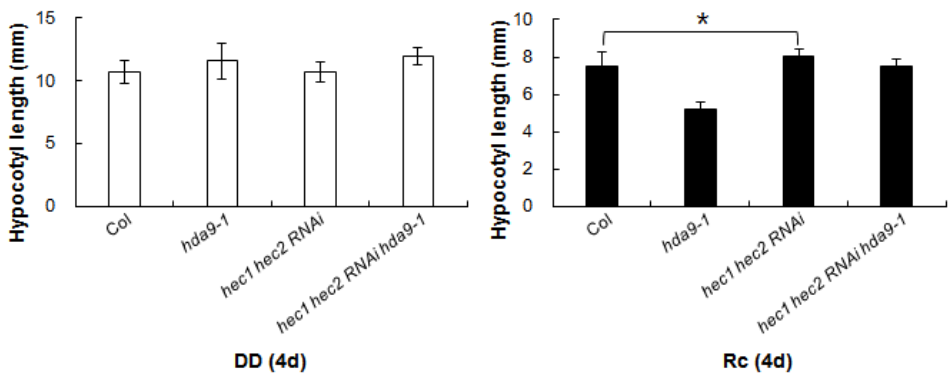

Fig.12 HECs are required for the short-hypocotyl phenotype of *hda9-1*.

Hypocotyl elongations of wild type Col, *hda9-1*, *hec1hec2 RNAi*, *hec1hec2 RNAi hda9-1*. Seedlings were grown for 4 days under constant dark (DD; left panel) or 40 μmol/m^2s of constant red light condition (Rc; right panel). Hypocotyl length was measured using ImageJ software. At least 20 individual seedlings were used for hypocotyl measurement. Bars indicate standard deviation of averages. Asterisks indicate statistically significant differences (*P <0.0005).

3.5 Discussion

Histone deacetylases have shown to be key players in differentiation and development of multicellular organisms. I and others previously reported an Arabidopsis RPD3/HDA1 class I histone deacetylases, HDA9 functions in repressing floral transition under unfavorable day-length condition. In this study I find an additional biological role of HDA9. HDA9 plays a role in germination, one of dramatic developmental transition during plant life cycle. Germination-relate gene expression studies, ChIP analyses for H3Ac levels and HDA9 binding and genetic studies for epistasis all pointed out that HDA9 controls the light-induced germination through repressing the expressions of HECs, positive regulators of light-induced germination.

Although the target genes and underlying mechanisms of HDA9-mediated regulation of flowering and germination are different, there appear some aspects in common between two events. HDA9 deacetylates chromatin of target genes (AGL19 for flowering and HECs for germination) when they are actively transcribed. This was supported by the ChIP results which show in both cases the increase in H3Ac level, the differences in H3Ac levels between wt and the mutant and HDA9 binding were more significant under the conditions that activate the expression of target genes. Thus the role of HDA9 in transcription, unlike the conventional idea of HDACs is to modulate the transcription activity of target chromatin by resetting the landscape of chromatin during active transcription. Similarly it was reported that Arabidopsis homologs of a component of Sin3-HDAC complex are recruited to *FT* chromatin only at the end of day when *FT* is

actively transcribed to dampen the *FT* expression level (Gu et al., 2013). My works suggest that above function of HDA9 in transcription act as a tool to fine-tune the timing of critical developmental transitions such as germination and flowering. Timing of germination and flowering are both exquisitely regulated by environmental stimuli. If the responses of plants to environmental stimuli are abnormal, either hyper-sensitive or hypo-sensitive, it would lead to improper timing of transitions which must be damaging to plants. The function of HDA9 to prevent hyper-activation of target gene expression in response to environmental stimuli would also prevent illegitimately early initiation of the downstream events and subsequent developmental transition. Although my work demonstrated that the recruitment of HDA9 to the *HECs* chromatin is light- dependent, its underlying mechanism of this remains unanswered. One possibility would be the light dependent expression of HDA9 in seeds. However the analyses of *HDA9* protein level in seeds either kept in dark or exposed to light (Fig. 3) showed that that is not the case. Another possibility would be that a red-light specific transcription factor(s) recruits HDA9 to the *HEC* chromatin. One of such candidates is LONG HYPOCOTYL 5 (HY5), a bZIP transcription factor which is known to directly bind to and activate the expression of the light induced genes (Chattopadhyay S., 1998). However, *HEC* transcript level was not changed by *hy5* mutation under red light (data not shown), indicating that the recruitment of HDA9 to *HECs* chromatin is not likely caused by *HY5*. It is also conceivable that HDA9 might be recruited via a component of the HDA9-containing complex that recognize the histone marks produced during transcription such as H3K4- and H3K36 methylation.

Previously it was reported that Eaf3/Rpd3C deacetylase complex can recognize H3K36 methylation mark and remove histone acetylation immediately subsequent to Pol II transcription, thus maintaining a repressive chromatin structure. Although the role of such deacetylation was known to prevent unwanted intragenic transcription initiation or cryptic transcription in yeast, it has not been clearly demonstrated in multicellular organisms. Therefore, it would be possible that HDA9 is recruited to actively transcribed chromatin in similar way but it role in the regulation of transcription is different from that in yeast. Further studies are required to decipher the molecular mechanism by which HDA9 is recruited to *HEC* chromatin in the light-dependent manner.

According to previous studies (Oh et al., 2008), PIF1 regulates gene transcription either positively or negatively depending on the target in seeds. Interestingly, a gene ChIP study (Oh et al., 2008) showed that some of light-induced genes (dark-repressed genes) are PIF1-repressed genes and I found HEC1 in the list of the genes belong to that category. My preliminary data showed that *HEC* mRNA levels were significantly increased by *pif1-2* mutation under far-red light and PIF1 protein was directly associated with *HEC* chromatin (data not shown). Thus, light promotes germination by removing PIF1 via two modes: degradation of PIF1 by activation of phyB and inhibition of PIF1 activity by increasing the level of its antagonistic interacting partners HECs. Thus, this HECs-PIF1 inhibitory circuit might serve as a safety mechanism to ensure germination by light and HDA9 refine it to prevent the start of germination by low fluence or short irradiation of light by regulating HECs levels.

References

Adamczyk BJ, Lehti-Shiu MD, Fernandez DE. 2007. The MADS domain factors AGL15 and AGL18 act redundantly as repressors of the floral transition in Arabidopsis. *Plant Journal* **50:** 1007-1019.

Adrian, J., Farrona, S., Reimer, J.J., Albani, M.C., Coupland, G. and Turck, F. 2010. cis-Regulatory elements and chromatin state coordinately control temporal and spatial expression of FLOWERING LOCUS T in Arabidopsis. *The Plant cell* **22:** 1425-1440.

Alexandre CM, Hennig L. 2008. FLC or not FLC: the other side of vernalization. *J Exp Bot* **59:**1127-1135

Amasino R. 2010. Seasonal and developmental timing of flowering. *Plant Journal* **61:** 1001-1013.

Aufsatz W, Mette MF, van der Winden J, Matzke M, Matzke AJM. 2002. HDA6, a putative histone deacetylase needed to enhance DNA methylation induced by double-standard RNA. *EMBO Journal* **21:** 6832-6841.

Aukerman MJ, Sakai H. 2003. Regulation of flowering time and floral organ identity by a MicroRNA and its APETALA2-like target genes. *Plant Cell* **15:** 2730-2741.

Benhamed M, Bertrand C, Servet C, Zhou DX. 2006. Arabidopsis GCN5, HD1, and TAF1/HAF2 interact to regulate histone acetylation required for light-

responsive gene expression. *Plant Cell* **18:** 2893-2903.

Blázquez MA, Weigel D. 2000. Integration of floral inductive signals in Arabidopsis. *Nature* **404:** 889-892.

Carey, B.W., Finley, L.W., Cross, J.R., Allis, C.D. and Thompson, C.B. 2015. Intracellular alpha-ketoglutarate maintains the pluripotency of embryonic stem cells. Nature **518:** 413-416.

Castillejo C, Pelaz S. 2008. The balance between CONSTANS and TEMPRANILLO activities determines *FT* expression to trigger flowering. *Current Biology* **18:** 1338-1343.

Chattopadhyay S, Ang LH, Puente P, Deng XW, Wei N. 1998. Arabidopsis bZIP protein HY5 directly interacts with light-responsive promoters in mediating light control of gene expression. *Plant Cell* **10:** 673-683.

Chen, H., Zhang, J., Neff, M.M., Hong, S.W., Zhang, H., Deng, X.W. and Xiong, L. 2008. Integration of light and abscisic acid signaling during seed germination and early seedling development. *Proceedings of the National Academy of Sciences of the United States of America* **105:** 4495-4500.

Cho, J.N., Ryu, J.Y., Jeong, Y.M., Park, J., Song, J.J., Amasino, R.M., Noh, B. and Noh, Y.S. 2012. Control of seed germination by light-induced histone arginine demethylation activity. *Developmental cell* **22:** 736-748.

Choi SM, Song HR, Han SK, Han M, Kim CY, Park J, Lee YH, Jeon JS, Noh

YS, Noh B. 2012. HDA19 is required for the repression of salicylic acid biosynthesis and salicylic acid-mediated defense responses in Arabidopsis. *Plant Journal* **71:** 135-146.

Cigliano, R.A., Cremona, G., Paparo, R., Termolino, P., Perrella, G., Gutzat, R., Consiglio, M.F. and Conicella, C. 2013. Histone deacetylase AtHDA7 is required for female gametophyte and embryo development in Arabidopsis. *Plant physiology* **163:** 431-440.

Clough SJ, Bent AF. 1998. Floral dip: a Simplified method for Agrobacterium-mediated transformation of *Arabidopsis thaliana*. *Plant Journal* **16:** 735-743.

Costas, C., de la Paz Sanchez, M., Stroud, H., Yu, Y., Oliveros, J.C., Feng, S., Benguria, A., Lopez-Vidriero, I., Zhang, X., Solano, R., Jacobsen, S.E. and Gutierrez, C. 2011. Genome-wide mapping of Arabidopsis thaliana origins of DNA replication and their associated epigenetic marks. *Nature structural & molecular biology* **18:** 395-400.

Cunliffe VT. 2008. Eloquent silence: developmental functions of Class I histone deacetylases. *Current Opinion in Genetics & Development* **18:** 404-410.

Dechaine, J.M., Gardner, G. and Weinig, C. 2009. Phytochromes differentially regulate seed germination responses to light quality and temperature cues during seed maturation. *Plant, cell & environment* **32:** 1297-1309.

Earley K, Lawrence RJ, Pontes O, Reuther R, Enciso A, Silva M, Neves N,

Gross M, Viegas W, Pikaard CS. 2006. Erasure of histone acetylation by Arabidopsis HDA6 mediates large-scale gene silencing in nucleolar dominance. *Genes & Development* **20:** 1283-1293.

Earley KW, Pontvianne F, Wierzbicki AT, Blevins T, Tucker S, Costa-Nunes P, Pontes O, Pikaard CS. 2010. Mechanisms of HDA6-mediated rRNA gene silencing: suppression of intergenic Pol II transcription and differential effects on maintenance versus siRNA-directed cytosine methylation. *Genes & Development* **24:** 1119-1132.

Fairchild CD, Schumaker MA, Quail PH. 2000. HFR1 encodes an atypical bHLH protein that acts in phytochrome A signal transduction. *Genes Dev* **14:** 2377-91.

Fong PM, Tian L, Chen J. 2006. *Arabidopsis thaliana* histone deaetylase 1 (AtHD1) is localized in euchromatic regions and demonstrates histone deacetylase activity in vitro. *Cell Research* **16:** 479-488.

Finch-Savage, W.E. and Leubner-Metzger, G. 2006. Seed dormancy and the control of germination. *The New phytologist* **171:** 501-523.

Gabriele, S., Rizza, A., Martone, J., Circelli, P., Costantino, P. and Vittorioso, P. 2010. The Dof protein DAG1 mediates PIL5 activity on seed germination by negatively regulating GA biosynthetic gene AtGA3ox1. *The Plant journal : for cell and molecular biology* **61:** 312-323.

Graeber, K., Linkies, A., Steinbrecher, T., Mummenhoff, K., Tarkowska, D.,

Tureckova, V., Ignatz, M., Sperber, K., Voegele, A., de Jong, H., Urbanova, T., Strnad, M. and Leubner-Metzger, G. 2014. DELAY OF GERMINATION 1 mediates a conserved coat-dormancy mechanism for the temperature- and gibberellin-dependent control of seed germination. *Proceedings of the National Academy of Sciences of the United States of America* **111:** E3571-3580.

Gremski K, Ditta G, Yanofsky MF.2007. The HECATE genes regulate female reproductive tract development in Arabidopsis thaliana. *Development* **134:** 3593-601

Grozinger CM, Schreiber SL. 2000. Regulation of histone deacetylase 4 and 5 and transcriptional activity by 14-3-3-dependent cellular localization. *Proceedings of the National Academy of Sciences, USA* **97:** 7835-7840.

Gu X, Jiang D, Wang Y, Bachmair A, He Y. 2009. Repression of the floral transition via histone H2B monoubiquitination. *Plant Journal* **57:** 522-533.

Gu X, Le C, Wang Y, Li Z, Jiang D, Wang Y, He Y. 2013. *Arabidopsis* FLC clade members form flowering-repressor complexes coordinating responses to endogenous and environmental cues. *Nature Communications* **4:** 1947.

Gu, X., Wang, Y. and He, Y. 2013. Photoperiodic regulation of flowering time through periodic histone deacetylation of the florigen gene FT. *PLoS biology* **11:** e1001649.

Gremski K, Ditta G, Yanofsky MF. 2007. HECATE genes regulate female reproductive tract development in Arabidopsis thaliana. *Development* **20:** 3593-601

Han, C. and Yang, P. 2015. Studies on the molecular mechanisms of seed germination. *Proteomics* **10:** 1671-1679

Han SK, Song JD, Noh YS, Noh B. 2007. Role of plant CBP/p300-like genes in the regulation of flowering time. *Plant Journal* **49:** 103-114.

Hayakawa T, Nakayama J. **2011.** Physiological roles of Class I HDAC complex and histone demethylases. *Journal of Biomedicine and Biotechnology* **2011:** 1-10.

He Y, Michaels SD, Amasino RM. 2003. Regulation of flowering time by histone acetylation in Arabidopsis. *Science* **302:** 1751-1754.

He Y. 2012. Chromatin regulation of flowering. *Trends Plant Sci* **17:** 556-562

Helliwell CA, Wood CC, Robertson M, Peacock WJ, Dennis ES. 2006. The Arabidopsis FLC protein interacts directly in vivo with *SOC1* and *FT* chromatin and is a part of a high-molecular-weight protein complex. *Plant Journal* **46:** 183-192.

Hollender C, Liu Z. 2008. Histone deacetylase genes in Arabidopsis development. *Journal of Integrative Plant Biology* **50:** 875-885.

Holdsworth, M.J., Bentsink, L. and Soppe, W.J. 2008. Molecular networks regulating Arabidopsis seed maturation, after-ripening, dormancy and

germination. *The New phytologist* **179:** 33-54.

Hu, Y. and Yu, D. 2014. BRASSINOSTEROID INSENSITIVE2 interacts with ABSCISIC ACID INSENSITIVE5 to mediate the antagonism of brassinosteroids to abscisic acid during seed germination in Arabidopsis. *The Plant cell* **26:** 4394-4408.

Jeong JH, Song HR, Ko JH, Jeong YM, Kwon YE, Seol JH, Amasino RM, Noh B, Noh YS. 2009. Repression of FLOWERING LOCUS T chromatin by functionally redundant histone H3 lysine 4 demethylases in Arabidopsis. *PLoS One* **25:** e8033

Jung JH, Seo YH, Seo PJ, Reyes JL, Yun J, Chua NH, Park CM. 2007. The GIGANTEA-regulated microRNA172 mediates photoperiodic flowering independent of CONSTANS in Arabidopsis. *Plant Cell* **19:** 2736-2748.

Jung, J.H., Park, J.H., Lee, S., To, T.K., Kim, J.M., Seki, M. and Park, C.M. 2013. The cold signaling attenuator HIGH EXPRESSION OF OSMOTICALLY RESPONSIVE GENE1 activates FLOWERING LOCUS C transcription via chromatin remodeling under short-term cold stress in Arabidopsis. *The Plant cell* **25:** 4378-4390.

Kang MJ, Jin HS, Noh YS, Noh B. 2015. Repression of flowering under a noninductive photoperiod by the HDA9-AGL19-FT module in Arabidopsis. *New Phytol* **206:** 281-294.

Kang, H., Oh, E., Choi, G. and Lee, D. 2010. Genome-wide DNA-binding

specificity of PIL5, an Arabidopsis basic Helix-Loop-Helix (bHLH) transcription factor. *International journal of data mining and bioinformatics* **4:** 588-599.

Kaufmann K, Muiño JM, Østerås M, Farinelli L, Krajewski P, Angenent GC. 2010. Chromatin immunoprecipitation (ChIP) of plant transcription factors followed by sequencing (ChIP-SEQ) or hybridization to whole genome arrays (ChIP-CHIP). *Nature Protocol* **5:** 457-472.

Kendall, S. 2012. Temp regulation of seed dormancy and germination in arabidopsis.

Kim, D.H., Yamaguchi, S., Lim, S., Oh, E., Park, J., Hanada, A., Kamiya, Y. and Choi, G. 2008. SOMNUS, a CCCH-type zinc finger protein in Arabidopsis, negatively regulates light-dependent seed germination downstream of PIL5. *The Plant cell* **20:** 1260-1277.

Kim, D.H. and Sung, S. 2010. The Plant Homeo Domain finger protein, VIN3-LIKE 2, is necessary for photoperiod-mediated epigenetic regulation of the floral repressor, MAF5. *Proceedings of the National Academy of Sciences of the United States of America* **107:** 17029-17034.

Kim, D.H. and Sung, S. 2013. Coordination of the vernalization response through a VIN3 and FLC gene family regulatory network in Arabidopsis. *Plan cell* **25:** 454-469.

Kim DH, Sung S. 2014. Genetic and Epigenetic Mechanisms Underlying

Vernalization. *Arabidopsis Book* **12:** e0171.

Kim JY, Oh JE, Noh YS, Noh B. 2015. Epigenetic control of juvenile-to-adult phase transition by the Arabidopsis SAGA-like complex. *Plant J* **83:** 537-545

Kim W, Latrasse D, Servet C, Zhou DX. 2013. Arabidopsis histone deacetylase HDA9 regulates flowering time through repression of AGL19. *Biochemical and Biophysical Research Communications* **432:** 394–398.

Kim KC, Lai Z, Fan B, Chen Z. 2008. *Arabidopsis* WRKY38 and WRKY62 transcription factors interact with histone deacetylase 19 in basal defense. *Plant Cell* **20:** 2357-2371.

Kim SY, Zhu T, Sung ZR. 2010. Epigenetic regulation of gene programs by EMF1 and EMF2 in Arabidopsis. *Plant Physiology* **152:** 516–528.

Kinkema M, Fan W, Dong X. 2000. Nuclear localization of NPR1 is required for activation of *PR* gene expression. *Plant Cell* **12:** 2339-2350.

Koornneef M, Alonso-Blanco C, Peeters AJM, Soppe W. 1998. Genetic control of flowering time in Arabidopsis. *Annual Review of Plant Physiology and Plant Molecular Biology* **49:** 345-370.

Koornneef M, Vrles HB, Hanhart C, Soppe W, Peeters T. 1994. The phenotype of some late-flowering mutants is enhanced by a locus on chromosome 5 that is not effective in the Landsberg erecta wild-type. *Plant Journal* **6:**

911–919.

Kurdistani SK, Robyr D, Tavazoie S, Grunstein M. 2002. Genome-wide binding map of the histone deacetylase Rpd3 in yeast. *Nature Genetics* **31:** 248-254.

Lee I, Michaels SD, Amasino RM. 1994. The late-flowering phenotype of *FRIGIDA* and mutations in *LUMINIDEPENDENS* is suppressed in the Landsberg *erecta* strain of Arabidopsis. *Plant Journal* **6:** 903-909.

Lee, N., Kang, H., Lee, D. and Choi, G. 2014. A histone methyltransferase inhibits seed germination by increasing PIF1 mRNA expression in imbibed seeds. *The Plant journal : for cell and molecular biology* **78:** 282-293.

Liu, P.P., Koizuka, N., Martin, R.C. and Nonogaki, H. 2005. The BME3 (Blue Micropylar End 3) GATA zinc finger transcription factor is a positive regulator of Arabidopsis seed germination. *The Plant journal : for cell and molecular biology* **44:** 960-971.

Liu X, Yu CW, Duan J, Luo M, Wang K, Tian G, Cui Y, Wu K. 2012. HDA6 directly interacts with DNA methyltransferase MET1 and maintains transposable element silencing in Arabidopsis. *Plant Physiology* **158:** 119-129.

Liu, X., Chen, C.Y., Wang, K.C., Luo, M., Tai, R., Yuan, L., Zhao, M., Yang, S., Tian, G., Cui, Y., Hsieh, H.L. and Wu, K. 2013. PHYTOCHROME INTERACTING FACTOR3 associates with the histone deacetylase

HDA15 in repression of chlorophyll biosynthesis and photosynthesis in etiolated Arabidopsis seedlings. *The Plant cell* **25:** 1258-1273.

Livak KJ, Schmittgen TD. 2001. Analysis of relative gene expression data using real-time quantitative PCR and the $2^{-\Delta\Delta CT}$ method. *Methods* **25:** 402-408.

Liu X, Yang S, Zhao M, Luo M, Yu CW, Chen CY, Tai R, Wu K. 2014. Transcriptional repression by histone deacetylases in plants. *Mol Plant* **7:**764-72.

Long JA, Ohno C, Simth ZR, Meyerowitz EM. 2006. TOPLESS regulates apical embryonic fate in Arabidopsis. *Science* **312:** 1520-1523.

Lu, X., Wontakal, S.N., Kavi, H., Kim, B.J., Guzzardo, P.M., Emelyanov, A.V., Xu, N., Hannon, G.J., Zavadil, J., Fyodorov, D.V. and Skoultchi, A.I. 2013. Drosophila H1 regulates the genetic activity of heterochromatin by recruitment of Su(var)3-9. *Science* **340:** 78-81.

Michaels SD, Amasino RM. 2001. Loss of FLOWERING LOCUS C activity eliminates the late flowering of *FRIGIDIA* and autonomous pathway mutants but not responsiveness to vernalization. *Plant Cell* **13:** 935-941.

Michales SD, Ditta G, Gustafson-Brown C, Pelaz S, Yanofsky M, Amasino R. 2003. AGL24 acts as a promoter of flowering in Arabidopsis and is positively regulates by vernalization. *Plant Journal* **33:** 867-874.

Molitor, A.M., Bu, Z., Yu, Y. and Shen, W.H. 2014. Arabidopsis AL PHD-PRC1

complexes promote seed germination through H3K4me3-to-H3K27me3 chromatin state switch in repression of seed developmental genes. *PLoS genetics* **10:** e1004091.

Moon J, Suh SS, Lee H, Choi KR, Hong CB, Paek NC, Kim SG, Lee I. 2003. The *SOC1* MADS-box gene integrates vernalization and gibberellin signals for flowering in Arabidopsis. *Plant Journal* **35:** 613-623.

Morris, K., Linkies, A., Muller, K., Oracz, K., Wang, X., Lynn, J.R., Leubner-Metzger, G. and Finch-Savage, W.E. 2011. Regulation of seed germination in the close Arabidopsis relative Lepidium sativum: a global tissue-specific transcript analysis. *Plant physiology* **155:** 1851-1870.

Nakabayashi, K., Bartsch, M., Xiang, Y., Miatton, E., Pellengahr, S., Yano, R., Seo, M. and Soppe, W.J. 2012. The time required for dormancy release in Arabidopsis is determined by DELAY OF GERMINATION1 protein levels in freshly harvested seeds. *The Plant cell* **24:** 2826-2838.

Nelson, D.C., Flematti, G.R., Ghisalberti, E.L., Dixon, K.W. and Smith, S.M. 2012. Regulation of seed germination and seedling growth by chemical signals from burning vegetation. *Annual review of plant biology* **63:** 107-130.

Noh B, Lee SH, Kim HJ, Yi G, Shin EA, Lee M, Jung KJ, Doyle MR, Amasino RM, Noh YS. 2004. Divergent roles of a pair of homologous jumonji/zinc-finger-class transcription factor proteins in the regulation of Arabidopsis flowering time. *Plant Cell* **16:** 2601-2613.

Noh B, Murphy AS, Spalding EP. 2001. *Multidrug resistance*-like genes of Arabidospis required for auxin transport and auxin-mediated development. *Plant Cell* **13:** 2441-2454.

Ogawa, M. 2003. Gibberellin Biosynthesis and Response during Arabidopsis Seed Germination. *The Plant Cell Online* **15:** 1591-1604.

Oh, E., Kang, H., Yamaguchi, S., Park, J., Lee, D., Kamiya, Y. and Choi, G. 2009. Genome-wide analysis of genes targeted by PHYTOCHROME INTERACTING FACTOR 3-LIKE5 during seed germination in Arabidopsis. *The Plant cell* **21**, 403-419.

Oh, E., Kim, J., Park, E., Kim, J.I., Kang, C. and Choi, G. 2004. PIL5, a phytochrome-interacting basic helix-loop-helix protein, is a key negative regulator of seed germination in Arabidopsis thaliana. *The Plant cell* **16**, 3045-3058.

Oh, E., Yamaguchi, S., Kamiya, Y., Bae, G., Chung, W.I. and Choi, G. 2006. Light activates the degradation of PIL5 protein to promote seed germination through gibberellin in Arabidopsis. *The Plant journal : for cell and molecular biology* **47**, 124-139.

Oh, E., Yamaguchi, S., Hu, J., Yusuke, J., Jung, B., Paik, I., Lee, H.S., Sun, T.P., Kamiya, Y. and Choi, G. 2007. PIL5, a phytochrome-interacting bHLH protein, regulates gibberellin responsiveness by binding directly to the GAI and RGA promoters in Arabidopsis seeds. *The Plant cell* **19:**1192-1208.

Pandey R, Muller A, Napoli CA, Selinger DA, Pikarrd CS, Richard EJ, Bender J, Mount DW, Jorgensen A. 2002. Analysis of histone acetyltransferase and histone deacetylase families of *Arabidopsis thaliana* suggests functional diversification of chromatin modification among multicellular eukaryotes. *Nucleic Acids Research* **30:** 5036-5055.

Park DH, Somers DE, Kim YS, Choy YH, Lim HK, Soh MS, Kim HJ, Kay SA, Nam HG. 1999. Control of circadian rhythms and photoperiodic flowering by the Arabidopsis *GIGANTEA* gene. *Science* **285:** 1579-1582.

Park, S.J., Kwak, K.J., Oh, T.R., Kim, Y.O. and Kang, H. 2009. Cold shock domain proteins affect seed germination and growth of Arabidopsis thaliana under abiotic stress conditions. *Plant & cell physiology* **50:** 869-878.

Penfield, S., Josse, E.M., Kannangara, R., Gilday, A.D., Halliday, K.J. and Graham, I.A. 2005. Cold and light control seed germination through the bHLH transcription factor SPATULA. *Current biology : CB* **15:** 1998-2006.

Perales M, Màs P. 2007. A functional link between rhythmic changes in chromatin structure and the Arabidopsis biological clock. *Plant Cell* **19:** 2111-2123.

Probst AV, Fagard M, Proux F, Mourrain P, Boutet S, Earley K, Lawrence RJ, Pikkard CS, Murfett J, Furner I, Vaucheret H, Scheid OM. 2004. Arabidopsis histone deacetylase HDA6 is required for maintenance of

transcriptional silencing and determines nuclear organization of rDNA repeats. *Plant Cell* **16:** 1021-1034.

Ramsey, S.A., Knijnenburg, T.A., Kennedy, K.A., Zak, D.E., Gilchrist, M., Gold, E.S., Johnson, C.D., Lampano, A.E., Litvak, V., Navarro, G., Stolyar, T., Aderem, A. and Shmulevich, I. 2010. Genome-wide histone acetylation data improve prediction of mammalian transcription factor binding sites. *Bioinformatics* **26:** 2071-2075.

Ratcliffe OJ, Kumimoto RW, Wong BJ, Riechmann JL. 2003. Analysis of the Arabidopsis *MADS AFFECTING FLOWERING* gene family: *MAF2* prevents vernnalization by short periods of cold. *Plant Cell* **15:** 1159-1169.

Rashid, A. and Deyholos, M.K. 2011. PELPK1 (At5g09530) contains a unique pentapeptide repeat and is a positive regulator of germination in Arabidopsis thaliana. *Plant cell reports* **30:** 1735-1745.

Rincon-Arano, H., Halow, J., Delrow, J.J., Parkhurst, S.M. and Groudine, M. 2012. UpSET recruits HDAC complexes and restricts chromatin accessibility and acetylation at promoter regions. *Cell* **151:** 1214-1228.

Rivera, C., Gurard-Levin, Z.A., Almouzni, G. and Loyola, A. 2014. Histone lysine methylation and chromatin replication. *Biochimica et biophysica acta* **1839:** 1433-1439.

Robin J. Probert. 2012 The Role of Temperature in the Regulation of Seed

Dormancy and Germination *Seeds: The Ecology of Regeneration in Plant Communities* **2:** 261-292

Sanchez Mde, L., Caro, E., Desvoyes, B., Ramirez-Parra, E. and Gutierrez, C. 2008. Chromatin dynamics during the plant cell cycle. *Seminars in cell & developmental biology* **19:** 537-546.

Santopolo, S., Boccaccini, A., Lorrai, R., Ruta, V., Capauto, D., Minutello, E., Serino, G., Costantino, P. and Vittorioso, P. 2015. DOF AFFECTING GERMINATION 2 is a positive regulator of light-mediated seed germination and is repressed by DOF AFFECTING GERMINATION 1. *BMC plant biology* **15:** 72.

Sassone-Corsi, P. 2013. Physiology. When metabolism and epigenetics converge. *Science* **339:** 148-150.

Schmid M, Uhlenhaut NH, Godard F, Demar M, Bressan R, Weigel D, Lohmann JU. 2003. Dissection of floral induction pathways using global expression analysis. *Development* **130:** 6001-6012.

Schönrock N, Bouveret R, Leroy O, Borghi L, Kohler C, Gruissem W, Hennig L. 2006. Plycomb-group proteins repress the floral activator *AGL19* in the *FLC*-independent vernalization pathway. *Genes & Development* **20:** 1667-1678.

Schuster C, Gaillochet C, Lohmann JU. 2015. Arabidopsis HECATE genes function in phytohormone control during gynoecium development.

Development **142:** 3343-3350

Servet, C., Conde e Silva, N. and Zhou, D.X. 2010. Histone acetyltransferase AtGCN5/HAG1 is a versatile regulator of developmental and inducible gene expression in Arabidopsis. *Mol Plant* **3:** 670-677.

Seo, M., Hanada, A., Kuwahara, A., Endo, A., Okamoto, M., Yamauchi, Y., North, H., Marion-Poll, A., Sun, T.P., Koshiba, T., et al. 2006. Regulation of hormone metabolism in Arabidopsis seeds: phytochrome regulation of abscisic acid metabolism and abscisic acid regulation of gibberellin metabolism. *Plant J* **48:** 354–366.

Seo, M., Nambara, E., Choi, G., and Yamaguchi, S. 2009. Interaction of light and hormone signals in germinating seeds. *Plant Mol. Biol* **69:** 463–472.

Sharma, V.M., Tomar, R.S., Dempsey, A.E. and Reese, J.C. 2007. Histone deacetylases RPD3 and HOS2 regulate the transcriptional activation of DNA damage-inducible genes. *Molecular and cellular biology* **27:** 3199-3210.

Shi, H., Wang, X., Mo, X., Tang, C., Zhong, S. and Deng, X.W. 2015. Arabidopsis DET1 degrades HFR1 but stabilizes PIF1 to precisely regulate seed germination. *Proceedings of the National Academy of Sciences of the United States of America* **112:** 3817-3822.

Shi, H., Zhong, S., Mo, X., Liu, N., Nezames, C.D. and Deng, X.W. 2013. HFR1 sequesters PIF1 to govern the transcriptional network underlying light-

initiated seed germination in Arabidopsis. *The Plant cell* **25:** 3770-3784.

Silva-Correia, J., Freitas, S., Tavares, R.M., Lino-Neto, T. and Azevedo, H. 2014. Phenotypic analysis of the Arabidopsis heat stress response during germination and early seedling development. *Plant methods* **10:** 7.

Shinomura, T., Nagatani, A., Chory, J., and Furuya, M. 1994. The induction of seed germination in Arabidopsis thaliana is regulated principally by phytochrome B and secondarily by phytochrome A. *Plant Physiol* **104:** 363–371.

Suzuki, Y., Kawazu, T., and Koyama, H. 2004. RNA isolation from siliques, dry seeds, and other tissues of Arabidopsis thaliana. *Biotechniques* **37:** 542.

Soh MS, Kim YM, Han SJ, Song PS. 2000. REP1, a basic helix-loop-helix protein, is required for a branch pathway of phytochrome A signaling in arabidopsis. *Plant Cell* **12:** 2061-2074.

Song, C.P. and Galbraith, D.W. 2006. AtSAP18, an orthologue of human SAP18, is involved in the regulation of salt stress and mediates transcriptional repression in Arabidopsis. *Plant molecular biology* **60:** 241-257.

Stamm, P. 2012. Insights into the molecular mech of RGL2 mediated inhibition of seed germination in arabidopsis. *BMC plant biology* **12:**179

Sung S, Schmitz RJ, Amasino RM. 2006. A PHD finger domain involved in both the verrnalization and photoperiod pathways in Arabidopsis. *Genes & Development* **20:** 3244-3248.

Sutendra, G., Kinnaird, A., Dromparis, P., Paulin, R., Stenson, T.H., Haromy, A., Hashimoto, K., Zhang, N., Flaim, E. and Michelakis, E.D. 2014. A nuclear pyruvate dehydrogenase complex is important for the generation of acetyl-CoA and histone acetylation. *Cell* **158:** 84-97.

Takada S, Goto K. 2003. TERMINAL FLOWER 2, a HETEROCHROMATIN PROTEION1-Like protein of Arabidopsis, counteracts the activation of *FLOWERING LOCUS T* by CONSTANTS in the vascular tissues of leaves to regulate flowering time. *Plant Cell* **15:** 2856-2865.

Tanaka M, Kikuchi A, Kamada H. 2008. The Arabidopsis histone deacetylases HDA6 and HDA19 contribute to the repression of embryonic properties after germination. *Plant Physiology* **146:** 149-161.

Tai HH, Tai GC, Beardmore T. 2005. Dynamic histone acetylation of late embryonic genes during seed germination. *Plant Mol Biol* **59:** 909-925.

Tian L, Chen ZL. 2001. Blocking histone deacetylation in Arabidopsis induces pleiotropic effects on plant gene regulation and development. *Proceedings of the National Academy of Sciences, USA* **98:** 200-205.

Tian L, Fong MP, Wang JJ, Wei NE, Jianf J, Doerge RW, Chen ZJ. 2005. Reversible histone acetylation and deacetylation mediate genome0wide, promoter-dependent and locus-specific changes in gene expression during plant development. *Genetics* **169:** 337-345.

Tian L, Wang J, Fong MP, Chen M, Cao H, Gelvin SB, Chen ZJ. 2003.

Genetic control of developmental changes induced by disruption of Arabidopsis histone deacetylase 1 (AtHD1) expression. *Genetics* **165:** 399-409.

Toyomasu, T., Kawaide, H., Mitsuhashi, W., Inoue, Y., and Kamiya, Y. 1998. Phytochrome regulates gibberellin biosynthesis during germination of photoblastic lettuce seeds. *Plant Physiol* **118:** 1517–1523.

To TK, Kim JM, Matsui A, Kurihara Y, Morosawa T, Ishida J, Tanaka M, Endo T, Kakutani T, Toyoda T, Kimura H, Yokoyama S, Shinozaki K, Seki M. 2011. Arabidopsis HDA6 regulates locus-directed heterochromatin silencing in cooperation with MET1. *PLoS Genetics* **7:** e1002055.

Torii KU, Mitsukawa N, Oosummi T, Matsuura Y, Yokoyamma R, Whittier RF, Komeda Y. 1996. The Arabidopsis *ERECTA* gene encodes a putative receptor protein kinase with extracellular kinase leucine-rich repeats. *Plant Cell* **8:** 735-746.

Turck F, Fornara F, Coupland G. 2008. Regulation and identity of florigen: FLOWERING LOCUS T moves center stage. *Annual Review of Plant Biology* **59:** 573-594.

van Dijk, K., Ding, Y., Malkaram, S., Riethoven, J.J., Liu, R., Yang, J., Laczko, P., Chen, H., Xia, Y., Ladunga, I., Avramova, Z. and Fromm, M. 2010. Dynamic changes in genome-wide histone H3 lysine 4 methylation patterns in response to dehydration stress in Arabidopsis thaliana. *BMC plant biology* **10:** 238.

van Zanten M, Zöll C, Wang Z, Philipp C, Carles A, Li Y, Kornet NG, Liu Y, Soppe WJ. 2014. HISTONE DEACETYLASE 9 represses seedling traits in Arabidopsis thaliana dry seeds. *Plant Journal* **80:** 475–488

Verdel A, Curtet S, Brocard MP, Rousseaux S, Lemercier C, Yoshida M, Khochbin S. 2000. Active maintenance of mHDA2/mHDA6 histone-deacetylase in the cytoplasm. *Current Biology* **10:** 747-749.

Villedieu-Percheron, E., Lachia, M., Jung, P.M., Screpanti, C., Fonne-Pfister, R., Wendeborn, S., Zurwerra, D. and De Mesmaeker, A. 2014. Chemicals inducing seed germination and early seedling development. *Chimia* **68:** 654-663.

Wang JW, Czech B, Weigel D. 2009a. miR156-regulated SPL transcription factors define an endogenous flowering pathway in *Arabidopsis thaliana*. *Cell* **138:** 738-749.

Wang, Y., Gu, X., Yuan, W., Schmitz, R.J. and He, Y. 2014. Photoperiodic control of the floral transition through a distinct polycomb repressive complex. *Developmental cell* **28:** 727-736

Wang Z, Cao H, Chen F, Liu Y. 2014. The roles of histone acetylation in seed performance and plant development. *Plant Physiol Biochem* **84:**125-33

Wang Z, Zang C, Cui K, Schones DE, Barski A, Peng W, Zhao K. 2009b. Genome-wide mapping of HATs and HDACs reveals distinct functions in

active and inactive genes. *Cell* **138:** 1019-1031.

Wang Z, Cao H, Sun Y, Li X, Chen F, Carles A, Li Y, Ding M, Zhang C, Deng X, Soppe WJ, Liu YX. 2013. Arabidopsis paired amphipathic helix proteins SNL1 and SNL2 redundantly regulate primary seed dormancy via abscisic acid-ethylene antagonism mediated by histone deacetylation. *Plant Cell* **25:**149-166.

Weitbrecht, K., Muller, K. and Leubner-Metzger, G. 2011. First off the mark: early seed germination. *Journal of experimental botany* **62:** 3289-3309.

Wu K, Zhang L, Zhou C, Yu CW, Chaikam V. 2008. HDA6 is required for jasmonate response, senescence and flowering in Arabidopsis. *Journal of Experimental Botany* **59:** 225-234.

Xu CR, Liu C, Wang YL, Li LC, Chen WQ, Xu ZH, Bai SN. 2005. Histone acetylation affects expression of cellular patterning genes in the Arabidopsis root epidermis. *Proceedings of the National Academy of Sciences, USA* **102:** 14469-14474.

Yamaguchi, S., Smith, M.W., Brown, R.G., Kamiya, Y., and Sun, T. 1998. Phytochrome regulation and differential expression of gibberellin 3betahydroxylase genes in germinating Arabidopsis seeds. *Plant Cell* **10:** 2115–2126.

Yamauchi, Y., Takeda-Kamiya, N., Hanada, A., Ogawa, M., Kuwahara, A., Seo, M., Kamiya, Y., and Yamaguchi, S. 2007. Contribution of gibberellin

deactivation by AtGA2ox2 to the suppression of germination of dark-imbibed Arabidopsis thaliana seeds. *Plant Cell Physiol* **48:** 555–561.

Yang KY, Kim YM, Lee S, Song PS, Soh MS. 2003. Overexpression of a mutant basic helix-loop-helix protein HFR1, HFR1-deltaN105, activates a branch pathway of light signaling in Arabidopsis. *Plant Physiol* **133:**1630-1642

Yang, X.J. and Seto, E. 2007. HATs and HDACs: from structure, function and regulation to novel strategies for therapy and prevention. *Oncogene* **26:** 5310-5318.

Yang XJ, Seto, E. 2008. The Rpd3/Hda1 family of lysine deacetylases: from bacteria and yeast to mice and men. *Nature Reviews Molecular Cell Biology* **9:** 206-218.

Yang, Y. and Karlson, D. 2013. AtCSP1 regulates germination timing promoted by low temperature. *FEBS letters* **587:** 2186-2192.

Yano, R., Takebayashi, Y., Nambara, E., Kamiya, Y. and Seo, M. 2013. Combining association mapping and transcriptomics identify HD2B histone deacetylase as a genetic factor associated with seed dormancy in Arabidopsis thaliana. *The Plant journal : for cell and molecular biology* **74:** 815-828.

Yelagandula, R., Stroud, H., Holec, S., Zhou, K., Feng, S., Zhong, X., Muthurajan, U.M., Nie, X., Kawashima, T., Groth, M., Luger, K., Jacobsen, S.E. and Berger, F. 2014. The histone variant H2A.W defines

heterochromatin and promotes chromatin condensation in Arabidopsis. *Cell* **158:** 98-109.

Yoo SK, Wu X, Lee JS, Ahn JH. 2011. AGAMOUS-LIKE 6 is a floral promoter that negatively regulates the *FLC/MAF* clade genes and positively regulates *FT* in Arabidopsis. *Plant Journal* **65:** 62-76.

Yoo SK, Chung KS, Kim J, Lee JH, Hong SM, Yoo SJ, Yoo SY, Lee JS, Ahn JH. 2005. CONSTANS activates *SUPPRESSOR OF OVEREXPRESSION OF CONSTANS 1* through *FLOWERING LOCUS T* to promote flowering in Arabidopsis. *Plant Physiology* **139:** 770-778.

Yu CW, Liu X, Luo M, Chen C, Lin X, Tian G, Lu Q, Cui Y, Wu K. 2011. HISTONE DEACETYLASE6 interacts with FLOWERING LOCUS D and regulates flowering in Arabidopsis. *Plant Physiology* **156:** 172-184.

Yu H, Xu Y, Tan EL, Kumar PP. 2002. AGAMOUS-LIKE 24, a dosage-dependent mediator of the flowering signals. *Proceedings of the National Academy of Sciences, USA* **99:** 16336-16341.

Zografos BR, Sung S. 2012. Vernalization-mediated chromatin changes. *J Exp Bot* 63:4343-4348.

Zhou C, Zhang L, Duan J, Miki B, Wu K. 2005. HISTONE DEACETYLASE 19 is involved in jasmonic acid and ethylene signaling of pathogen response in Arabidopsis. *Plant Cell* **17:** 1196-1204.

Zhou, J., Wang, X., He, K., Charron, J.B., Elling, A.A. and Deng, X.W. 2010.

Genome-wide profiling of histone H3 lysine 9 acetylation and dimethylation in Arabidopsis reveals correlation between multiple histone marks and gene expression. *Plant molecular biology* **72:** 585-595.

Zhu L. 2012. The HECATE proteins promote photomorphogenesis by negatively regulating the function of PIF1 in Arabidopsis, *PhD Thesis*

Zhou, Y., Tan, B., Luo, M., Li, Y., Liu, C., Chen, C., Yu, C.W., Yang, S., Dong, S., Ruan, J., Yuan, L., Zhang, Z., Zhao, L., Li, C., Chen, H., Cui, Y., Wu, K. and Huang, S. 2013. HISTONE DEACETYLASE19 interacts with HSL1 and participates in the repression of seed maturation genes in Arabidopsis seedlings. *The Plant cell* **25:** 134-148.

국문 초록

히스톤 아세틸화와 탈아세틸화는 유전자 발현을 결정하는 중요한 변형 중 하나이다. 최근 연구들에서 히스톤 탈아세틸화는 유전자 발현 억제뿐만 아니라, 아세틸화와 함께 유전자 발현 활성에도 밀접한 연관이 있다는 것이 보고되었다. 하지만 식물의 발달과정에서 유전자 발현 활성 조절에 필요한 히스톤 탈아세틸화 효소에 대해서는 현재까지 충분히 연구되어 있지 않다. 따라서 본 연구는 모델식물인 애기장대에서 유전자 발현활성의 균형을 유지하는데 HDA9이 필요하다는 것에 연구의 초점을 두었다.

식물에서 HAT과 HDAC 효소에 의한 히스톤 변형은 외부 환경에 반응하여 종자발아 및 개화시기 조절 등의 발달과정에 영향을 준다. 식물이 영양생장에서 생식생장으로 전이되는 과정은 성공적인 생식을 위해 중요하며, 이는 주요 유전자의 히스톤 변형을 동반한다. 본 연구에서는 단일 조건 특이적인 *hda9* 돌연변이체의 조기개화 현상이 광주기 의존적 개화 촉진 인자인 *AGL19* 과발현을 동반함을 확인하였다. 나아가 HDA9은 히스톤 탈아세틸화를 통해 단일 조건과 춘화 처리 신호에 의해 과발현될 *AGL19* 전사활성을 억제하고, 이어 개화 호르몬인 *FT* 전사활성에 영향을 주어 조기 개화를 제한함을 증명하였다.

개화뿐만 아니라, 종자가 주어진 환경에서 발아시기를 최적화 하는 일은 생존과 생장을 위한 중요한 과정 중 하나이다. 본 연구에서는 종자 발아 촉진 인자인 *HEC*가 적색광에 의해 유도되고, 과발현될 *HEC*를 HDA9이

히스톤 탈아세틸화를 통해 억제함을 확인하였다. 따라서, 적절한 *HEC* 전사활성을 유지하는데 히스톤 탈아세틸화가 필요함을 증명하였다. 더 나아가 HDA9-HEC-PIF1 모듈을 통해 HDA9이 비정상적인 종자발아 현상을 지연시킨다는 것을 규명하였다.

본 연구는 개화와 종자발아 등 식물의 발달과정에서 HDA9이 외부 환경요인에 의해 과발현될 AGL19, HEC 등의 전사활성의 균형을 유지시키기 위해 국부적으로 과활성화될 수 있는 염색질을 에피유전학적으로 재프로그래밍함에 중요한 인자임을 증명하였다. 이러한 HDA9 기능은 기존에 알려진 히스톤 탈아세틸화 효소들의 역할과 구분되는 독특한 것이며, 향후 애기장대의 발달 연구에 있어서 히스톤 탈아세틸화 효소들의 보다 다양한 기능이 규명될 가능성을 시사한다.

주요어: 히스톤 탈아세틸화, HDA9, AGL19, 개화시기, HEC, 종자발아

학 번: 2008-30102